ANNA NAOMI DE HAAS

Mapping space, episodes and values in the hippocampus

Mapping space, episodes and values in the hippocampus

Proefschrift

ter verkrijging van de graad van doctor
aan de Radboud Universiteit Nijmegen
op gezag van de rector magnificus prof. dr. J.H.J.M. van Krieken,
volgens besluit van het college van decanen
in het openbaar te verdedigen op

maandag 28 juni 2021
om 16:30 uur precies

door

Anna Naomi de Haas
geboren op 23 augustus 1990
te Gießen, Duitsland

Mapping space, episodes and values in the hippocampus
PhD thesis, Radboud University, Nijmegen.

Cover/layout | Proefschriftenbalie
Print | Ipskamp Printing

Promotoren

Prof. dr. Christian F.A Döller (Norges teknisk-naturvitenskapelige universitet, Trondheim, Noorwegen)

Prof. dr. Roshan Cools

Copromotor

Dr. Mona M. Garvert (Max Planck Institut für Kognitions- und Neurowissenschaften, Leipzig, Duitsland)

Manuscriptcommissie

Prof. dr. Guillén S.E. Fernández

Dr. H. Freyja Ólafsdóttir

Prof. dr. Gerhard Jocham (Heinrich Heine Universität Düsseldorf, Duitsland)

Mapping space, episodes and values in the hippocampus

Doctoral Thesis

to obtain the degree of doctor
from Radboud University Nijmegen
on the authority of the Rector Magnificus prof. dr. J.H.J.M. van Krieken,
according to the decision of the Council of Deans
to be defended in public on

Monday, June 28, 2021
at 16:30 hours

by

Anna Naomi de Haas
born on August 23, 1990
in Gießen, Germany

Supervisors

Prof. dr. Christian F.A Döller (Norges teknisk-naturvitenskapelige universitet, Trondheim, Norway)

Prof. dr. Roshan Cools

Co-supervisor

Dr. Mona M. Garvert (Max Planck Institut für Kognitions- und Neurowissenschaften, Leipzig, Germany)

Doctoral Thesis Committee

Prof. dr. Guillén S.E. Fernández

Dr. H. Freyja Ólafsdóttir

Prof. dr. Gerhard Jocham (Heinrich Heine Universität Düsseldorf, Germany)

To my generous grandparents Gerhard and Erdmuthe Höf

Contents

CHAPTER 1

General introduction

Aim

As is probably true for all PhD candidates, I had to overcome many obstacles to finish my thesis. However, one thing I always loved about it was living and working in Nijmegen. There are many little reasons for this, like the amount of excellent coffee places or the fact that no matter where you live, it takes less than 15 minutes to bike to work. Funnily enough though, the annual highlight of this cosy, midsize city is a week-long outdoor festival with more than a million visitors from around the world. I have fond memories of these events, for example sitting at the crowded edges of the river while watching fireworks with my friends. However, as we have already established in the very first sentence of this thesis: life often comes with obstacles. See, the actual cause behind the festival is a four-day march, where the participants have to walk a different (extremely long) trail every day. As a consequence, every day another set of streets is closed off for the general public. This leaves me (and many, many others) with the challenge to plan a daily detour to the office. At this point, you might start to wonder why I am telling you this story and how this all relates to the topic of my thesis.

I studied a very specific brain region: the hippocampus (Box 1). What fascinates me about the hippocampus is that it is involved in very different aspects of this story: remembering events like sitting at the river watching the fireworks and at the same time solving navigation problems like biking to the office. At the very core of this thesis, I wanted to investigate the question: How does the hippocampus support so seemingly different functions like memory and navigation?

For this purpose, I conducted three experiments in collaboration with other researchers. In the first experiment, we took a closer look at the mental map that the hippocampus forms of our environment. Think back to the story: I bike from my home to the office quite often. For this, I need to have a mental representation of Nijmegen (or at least parts of it). If I would lay out a map of Nijmegen in front of you, I could draw a straight line between my home and the office – the Euclidean distance. I could also draw the path I need to bike along to get to the office – the path distance. Remarkably, I found myself able to update the path distance very flexibly when I encountered new roadblocks during the festival, speaking to the flexible nature of these mental representations. In the first study, we looked at hippocampal representations of these different distance measures and how they are updated when shortcuts or detours are introduced.

In the second experiment, we looked at hippocampal processing of navigation and episodic memory at the same time. We tested the two opposing ideas that the hippocampus either uses the same coding mechanisms for both, navigation and memory, or that different subregions in the hippocampus are involved in either function,

respectively. The question was does the hippocampus process my memory of sitting at the river watching fireworks and me biking from home to the office similarly? Or do different parts of hippocampus code for one, but not the other.

In the third and final experiment, we asked the question whether hippocampal mechanisms are not only shared between memory and navigation but even translate to other cognitive functions. We tested the idea that the hippocampus not only forms a map of our actual physical environment, but also 'abstract' maps of different aspects of our world. For example, during the summer festival a lot of live music is performed simultaneously at different stages. So, I have to evaluate my options to decide which act I want to go to. There might be several aspects that influence my decision: e.g. how much do I like the style of music of the act and given that I am very short (especially for Dutch standards), how crowded will it be and therefore how likely is it for me to see anything. There are many ways to represent these two aspects. One of them is to draw a two-dimensional abstract space, where one axis represents how much I like the style of music and the other how likely I am to see the stage. In the third experiment, we wanted to test the idea that the hippocampus can apply the same mechanisms it uses to represent physical space to represent such an abstract space.

The hippocampus: two parallel lines of research

Remembering events from our life and navigating from one place to another are two core functions of everyday life. It is not surprising then, that both functions and their neural correlates have been studied for decades. Interestingly, a huge portion of both research fields have provided evidence that both functions seem to heavily rely on the hippocampus (Eichenbaum et al., 1992; O'Keefe & Nadel, 1978). Nevertheless, until recent years both research lines were mostly conducted in parallel. This was probably due to large differences in the methodological approaches. Historically, spatial memory and navigation have been mainly assessed using electrophysiology in rodents (Burgess, 2014; Hartley et al., 2014). However, episodic memory is almost exclusively investigated at the systems-level in humans, for example with haemodynamic neuroimaging techniques and clinical studies (Squire & Wixted, 2011). Only recent advances in important techniques like virtual reality have opened the possibility to study navigation in healthy humans in more depth (Epstein et al., 2017; Hartley et al., 2014). Bridging methodological approaches between navigation and episodic memory may allow us to gain new insight into general mechanisms of the hippocampus.

In the following text, I will first briefly summarize the literature illustrating the role of the hippocampus in episodic memory and in navigation, separately. Subsequently,

I will present ideas and studies that try to bridge these two lines of literature. Lastly, I want to motivate how these ideas connect to the work presented in this thesis.

Box 1: The hippocampus

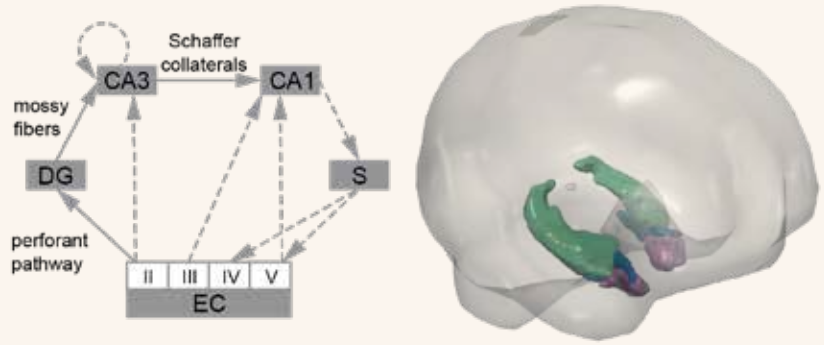

The hippocampus (depicted in green in the right half of the Figure) is located subcortically in the medial temporal lobe and is part of the limbic system (Kolb & Whishaw, 2009a). The name of this brain region is related to its curved shape, which is reminiscent of a seahorse (hippocampus is Greek for seahorse).

The hippocampus consists of two main anatomical substructures, the dentate gyrus (DG) and cornu Ammonis (consisting of the subfields CA1-CA4). The basic anatomy and (anatomical) connections of the hippocampus are well preserved across species (Clark & Squire, 2013).

The hippocampus is part of the hippocampal formation. It shares reciprocal connections with the other brain areas of this compound structure, namely the adjacent entorhinal cortex (EC, depicted in blue and purple in the right half of the Figure) and subiculum (S) (Felleman & van Essen, 1991; Squire & Zola-Morgan, 1991). Some of these connections are shown in the left half of the Figure, most notably the trisynaptic loop (solid lines). Here, layer II of the entorhinal cortex projects to the dentate gyrus of the hippocampus. Within the hippocampus, this input is projected to the cornu Ammonis (from CA3 to CA1). Via the hippocampal formation, the hippocampus is also highly connected with numerous other brain areas, such as the prefrontal cortex, thalamus and parahippocampal cortex (Kolb & Whishaw, 2009a).

There is an ongoing discussion about functional differences between the left and right hippocampus (Kühn & Gallinat, 2014). Furthermore, functional gradients have been discussed.

along the anterior-posterior axis in humans and the equivalent ventral-dorsal axis in rodents (Hirshhorn et al., 2012; Kühn & Gallinat, 2014; Nadel et al., 2013; Persson et al., 2018). In **chapter 3**, we take a closer look at potential differences between spatial and episodic memory across the hemispheres and along the anterior-posterior axis.

Figure is adapted with permission from Bellmund (2019).

The hippocampus and episodic memory

In his influential review, Tulving described episodic memory as our only option to travel back in time – at least mentally (Tulving, 2002). It is our ability to consciously reinstate three key components of an event in our mind: 'what', 'where' and 'when' (Tulving, 2002). It is easy to see how we could dissect my personal example from above into these three components: the what – looking at fireworks with my friends in a crowd with other people; the where – at the edges of the river Waal in Nijmegen; and the when – at night during the summer festival.
Furthermore, episodic memory is described as fundamentally different from other memory systems (Squire, 1982, 1992; Tulving, 2002). As mentioned before, episodic memory is described as a conscious process and therefore clearly distinct from subconscious, non-declarative memory systems like the acquisition of procedural skills, e.g. learning how to ride a bicycle (Cohen & Squire, 1980; Squire, 1982, 1992). However, not all conscious memory processes are episodic (Squire, 1992; Tulving, 2002). For example, I can consciously remember the fact that the name of the river in Nijmegen is 'Waal'. This semantic (fact-based) memory is very different to my recollection of a very specific event from my past (e.g. sitting at the Waal with friends and watching the fireworks). Taken together, episodic memory is the conscious recollection of experiences in their spatial and temporal context.

As mentioned before, the hippocampus is a key region involved in episodic memory. One of the most convincing and famous pieces of evidence for its important role comes from patient H.M.. H.M.'s bilateral medial temporal lobe (including the bilateral hippocampus) was surgically removed when he was a young man to stop his constantly occurring seizures (Scoville & Milner, 1957). As an unexpected consequence, he suffered from severe anterograde amnesia and partial retrograde amnesia, while most other cognitive functions were preserved (Scoville & Milner, 1957; Squire, 2009). This meant that after the surgery H.M. could no longer form new episodic memories and had trouble remembering any episodic events that happened relatively shortly before the surgery. What followed was decades of accumulating evidence from lesion, electrophysiological

to neuroimaging studies, confirming the importance of the hippocampus in episodic memory (Davachi, 2006; Ranganath, 2010; Rugg & Vilberg, 2013; Shastri, 2002; Squire, 2009; Tulving & Markowitsch, 1998).

Even though its importance is well established, what exact role the hippocampus plays in episodic memory is subject to ongoing research. One prominent theory posits that the role of the hippocampus is to bind and relate items to each other and into their context (Davachi, 2006; Eichenbaum et al., 1992; Eichenbaum & Cohen, 2014; Ranganath, 2010). In other words, it is not the retention of me and my friends watching the fireworks, but connecting this event to the spatiotemporal context it occurred in; i.e. sitting next to the river on a summer evening.
Interestingly, this idea of relational binding describes hippocampal mechanisms already more generally, i.e. not necessarily bound to one cognitive domain like episodic memory (Eichenbaum & Cohen, 2014). However, before we dive deeper into this topic of domain-general processing in the hippocampus, we should first discuss the other big line of hippocampal literature: space and navigation.

The hippocampus and space

We constantly move through the world and to do so in a goal-directed manner we need a mental representation of our environment (Hartley et al., 2014; Tolman, 1948). For example, I need to know where the University is with respect to my home. Otherwise, I couldn't find my way to the office and as a consequence never finish this thesis. Remembering important locations and how to get to them is a problem that not only humans must solve. For many species it is crucial to explore their environment and remember where they can find e.g. food or shelter (O'Keefe & Nadel, 1978). As a result combining electrophysiology with spatial cognition tasks became a powerful tool to understand how neural mechanisms enable us to form mental maps (Hartley et al., 2014; Moser et al., 2017). It is probably safe to say that our current level of understanding of hippocampal mechanisms would not have been possible without electrophysiological studies in freely moving rodents.
Leveraging single-cell recordings, one of the most important discoveries were hippocampal place cells (Burgess, 2014; Hartley et al., 2014; O'Keefe & Dostrovsky, 1971). As the name suggests, a place cell fires only if the navigator is in one specific location (or place) of the environment. The area in which the place cell fires is referred to as its place field (Hartley et al., 2014; O'Keefe & Burgess, 1996). Importantly, different place cells have different place fields, i.e. respond at different locations. This mechanism allows the hippocampus to map out the entire environment (O'Keefe & Nadel, 1978). For example, place fields not only differ in their location but also in

size. Therefore, the hippocampus cannot only map out our environment, but do so at different levels of granularity (Hartley et al., 2014; Kjelstrup et al., 2008). Interestingly, these differences in place field size form a topographical gradient, with an increase in field size of place cells along the ventral-dorsal axis in the rodent hippocampus (equivalent would be the anterior-posterior axis in humans; Kjelstrup et al., 2008). Furthermore, place cells are able to remap (Bostock et al., 1991; Leutgeb et al., 2005). Let us assume we track the activity of one place cell in three different rooms. It might have a place field in the north-west corner of the first room. In the second room it might respond to a completely different location (e.g. in the centre). In the third room it might have no place field at all. This example demonstrates that we cannot predict the place field of a place cell in one environment based on its place field in another environment – every environment seems to evoke its own specific mental map (Leutgeb et al., 2005).

It is important to note that hippocampal place cells are not the only spatially tuned cells that have been found in rodents. Spatially tuned cells in general show firing patterns that are driven by the spatial location or orientation of a navigator. The most prominent example besides place cells are grid cells. Grid cells can be found in the entorhinal cortex, which is highly connected and structurally close to the hippocampus (Burgess, 2014; Hafting et al., 2005; Hartley et al., 2014; Moser et al., 2008). In short, a grid cell does not respond to one specific location in an environment, but has multiple firing fields. These firing fields form a periodic, hexagonal grid spanning the entire environment (Burgess, 2014; Hafting et al., 2005; Hartley et al., 2014; Moser et al., 2008). Akin to place cells, the firing fields of different grid cells vary from each other in certain properties like e.g. orientation of the grid and spacing between firing fields (for a more detailed description of the firing properties of grid cells see: Bush et al., 2015; Hartley et al., 2014; Moser et al., 2017).

Although spatially tuned cells (like place cells) have mostly been studied in rodents, growing evidence suggests that the same processing mechanisms can be found in humans (Bellmund et al., 2016; Doeller et al., 2010; Ekstrom et al., 2003; Jacobs et al., 2013; Miller et al., 2013). Given the properties of spatially tuned cells, they are thought to be the building blocks for forming a flexible mental representation of our environment (Bellmund, Gärdenfors, et al., 2018; Bush et al., 2015; O'Keefe & Nadel, 1978).

Box 2: Life-simulation techniques

We wanted to bring the rich spatial and episodic experiences from the real world into the lab setting. Although this goal can never be fulfilled completely, life-simulation techniques like virtual reality (VR) and software packages such as 'the Sims' are useful tools. These types of stimulus material allow participants to have an immersive experience, while the experimenter still has a high level of experimental control.

In **chapters 2** and **3**, we let participants navigate in large-scale virtual environments. We wanted participants to freely navigate and have their own personal experience with the environment. At the same time, VR allowed us to keep control over the duration and number of interactions participants had with these environments and what types of problems they needed to solve.

In **chapter 3**, we also used the life-simulating game 'the Sims'. This game allowed us to create videos of life-like events. Here, we took advantage of the fact that we could present participants with naturalistic stories and simultaneously control all defining factors of an episode: the "when", the "what" and most importantly the "where".

In the following, I will describe virtual reality and 'the Sims' in a bit more detail.

Virtual reality

VR played a major role in translating and expanding what we know about the navigational system of the brain from electrophysiological studies in rodents to non-invasive neuroimaging methods in humans (Bohil et al., 2011; Burgess et al., 2002; Hartley et al., 2014).

The main advantage of VR is that it has relatively high ecological validity, while offering experimental control (Bohil et al., 2011). Participants are able to have an immersive experience in the virtual environment by actively engaging with it, instead of passively perceiving it. At the same time, the experimenter can control the type, duration and number of interactions the participants have with the environment.

Although VR is also a popular method in other cognitive research fields, it is probably most widely used for spatial cognition (Bohil et al., 2011). Non-invasive human neuroimaging techniques like fMRI and MEG require the participant to lay or sit still while data is recorded. This poses an obvious problem for studying navigation with these techniques. VR however, allows participants to navigate in virtual environments via a controller while their body remains still. Therefore it became such a popular tool for this field (Bohil et al., 2011; Burgess et al., 2002;

Hartley et al., 2014). The idea here is that even though the motor, vestibular and proprioceptive aspects of real-world navigation are different to its virtual counterpart, the cognitive and neural aspects are highly similar. This notion is supported by the multitude of human neuroimaging studies that use VR and find coding mechanisms of navigation that dovetail with electrophysiological studies in rodents (e.g. Doeller et al., 2010; Ekstrom et al., 2003; Jacobs et al., 2013; Miller et al., 2013).

The Sims

'The Sims' is a popular life-simulation game, in which the player can control the life of virtual characters (Nutt & Railton, 2003). An important component of the game is the ability to create the home of a character with a high degree of freedom regarding the interior and exterior design. Furthermore, the game allows to control the actions of the virtual characters and let them interact with objects and other characters (Nutt & Railton, 2003).

These characteristics make this game an interesting tool for studying episodic memory. Here, the experimenter can generate and control a virtual world and create naturalistic narratives with human-like characters. The built-in video tool of the game allows to capture these narratives and use them in an experimental setting. Although this method is not widely used yet, previous studies have shown that this type of stimulus material can induce rich episodic experiences (Collin et al., 2015; Milivojevic et al., 2015).

The hippocampus and the cognitive map

I hope that the literature reviewed so far, made a convincing case that the hippocampus plays a fundamental role in both episodic memory and spatial cognition. This brings us back to the original question of the thesis: how can the hippocampus support both of these functions? One possible and simple answer that has been suggested is that the hippocampus processes the two functions in parallel through different subregions (Burgess et al., 2002; Kühn & Gallinat, 2014; Poppenk et al., 2013). Proposed functional divisions in the hippocampus are based on differences between findings of the spatial and episodic literature. Most prominent ideas claim differences between hemispheres and across the anterior-posterior axis of the hippocampus (left and anterior hippocampus is often involved in episodic tasks vs. right and posterior hippocampus is often involved in spatial tasks, Kühn & Gallinat, 2014).

A somewhat opposing idea that has received more and more attention in the last couple of years is that the hippocampus forms maps that relate not only information in space, but also in time and maybe even more domains (Behrens et al., 2018; Bellmund, Gärdenfors, et al., 2018; Buzsáki & Moser, 2013; Epstein et al., 2017; Schiller et al., 2015; Stachenfeld et al., 2017). The idea of such a general cognitive map has already been proposed in the late 1940s (Tolman, 1948). After a series of behavioural experiments in rats, Tolman challenged the –at the time– popular theory that all of our behaviour is based on stimulus-response learning (Tolman, 1948). He demonstrated that rats could react adaptively and flexibly to a changing environment. For example, in one experiment rats repeatedly followed the rigid tracks of a maze to get to a food-rewarded location. During a probe trial, other arms in the maze opened, giving the rats the option to take a shorter, more direct path to the rewarded location. If rats only learned via stimulus response associations, they should follow the tracks of the path they previously got rewarded for. However, these rats took the arm with the most direct path to the rewarded location (even though they could not see the rewarded location from the decision point). These and other results motivated Tolman to postulate the idea that rats (and humans) form a cognitive map of their environment, in which they can draw inferences (Tolman, 1948). Even back then, Tolman presented cognitive maps not only as a model for spatial cognition, but as a general mechanism that allows to build mental models of our world.

It was decades later, after the discovery of place cells, that the hippocampus was brought into the spotlight as the neural basis for cognitive maps (O'Keefe & Nadel, 1978). As time progressed, spatially tuned cells from adjacent areas of the hippocampus were included into the debate about the neural basis of cognitive maps (Burgess et al., 2002; Ekstrom & Ranganath, 2018). Based on the nature of these types of cells, the suggested role of hippocampal cognitive maps was (mostly) reduced to space (Burgess et al., 2002; Ekstrom & Ranganath, 2018; Kumaran & Maguire, 2005; O'Keefe & Nadel, 1978). Within this line of thought, hippocampal involvement in episodic memory was attributed to the spatial component of an event (i.e. the "where"). This ignited a long-standing debate whether the function of the hippocampus goes beyond space. Strongest opposition came (unsurprisingly) from the episodic memory literature (Davachi, 2006; Eichenbaum et al., 1992, 1999; Eichenbaum & Cohen, 2014; Ranganath, 2010). The core alternative hypothesis stated that the main mechanism of the hippocampus is to relate and bind relevant items into their context (as mentioned above). One interesting theory based on this idea is that the hippocampus processes sequences in both space and time (Eichenbaum et al., 1999; Eichenbaum & Cohen, 2014). Accordingly, the hippocampus does not simply form a cognitive map of our spatial environment, but instead a 'memory space' where meaningful events are arranged and linked according to their spatial and temporal order.

Over time, these two opposing camps have grown much closer together. As a result, the term cognitive map is nowadays used in a much broader sense and incorporates a lot of ideas from Eichenbaum's 'memory space' and original propositions from Tolman. In more detail, the current idea of cognitive mapping is that computations supporting navigation are not specialized to the spatial domain, but are general, domain-unspecific mechanisms (Behrens et al., 2018; Bellmund, Gärdenfors, et al., 2018; Epstein et al., 2017; Schiller et al., 2015; Stachenfeld et al., 2017; Tolman, 1948). A cognitive map is in its essence a relational map (here Eichenbaum's ideas are clearly reflected), that allows predicting transitions from the current state to future states. These states can theoretically be any meaningful entity, from concrete positions in space or time to abstract concepts (Behrens et al., 2018; Bellmund, Gärdenfors, et al., 2018; Epstein et al., 2017; Schiller et al., 2015; Stachenfeld et al., 2017). In other words, so called spatially tuned cells are not bound to physical space, but are more general coding mechanisms of abstract spaces/maps. An example for such an abstract space would be the earlier discussed scenario, where I would evaluate my options between different performances during the summer festival along two aspects. Here, how much I like the music would represent one axis of the abstract space and how likely I am to see the stage would represent the second axis. By combining these two aspects, every option could be 'placed' in this abstract space. If the idea of a cognitive map is true, exploring my options through this abstract space should involve spatially tuned cells in a similar fashion as when I were to walk around in Nijmegen. In recent years, first proof-of-principle studies have been published. These studies showed involvement of the hippocampal formation in the mapping of e.g. time, concepts, social hierarchies and sound frequency (Aronov et al., 2017; Constantinescu et al., 2016; Garvert et al., 2017; Tavares et al., 2015; Theves et al., 2019). Furthermore, both evidence for grid cell like as well as place cell like coding has been found in the representation of these abstract cognitive maps (Aronov et al., 2017; Constantinescu et al., 2016).

Taken together, the idea of cognitive mapping states that the hippocampus shares mechanisms across cognitive domains, such as space and memory. These mechanisms allow us to form adaptive and flexible cognitive maps of our world.

Box 3: Measuring representational change with fMRI

Neural activity is accompanied by an increase in highly oxygenated blood flow to the activated area. Due to the different magnetic properties of oxygenated and deoxygenated haemoglobin, functional magnetic resonance imaging (fMRI) is able to detect relative increases and decreases in (de)oxygenated blood-

flow (Kolb & Whishaw, 2009b). Therefore, we use this blood-oxygenation-level dependent (BOLD) signal as an indirect measure of neural activity. Even though fMRI has a reasonable spatial resolution (in our experiments 1.5 mm isotropic voxel size) within the realm of non-invasive neuroimaging methods, the BOLD signal is sluggish and slow (Kolb & Whishaw, 2009b). As we wanted to test a healthy population and were mainly interested in the neural activity of a spatially defined region (the hippocampus) and less so in the temporal aspects of its processing mechanisms, fMRI was the method of choice.

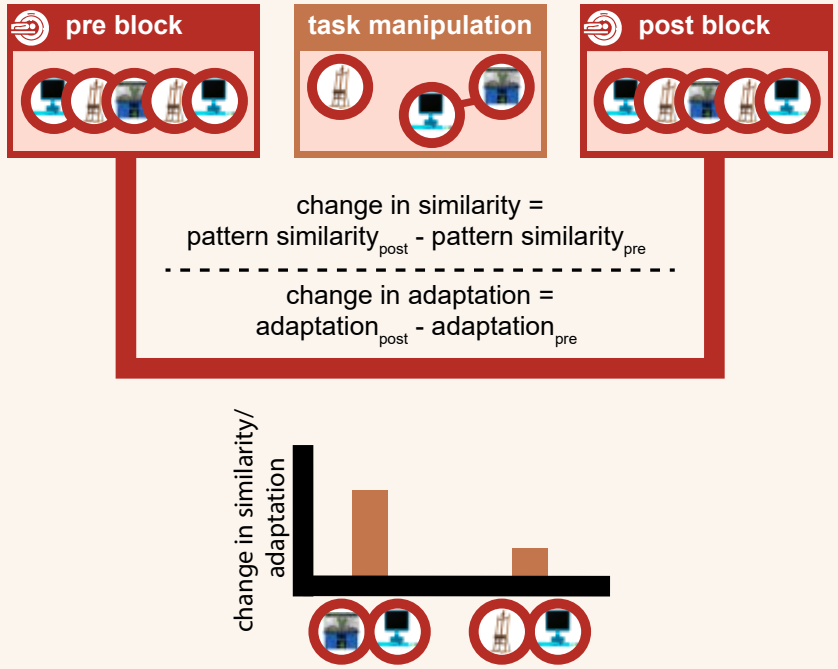

We used a similar structure for all of our experiments, when measuring fMRI data (Figure). In the main task(s) of the experiment, the relationships between items were manipulated (e.g. by learning the spatial distance separating two items in a virtual environment). The same items were presented pre and post the main task(s) in random order during a picture viewing task (except for **chapter 3**, where we only presented the items after the main tasks during post blocks). The order of the items was always randomized across participants, but constant between the pre and post blocks of the same participant. We used the pre and post blocks to measure the effects of the manipulations of the main task(s) on brain activity. The idea here was that, if an area is sensitive to the task manipula-

tion, the overlap of neural code between items should in turn change as a function of this manipulation. Throughout this thesis, we used two different measurements for this overlap in neural code: multivariate representational similarity analysis (RSA) and univariate repetition suppression, also referred to as adaptation analysis.

Representational similarity analysis

RSA is a form of multivariate pattern analysis (Kriegeskorte et al., 2008). This means that the pattern of activity of a set of voxels (referred to as searchlight or region of interest) is examined and compared between conditions. The idea here is, the bigger the neural overlap between conditions, the higher the similarity of the patterns of activity.

In our case, we were mainly interested in the similarity between activity patterns within the hippocampus. Therefore, we measured the item-specific activity pattern of hippocampal voxels during the pre and the post block. Next, we correlated each item-specific pattern of activity with every other item-specific pattern of activity as a proxy for neural similarity. This allowed us to track the changes in similarity from the pre to the post block. Lastly, we tested whether these changes occurred as a function of our task manipulations. We used RSA in **chapter 2** and **4**.

Adaptation analysis

Adaptation analysis leverages the repetition suppression effect. This effect refers to the fact that neurons suppress their response if two successive items share information this neuron is sensitive to (Barron et al., 2016; Grill-Spector et al., 2006; Krekelberg et al., 2006). In other words, higher overlap of neural code between the preceding item and the current item should result in greater suppression of the BOLD activity evoked by the current item presentation (Barron et al., 2016; Grill-Spector et al., 2006; Krekelberg et al., 2006). In our experiment, we could therefore measure this adaptation effect for each pair of items and tested how this effect changed from the pre to the post block. Akin to our RSA approach, we could then test whether the adaptation effect changed as a function of our interim task manipulation. We used adaptation analysis in **chapter 3** and **4**.

Outline

The idea of cognitive mapping is a powerful tool to study and understand the hippocampus. The role of this brain area in episodic memory and spatial cognition is

well established (Buzsáki & Moser, 2013; Eichenbaum et al., 1992; O'Keefe & Nadel, 1978). However, how the hippocampus successfully supports both of these functions is an ongoing debate. In this thesis, I want to contribute to this debate by exploring hippocampal mapping mechanisms in space, memory and beyond. To mimic the rich experiences underlying episodic memory and spatial navigation we used virtual reality and the life-simulation game 'the Sims' (Box 2). Combining fMRI with multi-voxel pattern analyses allowed us to test how our experimental manipulations affect hippocampal processing at a meso-anatomical and coarse temporal scale (Box 3).

In **chapter 2**, we took a closer look at hippocampal cognitive maps in space. In order for a cognitive map to be useful it needs to contain information about important locations and the relationships between them (Burgess et al., 2002; Epstein et al., 2017; McNaughton et al., 2006; O'Keefe & Nadel, 1978; Tolman, 1948). It has previously been shown that the hippocampus is able to map the distances between such relevant locations (Deuker et al., 2016; L. R. Howard et al., 2014; Morgan et al., 2011; Spiers & Barry, 2015). Here, we manipulated the actual navigated distance and the Euclidean distance between goal-locations in a large-scale virtual town. We wanted to test whether the hippocampus forms an integrative map of these different distance representations or whether it maps one, but not the other. Both types of distance measurements carry important information about the environment. On the one hand, Euclidean distance informs us about the allocentric relationship between goal-locations, which is independent of the navigator. On the other hand, path distance informs us about the egocentric route we have to take to get from one place to another. Furthermore, our aim was to test whether a hippocampal map can adapt to changes in the environment. After all, it was the flexible and adaptive behaviour of rats that inspired Tolman to postulate the idea of a cognitive map in the first place (Tolman, 1948). To this end, we changed how participants had to navigate between locations and tested the influence of these changes in path length on hippocampal mapping.

In **chapter 3** we tested the two opposing ideas that the hippocampus can support spatial and episodic memory either via common mechanisms (Bellmund, Gärdenfors, et al., 2018; Eichenbaum & Cohen, 2014; Epstein et al., 2017; Schiller et al., 2015) or processes either function in different subregions (Burgess et al., 2002; Kühn & Gallinat, 2014; Poppenk et al., 2013). To this end, we manipulated spatial and episodic context associations between items. If the hippocampus integrates spatial and episodic context information, we would expect that items that share both types of context information show higher representational overlap than items that share either a spatial or an episodic context. Furthermore, we tested whether items that share a spatial context showed neural overlap in different subregions of the hippocampus compared to items that share an episodic context. Specifically, we assessed episodic and spatial coding

differences between hemisphere (left vs. right hippocampus) and across the anterior-posterior axis of the hippocampus (Kühn & Gallinat, 2014).

In **chapter 4** we tested whether the hippocampus uses mechanisms supporting navigation in other cognitive domains as well (Behrens et al., 2018; Bellmund, Gärdenfors, et al., 2018; Epstein et al., 2017; Schiller et al., 2015; Stachenfeld et al., 2017). Recently, proof-of-principle studies have found 'spatial coding' in abstract spaces (Aronov et al., 2017; Constantinescu et al., 2016; Garvert et al., 2017; Tavares et al., 2015; Theves et al., 2019). These abstract spaces are typically defined along two physical feature dimensions (e.g. the length of a bird's leg or neck). If any physical feature dimension can be organized with a hippocampal map, this principle might also apply to more abstract concepts. We argue that values are good candidates for examining hippocampal coding of these more abstract (non-physical) maps. Values are not a sensory/physical feature, but a concept appearing constantly in our everyday lives. The concept of a value can take many forms, in our case we used numerical rewards. We leveraged the fact that these numeric reward values inherently form a continuous axis. These features facilitated an experimental design of a value map. We associated context items with two types of reward values. Either type of value represented one dimension of a value space. We tested whether the hippocampus maps distances in such a value space, akin to physical (or virtual) space.

In **chapter 5**, I summarize and discuss the results from the empirical **chapters 2-4**. The aim here is to contribute to the ongoing debate about cognitive mapping in the hippocampus and how the hippocampus can support a multitude of functions. I conclude **chapter 5** with an outlook on possible future directions in the field of hippocampal research.

CHAPTER 2

The hippocampus forms integrative and adaptive maps of space

This chapter is in preparation as:

A. N. de Haas, L. Ottink, C. F. Doeller. The hippocampus forms integrative and adaptive maps of space.

.

Abstract

The hippocampus is a key region for forming a mental map of our environment. To be useful for guiding navigation, such a map requires a representation of distances between landmarks, which can be used for flexibly computing relationships that have never been directly experienced. Here, we let participants perform an object-location task in a large-scale virtual environment and combined functional magnetic resonance imaging (fMRI) with representational similarity analysis to test how Euclidean and path distances between objects affect their neural similarity in the hippocampus. We found evidence that the left hippocampus forms a cognitive map that integrates Euclidean and path distances. One key characteristic of cognitive maps is their adaptive and flexible nature. We therefore let participants perform another object-location task in the same virtual environment. Importantly, here we changed the path distance between objects by relocating roadblocks in the environment. We found that hippocampal maps of response learners (i.e. people who navigate based on remembered sequences of egocentric turns) adapted as a function of these changes in path distance. Taken together, our study supports the idea that the hippocampus can create integrative and flexible cognitive maps of our world.

Introduction

Navigating successfully in our everyday lives requires a mental representation of our environment. Such a so-called cognitive map must contain information about relevant locations and the geometric relationships between them, such as distance and angle. Furthermore, it must facilitate flexible behaviour, for instances planning detours after changes in the environment occur (Burgess et al., 2002; Epstein et al., 2017; McNaughton et al., 2006; O'Keefe & Nadel, 1978; Tolman, 1948). Spatially tuned cells in the hippocampus and related structures (e.g. the entorhinal cortex) are thought to be the neural basis of these cognitive maps (Hafting et al., 2005; Hartley et al., 2014; O'Keefe & Dostrovsky, 1971; Taube et al., 1990). Decades of experimental evidence, including lesion, electrophysiological and neuroimaging studies strongly support the importance of the hippocampus in representing our spatial environment (Bellmund, Gärdenfors, et al., 2018; Burgess et al., 2002; Ekstrom et al., 2003; Epstein et al., 2017; Iglói et al., 2010; McNaughton et al., 2006; Morris et al., 1982; O'Keefe & Nadel, 1978; Sarel et al., 2017; Spiers et al., 2001; Wilson & McNaughton, 1993). One key finding are hippocampal place cells (O'Keefe & Dostrovsky, 1971). As the name suggests, a place cell fires only if the navigator is in one specific location (or place) of an environment. With different place cells responding to different locations, the hippocampus can map out the entire environment. Although spatially tuned cells (like place cells) have mostly been studied in rodents, growing evidence suggests that the same processing mechanisms form the building blocks of cognitive maps in humans (Bellmund et al., 2016; Doeller et al., 2010; Ekstrom et al., 2003; Jacobs et al., 2013; Miller et al., 2013). For example, neuroimaging studies in combination with virtual reality have demonstrated that the human hippocampus does indeed perform geometric computations in space. The hippocampus not only dynamically updates distance information to a goal-location during navigation, but also forms an offline map that represents distances between relevant locations (Deuker et al., 2016; L. R. Howard et al., 2014; Morgan et al., 2011; Spiers & Barry, 2015). Furthermore, converging evidence shows that univariate activity in the hippocampus correlates with the path distance between the navigator and the goal, in both highly familiar and relatively unfamiliar environments (L. R. Howard et al., 2014; Sherrill et al., 2013; Spiers & Barry, 2015; Viard et al., 2011). Simultaneously, univariate activity in the entorhinal cortex seems to index the Euclidean distance between the navigator and the goal location (L. R. Howard et al., 2014; Spiers & Barry, 2015; Spiers & Maguire, 2007).

Interestingly though, the role of the hippocampus in representing distance information goes beyond active navigation. Two fMRI studies suggest that the hippocampus stores an offline map that contains information about the temporal, path and Euclidean distance between relevant locations (Deuker et al., 2016; Morgan et al., 2011). Morgan

et al. (2011) found that hippocampal fMRI activity was modulated by the real-world distance between two successively presented, highly familiar landmarks. The authors used two variables as distance measurements: the objective Euclidean distance and the subjective estimation of the travel time by each participant. However, due to the grid-like layout of the environment, both variables were highly correlated, which makes it hard to distinguish what drives an effect of either distance measurement.

Excitingly, a couple years later Deuker et al. (2016) decoupled temporal and spatial distances while participants had to navigate from object to object in a predetermined sequence in a large-scale virtual city ('Donderstown'). Although normally the temporal and spatial distance would be correlated in such a design, the authors introduced teleporters to circumvent that problem. By teleporting participants instantly from one end to the other of the city, they introduced object-pairs with high spatial, but low temporal distances. Importantly, before and after the object-location task, participants were presented with all objects during a picture viewing task in the MRI scanner. This allowed the authors to test for changes in pattern similarity between object-pairs as a function of their respective distances. The results suggest that the hippocampus forms a spatio-temporal distance map of locations along a fixed path. Neural pattern similarity in the hippocampus increased the closer people remembered object-pairs to be in space and time.

In real-world navigation, both Euclidean and path distance are important features of a cognitive map. Path distances allow you to compute the shortest known path to a goal, while Euclidean distances enable you to compute novel shortcuts when the environment changes. Here, we asked whether Euclidean and path distance are simultaneously represented and how changes in the environment affect those distance representations. For this purpose, we let participants navigate freely and perform an object-location task in a smaller version of Donderstown (Bellmund, Deuker, et al., 2018; Deuker et al., 2016). Importantly, participants did not navigate along a predetermined sequence of locations as in the previous study. Instead, participants had to navigate repeatedly from every object-location to every other object-location in (pseudo-) random order. Furthermore, by introducing roadblocks into the city layout we were able to manipulate path distances between object-locations. The goal was to create object-pairs with distinguishable path and Euclidean distances. We were particularly interested whether an offline cognitive map in the hippocampus would only represent one of the two distance measurements or whether both types of information would be represented and maybe even integrated. Akin to Deuker et al. (2016), we used changes in neural pattern similarity between object-pairs as a proxy for this offline map (Figure 1A & B). Furthermore, we tested behavioural signatures of distance representations by asking participants to estimate the path and Euclidean distance between every object-pair.

Successful navigation requires one to react flexibly to changes in the environment (Spiers & Gilbert, 2015; Tolman, 1948). Imagine the standard route between your home and workplace is suddenly blocked by a construction site. An adaptive cognitive map should be sensitive to the fact that you need to change your route and be able to calculate a new path. Even though there is mixed evidence on the hippocampal role during these kind of detour problems, a well-controlled human neuroimaging study suggests that the hippocampus signals the change in path distance during active navigation (L. R. Howard et al., 2014; Spiers & Gilbert, 2015). Furthermore, evidence from single-unit recordings in rats shows that hippocampal place cells change their firing fields and therefore remap after changes in the path structure of the environment occur (Alvernhe et al., 2008, 2011). Here, we wanted to extend these previous studies and test how an offline hippocampal map is updated in humans. For this purpose, we let participants perform a second object-location task (remapping task) similar to the first one. Importantly, we kept the location of the objects constant across tasks, but changed the location of some of the roadblocks from the original object-location task (Figure 1A). Consequently, path distances between object-pairs could become shorter or longer while Euclidean Distance was unaffected. Again, we used changes in neural pattern similarity (from pre remapping task to post remapping task) as a proxy for updating the offline cognitive map (Figure 1A & C). In addition, participants had to re-estimate the path and Euclidean distance between every possible object-pair after the remapping task. This way, we could also test for an update in map representation on a behavioural level.

Even though we expected hippocampal involvement, its role in solving detour problems is not well established and there are mixed results from the literature (Spiers & Gilbert, 2015). This motivated us to explore the idea that differences between people in navigational strategies may affect detour-based remapping (and maybe even mapping) and its representations in the hippocampus. We were particularly interested whether egocentric navigators/response learners differed from allocentric navigators/place learners. Egocentric navigation is based on remembered sequences of left and right turns (i.e. responses) at landmarks, while allocentric navigation is based on the relationship between distal cues (i.e. places) in the environment (Astur et al., 2016; Burgess et al., 2002; Iglói et al., 2010; Klatzky, 1998). Previous research has shown that these two navigational strategies result in different neural signatures in the hippocampus (Iglói et al., 2010, 2015). Furthermore, it seems that strategy behaviour is not random, but stable (Astur et al., 2016). We therefore adapted a T-maze task used previously by Astur et al. (2016) to categorize our participants into response learners (egocentric navigation) and place learners (allocentric navigation). This task was independent from the rest of the experiment and therefore allowed us to test the potential influence of these strategies on the neural signatures of mapping and remapping.

Taken together, we used an extensive and rich design to test for offline representations of path and Euclidean distances in the hippocampus. We extended previous designs, by testing how these representations might undergo remapping after changes in the environment occur. Lastly, we explored whether different navigational strategies might yield different neural signatures of remapping (or even mapping) in the hippocampus.

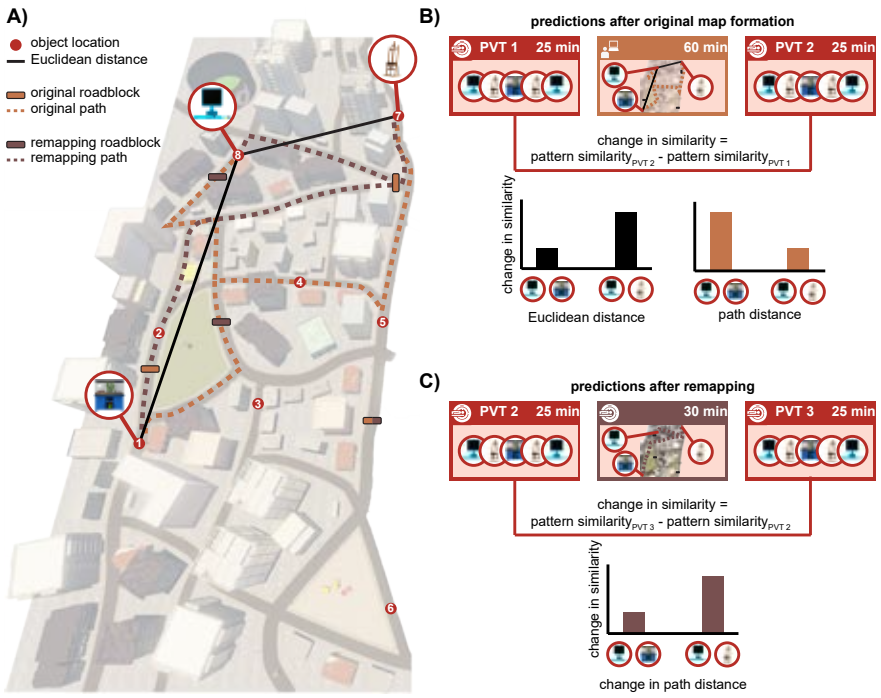

Figure 1 | Virtual city and the predictions based on the original map and subsequent remapping
(A) Bird-view of virtual city. Eight objects were placed in the virtual city (locations marked here by red dots). During two object-locations tasks, participants had to take the shortest possible route from every object to every other object. Participants encountered three roadblocks during navigation. Two of the three roadblocks changed location between the original object-location task and the remapping task. Changed routes could either become longer or shorter. The location and therefore the Euclidean distance between objects stayed constant between tasks.

(B) Predictions based on the Euclidean and path distances of the original map. Before and after the original object-location task, participants performed the identical picture viewing task in the MRI scanner. This allowed us to measure the change in neural pattern similarity between object-pairs. Here, we wanted to test whether neural pattern similarity changes as a function of Euclidean or/and path distance. In the example here, the object pair computer-terrarium (locations 8-1) has a higher Euclidean distance than the object-pair computer-easel (locations 8-7). The prediction based on Euclidean distances would therefore be that the object pair computer-terrarium (locations 8-1) becomes less similar than the object-pair computer-easel (locations 8-7). As the path distances show the opposite pattern between the two object-pairs, the prediction would be the other way around.

(C) Predictions based on the changes in path distances of the remapping. After the second picture-viewing task, participants performed the remapping task and a third identical picture viewing task. Again, this allowed us to measure the change in neural pattern similarity between object-pairs from pre to post remapping. Here, we wanted to test whether neural pattern similarity changes as a function of the remapping of path distances. In the example here, the distance between the object pair computer-terrarium (locations 8-1) got longer in the remapping task (compared to the original object-location task), whereas the distance between the object-pair computer-easel (locations 8-7) got shorter. The prediction based on the change in path distance would therefore be that the object pair computer-terrarium (locations 8-1) becomes less similar than the object-pair computer-easel (locations 8-7).

Results

Behavioural signatures of a cognitive map

We set out to test how a hippocampal map represents Euclidean and path distances and furthermore how these representations adapt to changes in the environment. To ensure that participants were familiar with the virtual environment, we let them complete an extensive training at the beginning of the experiment. Here, participants had to navigate repeatedly between eight goal-locations and complete recall trials in which they indicated where the eight goal-locations were in the city. Participants received positive feedback if they remembered a goal-location within an error-radius of ca. 2.6% of the total map length (see Methods for more details). In the subsequent object-location task, each goal-location was associated with an object, and participants had to navigate here from object-location to object-location (for an overview of all objects see Supplementary Figure 1). The goal of this extensive experience with the environment was to let participants form a map of the environment and let them learn distances between objects/goal-locations. However, for such neural distance representations to be interpretable it is important to first establish behavioural signatures of such a cognitive map. In other words, can our participants replicate Euclidean and path distances between relevant locations of the environment?

To answer this question, we let participants estimate the Euclidean and the path distances between object-pairs, respectively. Participants performed this distance recall task twice, after the object-location task and after the remapping task, respectively (Figure 2). We asked participants to estimate these distances on a scale from zero to 100. We instructed participants that zero would mean that two objects share the same location, whereas 100 represents the maximal distance two objects had in the preceding task. As a distance memory score, we correlated the estimated distances with the real distances for every participant. If participants can accurately remember Euclidean and path distances, then we would expect on average a high and positive score. As expected, all average scores were significantly greater than zero (Figure 3). More specifically, after the object-location task, average correlation between estimated and real path distance was $r = 0.83$ ($T_{(31)} = 21.91$, $p < 0.001$) and average cor-

Figure 2 | Overview of experimental sessions
On day 1, participants started the experiment with the first picture viewing task (PVT) in the MRI scanner. Here, we measured the baseline neural pattern similarity between object-pairs. The rest of the experiment on day 1 took place in the behavioural lab. Participants performed an extensive training task in the virtual city. They learned how to navigate ideally between eight goal-locations. Then they completed the Santa Barbara Sense of Direction Scale (a self-report measurement of navigational abilities) and a T-Maze task. The purpose of the T-Maze task was to have an independent measure of navigational strategies. On day 2 of the experiment, participants started in the behavioural lab with an object-location task. Participants had to associate the previously learned goal-locations with objects and navigate successfully between them. Afterwards, participants had to recall the path and Euclidean distance between every object-pair. Participants then had to perform three tasks in the MRI scanner. They started with the second PVT. Here we wanted to measure the effects of the path and Euclidean distance on neural pattern similarity between object-pairs. During a subsequent remapping task, participants had to learn new routes/paths between object-pairs. We then again recorded a PVT. Here we wanted to measure how the change in path distance affected the neural pattern similarity between object-pairs. After the scanning session, participants finished the experiment with a second distance recall task (same as the first one) and a bird-view placement task. Here, we presented participants with a bird-view picture of the virtual city and asked them to indicate the location of every object.

relation between estimated and real Euclidean distance was r= 0.79 ($T_{(31)}$= 18.28, p< 0.001). To control that participants really learned Euclidean and path distance as separate components, we also correlated remembered path distance with the real Euclidean distance and vice versa remembered Euclidean distance with the real path distance. Distance memory scores were significantly higher than their control counterparts (path distance vs. control: $T_{(31)}$= 5.77, p< 0.001, Euclidean distance vs. control: $T_{(31)}$= 6.53, p< 0.001). After the remapping task, the average correlation between estimated and real path distance was r= 0.80 ($T_{(31)}$= 14.76, p< 0.001) and the average correlation between estimated and real Euclidean distance was r= 0.76 ($T_{(31)}$= 16.14, p< 0.001). The same control analyses was applied here as after the object-location task. Distance memory scores after remapping were significantly higher than their control counterparts (path distance vs. control: $T_{(31)}$= 6.42, p< 0.001, Euclidean distance vs. control: $T_{(31)}$= 4.90, p< 0.001).
Taken together, these memory scores indicate that participants could replicate Euclidean and path distances as separate components.

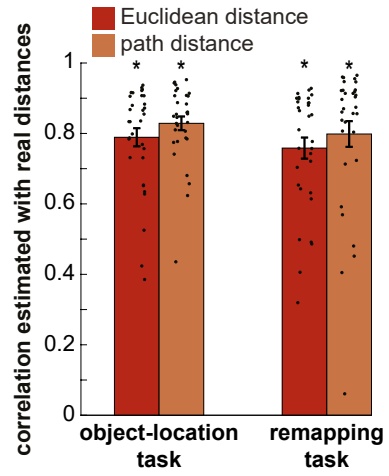

Figure 3 | Mean correlation between estimated and real distances
Participants estimated the Euclidean and path distance for every object-pair after the object-location task and after the remapping task. We correlated these distance estimations with the real distances for every participant. On a group level, all correlations were significantly higher than zero after Fisher transformation was applied (all p< 0.001). Dots represent single participant values. Error bars show the standard error of the mean. Asterisk symbolizes a significant effect (p< 0.05).

We used multidimensional scaling (MDS) to visualize the object-locations based on the Euclidean distance estimations and the path distance across all participants. Note that MDS estimates locations based on the assumption that the distance input is Euclidean. Therefore, we can easily compare the real locations of the objects in the virtual city with the locations based on the MDS model of the estimated Euclidean distances. This comparison is not possible based on the MDS model of the estimated path distances. However, by applying MDS to the objective path distances, we can translate the real object-locations to their locations in a 'path space' (i.e. a space where the path distances are treated as Euclidean distances).

Subsequently, this allows us to compare objective object-locations in this 'path space' to the locations based on the MDS model of the estimated path distances. To do this, we computed the average object-locations across all participant's MDS maps and compared these to the objective object-locations of the corresponding space (Figure 4). Figure 4 shows that participants distance estimations were accurate enough to reconstruct the actual object-locations of the Euclidean and path space. After the object-location task, the estimated and real locations in Euclidean space had an average error distance corresponding to 7.9% (sd= 4.2%) of the maximal Euclidean distance of an object-pair in the virtual city and in path space an average error distance corresponding to 6.7% (sd= 3.2%) of the maximal path distance of an object-pair in the virtual city. After the remapping task, the estimated and real locations in Euclidean space had an average error distance of 8.5% (sd= 5.1%) of the maximal Euclidean distance of an object-pair in the virtual city, and in path space an average error distance of 6.5% (sd= 3.0%) of the maximal path distance of an object-pair in the virtual city.

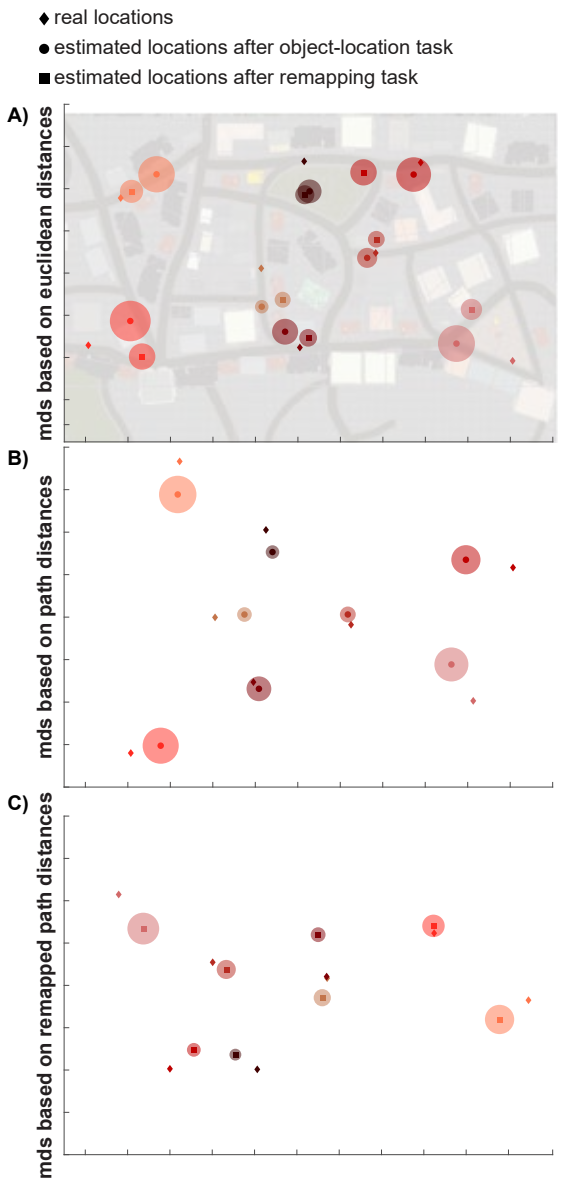

Figure 4 | Multidimensional scaling of Euclidean and path space
(A) Multidimensional scaling (MDS) of Euclidean space. Marked by the diamonds are the real object-locations in the virtual city. These objective object-locations are compared to the mean locations across the MDS output of the estimated Euclidean distances of all participants. Circles mark the mean estimated locations after the object-location task and squares mark the mean estimated locations after the remapping task. In the background is a bird's-eye view picture of the virtual city.

(B) Multidimensional scaling of path space after the object-location task. Marked by diamonds are the object-locations based on the MDS of the objective path distances of the object-location task. These objective object-locations are compared to the mean locations across the MDS output of the estimated path distances of all participants (marked by circles).

(C) Multidimensional scaling of path space after remapping. Marked by diamonds are the object-locations based on the MDS of the objective path distances of the remapping task. These objective object-locations are compared to the mean locations across the MDS output of the estimated path distances of all participants (marked by squares).

Each real location and corresponding estimated location have the same colour. Opaque circles around estimated locations represent the standard error of the mean.

For an overview of all objective distances and the distances based on the mean estimated MDS locations, see Supplementary Figure 2.

In addition to the distance recall tasks, we presented participants with a bird's-eye view of the virtual city at the end of the experiment (Figure 2 and Supplementary Figure 3). We tested participant's knowledge about object-locations directly by asking them to indicate the location of every object on the map (Figure 5). On average, participants had

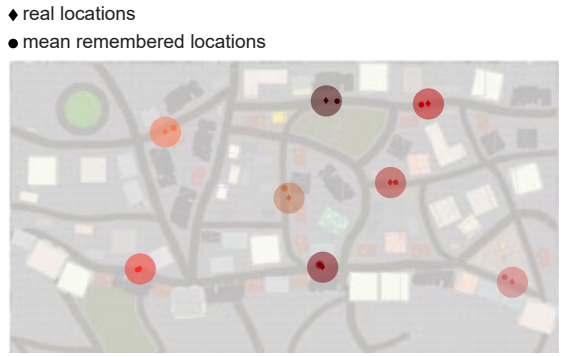

Figure 5 | Remembered locations of the bird-view task
Participants had to indicate all object-locations on a bird-view map. Here, the mean remem-bered location across all participants and the real locations are shown. The opaque circle around the real locations represents the area in which participants received positive feedback during training for remembering an object-location (radius of around 2.6% of map length). Each real location and corresponding estimated location have the same colour.

a distance error between the indicated and the real location corresponding to 2.5% (sd= 1.4%) of the total map length. This distance error was below the error-radius of 2.6% that was allowed in the training task.

Furthermore, we found a positive relationship with self-reported navigational abilities (measured here with the Santa-Barbara Sense of Direction Scale – SBSOD) and mean distance memory score of r= 0.56 (p= 0.001, Supplementary Figure 4). Additionally, we found a negative correlation between SBSOD-scores and mean placement error in the bird-view task of r= -0.33 that reached trend level (p= 0.072).
We also explored whether differences in navigational strategies was related to behavioural map representations. There was no significant differences for any of the distance memory scores (Euclidean distance: p= 0.29, path distance: p= 0.25, Euclidean distance after remapping: p= 0.40, path distance after remapping: p= 0.63) or mean placement error in the bird-view task (p= 0.33) between response and place learners. Lastly, there was also no significant difference between response and place learners for self-reported navigational abilities (p= 0.33).

Taken together, behavioural results indicate that participants could accurately remember object-locations and recreate the Euclidean and path distances between them.

The hippocampus maps and integrates Euclidean and path distances

We set out to investigate hippocampal representations of Euclidean and path distances. To do so, we analysed the changes in neural pattern similarity between object-pairs using representational similarity analysis (RSA; Kriegeskorte et al., 2008). More specifically, we calculated neural pattern similarity between object-pairs by correlating the neural activation pattern of every object with every other object, both before (PVT 1) and after (PVT 2) the object-location task (Figure 1B). Subsequently, we subtracted

the pattern similarity of PVT 1 from PVT 2 to test whether pattern similarity scaled as a function of Euclidean and/or path distance. We ensured that participants payed attention to the object presentations during all three PVTs of the experiments through an orthogonal oddball detection task. Participants performed at ceiling level during PVT 1 (correct responses: mean= 96.1%, sd= 17.5), PVT 2 (correct responses: mean= 98.7%, sd= 1.8) and PVT 3 (correct responses: mean= 98.1%, sd= 4.4).

Based on our a-priori hypothesis, we used the left and right hippocampus as regions of interest (ROI) in the analyses. Each ROI yielded one value for the change in neural pattern similarity per object-pair. In order to test how these changes are affected by distances, we (median-)split object-pairs into high (indicated by a 2 in the model) and low distance pairs (indicated by a 1 in the model) for both the Euclidean and the path distances (see Deuker et al., 2016). The prediction was that the representations of objects with a low distance should become more similar to each other than the representations of object-pairs with a high distance (Figure 1B). It has been shown that the hippocampus forms a combined representation of the spatial and temporal distances between goal locations (Deuker et al., 2016). As path distance is highly related to the average travel duration between objects in our design (object-location task: r= 0.99, remapping task r= 0.96), we also tested the effect of the combined Euclidean and path distance (defined as the product of the (median-split) Euclidean distances and the (median-split) path distances). Therefore, this interaction term was a proxy for a combined/integrative representation of Euclidean and path distances. It predicts lowest similarity for object pairs with both a high Euclidean and a high path distances, and vice versa highest similarity for object pairs with low Euclidean and low path distances. To account for shared variance between the Euclidean and path distance predictors (the two predictors correlated with r= 0.57), we used multiple linear regression. For every participant, we included the Euclidean distance categories, path distance categories and an interaction/combined term between the two as predictors for the change of pattern similarity between object-pairs. To estimate the effect for every predictor, we performed t-tests on the participant-specific betas. We found an effect for all three predictors in the left hippocampus (Euclidean distance categories: $T_{(29)}$= 2.3768, p= 0.024, path distance categories: $T_{(29)}$= 2.0255, p= 0.052 approaching significance, interaction of Euclidean and path distance categories: $T_{(29)}$= -2.5570, p= 0.016, Figure 6A). The direction of the integrative effect of Euclidean and path distances, as measured by the interaction term was as expected.

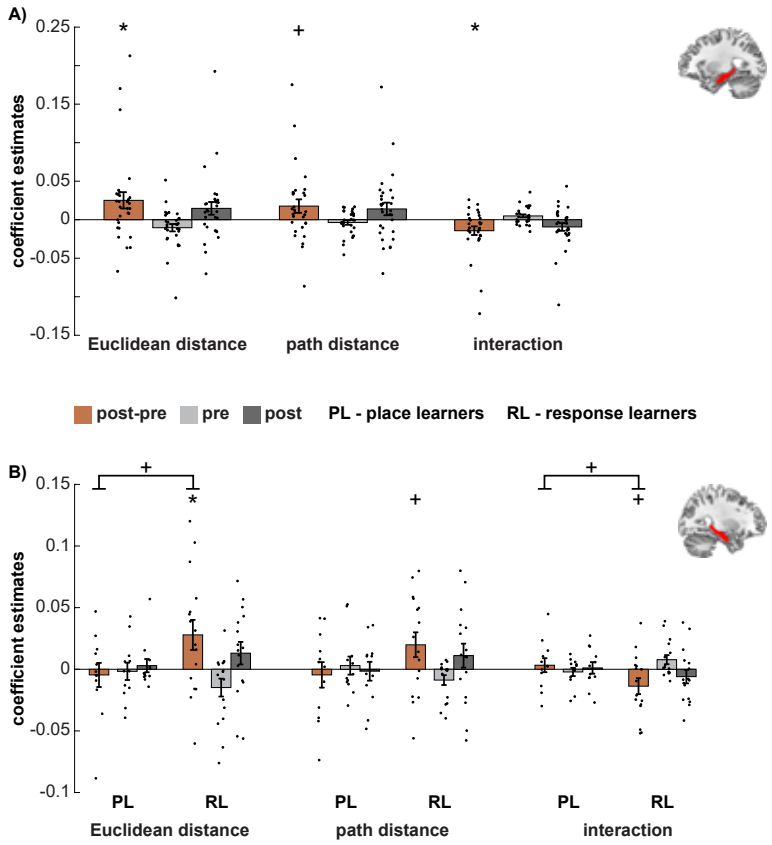

Figure 6 | Changes in neural pattern similarity as a function of Euclidean and path distance in the left and right hippocampus

(A) Changes in pattern similarity as a function of Euclidean and path distance in the left hippocampus. We calculated the changes in neural pattern similarity between object-pairs from pre (PVT 1) to post (PVT 2) the object-location task. We estimated on an individual level the effects of Euclidean distance category, path distance category and the interaction of Euclidean and path distances as predictors for these changes. We then tested on a group level whether these effects differ significantly from zero. To understand the effects better, we also show the betas (coefficient estimates) of each predictor from pre (PVT 1) and post (PVT 2), separately.

(B) Changes in pattern similarity as a function of Euclidean and path distance in the right hippocampus split for place learners (PL) and response learners (RL). We calculated the changes in neural pattern similarity between object-pairs from pre (PVT 1) to post (PVT 2) the object-location task. We estimated on an individual level the effects of Euclidean distance category, path distance category and the interaction of Euclidean and path distances as predictors for these changes. We then tested whether place learners and response learners differ regarding the effects of these predictors. We also performed post-hoc tests for effects for either group, separately. To understand the effects better, we also show the betas (coefficient estimates) of each predictor from pre (PVT 1) and post (PVT 2), separately.

Dots represent single participant values. Error bars show the standard error of the mean. Asterisk symbolizes a significant effect (p< 0.05). Cross symbolizes a trend effect (p< 0.1).

The lower the integrated Euclidean and path distance was between object-pairs, the higher the increase in similarity. However, the directions of the separate effects for the Euclidean and path distance were unexpected, with a higher increase in similarity for high distances than low distances. Furthermore, Euclidean distance representations in the left hippocampus, but neither path distance representations nor the representation of the interaction of Euclidean and path distances, correlated with SBSOD-scores – an indicator of self-reported navigational abilities (Euclidean distances: r= -0.385, p= 0.036; path distances: r= -0.310, p= 0.096; interaction Euclidean and path distances: r= 0.318, p= 0.087). Based on the allocentric nature of Euclidean distances and the egocentric nature of path distances, we additionally explored different map representation between place learners (egocentric navigators) and response learners (allocentric navigators; both groups were classified by an independent T-maze test). We found no differences between place and response learners for neural map representations in the left hippocampus (Euclidean distance categories: p= 0.613, path distance categories: p= 0.752 interaction of Euclidean and path distance categories: p= 0.659).

There was no effect for Euclidean or path distances in the right hippocampus, when testing across all participants (Euclidean distance category: p= 0.156, path distance category: p= 0.287, interaction of Euclidean and path distance category: p= 0.228). However, we observed a trend effect for differences between place and response learners for effects of Euclidean distance categories ($T_{(26)}$= -1.9786, p= 0.059) and the interaction between Euclidean and path distance categories ($T_{(26)}$= 1.9016, p= 0.068), but not path distance categories (p= 0.109, Figure 6B). Post-hoc tests reveal that these differences were probably driven by the response learners. Response learners showed significant or trend effects (Euclidean distance categories: $T_{(15)}$= 2.2957, p= 0.037, path distance categories: $T_{(15)}$= 1.9668, p= 0.068 interaction of Euclidean and path distance categories: $T_{(15)}$= -2.1259, p= 0.051, Figure 6B), whereas the place learners did not (Euclidean distance categories: p= 0.65, path distance categories: p= 0.67 interaction of Euclidean and path distance categories: p= 0.59, Figure 6B). As only response learners showed any indication for a distance map representation in the right hippocampus, we explored whether those correlated with self-reported navigational abilities. Here, we found no significant correlations between distance representations in the right hippocampus and SBSOD-scores (Euclidean distance categories: p= 0.32, path distance categories: p= 0.61, interaction of Euclidean and path distance categories: p= 0.37).

To explore peak-locations of the map representations in the hippocampus more precisely, we performed post-hoc searchlight analyses around each grey-matter voxel of both ROIs, separately (for more details see supplementary analyses and Supplementary Figure 5). No clear peak emerged.

We also explored representations of path and Euclidean distances outside of the hippocampus. Searchlight analyses on grey-matter voxels at the whole-brain level revealed no significant effects representations of Euclidean distance or path distance that survived correction (see Supplementary Figure 6 for non-thresholded effects). We also found no differences between place and response learners for any distance category effects that survived whole-brain correction (see Supplementary Figure 7 for non-thresholded effects).

Taken together, these results suggest that the left hippocampus forms an integrative map of Euclidean and path distances. These effects do not seem to be driven by any subregions in the left hippocampus. Furthermore, these representations were related to self-reported navigational abilities. We found a trend effect that response learners and not place learners use the right hippocampus to represent Euclidean distances and an integration of Euclidean and path distances. Again, these effects do not seem to be driven by any particular subregions in the right hippocampus. Whole-brain analyses revealed no evidence for distance map representations outside of the hippocampus.

The hippocampal distance map of response learners is sensitive to changes in the environment

The second main question of this study was whether a hippocampal map can react flexibly to changes in the environment. For this purpose, participants performed a remapping task after PVT 2 (Figure 2). This remapping task was similar in task structure to the first object-location task. Importantly though, here the position of two out of three roadblocks changed, while the object-locations were consistent with the first task. As a result, for a number of object-pairs path distances either increased or decreased (Figure 1A & C). To test how these changes affect offline map representations, participants completed a third picture-viewing task (PVT 3) after the remapping task (Figure 2). Here, our expectation was that object-pairs with decreased path length would become more similar from pre (PVT 2) to post (PVT 3) the remapping task, compared with object-pairs with increased path length (Figure 1C).

Effects of path changes were assessed in the left and right hippocampus ROIs. To this end, object-pairs that experienced a meaningful change in path distance were median split into an ‘increase’ and a ‘decrease group’ (see Methods for more details). For every participant, the mean similarity change in the decrease group was subtracted from the mean similarity change in the increase group. We then used a t-test to assess whether there was an effect of path length change on the neural similarity change in either the left and/or the right hippocampus.

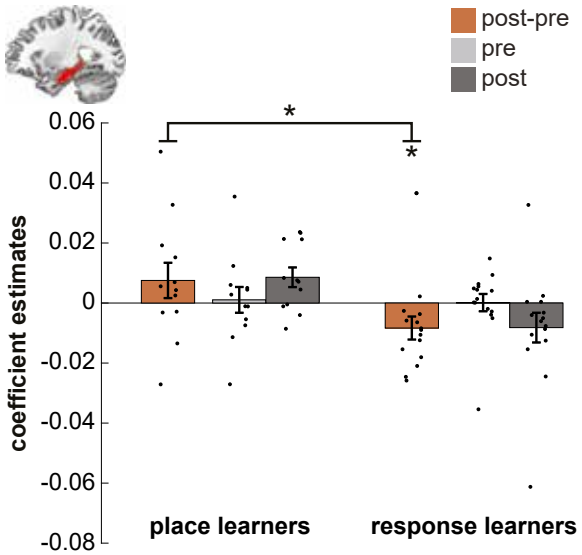

Figure 7 | Changes in neural pattern similarity as a function of change in path distance in the left hippocampus
Effects are split for place learners and response learners. We calculated the changes in neural pattern similarity between object-pairs from pre (PVT 2) to post (PVT 3) the remapping task. We estimated on an individual level the effects of object-pairs which path length increased vs. decreased. We then tested whether place learners and response learners differ from each other. We also performed post-hoc tests for effects of either group, separately. To understand the effects better, we also show the effects from pre (PVT 2) and post (PVT 3), separately.
Dots represent single participant values. Error bars show the standard error of the mean. Asterisk symbolizes a significant effect ($p < 0.05$).

When testing across all participants, there was no effect of change in path length for neither the left ($p = 0.462$), nor the right hippocampus ($p = 0.823$). However, we found a significant difference in path change representation between place and response learners in the left hippocampus ($T_{(25)} = 2.339$, $p = 0.028$, Figure 7), but not the right hippocampus ($p = 0.188$). Post-hoc tests revealed that this effect was driven by response learners: they showed a significant effect of change in path length in the left hippocampus ($T_{(14)} = -2.171$, $p = 0.048$, Figure 7) while place learners did not ($p = 0.227$, Figure 7). The direction of the effect for response learners was as expected, with object-pairs in the path length decrease group showing a higher increase in neural pattern similarity than object-pairs in the path length increase group. We found no significant correlation between SBSOD-scores and the effect of change in path length across response learners ($p = 0.839$).

To explore peak-locations of the change of map representations in the left hippocampus, we performed post-hoc searchlight analyses around each grey-matter voxel of this ROI (for more details see supplementary analyses and Supplementary Figure 8). We

found significant differences between place and response learners in the anterior left hippocampus.

Searchlight analyses on grey-matter voxels at the whole-brain level revealed no representations of changes in path length – neither across all participants, nor for differences between place and response learners (Supplementary Figure 9).

Taken together, we found that response and place learners exhibit differential sensitivity of their hippocampal map to changes in the environment. Specifically, the left hippocampus of response learners remaps based on changes in path lengths. Place learners on the other hand showed no effect. Whole-brain analyses revealed no evidence for remapping outside of the hippocampus.

Discussion

The results of the current study demonstrate that participants acquired map-knowledge about relevant locations and the Euclidean and path distances between these locations when navigating in a rich virtual environment. By associating goal-locations with objects, we were able to measure how Euclidean and path distances affect the neural pattern similarity between object-pairs as a proxy for an offline cognitive map representation. We found that the left hippocampus represents and integrates path and Euclidean distances.
Our second main interest was whether a distance map can adapt to changes in the environment. For this purpose, we changed path distances between object-pairs and tested how these changes affected neural pattern similarity. There was no effect of changes in path distance on hippocampal representations, when testing across all participants. However, there was a significant difference between place and response learners in representing changes of the environment in the left hippocampus. Response learners had a significant effect of distance changes, whereas place learners had not. We speculate that the neural representations of response learners (i.e. egocentric navigators) might be more sensitive to changes in the environment that induce a change in egocentric behaviour. There was no effect of changes in the environment outside of the hippocampus, when testing on whole-brain level.

The integrative map of the left hippocampus

Our results indicate that the left hippocampus forms an offline map that integrates Euclidean and path distance information. This is in line with two other fMRI studies testing offline map representations in the hippocampus (Deuker et al., 2016; Morgan et al., 2011). Morgan et al. (2011) found evidence for both Euclidean and remembered

distance travel time (comparable to path distances in our study) representations in the left hippocampus while participants were watching images of landmarks of a highly familiar environment. Importantly though, the environment of that study had a grid-like structure, resulting in an extremely high correlation (r= 0.9) between the two distances. In comparison, the street-layout of Donderstown is irregular and complex, as it is modelled after a medieval German town (Figure 1; Bellmund et al., 2016). Furthermore, roadblocks made Euclidean and path distances even more distinguishable and as a result our Euclidean and path distance predictors had a lower correlation (r= 0.57) than in the study by Morgan et al. (2011). Last, but not least using multiple linear regression allowed us to test the effects of either distance while simultaneously taking into account shared variance. Hence, our results provide more definitive evidence that both types of distance information are represented and integrated by the left hippocampus. This interpretation dovetails with the results of a previous study testing map representations of Donderstown (Deuker et al., 2016). Here, the authors also found significant effects of remembered Euclidean distance and for the interaction between remembered Euclidean distance and remembered distance travel time in the left hippocampus. A key difference between their design and ours is that in their study participants always navigated along one path and therefore encountered the objects within a predetermined order. This means that the elapsed time between the presentation of object A and B was always equal to the travel time from object A to object B. In comparison, we let participants navigate directly from one object to every other object in (pseudo-)random order. Therefore, the time elapsed between the presentation of object A and object B varied a lot during the experiment (as a varying number of other objects had to be visited in between) and was only equal to the travel time in trials were participants had to directly navigate from object A to object B. Nevertheless, our path distance measurement was by default related to time, as the speed of participants was constant. In short, our path distance can easily be translated into the time it needs to navigate from one object to another. Hence, given the consistency between our results in the other two discussed fMRI studies (Deuker et al., 2016; Morgan et al., 2011), we speculate that our results might reflect an interaction between time and space in the hippocampus. This idea is in line with popular theories about cognitive mapping in the hippocampus (Bellmund, Gärdenfors, et al., 2018; Eichenbaum, 2017; Eichenbaum & Cohen, 2014; Epstein et al., 2017; Schiller et al., 2015; Stachenfeld et al., 2017). Accordingly, the hippocampus represents and processes spatial and temporal information in similar ways. In a much broader sense, these ideas propose that the hippocampus has general processing mechanisms that are domain unspecific. We cannot directly test this idea in the current study as we tested for distance representations in the spatial domain. However, our results demonstrate that the left hippocampus forms a map that integrates different spatial relationships between relevant locations. This, at the very least, is coherent with the

idea that the hippocampus is able to form cognitive maps that entail and integrate a variety of information.

Interestingly, our results point towards a relationship between self-reported navigational abilities and Euclidean distance representation. We found that Euclidean distances were represented in the opposite direction as expected: higher distances resulted in a higher increase in similarity than lower distances. This positive, unexpected effect was negatively correlated with self-reported navigational abilities. This indicates that this unexpected pattern of distance representations is more pronounced the worse people (self-reportedly) navigate. It is important to note that the number of participants in the study was probably too small to interpret these effects of inter-individual differences with confidence. Nevertheless, these patterns of results point towards a more complex story of how cognitive maps might be represented in the hippocampus. Moving forward it might be beneficial to test the effects of navigational abilities in a more direct manner. We propose to pre-screen potential participants for extremely good and bad navigators. This approach circumvents the problem of the inflation of costs by simply increasing the number of participants for such an extensive design as ours (de Haas, 2018). Furthermore, it might shed light on whether different levels of navigational abilities might either lead to ‘more’ or ‘less’ map formation or lead to different forms of map formation (e.g. different directions of distance representations).

How changes in the environment affect the hippocampal cognitive map of response learners, but not place learners

Being flexible and adaptive are key characteristics that are attributed to cognitive maps (Behrens et al., 2018; Bellmund, Gärdenfors, et al., 2018; Tolman, 1948). In fact, it was the adaptive behaviour rats displayed towards changes in the environment that inspired Tolman to postulate the idea of cognitive maps in the first place (Tolman, 1948). Nevertheless, human neuroimaging studies about the effects of changes in spatial environment on hippocampal representations are rare. To our knowledge, these studies are limited to studying these effects during active navigation (e.g. Javadi et al., 2019; Maguire et al., 1998; for an overview see Spiers & Gilbert, 2015). We wanted to expand on this important literature by testing how changes in the environment affect offline hippocampal maps. We found that response learners updated representations in the left hippocampus based on the meaningful changes in path length that occurred in the remapping task (Figure 7). They did so significantly more than place learners. We found no evidence for hippocampal updating of path distances in place learners.

First and foremost, these results show that a hippocampal map is not rigid, but can adapt flexibly to changes in the environment. These updating abilities might be crucial for enabling us to live in an ever-changing world (Bellmund, Gärdenfors, et

al., 2018; Tolman, 1948). Furthermore, these findings support our earlier suggestion that navigational strategies might have an important influence on the nature of hippocampal cognitive maps. Interestingly, we also found trend-level differences between place and response learners for distance representations in right hippocampus (after the original object-location task). This emphasizes that it might be beneficial to investigate the influence of navigational strategies on hippocampal mapping in future studies. We were motivated to test for differences between navigational strategies during remapping because hippocampal involvement in solving detour problems is not consistently found (Spiers & Gilbert, 2015). Accordingly, frontal areas are more often reported as being involved during detour navigation than the hippocampus. Based on our results, we propose exploring whether inconsistencies in the literature might be due to differences between response and place learners.

Our findings also connect to the reported involvement of left hippocampus in sequential egocentric navigation (Iglói et al., 2010, 2015). For the remapping task, we changed the paths and hence the egocentric responses participants had to make to get from one object to another. We speculate therefore that the representations of response learners are more sensitive to these changes. In future studies it might be interesting to test how allocentric changes affect hippocampal map formation, by, for example changing the locations (and hence the Euclidean distance) of the objects. Based on our results, we speculate that navigational strategies might influence the sensitivity to these changes of hippocampal maps. Here we found that path (i.e. egocentric) changes affected egocentric navigators more than allocentric navigators. It might be that Euclidean (i.e. allocentric) changes impact allocentric navigators in a similar fashion as egocentric changes affect egocentric navigators.

Furthermore, it would be interesting to expand on this idea beyond the spatial domain. Recent studies have shown that the human hippocampus and adjacent regions can form maps of 'abstract' spaces (Constantinescu et al., 2016; Garvert et al., 2017; Tavares et al., 2015; Theves et al., 2019). For example, the hippocampus can track distances in a 2-dimensional feature space between object-pairs (Theves et al., 2019). If navigational strategies influence remapping in physical/virtual space, it is worth exploring how these inter-individual differences affect remapping in abstract spaces. Remapping here could, for example refer to the change in boundaries between concepts in an abstract space (e.g. by adapting the designs by Constantinescu et al., 2016; Theves et al., 2019).

Taken together, our results support the idea that offline hippocampal cognitive maps can adapt flexibly to changes in our environment. Furthermore, they highlight the important influence navigational strategies might have on map representations in the hippocampus.

Conclusions

We show that (especially the left) hippocampus forms an offline map of our environment that integrates Euclidean and path distance information. Importantly, we found evidence indicating that these offline maps can adapt flexibly to changes in the environment, at least in response learners. The results of this study highlight the important role that navigational strategies and abilities might play in the formation and updating of hippocampal maps.

Methods

Participants

32 healthy participants (16 women) completed the experiments. Participants were recruited via the university's online recruitment platform. Participants were between 18 and 32 years old (mean age= 22, sd= 3.1). At the beginning of the experiment, participants gave written informed consent to participate in the study and filled in a screening form to ensure that they did not meet any exclusion criteria for the MRI and behavioural labs. Participants were compensated at a rate of 8 Euro per hour of behavioural testing and 10 Euro per hour of MRI testing. The study was approved by the local ethics committee (CMO Regio Arnhem-Nijmegen, The Netherlands, nb. 2014/288).

Experimental sessions

The experiment took place on two consecutive days (for the timeline of the complete experiment see Figure 2). We wanted participants to form an offline map of a large-scale virtual environment. For this purpose, participants completed in total three navigation tasks in a virtual city. The virtual city was an adapted (smaller) version of 'Donderstown' (Bellmund, Deuker, et al., 2018; Deuker et al., 2016). We programmed all navigation tasks with Unreal Development Kit 3 (Unreal Engine 3, Epic Games, Inc.). Across all navigation tasks, participants had to navigate between eight goal-locations. These locations were marked with a black box. Goal-locations remained the same across all navigation tasks. Importantly, there were three roadblocks in the city. This way we could manipulate path distances between goal-locations (Figure 1A). The first navigation task was a training task and took place on day one of the experiment. The aim here was for participants to become familiar with the environment and to learn the shortest routes between the eight goal-locations. The second navigation task was an object-location task and took place on day two of the experiment. With the help of this task, participants associated every goal-location with an object. In more detail, participants had to navigate from goal-location to goal-location. When reaching a goal-location the location-specific object would appear. The layout of the city was identical

to the training task. The third navigation task was a remapping task and took place on day two of the experiment. Importantly, two out of the three roadblocks changed their location between the object-location task and the remapping task. Hence, participants had to find new routes between goal locations and as a result path distances between object-pairs changed. Otherwise, the structure of the remapping task was similar to the object-location task.

To index offline map representation of distances in the hippocampus, we measured the change in neural pattern similarity between object-pairs, similar to Deuker et al. (2016). To this end, participants performed three identical picture viewing tasks (PVT) while fMRI data was recorded. All eight objects were repeatedly presented during these PVTs. The first PVT took place at the start of the experiment on day one and was used as baseline measurement of neural pattern similarity between object-pairs. Because we were interested how Euclidean and path distances between object-pairs affected their neural pattern similarity, the second PVT took place after the object-location task on day two of the experiment. In order to measure how changes in path distances affect hippocampal representations, the third PVT took place after the remapping task.

In order to ensure that participants actually acquired knowledge about the map structure of the navigation tasks, we used two distance recall tasks and a bird-view task. Participants completed a distance recall task directly after the object-location task and after the scanning session (which included the remapping task) on day two. Here, we asked participants to estimate the Euclidean and path distance between every object-pair on a scale from zero to 100. We presented participants with a bird-view map of the virtual city at the very end of the experiment. We asked participants to indicate the location of every object on this map.

Finally, we assessed navigational abilities and strategies independent of the main navigation tasks. Participants filled out the Santa Barbara Sense of Direction Scale as a measurement for self-reported navigational abilities (Hegarty, 2002). Furthermore, we used a T-maze task (adapted from the version by Astur et al., 2016) to categorize participants into response and place learners. Both tasks were completed after the training task on day one.

Navigation tasks

General set-up of the environment

Participants completed the three navigation tasks in the same virtual environment (Figure 1A). All active components of the environment and the navigation tasks were programmed and created in Unreal Development Kit 3 (Unreal Engine 3, Epic Games, Inc.). The environment had a length of ca. 19500 virtual distance points and a width

of ca. 8760 virtual distance points. Throughout all tasks, participants were only able to navigate on the streets of the environment. Participants navigated with a constant speed of 600 virtual distance points per second (it took around 33 seconds to navigate from one end of the city to the other along the most direct path). Participants completed all tasks from a first-person perspective and with a viewpoint-height of 90 virtual distance points. In order to move forward, participants could use the upward arrow-key on the keyboard and to rotate they could use the left and right arrow key. In the MRI scanner, participants indicated their responses with a button box with their right hand. Here, the middle button was used to move forward and the left and right button was used to rotate.

There were eight goal-locations in the virtual environment. All goal-locations were marked by a black box and were placed on the street grid of the virtual environment (Figure 1A). Each black box had the dimensions of 64x64x64 virtual distance points. The goal-locations remained constant across all three tasks. Euclidean distance between goal-locations varied between 2760 and 13242 virtual distance points. Path distance between goal-locations varied between 3362 and 17990 virtual distance points up until remapping. For the remapping task, path distance between goal-locations varied between 3117 and 20873 virtual distance points (see Supplementary Figure 2A for an overview of all Euclidean and path distances between goal-locations). There were three roadblocks in the virtual environment. Two of them changed location between the object-location task and the remapping task (Figure 1A). This resulted in changes in path distance ranging from -8517 to 7821 virtual distance points. Participants could not continue navigating on the street when encountering a roadblock and had to change direction to find another path. Roadblocks had an approximate height of the viewpoint of the player and a thickness of 56 virtual distance points.

Throughout the street grid of the city, we placed location trackers. These trackers were invisible and penetrable for participants. Location trackers could register when a participant walked through them. This allowed the game to track whether a participant took the shortest route between two goal-locations and display the appropriate feedback at the end of a trial. We also logged the continuous location of the participant in the virtual environment, allowing us to recreate their navigation pattern after the experiment.

Training task

The aim of the training task was for participants to become familiar with the virtual environment. Particularly, we wanted participants to learn the eight goal-locations and the shortest route between them. For this purpose, trials in the training tasks consisted of participants navigating from one goal-location to another (Figure 8A & C). When reaching the correct goal-location, participants received feedback about whether

they took the shortest possible route. There was a total of 112 trials. The order from which goal-location participants had to navigate to the next goal-location was pseudo-randomized. Every goal-location was the starting point and destination point an equal amount of times over the course of the experiment (in total 14 times). Furthermore, from every goal-location, participants navigated an equal amount of times to every other goal-location (in total two times). A navigation trial consisted of the following steps:

1 Participants saw instructions on the screen to go to the next box and find the shortest possible route for 1000 ms. The target box was identifiable by turning from black to multi-coloured for the duration of the trial.
2 Participants could start to navigate freely in order to find the target box. During navigation, participants received feedback about the Euclidean distance between their current location and the location of the target box. This feedback resembled a Wifi-signal. The closer the participant was to the target box, the stronger the signal became (i.e. the more bars appeared, with a maximum of eight bars). The signal was scaled to the maximum Euclidean distance of the experiment.
3 Once participants walked into the target box (reached the destination), they received feedback about whether or not they had taken the shortest possible route. This feedback was presented for 2000 ms.
4 The trial ended and the target box would become the start location of the next trial.

The 112 navigation trials were split into four blocks (of 28 trials). After each block, we tested participants' knowledge about the locations of the eight boxes. All blocks were removed from the environment for this recall phase. Participants were asked to remember the location of every box. Participants could indicate their answers by pressing a button to signal that they were at a box-location. If they remembered the location of a box to be within a radius of 500 virtual distance points (about 2.6% of total map length), participants received positive feedback. Otherwise, the box would appear at its correct location in multi-colour. Before continuing with the task, participants had to walk to the miss-located box and touch it. During the recall phase, participants saw the number of locations they still had to find.

Out of the 32 participants, 28 completed all four blocks of the task. As the task was self-paced, we stopped the task for four participants because the allotted lab time ran out. Two of these participants completed two blocks and the other two completed three blocks. There were no timing issues with the navigation tasks on the following day. On average the duration of the training task was 93 minutes (sd= 14 minutes). Participants got faster during the task, with the first block taking on average 26 minutes (sd= 8 minutes) and the last block taking on average 20 minutes (sd= 3 minutes). From block to block, participants also increased the number of trials in which they took the shortest possible route (first block: average= 34%, sd= 14%, second block: average= 47%, sd=

12%, third block: average= 60%, sd= 12%, fourth block: average= 61%, sd= 16%). In the first block, participants took on average the shortest route in 34% (sd= 14%) of trials. In the last block, participants took on average the shortest route in 61% (sd= 16%) of trials. Over the whole task, participants took on average the shortest route in 49% (sd= 12%) of trials. Lastly, participants improved their knowledge about box-locations from block to block, reflected in an increase in correctly placed boxes (first block: average= 53%, sd= 17%, second block: average= 70%, sd= 20%, third block: average= 88%, sd= 14%, fourth block: average= 89%, sd= 17%).

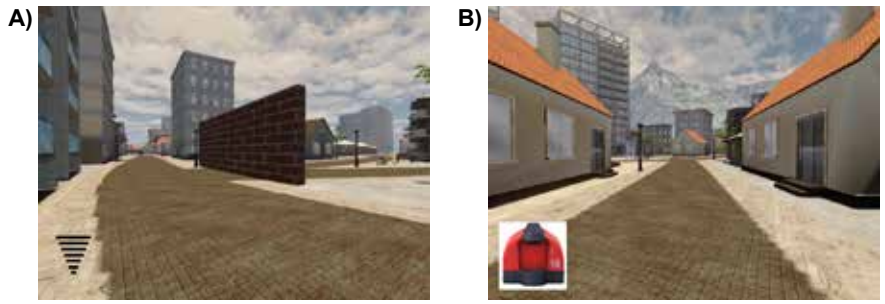

Figure 8 | Screenshots of navigation tasks from the perspective of the participant
(A) Navigation phase during the training task and the first half of the object-location task. Participants could freely navigate the streets of the virtual environment. The participant got feedback about their distance to the goal-location in the form of a wifi-like signal in the left lower corner of the screen. The more bars appeared on the screen, the closer a participant was to the goal-location (max. eight bars). Also shown in the image is a roadblock in the form of a brick-wall in the image.

(B) Navigation phase during the second half of the object-location task and the remapping task. Participants could freely navigate on the streets of the virtual environment. Instead of the wifi-like signal, participants saw the object of the goal-location. Participants had to recall the location of the object to successfully navigate to the correct box.

(C) The box of the goal-location would turn from black to multi-coloured. Participants had to walk into the box of the goal-location to finish the navigation trial.

Object-Location task

The object-location task was similar to the training task. Again, participants had to navigate from goal-location to goal-location and find the shortest possible route between them. A key difference however, was that every location/box was associated with one object, respectively.

Participants were presented with the object for 2000 ms, once they arrived at the target box. In total there were 112 trials – same as for the training task. The rules for the pseudo-randomization were the same as for the training task. There were no recall blocks for box locations. However, the task was split into two. In the first half, participants received feedback about their distance to the target-box while navigating (identical to the training task). In the second half, participants saw the object of the target box in place of the distance feedback (Figure 8B). Participants were instructed to go to the location of that object. With this, we wanted to encourage participants to learn the object-locations, instead of relying on the distance signal.

For each participant, the eight objects were randomly picked out of a pool of twelve objects (Supplementary Figure 1). Object-location associations were randomized across participants as well.

All participants completed the object-location task. On average the task took 64 minutes (sd= 10 minutes). The first half of the task took on average 35 minutes (sd= 5 minutes) and the second half 29 minutes (sd= 6 minutes). Participants improved over the task in finding the shortest possible route (first half: 62% of trials (sd= 13%), second half: 87% of trials (sd= 14%).

Remapping task

The remapping task was similar to the second half of the object-location task. In fact, the structure of the tasks and trials was identical to the second half of the object-location task (Figure 8B & C). The key difference was that the location of two out of the three roadblocks had changed (Figure 1A). Therefore, the shortest route could change between the objects/boxes. In order to receive positive feedback, participants had to find these new routes. In total, there were 56 pseudo-randomized trials. Rules for the pseudo-randomization were the same as for the training and object-location task. This resulted in seven trials per box/object as starting point and destination. Participants navigated from every object/box to every other object/box once during the remapping task.

All participants completed the remapping task in the MRI scanner. On average the task took 30 minutes (sd= 3 minutes). Participants took the shortest route on 74% (sd= 9%) of trials.

Testing knowledge about the map

We tested participants' knowledge about the map on three different occasions. We asked participants to estimate the Euclidean and path distance for every object-pair after the object-location task and after the remapping task, respectively (distance recall task). Lastly, we asked participants at the end of the whole experiment to indicate the location of every object on a bird-view map of the city (bird-view placement task).

For the distance recall task, we first asked participants to estimate all Euclidean distances between object-pairs and then to estimate all path distances between object pairs (in total 28 trials per distance estimation). The order of object-pairs was completely randomized across participants. For both estimations, we instructed participants to indicate the distance by entering a number between 0 and 100. We told participants that 0 would mean both objects share the same location, whereas 100 represents the longest possible distance between two objects. The task was completely self-paced. The task was programmed in neurobs Presentation (version 16.4, **www.neurobs.com/presentation**). We scored participants' performance by correlating the estimated distances with the actual distances between object-pairs.

For the bird-view placement task, participants were presented with a picture of the bird-view map of the street-layout of the city (Supplementary Figure 3). All buildings and landmarks had been removed from the picture. The street-layout was overlaid with a regular grid to help participants to indicate the locations better. Next to the picture of the street-layout, participants saw the eight objects with a number next to every object. We asked participants to indicate the location of each object by writing its corresponding number onto the map (paper-pencil format). We scored participants' performances by calculating the mean placement error (distance) between the recalled location and the actual location of every object.

Picture viewing tasks

In order to measure changes in neural pattern similarity, participants completed three (identical) picture viewing tasks (PVTs) in the MRI scanner. During a picture viewing task, pictures of the objects participants encountered in the virtual city appeared on the screen one at a time (Figure 9). In order to keep participants' attention on the objects during the PVTs, participants had to perform an oddball task. The oddball was the picture of an object (a bathtub) that did not appear in the rest of the experiment. Participants had to press one of two buttons if the oddball object was presented (catch trials) and the other button if any other object was presented (regular trials). Button-contingencies were randomized across participants, but were always done with the right index and middle finger. This oddball task was orthogonal to later analyses of the PVTs. Participants performed at ceiling on the cover task in all PVTs (PVT 1: mean= 96.1%, sd= 17.5, PVT 2: mean= 98.7%, sd= 1.8, PVT 3: mean= 98.1, sd= 4.4).

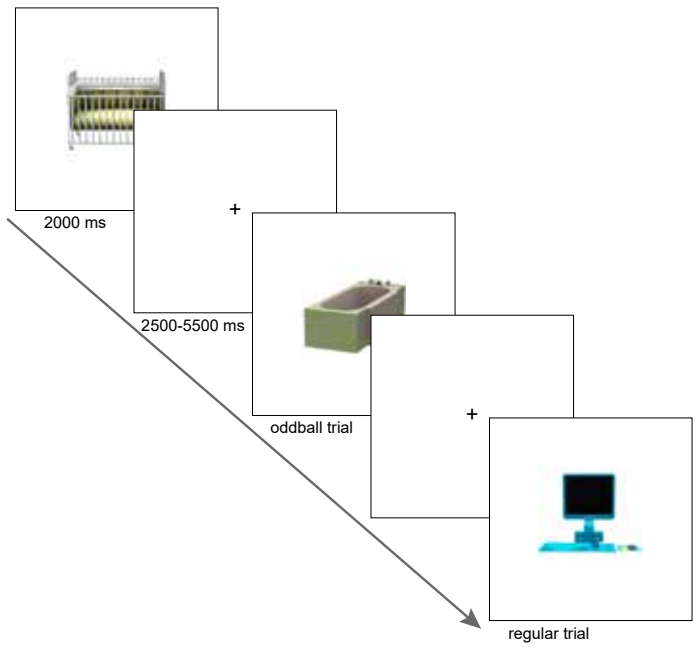

Figure 9 | Trial structure of the picture viewing tasks
The eight objects a participant encountered in the navigation tasks were presented in random order during the PVT. The order of object presentation was identical across all PVTs of the same participant. Objects were presented for 2000 ms at the centre of the screen. Between object presentations a black fixation cross was presented at the centre of the screen. Duration of the fixation cross was either 2500, 4000, or 5500 ms. Participants had to press one of two buttons if the presented object was the oddball object (bathtub). They pressed the other button if any other object was presented. Button contingencies were randomized across participants.

The order of the objects was pseudo-randomized for every participant, but held constant across picture viewing tasks of the same participant. All eight objects that a participant encountered in the object-location and remapping task were presented 20 times, respectively during a PVT. An object presentation took 2000 ms and the object was presented at the centre of a white screen. The order of the objects was pseudo-randomized, so that all objects were presented every mini-block of eight regular trials. Furthermore, an object could never repeat back-to-back. We added 32 catch-trials in which the oddball was presented. Hence, in total each PVT consisted of 192 trials. The oddball probability was constant across the experiment (oddball followed every regular object 4 times, probability was therefore 20%). Similarly, catch trials were equally distributed across the PVT with the same probability of appearing within every 20% of the task. We did this to keep attention high throughout the whole PVT.
After every trial, a black fixation cross appeared at the centre of the screen. The duration of these ITIs was jittered between one and three scanner pulses (TR was 1.5 seconds) plus 1 second. The order of the ITI-durations was pseudo-randomized in a

manner that all ITIs appeared as equally often as possible across all trials (the ITI of a catch trial was randomly chosen). Furthermore, the average ITI duration within every 20% of the task was not allowed to deviate more than one standard deviation of the average ITI duration of the whole PVT. The purpose of these pseudo-randomizations was to ensure that there was no temporal bias of ITI duration between objects or within the PVT.
After every block of 60 non-catch trials, participants had a 20 second break, in which they received feedback about their performance on the previous block and a reminder of the button-contingencies.
All PVTs were programmed in and presented with neurobs Presentation (version 16.4, www.neurobs.com/presentation).

Navigation assessment tasks

Santa-Barbara Sense of Direction Scale

The SBSOD is a self-referential questionnaire about navigational abilities (Hegarty, 2002). Participants completed the questionnaire on a computer. The 15 Likert-type questions were presented subsequently at the centre of the screen. Participants could take as much time as they wanted per question. Under each question was a 7-point scale reaching from ‘strongly agree’ (1) to ‘strongly disagree’ (7). Each number on the scale was surrounded by a grey frame. At the start of each trial ‘1’ was within a red frame. Participants could move this red frame along the scale with the left and right arrow keys to indicate their answer. By pressing enter, they would confirm that the currently selected number was their final answer and the next question would appear. When scoring participants’ answers, we reversed positive items, so that a higher score translated to higher self-reported navigational abilities. The final score was the mean of all (reversed positive and non-reversed negative) items. On average participants had a score of 4.49 (sd= 1.18).
The task was programmed in and presented with neurobs Presentation (version 16.4 www.neurobs.com/presentation).

T-Maze task

The T-Maze task was adapted from Astur et al. (2016). The goal of the task was to categorize participants into place and response learners. The task took place in a virtual room and was developed and programmed with Unreal Development Kit 3 (Unreal Engine 3, Epic Games, Inc.).

We placed a T-shaped platform in the room (Figure 10). Around the platform, we placed several objects in the room in order for participants to orientate themselves. We placed a multi-coloured box in either arm of the T-Maze, respectively. We instructed participants that one of the two boxes was rewarded, whereas the other was not. At the

beginning of a trial, participants were placed at the bottom of the T-Maze. Participants could freely navigate on the platform with the help of the arrow keys (akin to the navigation tasks) and additionally rotate with the mouse. Once participants arrived at one of the two boxes, they received either positive or negative feedback for 2000 ms. If participants walked to the rewarded box, they were presented with a green happy smiley, otherwise they were presented with a red sad smiley. After the feedback, participants were presented with a black fixation cross on a white screen for 5000 ms and the next trial started.

Figure 10 | T-Maze
Participants had to navigate in a virtual room from the bottom of a T-Maze to one of two arms. In both arms, a coloured box was placed. One box was rewarded, whereas the other was not. In two probe trials, the T-Maze was rotated 180°. This is indicated in the image by the dashed line around the new position of the higher arm of the T-Maze. Participants were classified as place learners if they went to the position in the room of the box that was rewarded in previous trials. Participants were classified as response learners if they took the same turn (left or right) at the end of the of the T-Maze as in previously rewarded trials.

In total, there were 10 trials. Two out of the 10 trials were probe trials. During these probe trials, the T-platform was rotated 180°. The idea here was that participants could either walk to the same location in reference to the room (allocentric/place learners) as in previous rewarded trials or make the same turn as in previous rewarded trials (egocentric/response learners). As we did not want to reward one strategy over the other, both choices were rewarded in probe trials. Akin to Astur et al. (2016) the first probe trial was either after 3, 5, or 7 normal trials (randomly chosen across participants), the second probe trial was always the last trial of the task. At the beginning of the task, participants were placed at the bottom of the T-Maze and were instructed to look around and get familiar with the environment for 20 seconds. In that time, participants

could not move away from the position they were in, but were able to rotate.
Out of the 32 participants 13 were classified as place learners, 17 were classified as response learners and 2 were classified as mix learners (based on inconsistent choices across the two probe trials). We excluded the mixed learners from analyses, when comparing place and response learners.

MRI Image acquisition

Functional T2*-weighted and anatomical images were acquired on a Magnetom Prisma or PrismaFit 3 Tesla magnetic resonance tomograph (Siemens, Erlangen, Germany) with a 32-channel head coil. Due to the extensive nature of the study and booking load of the PrismaFit scanner, we decided to collect four out of the 32 data-sets on the Prisma scanner. Both sessions within each participant were scanned on the same scanner. Functional images were acquired with a 4D multiband sequence with 84 slices (multi-slice mode, interleaved), TR= 1500 ms, TE= 28 ms, flip angle= 65 deg, acceleration factor PE= 2, FOV= 210 x 210 x 168 mm and an isotropic voxel size of 2 mm. An anatomical image of the brain was acquired, using a T1 sequence (MPRAGE) with TR= 2300 ms, TE= 3.03 ms, flip angle= 8 deg , FOV= 256 x 256 x 192 mm and an isotropic voxel size of 1 mm. If time limit of scanning was not reached yet at the end of each scanning session two separate phase and magnitude images were acquired in order to correct for distortions with a gradient field map (multiband sequence with TR= 1020 ms, TE= 10 ms, flip angle= 45 deg and a voxel size of 3.5 x 3.5 x 2.0 mm).

fMRI preprocessing

Functional images of the three functional runs (one per PVT) were preprocessed with help of the FSL toolbox (version 5.0.4, http://fsl.fmrib.ox.ac.uk/fsl/fslwiki/). Motion correction (three rotation and three translation estimations) and a high pass filter (cut-off: 100s) were applied to the images. The anatomical scan of each participant was downsampled to the voxel size of the functional scans (2 mm isotropic). In order to have a common reference space for the first-level analysis, all functional scans were linearly registered to the down-sampled anatomical scan.
After preprocessing, we excluded participants from further analysis of a functional run based on the following criteria: 1. No appropriate responses during the PVT (minimum inclusion criteria was pressing both possible buttons, no participant was excluded). 2. More than 10% of the volumes of a functional run had movement above 3 mm (two participants excluded from analyses of PVT 2 and an additional participant excluded from PVT 3). Taken together, 30 participants (12 place learners, 16 response learners and 2 mixed) were included for analysing changes from PVT 1 to PVT 2 and 29 participants (12 place learners, 15 response learners and 2 mixed) were included for analysing changes from PVT 2 to PVT 3.

First-level analyses

We used representational similarity analysis (RSA) to measure changes in neural similarity between object-pairs as a proxy for a cognitive map (Deuker et al., 2016; Kriegeskorte et al., 2008). To this end, we estimated object-specific activation by modelling the onset and duration for each object in a GLM (one GLM per PVT). To account for the other events during the PVTs, we set up additional regressors. All catch trials (oddball trials) were modelled in a single separate regressor. Additionally, we modelled button presses with the index and middle finger in two separate regressors with a stick function. The beginning of the task was modelled with the duration from start time of scanning until the first object presentation. The end of the task was modelled with the duration from the end of the last object presentation until end of scanning. Furthermore, all block breaks were modelled in one regressor with the duration from the end of the last object presentation before the break until the first object presentation after the break. Lastly, we accounted for movement by adding six movement parameters (estimated during preprocessing) and added an additional regressor for each volume that exceeded a movement of 3 mm (on average 1.7 volumes per run sd= 7.6).

ROI-Analyses

We performed analyses on anatomical masks of the left and right hippocampus. Both hippocampus masks were based on the Harvard-Oxford subcortical structural atlas (https://fsl.fmrib.ox.ac.uk/fsl/fslwiki/Atlases). Included voxels had to fulfil two criteria: a minimum probability of 25% to be hippocampus voxels and no higher probability to belong to a region other than the hippocampus. We only included grey-matter voxels into our masks. As these masks were in MNI space, we translated the object-specific parameter estimates of every PVT into MNI space. To estimate neural similarity between object-pairs, we correlated the parameter estimates of every object with the parameter estimates of every other object across all voxels within the ROI mask (Spearman's correlation coefficient). Subsequently, we could then subtract these correlation values of a pre-navigation-task PVT from a post-navigation-task PVT (e.g. 2-1, 3-2) as index for change in neural similarity. As we were interested how these changes in neural similarity were affected by distances in the map, we used multiple linear regression with different distance models as predictors. Using multiple linear regression allowed us to account for shared variance between different distance measurements. Specifically, we first measured the effect of Euclidean and path distance on change in neural similarity from PVT 1 to PVT 2. We performed a median split on object-pairs based on their Euclidean and their path distances, respectively. We set the weight for low distances to 1 and for high distances to 2. We entered as predictors the weight for Euclidean distance, the weight for path distance and an interaction term between the two and added a constant term. The interaction was the product of the

Euclidean prediction and the path prediction (so the highest weight for object-pairs that have a high Euclidean and a high path distance and the lowest weight for object-pairs with a low Euclidean and low path distance). As a result, we obtained a beta estimate for every predictor per ROI per participant.

As a second step, we assessed how changes in similarity from PVT 2 to PVT 3 were affected by changes in path distances. We only included object-pairs that experienced a meaningful change in path distance. We defined a meaningful change as a distance change higher than 1000 virtual distance points. We chose this cut-off as participants received positive feedback about placing the goal-locations within a radius of 500 virtual distance points during the training (2 object-locations * allowed error of 500 virtual distance points). As a result, 15 object-pairs were included into the analyses. We performed a median-split on these object-pairs into a (relative) decrease group and a (relative) increase group. We then calculated the mean change in neural similarity across all object-pairs of one group. Subsequently, we subtracted the mean change in neural similarity of decrease object-pairs from increase object-pairs. As a result, we obtained one value per ROI per participant.

Searchlight Analyses

We performed searchlight analyses on the whole-brain level and within the ROIs (for voxel-wise output). We included into the searchlight a grey-matter mask, which was based on the participant-specific downsampled anatomical scan. The searchlight had a radius of 3 voxels and was thresholded to include a minimum of 30 grey-matter voxels. RSA analysis within a searchlight was analogous to the analysis within an ROI. We correlated the parameter estimates of every object with the parameter estimates of every other object across all voxels within a searchlight. The resulting correlations were written back into the centre voxel of the searchlight. The rest of the steps were identical to the ROI analyses. Before second-level analyses we spatially normalized the relevant outputs from the searchlight analyses to MNI anatomical space and afterwards smoothed them using a 4 mm full-width at half maximum Gaussian kernel.

Second-level analyses

For the ROI analyses, we had one entry per participant per test and used a one-sample t-test when testing across all participants and a two-sample t-test when testing for differences between place and response learners. We also performed correlations with the ROI betas and the SBSOD-scores across all participants and (where applicable) across all participants within the same navigation-strategy group (place or response learners).

For the searchlight analyses we used a one-sample permutation test when testing across all participants and a two-sample permutation test when testing for differences between place and response learners. Output images from the first level analyses were

entered as input, as well as a whole-brain or ROI mask which only included grey-matter voxels where all participants had an entry. 10000 random sign flips were performed to estimate the null distribution. We used threshold-free cluster enhancement and corrected for multiple comparison with family-wise error rate ($p< 0.05$).

Behavioural analyses

Behavioural signatures of a cognitive map of distances were assessed using distance recall tasks. We used one-sample t-tests to test for an effect of the scores of all distance recall tasks after applying Fisher transformation to the correlation coefficients. As control analyses we correlated the estimated Euclidean distance with the real path distance and vice versa, the estimated path distance with the real Euclidean distance after the object-location task and remapping task, respectively. We used a paired-sample t-test to test whether memory scores were significantly higher than their control counterparts. To visualize the effects of the distance recall tasks, we used multidimensional scaling (MDS). We first applied MDS on the distance estimations for Euclidean and path distances for every participant, separately. We then calculated the mean location for every goal-location across all participants. To estimate locations in path space, we also applied MDS to the objective path distances.

We correlated both mean score of the distance recall task (after Fisher transformation) and the bird-view placement task with self-reported navigational abilities (SBSOD-scores) across participants.

To test for behavioural differences between place and response learners in representing distances, we used two-sample t-tests on all scores of the distance recall task (after Fisher transformation) and the bird-view placement task. We also used a two-sample t-test to test for differences regarding self-reported navigational abilities (SBSOD-scores).

Supplementary analyses

Searchlight analyses of map formation in the hippocampus

We found representations of Euclidean and path distances on ROI level in the left hippocampus (Figure 6B). Here, we performed post-hoc searchlight analyses around each grey-matter voxel of the left and right hippocampus ROIs, separately to localise the map representations in the hippocampus more precisely. In more detail, we performed the same multiple linear regression as on ROI level (see Methods and Results section), within every searchlight (sphere with a radius of 3 voxels) of the ROI. The searchlight is a sphere around a centre voxel and moves its centre from grey-matter voxel to grey-matter voxel. The results of every searchlight are read back into the centre voxel. To test for group effects, we used one-sample and two-sample permutation tests and corrected for multiple testing in each ROI using FWE.

No searchlight effects in the left hippocampus survived correction. However, effects of all three – Euclidean, path and interaction of Euclidean and path distance categories had the same posterior peak location (see Supplementary Figure 5A for non-thresholded effects, peak location at : -22 X -38 Y -4 Z MNI space). No searchlight effects for differences between place and response learners in the right hippocampus survived correction (see Supplementary Figure 5B for non-thresholded effects).

Searchlight analyses of remapping in the hippocampus

We found that response, but not place learners represent changes in path length from pre to post the remapping task (Figure 7). To visualize and understand the effect of path distance change better, we performed post-hoc searchlight analyses in the left hippocampus. In more detail, within every searchlight (sphere with a radius of 3 voxels) of the ROI we subtracted the mean change in similarity from object-pairs in the decrease group from the mean change in similarity from object-pairs in the increase group for every participant. Here, the corresponding difference was read back into the centre voxel of every searchlight. To test for differences between place and response learners, we used two-sample permutation tests and corrected for multiple testing in the ROI using FWE.

We found a significant cluster in the anterior left hippocampus (peak at -22 X -12 Y -20 Z, $T_{(25)}= 3.573$, $p_{FWE}= 0.025$, see Supplementary Figure 8 for non-thresholded effects). We also performed searchlight analyses within the left hippocampus for the response and place learners, separately. We found a significant cluster in the anterior left hippocampus for response learners (peak at -20 X -10 Y -20 Z, $T_{(14)}= -4.567$, $p_{FWE}= 0.008$, see Supplementary Figure 8 for non-thresholded effects). We found no significant effects for place learners (see Supplementary Figure 8 for non-thresholded effects).

Supplementary figures

Supplementary Figure 1 | Objects used in the experiment
Eight out of twelve objects were randomly chosen for each participant. Each object was associated with one of the eight goal-locations in the virtual environment. The objects were: a baby bed, a coffee maker, a bookshelf, a fridge, a computer, a dart board, a mirror, a terrarium, an easel, a sink, a TV and a stereo.

A) objective distance matrizes **B) mean estimated distance matrizes**

Euclidean distances for object-location task

	1	2	3	4	5	6	7	8
1	0	3633	3164	5978	6919	6849	11951	9418
2		0	3638	3615	5844	9022	9012	5834
3			0	3601	3793	5447	9485	8134
4				0	2760	8356	6000	4905
5					0	6644	6595	7294
6						0	13228	13242
7							0	4949
8								0

	1	2	3	4	5	6	7	8
1	0	3286	2990	6303	6368	5489	9964	8022
2		0	2759	3926	4489	6643	6923	4806
3			0	3634	3463	3891	7651	7078
4				0	1077	6203	4120	5297
5					0	5375	4837	6372
6						0	10212	10781
7							0	4681
8								0

Euclidean distances for remapping task

	1	2	3	4	5	6	7	8
1	0	3633	3164	5978	6919	6849	11951	9418
2		0	3638	3615	5844	9022	9012	5834
3			0	3601	3793	5447	9485	8134
4				0	2760	8356	6000	4905
5					0	6644	6595	7294
6						0	13228	13242
7							0	4949
8								0

	1	2	3	4	5	6	7	8
1	0	1963	2138	4729	5475	5459	9004	7259
2		0	2632	3368	4492	6318	7175	5402
3			0	3484	3754	3691	8176	7779
4				0	1434	5892	4728	5812
5					0	5168	5208	7173
6						0	10372	11225
7							0	5193
8								0

path distances for object-location task

	1	2	3	4	5	6	7	8
1	0	12190	6978	12820	12052	9773	17990	16493
2		0	5942	4176	7570	11942	12691	6366
3			0	6723	5131	6585	11222	10009
4				0	3362	12647	9153	8134
5					0	11664	6941	11344
6						0	17237	16412
7							0	16156
8								0

	1	2	3	4	5	6	7	8
1	0	8198	5511	9660	10329	4474	15133	12512
2		0	4144	2898	5818	8948	9467	4693
3			0	4377	4906	4869	9677	8814
4				0	3204	9014	6591	5814
5					0	8216	4806	8916
6						0	12781	13641
7							0	10663
8								0

path distances for remapping task

	1	2	3	4	5	6	7	8
1	0	3673	4686	8082	7920	9715	14554	17925
2		0	5976	4087	7225	12518	11149	14188
3			0	7590	4588	6369	11173	14555
4				0	3116	13727	7915	10791
5					0	10801	6686	10235
6						0	17493	20873
7							0	7739
8								0

	1	2	3	4	5	6	7	8
1	0	2064	4273	6837	8356	6476	13308	15154
2		0	4226	5124	7187	7699	11654	13144
3			0	4937	4845	4561	10445	13704
4				0	3112	9463	6529	8809
5					0	8629	5705	9875
6						0	14314	18134
7							0	5651
8								0

Supplementary Figure 2 | Objective and mean estimated distances between goal-locations for the object-location task and remapping task
(A) Objective Euclidean and path distance between goal-locations for the object-location task and the remapping task.

(B) Mean estimated Euclidean and path distance between goal-locations for the object-location task and the remapping task. Distance estimations from participants were used for multidimensional scaling. Across all participants, the mean location for every object was computed. Here, the distances between these mean estimated locations are displayed.

Distances are in virtual distance points. Location numbers are shown at the top and the left of every distance matrix. See Figure 1 as reference for the location numbers. The corresponding objective and estimated distance matrices are next to each other.

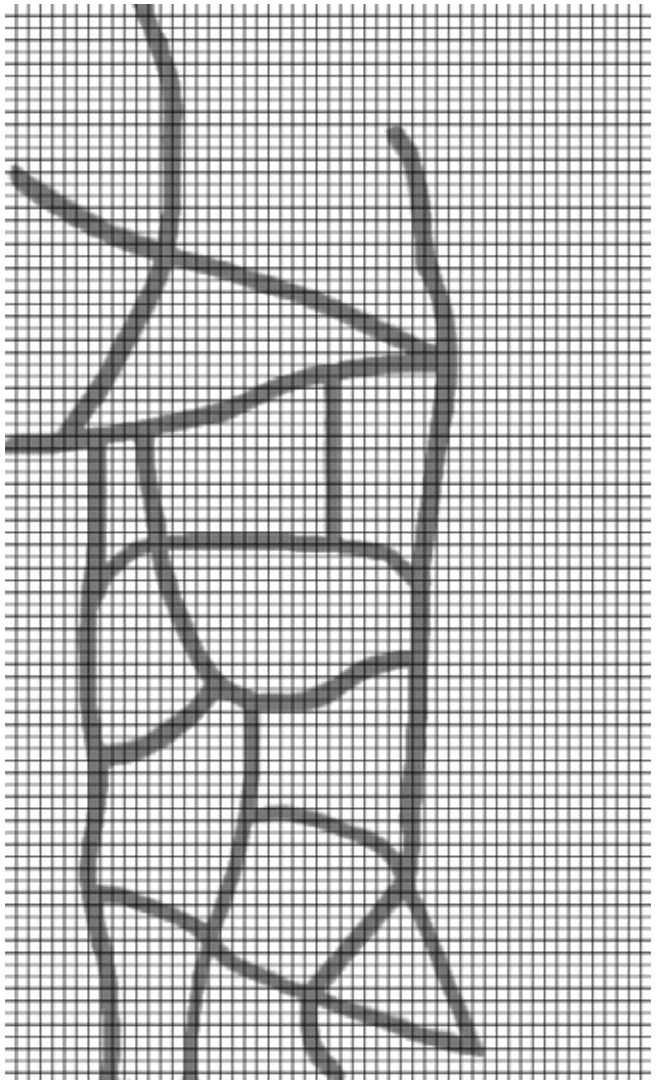

Supplementary Figure 3 | Street-layout of the virtual environment for the bird-view placement task
Participants had to indicate where on the street-layout the objects were located with a paper-pencil version of this image. We added a regular grid on top of the image of the street-layout.

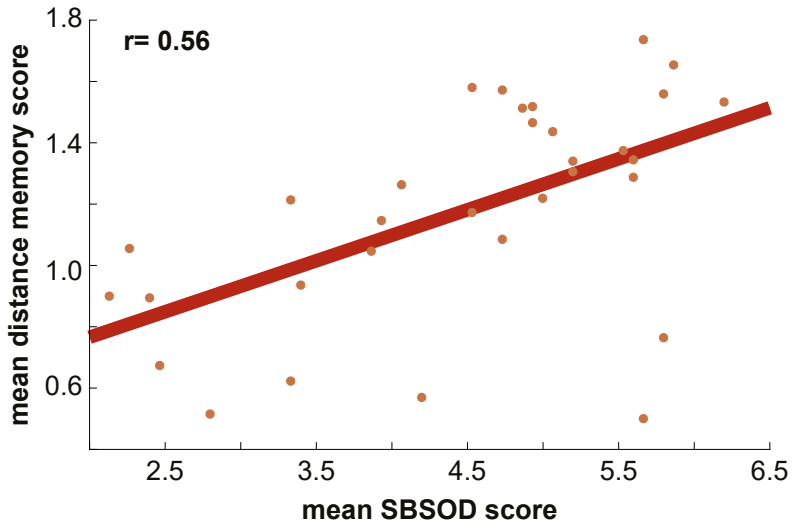

Supplementary Figure 4 | Correlation between mean distance memory score and mean SBSOD score
Mean distance memory score (Fisher transformed) was positively correlated with self-reported navigational abilities (measured here with the Santa Barbara Sense of Direction Scale – SBSOD). Correlation coefficient was r= 0.56, p= 0.001. Dots represent single participant values.

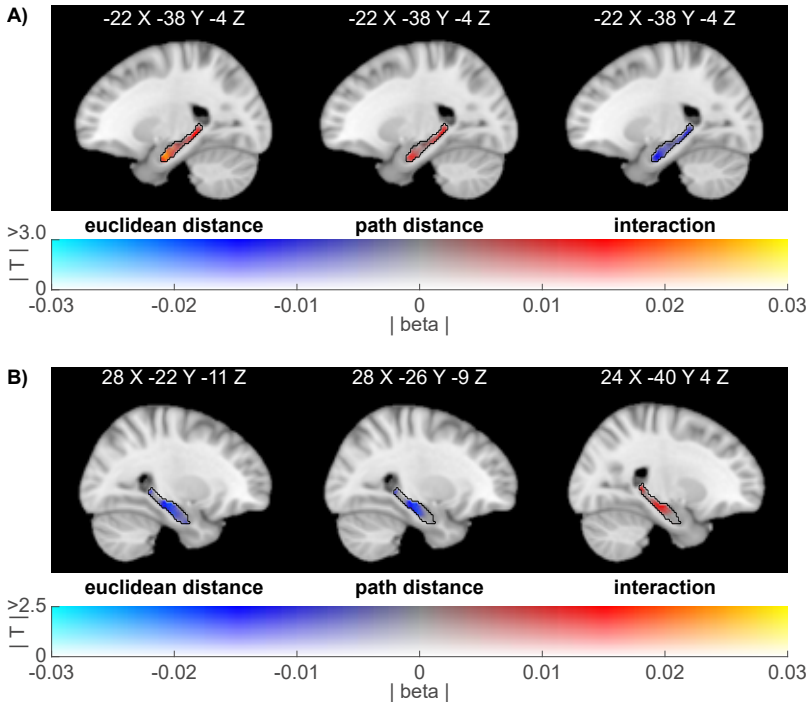

Supplementary Figure 5 | Searchlight results for distance categories effects on change in neural similarity from before to after the object-location task in the left and right hippocampus
(A) Effects of distance categories on change in neural similarity from before (PVT 1) to after (PVT 2) the object-location task, split for Euclidean distance, path distance and interaction between the two. No effects survived small-volume correction in the left hippocampus. Peak voxel coordinates are given in MNI space.

(B) Differences between place and response learners for effects of distance categories on change in neural similarity from before (PVT 1) to after (PVT 2) the object-location task. Effects are split for Euclidean distance, path distance and interaction between the two. No effects survived small-volume correction in the right hippocampus. Peak voxel coordinates are given in MNI space.

All images were created using a dual-coded design (Allen et al., 2012; Zandbelt, 2017). This allowed showing both, the mean beta coefficient (blue-red) and the T stats (opacity).

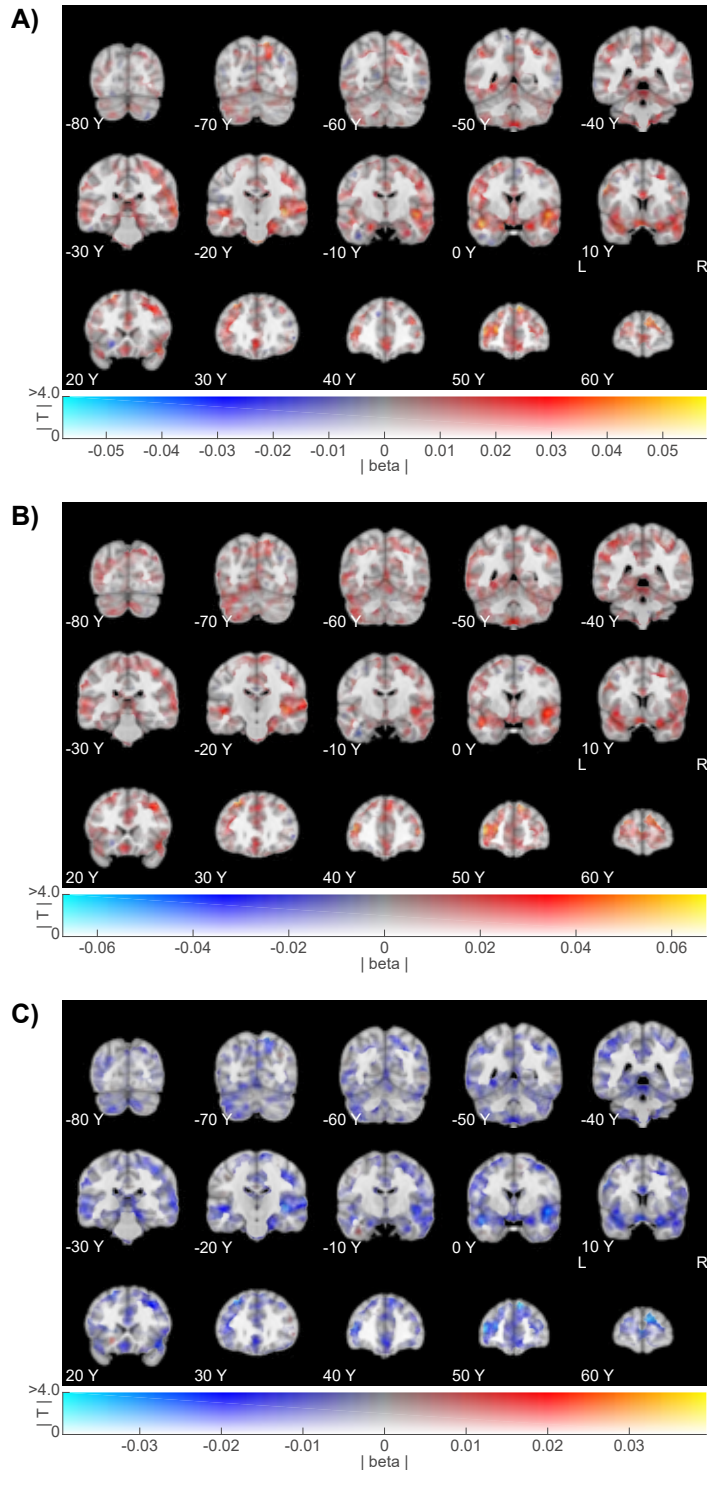

Supplementary Figure 6 | Whole brain effects of distance categories on change in neural similarity from before to after the object-location task
(A) Effects of Euclidean distance categories on change in neural similarity from before (PVT 1) to after (PVT 2) the object-location task. No effects survived whole-brain correction.

(B) Effects of path distance categories on change in neural similarity from before (PVT 1) to after (PVT 2) the object-location task. No effects survived whole-brain correction.

(C) Effects of interaction distance categories on change in neural similarity from before (PVT 1) to after (PVT 2) the object-location task. No effects survived whole-brain correction.

All images were created using a dual-coded design (Allen et al., 2012; Zandbelt, 2017). This allowed showing both, the mean beta coefficient (blue-red) and the T stats (opacity). Y-coordinates are in MNI space.

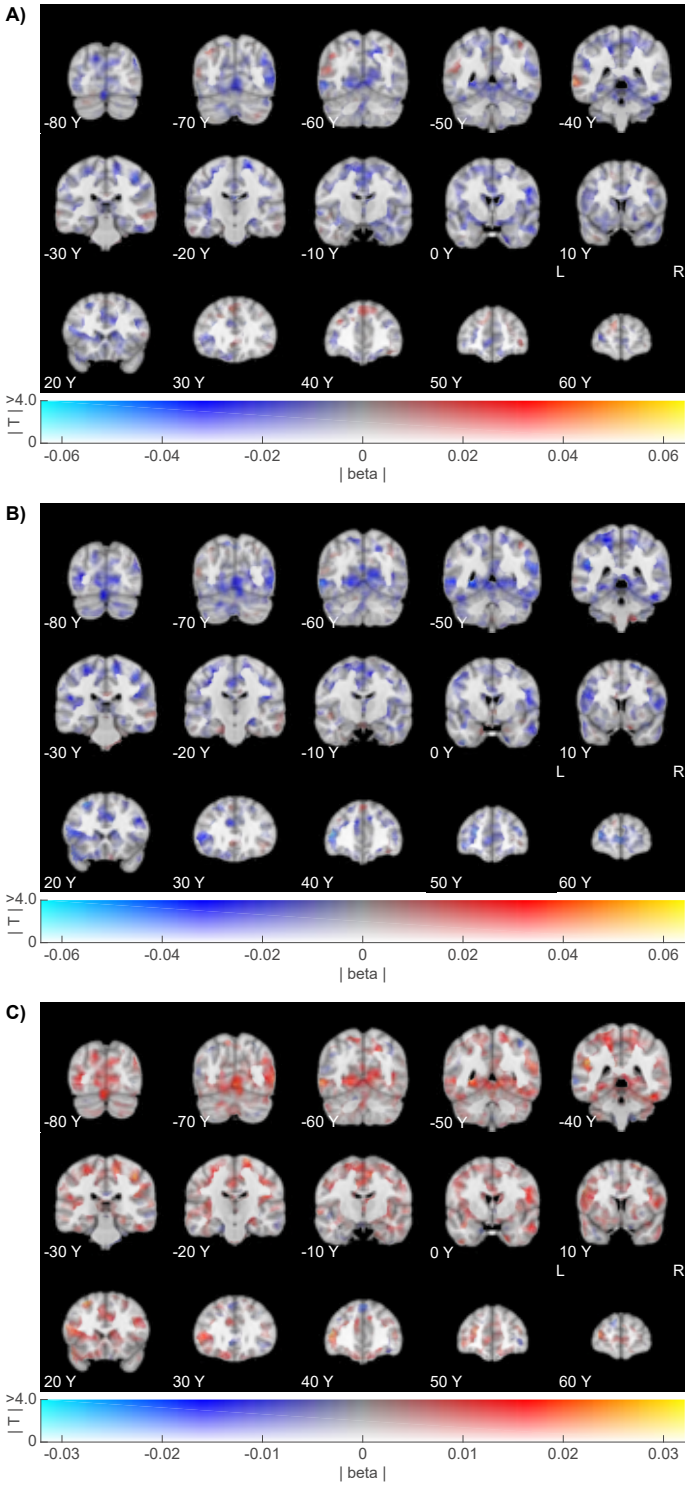

Supplementary Figure 7 | Whole brain effects for differences between response and place learners in distance representations
(A) Differences between response and place learners for effects of Euclidean distance categories on change in neural similarity from before (PVT 1) to after (PVT 2) the object-location task. No effects survived whole-brain correction.

(B) Differences between response and place learners for effects of path distance categories on change in neural similarity from before (PVT 1) to after (PVT 2) the object-location task. No effects survived whole-brain correction.

(C) Differences between response and place learners for effects of interaction distance categories on change in neural similarity from before (PVT 1) to after (PVT 2) the object-location task. No effects survived whole-brain correction.

All images were created using a dual-coded design (Allen et al., 2012; Zandbelt, 2017). This allowed showing both, the mean beta coefficient (blue-red) and the T stats (opacity). Y-coordinates are in MNI space.

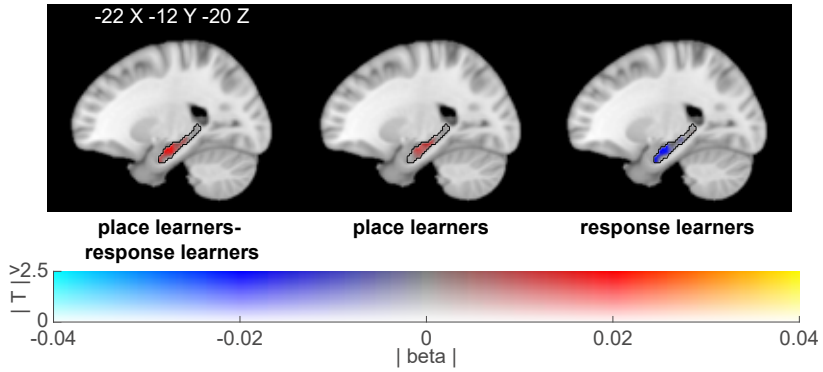

Supplementary Figure 8 | Searchlight results for changes in neural pattern similarity as a function of change in path distance in the left hippocampus
We estimated on an individual level the effects of object-pairs which path length increased vs. decreased on changes in neural pattern similarity from pre (PVT 2) to post (PVT 3) the remapping task. Effects are shown for the difference between place learners and response learners and separately for both groups. Images are centred to the peak voxel for the difference between place and response learners (coordinates are in MNI space.). All images were created using a dual-coded design (Allen et al., 2012; Zandbelt, 2017). This allowed showing both, the mean beta coefficient (blue-red) and the T stats (opacity).

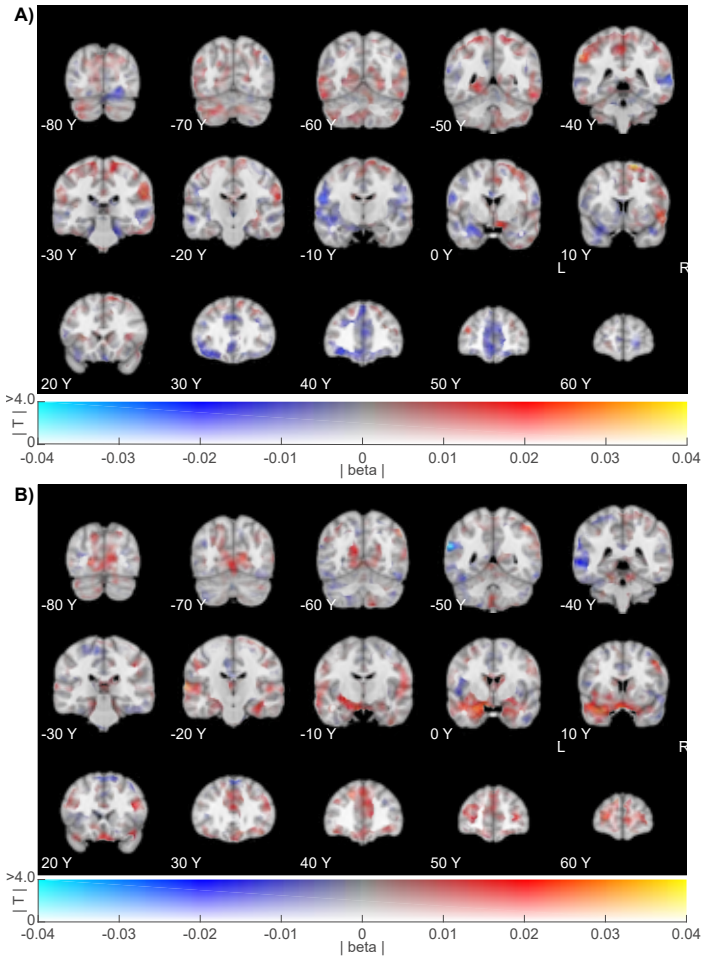

Supplementary Figure 9 | Whole brain effects for change in path distance on change in neural similarity from before to after the remapping task
(A) Effects of change in path distance on change in neural similarity from before (PVT 2) to after (PVT 3) the remapping task. No effects survived whole-brain correction.

(B) Differences between path and response learners for representing change in path distance (measured as in (A)). No effects survived whole-brain correction.

All images were created using a dual-coded design (Allen et al., 2012; Zandbelt, 2017). This allowed showing both, the mean beta coefficient (blue-red) and the T stats (opacity). Y-coordinates are in MNI space.

CHAPTER 3

Navigating our memories: how space and episodes combine in the hippocampus

This chapter is in preparation as:

A. N. de Haas, A. Nitsch, M. Garvert, L. Deuker, C. F. Doeller. Navigating our memories: how space and episode combine in the hippocampus.

.

Abstract

Spatial and episodic memory are two core forms of memory. Spatial memory allows the formation of a map-like representation of our environment, whereas episodic memory allows remembering specific events of our life. Interestingly, these seemingly different functions rely on the same brain structure: the hippocampus. So far, it remains unclear what the relationship between these two forms of memory is and how the hippocampus can support both of these functions. We tested the opposing hypotheses that the hippocampus underlies these two systems either via a common coding mechanism or via a parallel processing mechanism. To this end, we combined virtual reality and a life-simulation game with fMRI. This allowed us to simultaneously manipulate and control spatial and episodic context associations between items. Our results show an integration of spatial and episodic memory in the hippocampus. Neural adaptation effects in the hippocampus scaled with the overlapping episodic and spatial context information between items. At the same time, we found no evidence for differences between spatial and episodic memory in hippocampal subregions (neither across hemispheres, nor along the anterior-posterior axis). This is in line with the idea of a common coding mechanism and supports the notion that hippocampal processing mechanisms are not bound to one cognitive domain.

Introduction

In order to function in everyday life, we rely on our memories. Two core mnemonic systems are episodic and spatial memory. Spatial memory enables us to form a map-like representation of our environment, including the relationships among distinct locations, such as the location of our home and workplace and the possible routes between them (Epstein et al., 2017; Hartley et al., 2014; Tolman, 1948). In contrast, episodic memory allows us to remember what happened where and when during specific events, for example our last birthday party (Davachi, 2006; Tulving, 2002). Interestingly, these seemingly different functions both rely on the same brain structure: the hippocampus (Burgess, 2014; Buzsáki & Moser, 2013; Ekstrom et al., 2003; Kraus et al., 2013; Ranganath, 2010). To date, it remains elusive what the relationship between these two forms of memory is and how the hippocampus supports both of them at the same time.

Proposed hypotheses in the literature can be separated into two broad classes: the hypothesis of a *parallel processing mechanism* and the hypothesis of a *common coding mechanism.*

The main idea of a parallel processing mechanism is that neuronal populations processing episodic and spatial memory are differently distributed within the hippocampus (Burgess et al., 2002; Ezzati et al., 2016; Kühn & Gallinat, 2014; Poppenk et al., 2013). There are two prevailing ideas of how exactly representations of episodic and spatial memory are distributed within the hippocampus. Hemispheric specialization of spatial and episodic memory is one proposed parallel processing mechanism (Burgess et al., 2002; Ezzati et al., 2016; Spiers et al., 2001). According to this idea, spatial memory is related to the right hippocampus and episodic memory is associated with the left hippocampus. Another hypothesis proposes that episodic and spatial memory are differentially distributed along the longitudinal axis of the hippocampus, with processing of episodic memory located anteriorly and processing of spatial memory located in the posterior hippocampus (Hirshhorn et al., 2012; Nadel et al., 2013; Persson et al., 2018). Both ideas coincide with an extensive meta-analysis (Kühn & Gallinat, 2014). On the one hand, encoding of episodic memory is related to activity in the left hippocampus, whereas retrieval of episodic information is related to (bilateral) anterior activity. On the other hand, encoding of spatial memory is related to activity in the right hippocampus and retrieval of spatial information is related to (bilateral) posterior activity. However, this meta-analysis included experiments with either only a spatial or an episodic task – never both. Therefore, the interpretation of the results is limited due to possible systematic differences between spatial and episodic memory experiments.

An alternative view posits that the hippocampus supports a common coding mechanism of spatial and episodic memory (Bellmund, Gärdenfors, et al., 2018; Eichenbaum, 2014, 2017; Eichenbaum & Cohen, 2014; Epstein et al., 2017; Schiller et al., 2015). According to this idea, spatial and episodic memory are processed in (nearly) identical ways and hence their representations are distributed equally across the (bilateral) hippocampus. One prominent theory holds that spatial and episodic memory rely on a map like representation (often referred to as cognitive map or memory space) which holds information about transitions of either places or events/time, respectively (Behrens et al., 2018; Bellmund, Gärdenfors, et al., 2018; Eichenbaum & Cohen, 2014; Olsen et al., 2012; Stachenfeld et al., 2017). This is supported by experiments in rodents showing replay in the hippocampus for the sequences of both, recent spatial and temporal experiences (Diba & Buzsáki, 2007; Foster & Wilson, 2006). Additionally, rodent studies have demonstrated that the same hippocampal cells might code for specific points in time and in space by functioning either as time or as place cells, respectively (Eichenbaum, 2014; Kraus et al., 2013; MacDonald et al., 2011). Correspondingly, recent human neuroimaging studies showed similar effects in the hippocampus for spatial and temporal aspects of navigation (Deuker et al., 2016; Kyle et al., 2015; Nielson et al., 2015).

Determining which of these hypotheses more accurately reflects processing in the hippocampus might broaden our understanding of this brain area. Even though the hippocampus is one of the central brain areas involved in memory, many questions about its processing mechanisms remain unsolved. One core question is whether the hippocampus is a single working unit with domain-unspecific processing mechanisms (in line with the common coding hypothesis; Bellmund et al., 2018; Eichenbaum & Cohen, 2014; Epstein et al., 2017; Schiller et al., 2015) or whether it can be segregated into functional subunits or modules (in line with the parallel processing hypothesis; Burgess et al., 2002; Kühn & Gallinat, 2014; Poppenk et al., 2013). However, adjudicating between these hypotheses has been previously hindered by methodological limitations. One the one hand, spatial memory has been –historically– mainly assessed using electrophysiology in rodents (Burgess, 2014). On the other hand, episodic memory is almost exclusively investigated at the systems-level in humans, for example with hemodynamic neuroimaging techniques and lesion studies (Squire & Wixted, 2011). Studies investigating spatial memory with comparable methods have only been increasing in recent years with the introduction of virtual reality to neuroimaging (Hartley et al., 2014). It is not surprising then, that there is only a small number of studies investigating spatial and episodic memory at the same time and with the same methods (Burgess et al., 2001; Deuker et al., 2016; Dimsdale-Zucker et al., 2018; Hirshhorn et al., 2012; Kyle et al., 2015; Nielson et al., 2015). Furthermore, most of these experiments test episodic effects via the temporal relationship of events

during (passive or active) navigation (Deuker et al., 2016; Dimsdale-Zucker et al., 2018; Hirshhorn et al., 2012; Kyle et al., 2015; Nielson et al., 2015).

Here, we aim to expand these experimental approaches and compare neural processing of episodic and spatial memory in a single experiment. We not only let participants navigate in a virtual environment to test spatial memory, but also used a life-simulation game to examine episodic memory. This method has been shown to create rich episodic experiences (Collin et al., 2015). Furthermore, by using both of these techniques we were able to experimentally manipulate and control both, the episodic and spatial contexts of objects. This design is unique in that we were able to hold spatial aspects constant across different episodic contexts and vice versa, episodic aspects constant across different spatial contexts. Therefore, we could not only directly compare spatial and episodic context processing, but also assess their interaction. We used fMRI and adaptation analysis (Barron et al., 2016; Grill-Spector et al., 2006; Krekelberg et al., 2006) to investigate the effect of these manipulations on the neural representations in the hippocampus and its potential subregions (across the hemispheres and along the anterior-posterior axis). This in turn made it possible to test different predictions of the parallel processing mechanism and common coding mechanism concerning the adaptation effect for spatial and episodic context associations and the location of these changes in the hippocampus (Figure 1).

Methods

Participants

38 healthy participants were recruited to participate in the study via the university's online recruitment platform. Two participants stopped the experiment due to motion sickness after the spatial task and were not included in any analyses, resulting in a total sample size of 36 (20 women). Participants were between 19 and 32 years old (mean age= 23, sd= 3.4). At the beginning of the experiment, participants gave written informed consent to participate in the study and filled in a screening form to ensure that they did not meet any exclusion criteria for the MRI and behavioural labs. Participants were compensated at a rate of 8 Euro per hour of behavioural testing and 10 Euro per hour of MRI testing. The study was approved by the local ethics committee (CMO Regio Arnhem-Nijmegen, The Netherlands, nb. 2014/288).

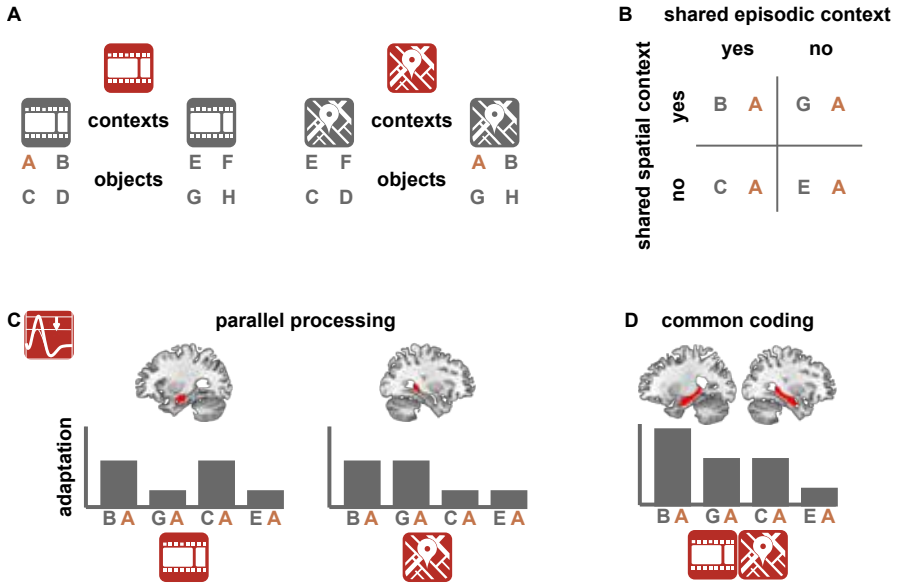

Figure 1 | Distribution of objects across task contexts and the resulting predictions of the parallel processing and common coding model

(A) Both, the episodic (represented by movie icon) and spatial task (represented by map icon) were divided into two contexts, respectively. Each regular object appeared in both tasks, but only in one episodic and one spatial context (see object A as an example). Half of all objects appeared in either context of a task.

(B) The distribution of objects across the task contexts resulted in a 2x2 design. For example, object A can be paired with an object that it shares no context with (object E), an object it shares only an episodic context with (object C), an object it only shares a spatial context with (object G) and an object it shares both a spatial and episodic context with (object B).

(C) The parallel processing model predicts a higher adaptation effect in the anterior and/or left hippocampus for pairs of objects that shared an episodic context (here in the example B-A and C-A) compared to pairs of objects that shared no episodic context (here in the example G-A and E-A). Furthermore, it predicts a higher adaptation effect in the posterior and/or right hippocampus for pairs of objects that shared a spatial context (here in the example B-A and G-A) compared to pairs of objects that shared no spatial context (here in the example C-A and E-A).

(D) The common coding model makes no predictions about subregions of the hippocampus. It predicts the highest adaptation effect in the hippocampus for pairs of objects that shared both an episodic and spatial context (here in the example B-A). Furthermore, it predicts the second highest adaptation effect for pairs of objects that shared either a spatial context (here in the example G-A) or an episodic context (here in the example

General procedure

The aim of this study was to compare neural processing of episodic and spatial memory in a single experiment (for an overview of the experimental sessions see Figure 2). We combined virtual reality and a life-simulation game to experimentally manipulate and control both, episodic and spatial context associations. We used fMRI adaptation analysis to investigate the effect of these manipulations on the neural representation in the hippocampus and its subregions (across hemispheres and along the anterior-posterior axis). As has been done before, we manipulated the relationships between objects as a proxy for spatial and episodic memory (Deuker et al., 2016). In a 2x2 design, objects were associated with one of two neighbourhoods (spatial contexts in the spatial task) and with one of two stories (episodic contexts in the episodic task; Figure 1 and Figure 3).

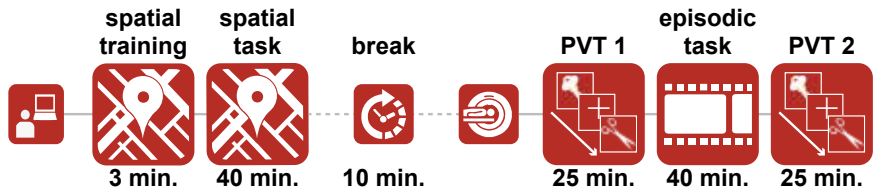

Figure 2 | Overview of experimental sessions

Participants completed one of two association tasks in a behavioural lab (here in the example the spatial task, order was counterbalanced across participants). Before entering the MRI scanner, participants were encouraged to take a 10 minute break. In the scanner, participants completed three tasks: the picture viewing task 1 (PVT 1), the second object association task (in this example the episodic task) and the picture viewing task 2 (PVT 2). Participants who completed the spatial task in the behavioural lab did the 3 minute training for the spatial task directly beforehand (as depicted in this example). Participants who completed the spatial task in the MRI scanner did the 3 minute training for the spatial task directly after the episodic task in the behavioural lab.

In total, twelve objects were presented throughout the whole experiment (for an overview of all objects see Figure 5). Eight regular objects were shown in both tasks and divided equally across the two spatial and the two episodic contexts, respectively. This resulted in four different types of pairs of regular objects, sharing either no context, only a spatial context, only an episodic context, or both a spatial and episodic context (Figure 1).

We added four control objects to the experiment (two spatial control objects and two episodic control objects). The spatial control objects appeared in both contexts of the spatial task and the episodic control objects appeared in both contexts of the episodic task, respectively. Spatial control objects would not appear in the episodic task and correspondingly, episodic control objects would not appear in the spatial task. This way the control pairs had the same number of context associations as regular pairs that shared both an episodic and spatial context. The purpose of the control objects was to

test whether any effects of the regular pairs are (purely) driven by association strength (Supplementary Figure 1). All twelve objects were randomly assigned to the conditions for each participant.

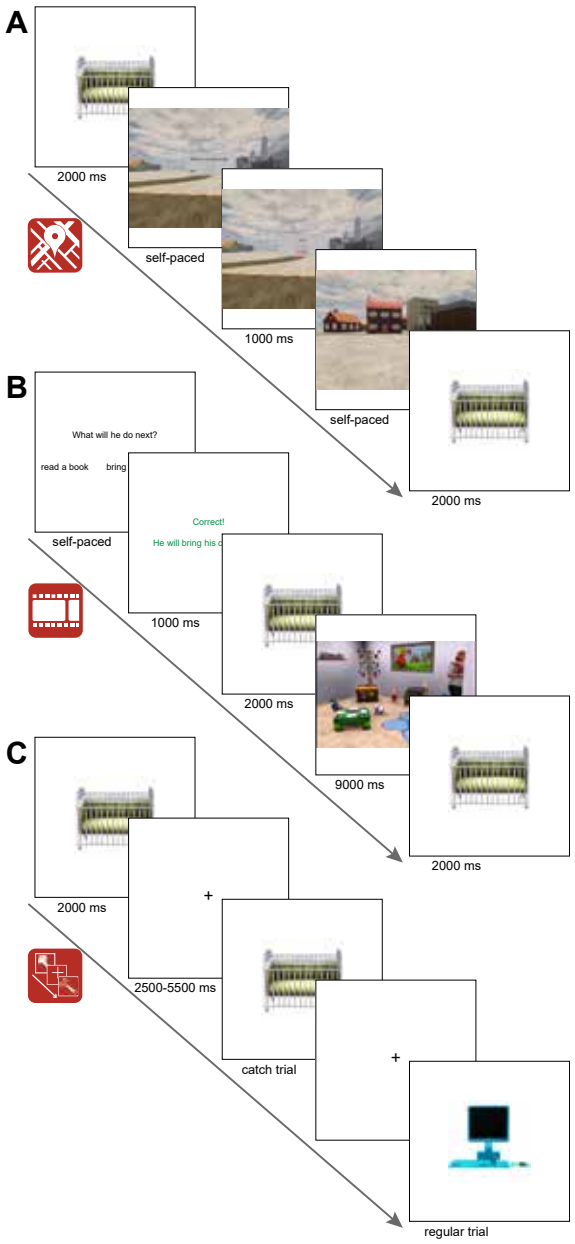

Figure 3 | Trials structure of all main tasks

(A) Trial structure of the spatial task. Participants saw one of ten objects for 2000 ms at the centre of the screen. Participants then had to indicate whether to deliver the object to the store on the left or the right of the starting warehouse (there was no time-out). After giving an answer, participants received feedback and instruction of where to deliver the object to (left or right). Participants then navigated freely to the correct location (there was no time-out). Once they arrived at the target location, the object was presented for a second time at the centre of the screen for 2000 ms.

(B) Trial structure of the episodic task. Participants needed to indicate what the next object-associated action in a current story was (there was no time-out). After giving an answer, participants received feedback and saw the correct object-associated action. The object (one out of ten possible objects) that was associated with that action appeared at the centre of the screen for 2000 ms. Then a video of the action was presented for 9000 ms. Once the video ended, the object was presented for a second time at the centre of the screen for 2000 ms.

(C) Trial structure of the picture viewing task.
Twelve different objects were presented in a random order during the PVT. Objects were presented for 2000 ms at the centre of the screen. Between object presentation a black fixation cross was presented at the centre of the screen. Duration of the fixation cross was either 2500, 4000, or 5500 ms. Participants had to press one of two buttons if the presented object was the same as the previous one (catch trial). They pressed the other button if the object was a different one from the previously presented object (regular trial). Button contingencies were randomized across participants.

We presented all twelve objects in random order after the completion of the spatial and episodic task, respectively (Figure 2 and Figure 3C). With these two picture viewing tasks (PVT) we were able to measure adaptation effects (Barron et al., 2016; Grill-Spector et al., 2006; Krekelberg et al., 2006) of spatial and episodic object associations. This enabled us to test directly different predictions of the parallel processing mechanism and the common coding mechanism (Figure 1).

Participants performed the first association task (spatial or episodic – counterbalanced across participants) in a behavioural lab. Participants completed all subsequent tasks inside the MRI scanner and were encouraged to take a 10 minute break between the behavioural and scanning session. Before entering the scanner, participants received instructions for the subsequent tasks. Participants performed three tasks in the scanner: PVT 1, the second association task and PVT 2. For the scope of this report, we only included PVT 1 and PVT 2 in the functional analyses.

Spatial task

The goal of the spatial task was to associate objects with one of two spatial contexts. For this purpose, participants had to navigate in a virtual city and deliver objects to two distinct neighbourhoods (i.e. spatial contexts). To make the neighbourhoods distinguishable, we created one with mostly skyscrapers and the other using one- and two-story houses (Figure 4).

Figure 4 | Virtual city of the spatial task

The virtual city was divided into two neighbourhoods. Two identical warehouses were located between the two neighbourhoods (marked by golden x), facing each other. Participants had to pick up objects from the two warehouses and deliver them to the correct target store. There was one target store per neighbourhood (marked by red x). Euclidean distances between both warehouses and both target stores were identical.

Importantly though, each neighbourhood had an identical looking store as a target location. Four out of ten objects had to be delivered to the store in neighbourhood A, another four to the store in neighbourhood B. There were two additional control objects, which had to be delivered to both neighbourhoods. Object-neighbourhood associations were randomized across participants. At the start of a trial, an object had to be picked up from one of two warehouses. These warehouses were located between the two neighbourhoods and had the same Euclidean distance to both target stores. On average participants needed 10.1 seconds to navigate from a warehouse to a target store (the average navigation time between either store/warehouse combination differed maximally one second from this average navigation time). Furthermore, the warehouses were facing each other. With this set up, the neighbourhood/store that was on the left side of one warehouse was on the right side of the other warehouse (for a bird's-eye view of the city see Figure 4). This allowed us to prevent associations between objects and specific actions like "going left"/"going right". Instead, the distinctive feature between objects was their spatial context, i.e. the neighbourhood. At the beginning of the task, participants had no knowledge about the specific object-neighbourhood associations and had to acquire this knowledge over the course of 96 delivery trials. A delivery trial consisted of the following steps (see also Figure 3A):

1 Picture of the current object was presented at the centre of a white screen for 2000 ms.
2 Participants were placed at one of the two warehouses and had to indicate whether the object had to be delivered to the neighbourhood that was on the left or the right side of the current warehouse. Participants could rotate but not change their location until they gave an answer via a button press (there was no time-out).
3 The given answer ("left" or "right") was highlighted for 500 ms.
4 Feedback and instructions where to go were shown for 1000 ms (e.g. "Correct! Go left" or "False! Go left."). Positive feedback was shown in green, negative feedback was shown in red.
5 Participants could freely navigate until they arrived at the correct target location. Participants received warnings in case they navigated away instead of towards the correct target store. A critical distance to trigger a warning was defined as the Euclidean distance between the warehouse and the correct target store plus a third of this distance. Two possible scenarios could trigger warnings: participant walking towards the wrong target store (warning displayed in red with correct direction, e.g. "Go left!") or by participant surpassing the target store and walking too far into the correct neighbourhood (warning displayed in red: "Too far. Go back.")
6 After walking into the target store the object counted as delivered and appeared at the centre of a white screen for 2000 ms.

Delivery trials were divided into four blocks of 24 trials. In each block, all regular objects (i.e. the eight objects only associated with one of the two neighbourhoods) were presented in two delivery trials. The two control objects were presented in four delivery trials in each block, with two trials having store A as target location and two trials with store B as target location. This allowed for all specific object-neighbourhood associations to be experienced equally often across the whole task. Furthermore, both warehouses appeared equally often as starting location in each block and for every object-neighbourhood association. Other than these restrictions, the order of object delivery trials within a block was completely randomized.
After every delivery trial, an inter-trial interval (ITI) was presented in the form of a black fixation cross at the centre of a white screen. The duration of these ITIs was jittered between one and three scanner pulses (TR was 1.5 seconds) plus 1 second. The order of the ITI-durations was pseudo-randomized in a manner that all ITIs appeared as equally often as possible for every object. Furthermore, the average ITI duration of a block was not allowed to deviate more than one standard deviation of the average ITI duration of all blocks. The purpose of these pseudo-randomizations was to ensure no temporal bias of ITI duration between objects or between task blocks.

In order to keep participants motivated, we provided them with feedback about their performance after every six trials for 5000 ms. The feedback consisted of the percentage of correct answers in the last six trials (e.g. "You scored 50% in the last block. Keep going!"). Additionally, after every block of 24 trials, participants had to perform a memory test. For each unique combination of an object and a neighbourhood, they had to indicate whether they were associated with each other (Supplementary Figure 2). All twelve objects of the whole experiment (including the two episodic control objects) appeared in the memory test, resulting in 24 memory trials. The test was completely self-paced and participants could indicate their answer by pressing one of two buttons ("yes" or "no"). Their given answer was highlighted for 500 ms. Participants received only feedback about their total score at the end of each memory test. Feedback was presented for 3000 ms and consisted of the percentage of correct answers and a motivating statement (in case of 100%: "Perfect score!"; in case of 75% and higher: "Great job! Try to get a perfect score next time."; in case of less than 75%: "Stay motivated and you can score even higher next time.").
Before the task started, we let participants navigate freely in the virtual city for 3 minutes. We wanted participants to know all main locations (warehouses and stores) and how to navigate between them before the start of the spatial task. For this purpose, traffic cones marked all main locations during the training task. To save time in the scanner, all participants performed the training task in the behavioural lab, regardless of whether a participant was in the group that performed the main spatial task in the MRI lab or in the group that performed it in the behavioural lab.

On average the spatial task took 40.0 minutes (sd= 3.6 min). The task was programmed in Unreal Development Kit 3 (Unreal Engine 3, Epic Games, Inc.).

Episodic task

The goal of the episodic task was to associate objects with one of two episodic contexts. Importantly, we tried to make the spatial and episodic tasks as comparable as possible. The general structure of the two tasks was the same in terms of number of trials & blocks, duration and pseudo-randomization of ITIs, memory tests, and intermittent performance feedback. Furthermore, akin to the spatial task, in the episodic task, the eight regular objects were divided over two episodic contexts and two control objects were associated with both episodic contexts. Here, the two episodic contexts were two stories in the life of a fictional character. Each story consisted of a sequence of six object-associated actions (e.g. the action "watching a movie" associated with the object TV; for each object-action pairing see Figure 5).

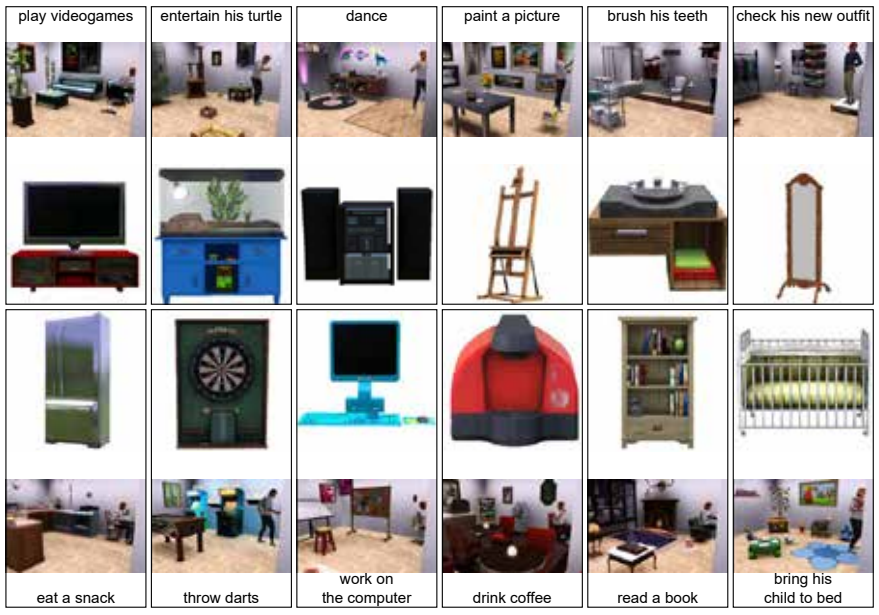

Figure 5 | Experimental objects and their associated actions in the episodic task
Twelve objects were presented throughout the experiment. These objects were: a TV, a terrarium, a stereo, an easel, a sink, a mirror, a fridge, a dart board, a computer, a coffee maker, a bookshelf and a baby bed. For each object, a video was created showing an action associated with the object. Depicted here are a screenshot of the corresponding video and the description of the action below each object. The videos were used in the episodic task.

Within a story, four actions were unique to the story (actions associated with regular objects) and two actions also appeared in the other story (actions associated with control objects). Object-story associations were randomized across participants. Participants were asked to learn the action sequence of these two stories. At the beginning of a trial, participants had to predict the following object-associated action in the sequence of a story. The object-associated actions were presented as short videos. Videos were created using the video game the Sims 3 (www.thesims3.com). Every action was filmed in the same room and from the same angle and distance to the protagonist. The physical layout (walls and floor) remained constant across all actions. However, the interior of the room was changed for every action (e.g. interior of a living room, when the action was watching a movie vs. interior of a kitchen, when the action was making a meal; for a screenshot of each video see Figure 5). As a cover story, we told the participants that they were watching two plays, taking place on the same stage. Furthermore, we made sure that the objects were never displayed in the videos. This was done to match the episodic task to the spatial task (objects are also never seen during the navigation phase in the spatial task). To achieve this, we placed all objects at the same location behind a visible wall and participants were instructed about this location. Furthermore, all actions of the fictional character were performed at the same location in front of the objects (meaning videos displayed the fictional character from the side and never from the front). This allowed us to keep the spatial aspect constant across stories. The aim was that the distinct feature between objects was the episodic context, i.e. the story. At the beginning of the task, participants had no knowledge about the specific object-story associations and had to learn them through the prediction trials. A prediction trial consisted of the following steps (see also Figure 3B):

1 Participants had to answer what the fictional character will do next ("What will he do next?"). Two possible answers were displayed on the screen; the correct action and a foil action. The question was displayed until participants gave an answer (there was no time-out).
2 The given answer was highlighted for 500 ms.
3 Feedback and the correct action were shown for 1000 ms (e.g. "Correct! He will read a book" or "False! He will read a book."). Positive feedback was shown in green; negative feedback was shown in red.
4 Picture of the object associated with the action (e.g. bookshelf) was presented at the centre of a white screen for 2000 ms.
5 A video was displayed showing the action for 9000 ms. The duration was chosen to approximately match the time needed for the navigation phase in the spatial task (based on pilot data).
6 Picture of the object associated with the action (e.g. bookshelf) was presented for a second time at the centre of a white screen for 2000 ms.

Akin to the spatial task, the episodic task was divided into four blocks. In each block, both stories were presented twice (six trials per story, resulting in 24 trials per block). The order of stories was pseudo-randomized, so that both stories appeared in the first and second half of a block. Both stories had a label ("Story 1" or "Story 2"), which was shown at the beginning of a story for 1500 ms at the centre of the screen.

During prediction trials participants had to choose between the correct action in the story sequence and a foil action. The side of the screen on which the correct action was displayed (i.e. the appropriate button response) was pseudo-randomized, so that it appeared equally often on either side of the screen within a block. The foil action was an action that also appeared in either story. We pseudo-randomized the foil actions in a manner that all actions appeared as equally often as possible as answers across the whole task. Actions associated with control objects were less likely chosen as foil answer because they appeared twice as much as correct answers than actions associated with regular objects. Furthermore, for each action every potential foil answer occurred as equally often as possible.

After every prediction trial a fixation cross was presented at the centre of a white screen. The durations of these ITIs and their pseudo-randomization were identical to the ITIs of the spatial task.

To keep participants motivated, we provided them with feedback about their performance after every story for 5000 ms. The feedback consisted of the percentage of correct answers in the last story (e.g. "You scored 50% in the last block. Keep going!"). Furthermore, after every block of four stories, participants had to perform a memory test. The memory test was identical to the spatial memory tests. The only difference was that participants had to indicate whether an object belonged to a certain story in place of a neighbourhood (Supplementary Figure 2).

On average the whole task took 40.0 minutes (sd= 1.9 min). The task was programmed in and presented with neurobs Presentation (version 16.4, www.neurobs.com/presentation).

Picture viewing task

Participants completed two identical PVTs in the MRI scanner, one after each association task, respectively. Participants were told that they would see a stream of objects. To ensure that participants paid attention to the objects, they had to do a 1-back task, comparing the current object to the preceding one (Figure 3C). Participants had to press one of two buttons if the current object was the same as the preceding one (catch trials) and the other button if the objects were not the same. Button contingencies were randomized across participants, but were always done with the right index and middle finger. This 1-back task was orthogonal to later analyses of the PVTs. Participants

performed high on the cover task in both PVTs (PVT 1: mean= 87.4%, sd= 17.7, PVT 2: mean= 91.9%, sd= 14.9).

The twelve objects from the spatial and episodic association tasks were presented during the PVT at the centre of a white screen. Pictures of the objects had a pixel size of 512 by 512. Each PVT consisted of 208 trials with a trial duration of 2 seconds (Figure 3C). The order of the objects was pseudo-randomized across participants. However, the order of objects in PVT 1 and PVT 2 was identical for each participant. Each PVT was divided into four blocks of 52 trials. After each block, participants had a 20 second break, in which they received feedback about their performance on the previous block and a reminder of the button-contingencies. 24 of the 208 trials were catch trials (self-repetitions, around 11.5% of all trials) and these trials were evenly distributed across the twelve different objects (two per object) and the four blocks (six per block).

We pseudo-randomized the order of the object presentation with the purpose to maximize power for the adaptation analysis. Here, the idea was that the higher the overlap of neural code between the preceding object and the current object, the greater the suppression of the BOLD activity evoked by the current object presentation (Barron et al., 2016; Grill-Spector et al., 2006; Krekelberg et al., 2006). Hence, we ensured that all objects were preceded by all other objects they formed a relevant pair with. We split each of the four PVT blocks into regular object trials and control object trials (first 33 non-catch trials only showed the eight regular objects, last 13 non-catch trials only showed the four control objects). This allowed us to have the maximum number of relevant object transitions, as we were not interested in adaption effects between regular and control objects. For the regular objects, we had four different types of object pairs, sharing: no context, only a spatial context, only an episodic context, sharing both a spatial and episodic context. We pseudo-randomized the order so that all types of object pairs preceded each other equally often in each block (eight times per type of object pair). Furthermore, all regular objects appeared four times in each block. For each type of object pair, each possible combination of objects preceded each other as equally as possible across the whole task and within a block (maximum differences in combinations within type of object pairs in each block was 1). Lastly, for each object pair, either object was the preceding one in two out of the four blocks, respectively. There were three different types of object pairs for control objects, sharing: two episodic contexts, two spatial contexts or no contexts. Each type of control pair preceded each other four times during a block. Each control object appeared three times during a block. The rest of the pseudo-randomization was analogous to the pseudo-randomization of the regular objects.

After every object presentation, a black fixation cross appeared at the centre of the screen (fixation cross was presented as text object with a font size of 20). The duration of these ITIs was jittered between one and three scanner pulses (TR was 1.5 seconds)

plus 1 second. The order of the ITI-durations was pseudo-randomized in a manner that all ITIs appeared as equally often as possible across all non-catch trials of an object (the ITI of a catch trial was randomly chosen). Furthermore, the average ITI duration of a block was not allowed to deviate more than one standard deviation of the average ITI duration of the whole PVT. The purpose of these pseudo-randomizations was to ensure that there was no temporal bias of ITI duration between objects or within the PVT.

The task was programmed in and presented with neurobs Presentation (version 16.4, www.neurobs.com/presentation).

MRI Image acquisition

Functional T2*-weighted and anatomical images were acquired on a Magnetom Prisma 3 Tesla magnetic resonance tomograph (Siemens, Erlangen, Germany) with a 32-channel head coil. Functional images were acquired with a 4D multiband sequence with 84 slices (multi-slice mode, interleaved), TR= 1500 ms, TE= 28 ms, flip angle= 65 deg, acceleration factor PE= 2, FOV= 210 mm and an isotropic voxel size of 2 mm. An anatomical image of the brain was acquired, using a T1 sequence (MPRAGE) with TR= 2300 ms, TE= 3.03 ms, flip angle= 8 deg, FOV= 256 x 256 x 192 mm and an isotropic voxel size of 1 mm. If a time limit of 2 hours was not reached yet at the end of the scanning session, two separate phase and magnitude images were acquired in order to correct for distortions with a gradient field map (multiband sequence with TR= 1020 ms, TE= 10 ms, flip angle= 45 deg, and a voxel size of 3.5 x 3.5 x 2.0 mm).

fMRI preprocessing

Functional images of the two functional runs (one per PVT) were preprocessed with help of the FSL toolbox (version 5.0.4, http://fsl.fmrib.ox.ac.uk/fsl/fslwiki/). Motion correction and a high pass filter (cut-off: 100 s) were applied to the images. The anatomical scan of each participant was downsampled to the voxel size of the functional scans (2 mm isotropic). In order to have a common reference space for the first-level analysis, both functional scans were linearly registered to the downsampled anatomical scan. After preprocessing, the functional output of each run was visually examined for artefacts (e.g. distortions throughout the whole brain). Volumes that had artefacts or/and exceeded a movement cut-off of 3 mm were taken into account in later first-level GLMs with a volume-specific regressor (on average 6.2 volumes affected per run, sd= 11.7). This was additional to the six movement parameters we included into all first-level GLMs. After preprocessing, we excluded participants from further analysis of a functional run based on the following criteria: 1. Mistakes during recording or incomplete log files (one participant excluded from PVT 2). 2. No appropriate responses during the PVT (minimum inclusion criteria was pressing both possible buttons, no participant was excluded). 3. A memory score under 60% at the end of an association

task. All PVTs after the memory test were excluded (one participant excluded from PVT 2). 4. More than 10% of the volumes of a functional run had to be excluded/regressed out due to movement and/or artefacts (one participant excluded from PVT 1, and four participants excluded from PVT 2). Taken together, 35 participants were included for PVT 1. Here, 20 participants completed the episodic task first and 15 the spatial task first. For PVT 2, 30 participants were included.

First-level analyses

As mentioned earlier, we used adaptation analysis to measure the effect of episodic and spatial context associations between pairs of objects. Adaptation analysis leverages repetition suppression. Repetition suppression refers to the effect that the preceding item can alter the univariate activity evoked by the current item. In more detail, activity is suppressed in areas that encode overlapping representations between the preceding and the current item (Barron et al., 2016; Grill-Spector et al., 2006; Krekelberg et al., 2006). Expanding on this, during our PVTs we expected that the suppression of univariate activity of an object scales with the spatial and/or episodic representation it shares with the preceding object. This allowed us to test different predictions from the common coding model and parallel processing model during PVT 1 and PVT 2 (Figure 1).

Testing the common coding model

Predictions from the common coding model are most effectively tested in PVT 2. In line with the model, we would expect the highest adaptation effect (in the hippocampus) for pairs of objects that share both a spatial and episodic context. We then would expect the second highest adaptation effect for pairs of objects that share one of the contexts and the lowest adaptation effect for pairs of objects that share no context (Figure 1). We weighted all three categories of pairs of objects accordingly in the first-level GLMs. In more detail, the weights before demeaning were set to 2 for pairs of objects that shared no context, to 3 for pairs of objects that shared one context and to 4 for pairs of objects that shared both a spatial and episodic context. We used control objects to also test for general effects of association strength. Control objects occur as often together as pairs of objects that share both, a spatial and episodic context (in either the spatial or the episodic task). In our control model the weight of pairs of control objects of the same task corresponded to the weight of pairs of regular objects sharing both, a spatial and an episodic context (i.e. regular pairs of objects with the same association strength). Furthermore, the weight of pairs of control objects that share no context corresponded to the weight of pairs of regular objects sharing no context (i.e. regular pairs of objects with the same association strength). To take a closer look at overlapping effects of space and episode in PVT 2, we created functional ROIs based on the effects of pairs of objects that shared only an episodic or only a spatial context, respectively. We based

these ROIs on the pair-wise GLM (see below), in which we contrasted these 'spatial' and 'episodic' object pairs with pairs of objects that shared no context, respectively. For either ROI, the voxel-wise output in the hippocampus was threshold at $p_{uncorr.} < 0.01$. We then tested for an effect of the spatial contrast in the episodic ROI and vice versa.

For PVT 1, we tested the assumption that pairs of objects that share a context have a more similar representation and therefore higher adaptation in the hippocampus than pairs of objects that share no context. Importantly, in this model, we did not differentiate between the group of participants that completed the spatial task at this point from the group of participants that completed the episodic task. As a control, we also tested whether there is any evidence that either (the spatial or episodic) group could drive such an effect, by testing for significant differences between them.

Testing the parallel processing model

Predictions from the parallel processing model are most effectively tested in PVT 1. At this point, there are no possible interactions between the spatial and episodic task because participants have only completed one of the two tasks, respectively. The general model is the same as for the common coding model (higher adaptation for pairs of objects sharing a context vs. no context). However, here we assume that there is an interaction between the subregions of the hippocampus and the two groups (Figure 1). More specifically, here we test for differences between the two groups along the anterior-posterior axis and the hemispheres (left vs. right) of the hippocampus.

For PVT 2, testing differences between spatial and episodic processing is preferably done by comparing pairs of objects that only share a spatial context and pairs of objects that only share an episodic context. In contrast, pairs of objects that share both, an episodic and spatial context are not ideal to test for pure spatial or pure episodic effects.

For all our analyses, we set up two different GLMs: object-wise and pair-wise. In short, the object-wise GLM models the relationship of each object with every other object within an object-specific regressor and therefore we can only look at the output of a main effect of episodic and spatial context association. The pair-wise GLM, on the other hand models each specific object pairs separately and therefore we can categorize regressors of specific object pairs based on their spatial and episodic association (for more information see below). Because we cannot disentangle different categories of pairs of objects in the object-wise GLMs, we took advantage of the pair-wise GLM. Here, we could directly compare whether there is an interaction between the subregions of the hippocampus and episodic and spatial object pairs. More specifically, here we tested for differences between pairs of object that share a spatial context and pairs of objects that share an episodic context along the anterior-posterior axis and the hemispheres (left vs. right) of the hippocampus. Next to this main analysis, we wanted to maximize power and repeated the analysis with all pairs of objects. Again, we tested

for an interaction between subregions of the hippocampus, but this time with all four object categories.

General set up of GLMs and ROI analyses

In general, we used two different types of GLMs to measure the adaptation effect: one with object-based regressors and one with pair-based regressors. The object-based GLMs have the following general set-up: A parametric regressor per object is used to measure the adaptation effect. This parametric regressor weights the onsets (and duration) of all regular trials by the relationship the current object has to the object of the preceding trial (weight depending on predicted relationship by either parallel processing model or common coding model, as described above). Furthermore, to account for general effects of the object presentation, all onsets and duration of regular trials are modelled in a separate regressor for each object. Each parametric regressor is demeaned, in order to orthogonalize it to its corresponding onset regressor. To estimate the adaptation effect for each participant, all parametric regressors of regular or control objects are included in a contrast (set to one). The main advantage of the object-based GLMs is that any general object presentation effects are accounted for by the onset regressors and cannot be explained by the parametric regressor.

However, this type of GLM loses information about the specific effects of different pairs of objects (e.g. the specific effect of pairs of objects that share an episodic context). Therefore, we also used pair-based GLMs, with the following general setup: Each possible pair of regular objects and of control objects is modelled in a separate onset regressor. For example, for pair A-B the regressor models the onset and duration of every trial that object B is presented under the condition that it was directly preceded by object A. To estimate the adaptation effect for each participant, all onset regressors of pairs of interest are included in a contrast and weighted by the relation of the pair (weight depending on the model). The main disadvantage of this type of model is that it cannot account for any general effects of the object presentations. Therefore, we used the pair-wise GLMs mainly to validate and visualize the results of the object-wise GLMs (if otherwise, it will be stated).

In both types of GLMs, we modelled all other events of the PVT with separate regressors. We added one regressor per object for its catch trials (self-repetition). Both types of button presses were modelled separately with a stick duration. The beginning of the task was modelled with the duration from start time of scanning until the first object presentation. The end of the task was modelled with the duration from the end of the last object presentation until end of scanning. Lastly, all block breaks were modelled in one onset regressor with the duration from the end of the last object presentation before the break until the first object presentation after the break.

We spatially normalized the relevant outputs from both types of GLMs (contrast estimates and/or parameter estimates) to MNI anatomical space and afterwards smoothed them using a 6 mm full-width at half maximum Gaussian kernel.

For the ROI analyses of the object-wise GLMs, we used the spatially normalized voxel-wise output of the contrast estimate(s). We then calculated for each participant the mean contrast estimate across all ROI voxels. For the ROI analyses of the pair-wise GLMs, we used the spatially normalized voxel-wise output of the relevant parameter estimates. We then calculated the mean parameter estimate across all ROI voxels for each participant. To account for any general effects of the presentation of a specific object, we first sorted all parameter estimates by their specific object successor (so every parameter estimate where object A is followed by any other object). Then, we demeaned each set of parameter estimates. Importantly, we had two parameter estimates per object pair (A followed by B and B followed by A). We took the average of these two ROI parameter estimates to have a single estimation of the effect per pair. To estimate the effect of a model (e.g. pairs of objects that share a context vs. no context) for every participant, we entered these parameter estimates per pair into a linear regression. We also grouped parameter estimates by category (e.g. sharing an episodic context) and calculated the mean for visualizing purposes. Both, the output of the category mean and the output from the linear regression were used in second level analyses of the ROI.

Second-level analyses

For the ROI analyses of the common coding model, we used a one-sample t-test for the main analyses and a two-sample t-test (episodic vs. spatial group) for the control analyses of PVT 1 (because the model predicts direction of the effect, we tested one-sided). For the ROI analyses of the parallel processing model, we used a 2x2x2 repeated measurement ANOVA. For both PVT 1 and PVT 2 we tested for the within-subject factors axis (anterior vs. posterior) and hemisphere (left vs. right). For PVT 1, we added the between-subject factor group (episodic vs. spatial). For PVT 2, we added the within-subject factor shared context (episodic vs. spatial). As mentioned above, we repeated this analysis for PVT 2 with the within-subject factor object pair category (no context shared, episodic context shared, spatial context shared, episodic and spatial context shared).

If we found ROI effects, we performed post-hoc voxel-wise analyses within the ROIs to visualize possible seed locations of these effects.
For the whole-brain analyses and voxel-wise analyses within the ROIs we used one-sample and two-sample permutation tests. Output images from the first level analyses were entered as input. We also included either a whole-brain mask or a ROI mask,

which only included voxels where all participants had an entry. For the permutation tests, 10000 random sign flips were performed to estimate the null distribution. We used threshold-free cluster enhancement and corrected for multiple comparison with family-wise error rate ($p_{FWE} < 0.05$).

Anatomical regions of interest

We used a bilateral hippocampal mask, provided by the WFU pickatlas (Maldjian et al., 2003). We created ROIs for the left and right hippocampus separately, as well as the anterior and posterior subregion. Following Collin et al. (2015) and Theves et al. (2019), the posterior portion of the hippocampus ranged from Y= −40 to −30 and the anterior portion of the hippocampus ranged from Y= −18 to −4 (ROI masks are shown in Figure 1C and D).

Results

Evidence for common coding in the hippocampus

We set out to investigate whether spatial and episodic memory are represented similarly in the hippocampus according to a common coding model. To this end, we tested in our first main analysis whether adaptation in the hippocampus scaled with the spatial and episodic context associations between object pairs (no context shared, one – spatial *or* episodic context shared, both – spatial *and* episodic context shared) after participants performed both, the spatial and episodic task (Figure 1D). In line with this prediction, we found that neural activity in response to an object decreased in the (bilateral) hippocampus ROI in relation to its context association with the preceding object as predicted by the common coding model ($T_{(29)} = -2.5919$, p= 0.007; Figure 6A & B). Figure 6A depicts the main effect of the common coding model described here (i.e. the effects of the object-wise regressors modelling the spatial and episodic context associations). Figure 6B depicts the effects split for each type of object pair from our secondary control analysis based on the pair-wise regressors (see below).

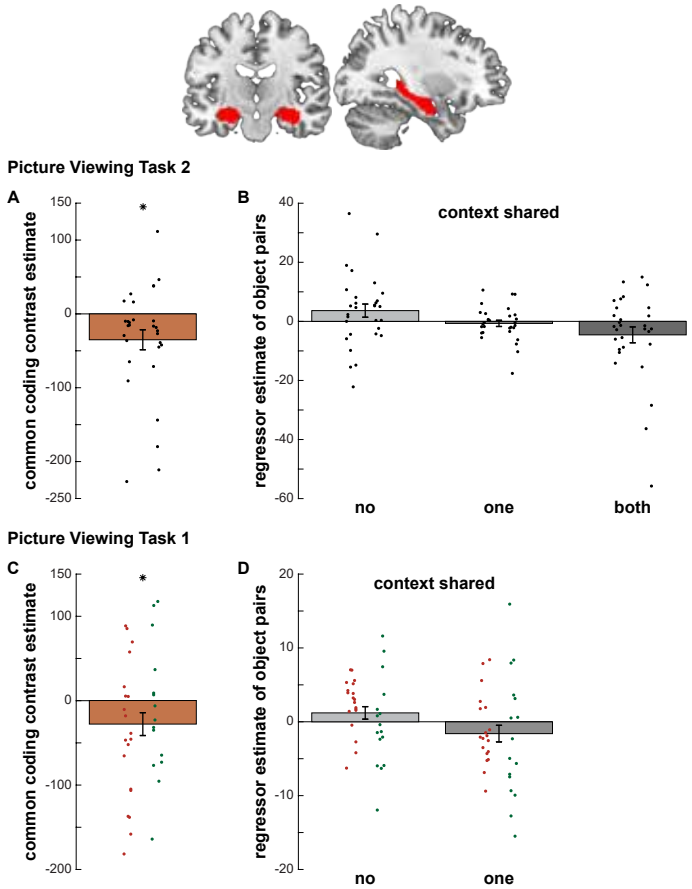

Figure 6 | Common coding in the hippocampus
(A) Contrast estimate of common coding effect in the hippocampus during PVT 2 ($T_{(29)}$= -2.8820, p= 0.0037). At this point participants had completed both, the spatial and episodic task. The contrast is based on common coding model which predicts an adaptation effect that scales with the context associations between object pairs (no context shared, one (spatial or episodic) context shared, both (episodic and spatial) contexts shared).

(B) Visualization of effect from (A). Depicted are the mean estimates of object pairs regressors, separately for pairs sharing no context, one (separately for spatial and episodic) context, and both (spatial and episodic) contexts.

(C) Contrast estimate of common coding effect in the hippocampus during PVT 1 ($T_{(34)}$= -2.2586, p= 0.0152). At this point participants had completed either the spatial or the episodic association task. The contrast is based on common coding model which predicts a higher adaptation effect for object pairs sharing a context than objects sharing no context (regardless of spatial or episodic context).

(D) Visualization of effect from (C). Estimates of object pairs regressors, divided by pairs sharing no context and one (spatial or episodic) context.

Dots represent single participant values. If applicable, red dots on the left side of the error bar represent participants that completed the episodic task first. If applicable, green dots on the right side of the error bar represent participants that completed the spatial task first. Error bars show the standard error of the mean. Asterisk symbolizes a significant effect (p< 0.05).

Our second main analysis tested whether we could already see supporting evidence after participants had only completed one (the spatial or episodic) task. Here, we expected a higher adaptation effect in the hippocampus for pairs of objects that shared a context (space or episode) than for pairs of objects that shared no context. According to the common coding model, this effect should be irrespective of which task a participant had completed. As expected, we found that neural activity in response to an object decreased more in the hippocampus when it was preceded by an object it shared a context with compared to an object it shared no context with ($T_{(34)}$= -2.0623, p= 0.023; Figure 6C & D). Importantly, we performed a post-hoc control analysis, showing that there was no significant difference between participants having completed the episodic task and participants having completed the spatial task ($T_{(33)}$= -0.9367, p= 0.36).

As the spatial and episodic relationship between objects scaled with the number of context associations (no, one and two), we controlled whether association strength drives the effect for a common coding model. To this end, we tested the adaption effects of pairs of control objects. Control objects either share two context association in the same task (space or episode) or no context association. Accordingly, if association strength drives the effect, control pairs with two context associations should have a higher adaption effect than control pairs that have no context associations. However, we found no significant evidence for an effect of association strength in the hippocampus, for neither PVT 1 ($T_{(34)}$= -0.3450, p= 0.37), nor PVT 2 ($T_{(29)}$= -0.8025, p= 0.21). Furthermore, the mean adaption effect for a common coding mechanism during PVT 2 in the hippocampus was significantly greater than the mean adaption effect for control objects ($T_{(29)}$= -2.3420, p= 0.026). The comparison between the mean adaptation effect for regular objects and control objects during PVT 1 reached trend level ($T_{(34)}$= -1.7857, p= 0.083).

To validate our results, we repeated our analyses in a secondary analyses with the pair-wise GLM (see Methods for details). In short, here we modelled every object pair in a separate regressor and then contrasted these regressors by scaling their weight with their spatial and episodic relationship (no context association, one – spatial *or* episodic context shared, spatial *and* episodic context shared). In line with our previous results, we found a significant effect for the common coding model in the hippocampus during PVT 2 ($T_{(29)}$= -1.9612, p= 0.030). For PVT 1, we found a trend effect in the hippocampus ($T_{(34)}$= -1.4240, p= 0.082).

The approach of the pair-wise GLM allowed us to specifically take a closer look at the pairs of objects that share either a spatial or an episodic context. According to the common coding model, the adaptation effect in the hippocampus should be comparable

between these two categories of object pairs. Therefore, we performed additional post-hoc analyses in which we created functional ROIs in the hippocampus, based on the adaptation effect of 'spatial' object pairs (contrast of object pairs that share a spatial context with pairs of objects that share no context) and 'episodic' object pairs (contrast of object pairs that share an episodic context with pairs of objects that share no context). We included voxels in either ROI that met the threshold of $p_{uncorr.} < 0.01$. We then used the 'spatial' ROI to test for an episodic adaptation effect and vice versa. Our results indicate that there is at least partial overlap between both effects. We found a significant 'spatial' effect in the episodic ROI ($T_{(29)} = -3.1938$, $p = 0.002$), whereas the episodic effect in the spatial ROI was approaching trend level ($T_{(29)} = -1.2994$, $p = 0.102$).

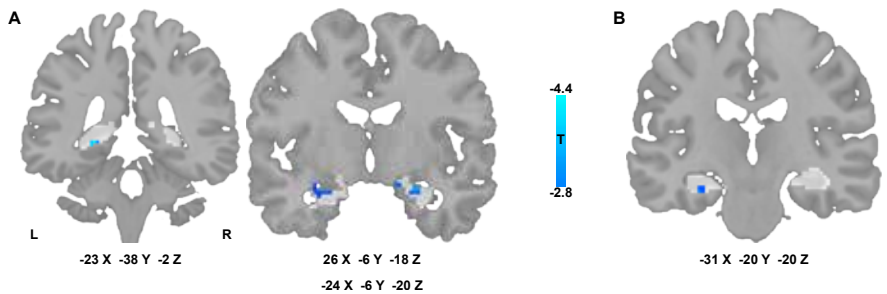

Figure 7 | Voxel wise effect of common coding in the hippocampus
(A) Negative modulation of activity in the hippocampus by context associations between object pairs (sharing no context, sharing one (episodic or spatial) context, sharing both, an episodic and a spatial context) PVT 2. At this point participants had completed both, the spatial and episodic association task. Clusters depicted are statistically significant after correcting for multiple comparisons using small volume correction ($p_{FWE} < 0.05$, left posterior peak $T_{(29)} = -4.323$, right anterior peak $T_{(29)} = -3.873$, left anterior peak $T_{(29)} = -3.425$), but image is thresholded at $p_{uncorr.} < 0.001$ for visualization. Coordinates for the peak voxels are given in MNI space. Image is masked for hippocampal voxels.

(B) Negative modulation of activity in the hippocampus by context associations between object pairs (sharing no context or sharing one (episodic or spatial) context) during PVT 1. At this point participants had completed one association task – either the spatial or the episodic association task. Cluster depicted is thresholded at $p_{uncorr.} < 0.001$, the peak was approaching small volume corrected significance (left anterior peak $p_{FWE} = 0.055$, $T_{(29)} = -3.579$). Coordinates for the peak voxel are given in MNI space. Image is masked for hippocampal voxels.

We were mainly interested in hippocampus effects on an ROI level. However, we performed post-hoc voxel-wise analyses within the hippocampus in order to visualize (potential) seed locations of the ROI effects. The strongest effects of PVT 2 were located in the left posterior and bilateral anterior hippocampus (all peak voxels $p_{FWE} < 0.05$, Figure 7A). The strongest effect of PVT 1 was located in the anterior, bordering middle left hippocampus (peak voxel $p_{FWE} = 0.055$, Figure 7B). Furthermore, we checked for peak locations for the spatial and episodic group separately. Neither group had a significant cluster in the hippocampus ($p_{FWE} > 0.05$); however for both groups the overall

peak cluster was located in the left hippocampus. While the episodic peak was clearly anterior, the spatial peak was bordering between the anterior and middle part of the hippocampus (peak spatial group: -29x -19 y -18z MNI space, $T_{(14)} = -2.972$, peak episodic group: -32x -9 y -26z MNI space, $T_{(19)} = -3.701$, Supplementary Figure 3).

Taken together, we found evidence for a common coding mechanism after participants completed both, the spatial and episodic task. Furthermore, we see a general effect of context association after participants only completed one of the two tasks. We did not find any evidence that this effect was driven by participants that completed the spatial task or by participants that completed the episodic task at this point.

No evidence for parallel processing in the hippocampus

To test our alternative account, we set out to investigate whether spatial and episodic memory are represented differently in hippocampal subregions according to a parallel processing model. To this end, we specifically tested for a difference in processing spatial and episodic context associations between the left and right hippocampus and/or the anterior and posterior hippocampus. Accordingly, we split the participants into a spatial and an episodic group after they completed (only) the corresponding task. Here, we expected an interaction of adaptation effects (pairs of objects sharing a context vs. no context) between group and hippocampal subregions during PVT 1 (Figure 1). We found no interactions between the groups and hemisphere ($p = 0.39$), anterior-posterior axis ($p = 0.34$), or hemisphere and anterior-posterior axis of the hippocampus ($p = 0.30$, Supplementary Figure 4).

To further investigate a possible parallel processing mechanism in the hippocampus, we tested for differences between spatial and episodic context associations after participants completed both (the spatial and episodic) task. For this purpose, we contrasted adaption effects for pairs of objects that (only) shared a spatial context with pairs of objects that (only) shared an episodic context. Here, we expected an interaction effect between the type of context association (spatial vs. episodic) and hippocampal subregions. We found no significant interactions for object pairs that shared (only) a spatial context vs. object that shared (only) an episodic context with hemisphere ($p = 0.53$), anterior-posterior axis ($p = 0.41$) or hemisphere and anterior-posterior axis of the hippocampus ($p = 0.59$, Supplementary Figure 5). As noted above, we only used two of the four possible categories of object pairs for this analysis, as it allowed contrasting spatial and episodic effects most clearly. However, to maximize power, we repeated our analysis with all four categories of object pairs (Figure 1). Again, we found no significant interactions of object category with the hemisphere ($p = 0.835$), anterior-posterior axis ($p = 0.21$) or hemisphere and anterior-posterior axis of the hippocampus ($p = 0.99$). Taken together, we found no supporting evidence for a parallel processing mechanism in the hippocampus.

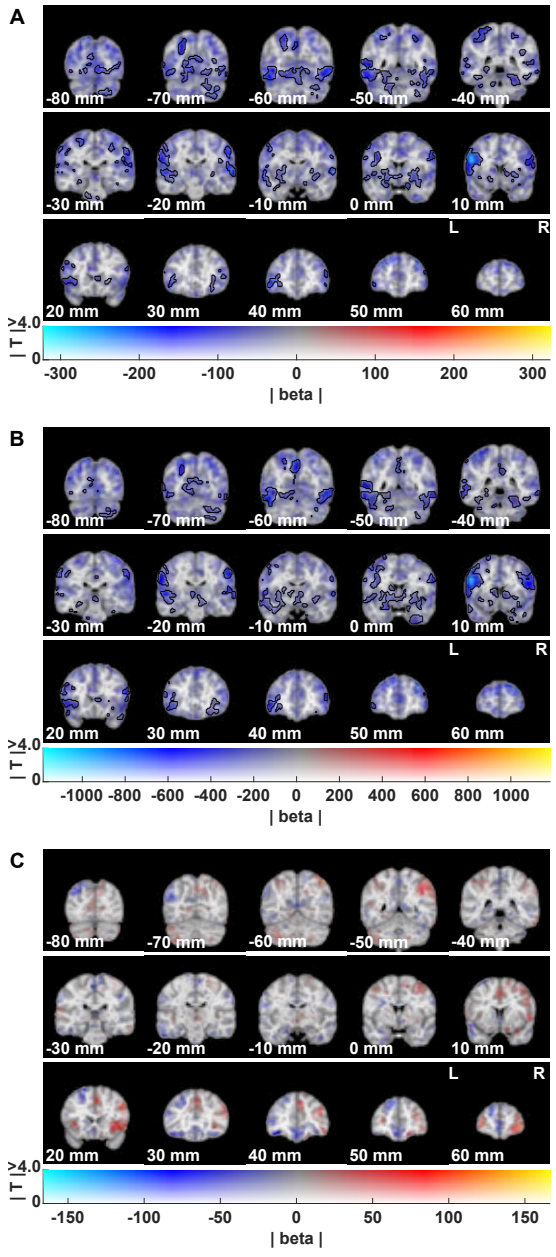

Figure 8 | Whole-brain results for common coding of spatial and episodic context associations during PVT 2

(A) Modulation of activity by spatial and episodic context associations between object pairs (no context shared, one (episodic or spatial) context shared, both episodic and spatial context shared) during picture viewing task 2. Data were modeled with an object-wise GLM. Effects that survived whole-brain correction are marked by black edges.

(B) Same modulation depicted as in (A), but here data were modeled with a pair-wise GLM. Effects that survived whole-brain correction are marked by black edges.

(C) Modulation of activity by strength of context association between control pairs (no shared context vs. sharing both task contexts –either spatial or episodic) during picture viewing task 2. Data were modeled with an object-wise GLM. No effects survived whole-brain correction.

All images were created using a dual-coded design (Allen et al., 2012; Zandbelt, 2017). This allowed showing both, the mean beta coefficient (blue-red) and the T stats (opacity). Y-coordinates are in MNI space.

Evidence for common coding, but not parallel processing on whole-brain level

Even though our key predictions were based on the hippocampus, we extended our analyses to the whole-brain level. In other words, we explored the neural differences and similarities in the processing of spatial and episodic context associations beyond the hippocampus.

Several clusters showed a significant adaptation effect that scaled with the combined spatial and episodic context associations during PVT 2, reaching from temporo-parietal regions to the frontal lobe (for non-thresholded map see Figure 8A). To validate our results, we repeated our analyses with the pair-wise GLM (for non-thresholded map see Figure 8B).

Clusters surviving correction for multiple comparisons largely overlapped with the initial results (see Supplementary Table 1 for a list of clusters that survived correction in both types of GLMs). However, we found no significant effect for control objects during PVT 2 (p_{FWE}> 0.05, for non-thresholded map see Figure 8C). We found no significant adaptation effect of a common coding mechanism for regular or control objects during PVT1 (p_{FWE}> 0.05, for non-thresholded map see Supplementary Figure 6).

We found no significant difference between participants that had completed the spatial task first and participants that had completed the episodic task first during PVT1, neither for regular nor control objects (p_{FWE}> 0.05, for non-thresholded map see Supplementary Figure 7A & B). For PVT 2, contrasting pairs of objects that only shared a spatial context with pairs of objects that only shared an episodic context also yielded no effect surviving correction (p_{FWE}> 0.05, for non-thresholded map see Supplementary Figure 7C). Neither did the comparison of spatial control objects with episodic control objects (p_{FWE}> 0.05, for non-thresholded map see Supplementary Figure 7D).

Participants learned spatial and episodic context associations at ceiling level

We designed the spatial and episodic task with the goal that participants form strong object-context associations. This goal was achieved, as participants remembered context associations of regular objects at ceiling level, at the end of both the episodic (mean= 99.48%, sd= 2.30) and spatial task (mean= 97.50%, sd= 8.99). Participants remembered the context associations of control objects at ceiling after the episodic task (mean= 99.31%, sd= 2.90) and very well after the spatial task (mean= 88.93%, sd= 19.83; for all mean memory scores of all blocks see Figure 9A). Nevertheless, on average participants seemed to reach ceiling performance in the episodic task in earlier memory blocks than in the spatial task (there was a significant task*memory block interaction for regular objects $F_{(2.04,\ 69.40)}$= 3.919, p= 0.024 and control objects $F_{(2.27,\ 77.21)}$= 13.702, p< 0.001).

Figure 9 | Recall of context associations of objects during the episodic and spatial task
(A) Mean percentage of correct memory trials in the memory test after each task block. During a memory trial, participants had to indicate whether an object belonged to a context. Scores are split for the episodic and spatial task and for regular and control objects.

(B) Mean percentage of correct prediction trials during each task block. During a prediction trial in the episodic task, participants had to predict which object-associated action appeared next in the story. During the spatial task, participants had to predict to which neighbourhood they had to deliver the current object. Scores are split for the episodic and spatial task and for regular and control objects. Scores for the spatial control objects are not displayed because both possible context (neighbourhood) predictions were equally true.

Dots represent single participant values. Error bars show the standard error of the mean. The line at 50% marks chance level.

Additional evidence for strong object-context associations came from participants' performance during the spatial and episodic task. Participants performed at ceiling during the prediction trials in the final block of both the episodic (regular objects: mean= 98.61%, sd= 3.03; control objects: mean= 98.96%, sd= 3.50) and spatial task (regular objects: mean= 94.11%, sd= 11.34). Note, that we did not score prediction trials for spatial control objects because either answer was correct. For all mean prediction scores of all blocks see Figure 9B. Again, results indicate that participants reached

ceiling performance in the episodic task in earlier blocks than in the spatial task (there was a significant task*block interaction for regular objects $F_{(1.96, 66.67)}$= 6.886, p= 0.002).

Taken together, participants showed strong object-context associations at the end of both, the spatial and episodic task.

Discussion

In line with the idea of a common coding mechanism, our results suggest that there is considerable overlap between episodic and spatial memory representations in the hippocampus. As a key result, we found an interaction between spatial and episodic context associations in the hippocampus during PVT 2. Adaptation scaled with the context associations, from the highest effect for pairs of objects that shared both, a spatial and episodic context, to the lowest effect for pairs of objects that shared no context. This is line with the findings from PVT 1, where we found a general higher adaptation effect across the spatial and episodic group in the bilateral hippocampus ROI for objects sharing a context than objects sharing no context. We found no evidence supporting the idea of a parallel processing mechanism. There was no effect of spatial vs. episodic context associations, neither along the anterior-posterior axis of the hippocampus nor across the hemispheres of the hippocampus (left vs. right).

Common coding of space and episodes as evidence for cognitive mapping

The idea of a common coding mechanism for spatial and episodic memory can be extended into the much broader idea of cognitive mapping. Cognitive mapping has become an umbrella term for the idea that the hippocampus forms a map or model of our world that goes beyond the spatial domain (Behrens et al., 2018; Bellmund, Gärdenfors, et al., 2018; Buzsáki & Moser, 2013; Epstein et al., 2017; Olsen et al., 2012; Schiller et al., 2015; Stachenfeld et al., 2017; Tolman, 1948). More specifically, a cognitive map is a relational or transitional map between different states. These states can theoretically be any meaningful entity, from concrete positions in space or time to abstract concepts. So called spatially tuned cells (e.g. hippocampal place cells or entorhinal grid cells) are thought to be the underlying neural mechanism of these cognitive maps (Behrens et al., 2018; Bellmund, Gärdenfors, et al., 2018; Buzsáki & Moser, 2013; Epstein et al., 2017; Schiller et al., 2015; Stachenfeld et al., 2017). In recent years, a number of exciting studies in both humans and in rodents demonstrated hippocampal and entorhinal coding of cognitive maps akin to spatial navigation (Aronov et al., 2017; Constantinescu et al., 2016; Deuker et al., 2016; Garvert et al., 2017; Nau et al., 2018; Tavares et al., 2015; Theves et al., 2019). For example, one fMRI study found grid-like coding while

participants were transitioning through concept space – paralleling the grid-like signal found in another fMRI study where participants were navigating a virtual arena (Constantinescu et al., 2016; Doeller et al., 2010). Likewise, other fMRI studies have demonstrated that the hippocampus does not only code for distances in space, but also in the temporal domain and even combines the two types of information (Deuker et al., 2016; Kyle et al., 2015; Nielson et al., 2015). Although, we did not test for coding akin to spatially tuned cells in our experiment, our results dovetail with these findings. The evidence for a common coding mechanism combined with the lack of evidence for parallel processing of spatial and episodic memory suggest that the hippocampus has mechanisms that are not bound to one cognitive domain.

The combination of spatial and episodic information is more than the sum of their associations

We interpret our results in line with a common coding mechanism and more broadly as consistent with the idea of cognitive mapping. Nevertheless, one might argue that our common coding effect reflects the amount of combinations or association strength an object pair experiences, more so than an interaction between space and episode. This is because space-episode pairs (pairs of objects that share both – a spatial and episodic context) share more context associations than any other regular object pair (Figure 1). However, we directly address this criticism by comparing our common coding effect with our control pairs. Control pairs share the same number of context associations as the space-episode pairs, but only in one domain (space or episode; Supplementary Figure 1). Not only was there no significant evidence for an adaptation effect for control objects, the common coding effect was significantly stronger in PVT 2 (and at trend level in PVT 1). We believe that control objects might have been processed differently because a control object in itself does not carry information about a context. During the association tasks, a control object does not tell you which context you are in right now (because both contexts are equally likely), whereas a regular object does. What is more, the hippocampus is known to be involved in contextual learning (Davachi, 2006; Frankland et al., 1998; Kennedy & Shapiro, 2004; Rugg et al., 2012). We therefore argue that the common coding effect for regular objects is more than a pure effect of association strength. Instead, it truly reflects the processing of spatial and episodic context information.

Peaks in the hippocampus for the interaction of space and episode

Generally speaking, the idea of a common coding mechanism (and in a broader sense the idea of cognitive mapping) makes no predictions about peak regions in the hippocampus for the combination of space and episode. Accordingly, we tested for common coding effects with an ROI approach across the entire hippocampus.

Nevertheless, we decided to further explore these bilateral hippocampus ROI effects and describe voxel-wise peak effects within this ROI. For the interaction between space and episodes, we found peaks in the left posterior and bilateral anterior hippocampus (Figure 7). Especially the effects in anterior hippocampus make sense in the light of other findings, showing a general memory integration effect in this region (Collin et al., 2015, 2017; Schlichting et al., 2015). Here, the anterior hippocampus formed a joined representation for events that were only indirectly linked.

Furthermore, our results somewhat overlap with other studies testing temporal and spatial interactions in the hippocampus (Deuker et al., 2016; Kyle et al., 2015; Nielson et al., 2015). In two of these fMRI studies, participants learned spatio-temporal distances between locations in a virtual city (Deuker et al., 2016; Kyle et al., 2015). Results showed that multivariate pattern similarity scaled with both spatial and temporal distances in the right anterior hippocampus. In an fMRI study based on real-life events, participants' movement pattern through a city was recorded over several days. In a subsequent fMRI session, participants were presented with pictures from the recorded events. Results showed that the left anterior hippocampus coded for distances in time and space between these events. Our results suggest that the bilateral anterior hippocampus' role in combining space and time (or episodic information) expands beyond spatial-temporal distance coding of events in space. Here, we demonstrate that episodic context information is integrated with spatial context information in the hippocampus, even with no navigational aspects in the episodic task. Furthermore, because we kept spatial information constant across episodic contexts, our results reflect episodic context processing that goes beyond the spatial domain (i.e. where something happens). In another fMRI study, participants learned episodic and spatial relationships between objects by watching videos of trajectories through a virtual environment (Dimsdale-Zucker et al., 2018). Each unique video was defined as an episodic context and it took place in one of two houses (spatial contexts). In each video, different objects appeared along the path. With this design, all objects that shared an episodic context also shared automatically a spatial context (that was not constant across all other episodes as in our design). The authors found that the left CA1 (a region that traverses along the longitudinal axis of the hippocampus) showed higher pattern similarity for pairs of objects that shared an episodic context than pairs of objects that did not share an episodic context. However, it cannot be excluded that these results are due to an interaction of spatial and episodic information. Although we did not specifically look at CA1 as a hippocampal subfield, the fact that we found peaks along the longitudinal axis of the left hippocampus facilitates this interpretation.

It is important to note that our main goal (and analyses) was to establish whether a common coding mechanism exists in the hippocampus and not its location. We also

did not directly test whether some regions are more involved in a common coding mechanism than others. Nevertheless, our voxel-wise results in combination with other fMRI studies open up the possibility that there are subregions of the hippocampus like the bilateral anterior hippocampus that play a special role in the combination of space and episode.

No evidence for parallel processing

We did not find evidence that there are systematic differences between hippocampal subregions in processing spatial and episodic memory. This absence of evidence neither allows us to conclude that there are no such differences, nor can it be understood as direct evidence for common coding or cognitive mapping. Nevertheless, at the very least it is consistent with the idea of cognitive mapping and does not strengthen any alternative ideas on hippocampal mechanisms like parallel processing. What is more, a number of studies that test for spatial and temporal distance coding in humans, find evidence that is concurrent with the idea that both types of information are combined in the hippocampus rather than processed separately (Deuker et al., 2016; Kyle et al., 2015; Nielson et al., 2015). Additionally, the majority of studies that directly compared spatial and episodic/temporal processing statistically did not find differences between the two in the hippocampus (Burgess et al., 2001; Kyle et al., 2015; Nielson et al., 2015). Nevertheless, there is some evidence for parallel processing from neuroimaging studies that include both spatial and episodic memory in their design (Dimsdale-Zucker et al., 2018; Hirshhorn et al., 2012). As mentioned above, Dimsdale-Zucker et al. (2018) let participants learn episodic and spatial relationships between objects by watching videos of trajectories through a virtual environment. They did find that episodic relationships between objects were coded in CA1 of the left hippocampus. However, as discussed earlier, all objects that shared an episodic context also shared a spatial context in this study. Therefore, it is hard to interpret whether this effect truly reflects a purely episodic processing in this subfield of the hippocampus or an interaction between the spatial and episodic information.

In another fMRI study, participants were presented with landmarks from their city of residence (Hirshhorn et al., 2012). More specifically, participants had to either compare landmarks based on either their spatial location (spatial condition) or based on how long ago the participant had passed/visited these landmarks (episodic condition). Results showed overlapping clusters between these conditions in the left and right hippocampus. However, the authors also found uniquely activated regions in the hippocampus for the episodic condition (along the axis of the left hippocampus and right anterior) and spatial condition (right posterior hippocampus), respectively. Importantly, with this design, the authors could not control for spatial aspects in the episodic recall. When participants were asked to remember the time point of their

last visit or passing of a landmark, they probably also recalled spatial aspects of this event – especially since these events are anchored to a spatial location. The spatial condition might not be a perfect control for these aspects since participants were asked to compare locations of landmarks in an allocentric, knowledge-based fashion (e.g. which landmark is further north). This is very different to the egocentric experience of an episode. Taken together, although both studies showed episodic specific activations in subregions of the hippocampus, their designs do not allow excluding spatial and episodic interactions.

The most convincing argument for a parallel processing mechanism however comes from the accumulative evidence from experiments that study either spatial memory/navigation or episodic memory. There seem to be systematic differences between subregions in the hippocampus that are found to be involved between the two sets of studies. This was established (as already discussed in the introduction) by a meta-analysis that tested these effects across a number of human neuroimaging studies that either involved spatial or episodic memory (Kühn & Gallinat, 2014). However, this type of evidence does not allow concluding that there are actual statistical differences between subregions of the hippocampus in processing spatial and episodic memory. Detecting these differences might require more power than studies directly comparing spatial and episodic processes have provided in the past. We cannot exclude the possibility that our results point more towards a common coding mechanism than a parallel processing mechanism because the former might require less power to detect than the latter. Another important limitation of comparing studies that test effects of either episodic memory or spatial memory is that there might be systematic differences in methods and materials, even when restricting the literature to human neuroimaging. Indeed, when taking a closer look, episodic memory is most commonly tested with the encoding/retrieval of words or pictures and spatial memory with mental or virtual navigation (Kühn & Gallinat, 2014). One could argue that these studies are very different from each other in terms of how active/passive the participant experiences the stimulus material, the richness of the stimulus material, the level of engagement etc. This points towards the ongoing need of well-controlled studies that directly compare both processes.

Taken together, the results of our study do not allow concluding that there is no parallel processing mechanism in the hippocampus. However, the lack of evidence in our study is in line with other studies directly comparing spatial and episodic memory. At the very least, detecting differences between spatial and episodic processes in the hippocampus requires more power than we and other studies have provided in the past.

Common coding in the temporo-parietal regions and frontal lobe

Our main goal was to contribute to the question whether the hippocampus combines space and episode or whether it can be divided into functional subregions. Nevertheless, we added whole-brain analyses to explore effects outside of the hippocampus. We only found effects for an interaction of space and episode in PVT 2 (Figure 8A & B; see Supplementary Figure 6 and Supplementary Figure 7 for whole-brain analyses that did not reach significance). Akin to our hippocampal results, we did not find significant whole-brain effects for control objects. We cannot exclude the possibility that the whole-brain effects are due to the number of associations pairs of objects experience (see the non-thresholded effects in Figure 8). However, we suspect that the whole-brain effect reflects a true processing of spatial and episodic context information. We found effects across a variety of brain areas, especially in temporo-parietal regions and the left frontal lobe (Figure 8A & B and Supplementary Table 1). This is somewhat overlapping with a previous study that looked at the retrieval of spatial context of episodic events (Burgess et al., 2001). In this study, participants were placed in a virtual environment and received different set of objects from two different people in two different spatial contexts. During the recall of the spatial context of these episodic events, the authors found a network in temporo-parietal regions and the prefrontal cortex. They found a similar (but smaller) network for the retrieval of the information about the person of these episodic events. These results in combination with ours indicate that there might be a bigger network reaching from more posterior temporo-parietal regions to more anterior frontal regions, which processes both spatial and episodic context information. Furthermore, a lot of the regions included in this network, have been associated with spatial or episodic functions in other studies, with amongst other the parahippocampus, temporal cortex, precentral gyrus, inferior & superior frontal gyrus, precuneus, and insula (Bellmund et al., 2016; Cavanna & Trimble, 2006; Doeller et al., 2010; Ghaem et al., 1997; Greenberg et al., 2005; Hayes et al., 2007; Maguire et al., 1998; Nyberg et al., 1996).

We also suspect, that the effects in the frontal and striatal regions might be related to their role in concept/category processing (Lie et al., 2006; Seger & Cincotta, 2002; Seger & Miller, 2010). This might have been due to the nature of our association tasks. Here, participants had to repeatedly give responses to objects (or associated actions) that were based on the context the object belonged to. Furthermore, we directly asked participants throughout the memory tasks whether an object belonged to a context. This might have led to a categorization of objects based on their associated task context. Manipulating the spatial and temporal/episodic relationship between objects in a continuous manner instead of a discrete (like contexts) might circumvent possible categorization effects. Unfortunately, studies who have used this sort of design in the past, did not report whole-brain results (Deuker et al., 2016; Kyle et al., 2015; Nielson et al., 2015).

Conclusions

Even though our whole-brain results point toward interactions of spatial and episodic memory beyond the hippocampus, we specifically focused on the question how the hippocampus processes these two types of memory. Our results are consistent with an interaction between spatial and episodic memory in the hippocampus. At the same time, we found no evidence for differences between spatial and episodic memory in hippocampal subregions. This pattern of results is in line with the idea of a common coding mechanism. Furthermore, the notion that spatial and episodic memory are processed similarly feeds into the broader idea of cognitive mapping. Accordingly, our results support the idea that the hippocampus forms a map of relationships/transitions we encounter in the world across domains.

Supplementary figures

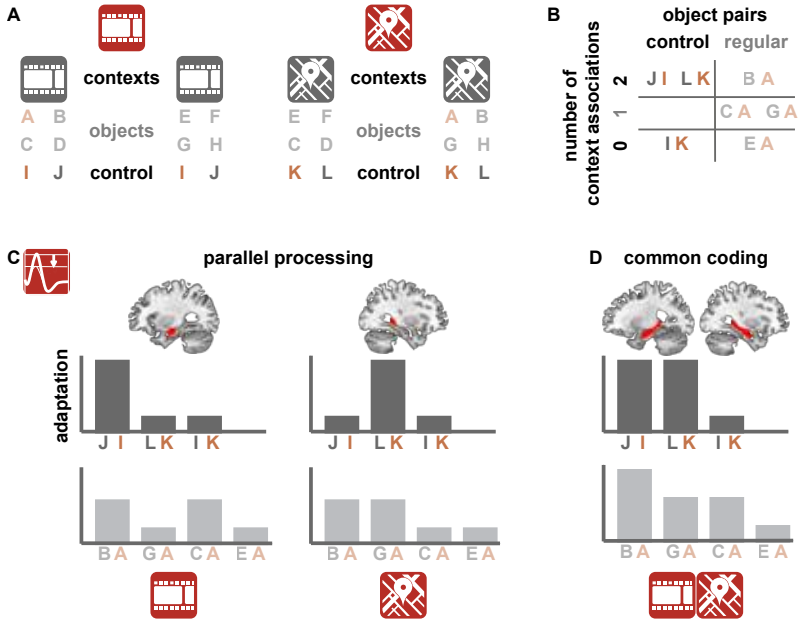

Supplementary Figure 1 | Control predictions for association strength
(A) A set of two control objects appeared only in either the spatial or the episodic task, respectively. Episodic control objects appeared in both episodic contexts (here J-I), spatial control objects appeared in both spatial contexts (here L-K). You can also see the distribution of regular objects across the task contexts (information for regular objects is shown here in paler colours, for more information see Figure 1).

(B) The purpose of the control objects was to test effects of association strength (i.e. number of context associations). Pairs of control objects from the same task share two context associations (here, L-K and J-I). This is the same number of context associations as regular pairs that share both, a spatial and episodic context (here B-A). Pairs of control objects from different tasks (mixed control pair, here I-K) share no context associations (same as regular pair E-A).

(C) The parallel processing model predicts a higher adaptation effect in the anterior and/or left hippocampus for episodic control objects (here in the example J-I) compared to spatial control pairs and mixed control pairs (here in the example L-K and I-K). Furthermore, it predicts a higher adaptation effect in the posterior and/or right hippocampus for spatial control objects (here in the example L-K) compared to episodic control pairs and mixed control pairs (here in the example J-I and I-K). Importantly, if a parallel processing effect is driven by association strength, then the adaption effect for control pairs from the same task should be higher than pairs of regular objects that share only one specific context (e.g. J-I vs C-A in the episodic condition and L-K and G-A in the spatial condition).

(D) The common coding model makes no predictions about subregions of the hippocampus. It predicts a higher adaptation effect for control pairs form the same task than mixed control pairs (here in the example J-I & L-K vs. I-K). Importantly, if a common coding effect is driven by association strength, then control pairs of the same task should have the same adaption effect than regular pairs of objects that share both, an episodic and spatial context (all of these pairs share two context associations, here in the example J-I, L-K & B-A).

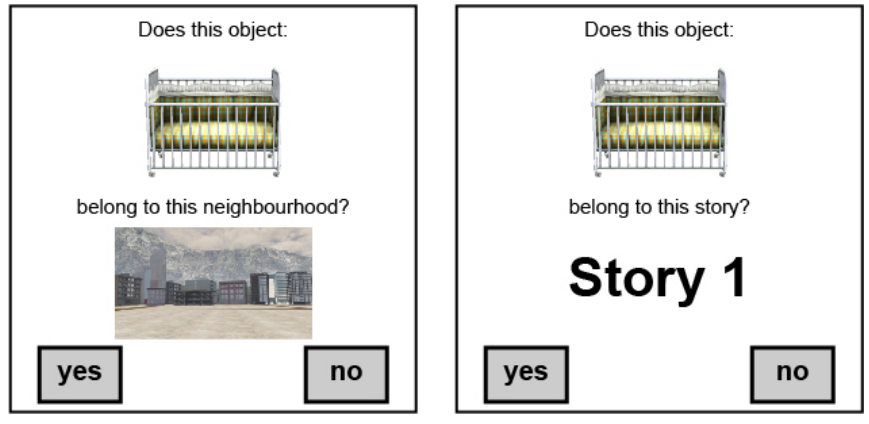

Supplementary Figure 2 | Memory trials of the spatial and episodic task
Both, the spatial and episodic task were divided into four blocks. After each block, participants had to complete 24 memory trials. Each trial consisted of a unique combination of one of the twelve objects and one of the two task contexts (neighbourhood in the spatial task and story in the episodic task). In each trial, participants had to indicate whether the object belonged to the task context with a button press.

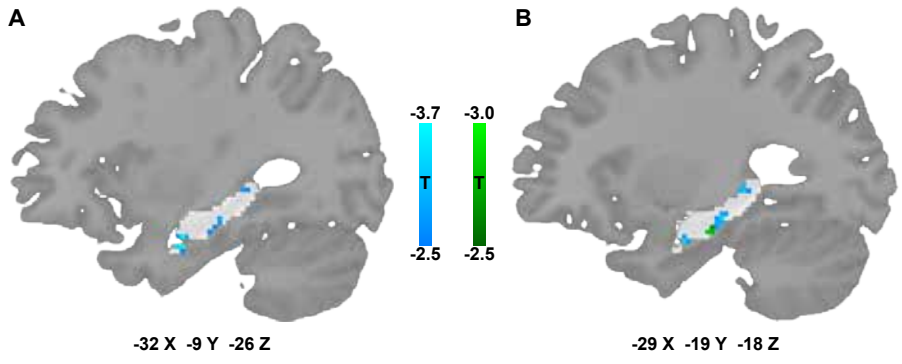

Supplementary Figure 3 | Voxel-wise effect of context associations for the episodic and spatial group
Negative modulation of activity in the hippocampus by context associations between object pairs after participants performed either the episodic or the spatial task (shared context vs. no shared context). Analyses were on PVT 1. No effects survived correction (p_{FWE}> 0.05), the image is thresholded at $p_{uncorr.}$< 0.001 for visualization. T-stats in blue are from the episodic group, T-stats in green are from the spatial group.

(A) depicts the peak for the episodic group ($T_{(19)}$= -3.701).

(B) depicts the peak for the spatial group ($T_{(14)}$= -2.972).

Coordinates for the peak voxels are given in MNI space. Image is masked for hippocampal voxels.

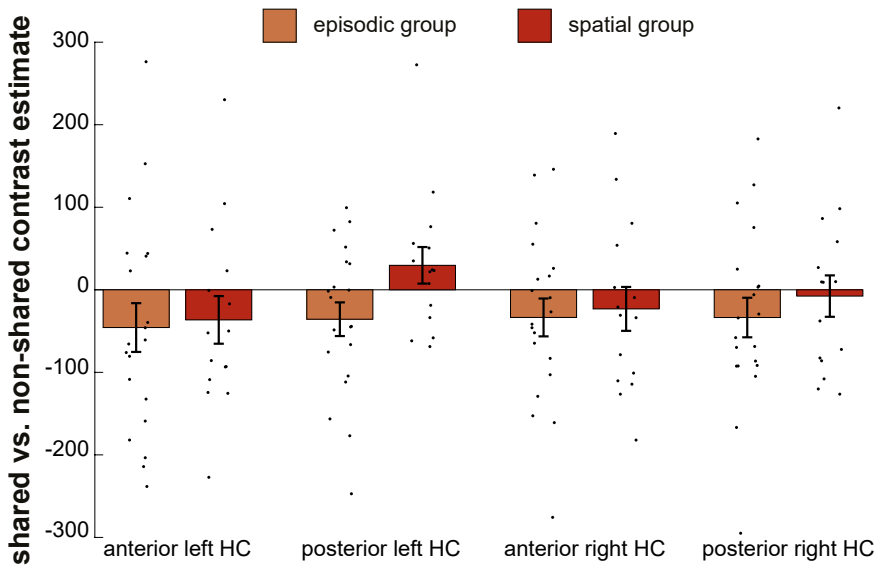

Supplementary Figure 4 | Parallel processing during PVT 1 in hippocampal subregions
Depicted are the mean contrast estimates of the contrast shared context vs non-shared context, divided by group (spatial vs. episodic group) and hippocampal subregions. There was no significant interaction between group and hemisphere (p= 0.39), anterior-posterior axis (p= 0.34) or hemisphere and anterior-posterior axis (p= 0.30). Dots represent single participant values. Error bars show the standard error of the mean.

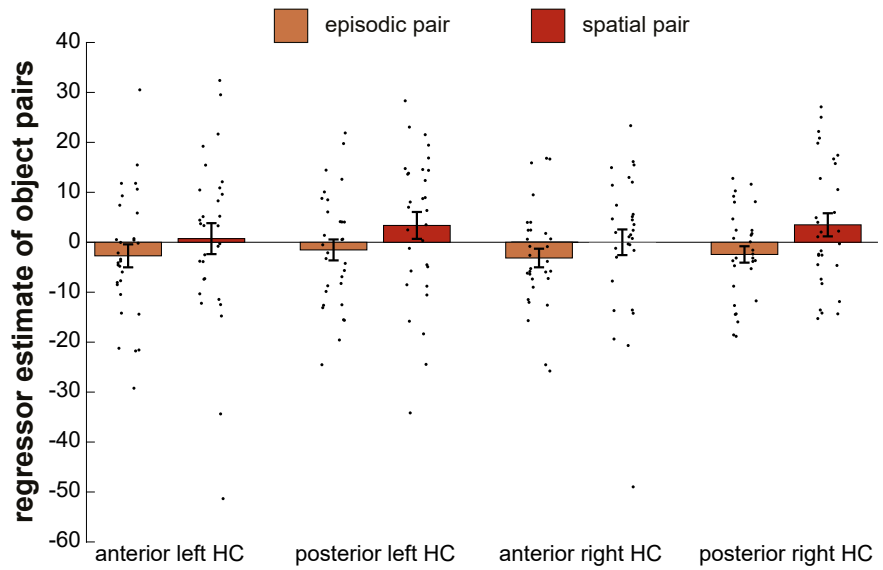

Supplementary Figure 5 | Parallel processing during PVT 2 in hippocampal subregions
Depicted are the mean regressor estimates of object pair regressors, divided by shared context (spatial vs. episodic) and hippocampal subregions. There was no significant interaction between context mode and either hemisphere (p= 0.53), anterior-posterior axis (p= 0.41) or hemisphere and anterior-posterior axis (p= 0.59). Dots represent single participant values. Error bars show the standard error of the mean.

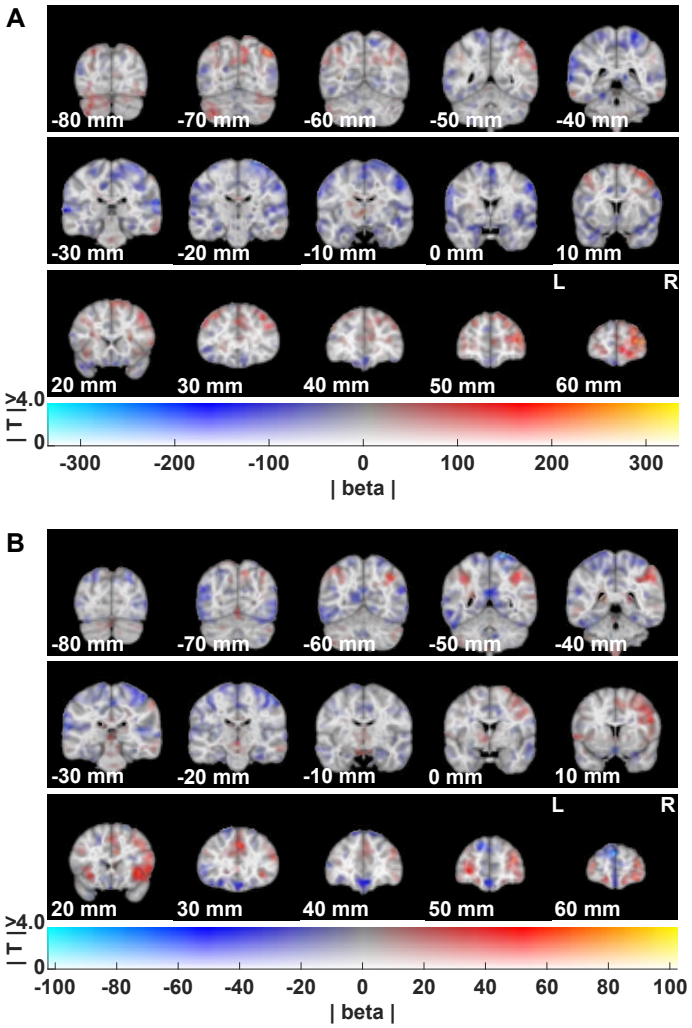

Supplementary Figure 6 | Whole-brain results for common coding of spatial and episodic context associations during PVT 1
(A) Modulation of activity by spatial and episodic context associations between object pairs (no context shared vs. one (episodic or spatial) context shared) during PVT 1. No effects survived whole-brain correction.

(B) Modulation of activity by context associations between control pairs (no context shared vs. both task contexts shared – either both spatial or both episodic contexts, depending which task the participant completed at this point) during PVT 1. No effects survived whole-brain correction.

All images were created using a dual-coded design (Allen et al., 2012; Zandbelt, 2017). This allowed showing both, the mean beta coefficient (blue-red) and the T stats (opacity). Y-coordinates are in MNI space.

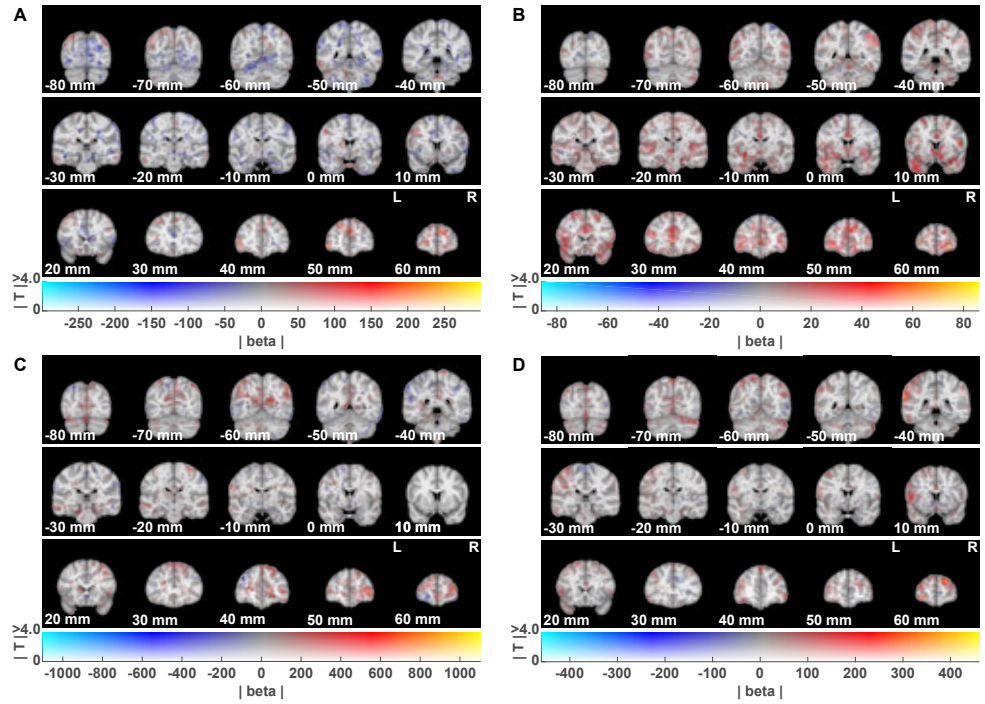

Supplementary Figure 7 | Whole brain results for parallel processing of spatial and episodic context associations during PVT 1 and PVT 2
(A) Group contrast during PVT 1 between participants that have completed the spatial task first and participants that have completed the episodic task first. Negative betas mean higher adaptation effect of strength of context association (shared one context vs. shared no context) for the episodic group than the spatial group (vice versa for positive betas). No effects survived whole-brain correction.

(B) Group contrast during PVT 1 between participants that have completed the spatial task first and participants that have completed the episodic task first. Negative betas mean higher adaptation effect of strength context association of control objects (shared both task contexts vs. shared no context) for the episodic group than the spatial group (vice versa for positive betas). No effects survived whole-brain correction.

(C) Contrast during PVT 2 of pairs of objects that share (solely) an episodic context with pairs of object that share (solely) a spatial context. Negative betas mean higher adaptation effect for pairs of objects sharing an episodic context than pairs of objects sharing a spatial context (vice versa for positive betas). No effects survived whole-brain correction.

(D) Contrast during PVT 2 of pairs of control objects that share both episodic contexts with pairs of control objects that share both spatial contexts. Negative betas mean higher adaptation effect for episodic control pairs than spatial control pairs context (vice versa for positive betas). No effects survived whole-brain correction.

All images were created using a dual-coded design (Allen et al., 2012; Zandbelt, 2017). This allowed showing both, the mean beta coefficient (blue-red) and the T stats (opacity). Y-coordinates are in MNI space.

Supplementary Table 1 | Significant clusters for common coding effect during PVT 2
Voxels within the clusters survived FWE wholebrain correction in both the object-wise and pair-wise GLM. Results are based on common coding adaptation effect during PVT 2. The peak position (MNI space) and the T-value refer to the local maxima within the cluster (only local maxima reported with a minimum distance of 50 mm between them). Local maxima for the object-wise GLM are highlighted in red. Cluster size is the number of voxels within the cluster (only clusters listed here with a size bigger than 5). Brain regions listed are based on labels from the Harvard Oxford Cortical and Subcortical Brain Atlas.

cluster	local peak in MNI			T value	cluster size	brain regions
	X	Y	Z			
1	-48	44	-6	$T_{(29)}$= -4.988	6892	Frontal Pole Insular Cortex Middle Frontal Gyrus Inferior Frontal Gyrus, pars triangularis Inferior Frontal Gyrus, pars opercularis Precentral Gyrus Temporal Pole Superior Temporal Gyrus, anterior division Superior Temporal Gyrus, posterior division Middle Temporal Gyrus, anterior division Middle Temporal Gyrus, posterior division Middle Temporal Gyrus, temporo-occipital part Inferior Temporal Gyrus, anterior division Inferior Temporal Gyrus, posterior division Inferior Temporal Gyrus, temporo-occipital part Supramarginal Gyrus, posterior division Angular Gyrus Lateral Occipital Cortex, superior division Lateral Occipital Cortex, inferior division Intracalcarine Cortex Subcallosal Cortex Cingulate Gyrus, anterior division Cingulate Gyrus, posterior division Precuneous Cortex Cuneal Cortex Frontal Orbital Cortex Parahippocampal Gyrus, anterior division Parahippocampal Gyrus, posterior division Lingual Gyrus Temporal Fusiform Cortex, anterior division Temporal Fusiform Cortex, posterior division Temporal Occipital Fusiform Cortex Occipital Fusiform Gyrus Frontal Operculum Cortex Central Opercular Cortex Planum Polare Heschl's Gyrus Planum Temporale Supracalcarine Cortex Occipital Pole Cerebellum Left Putamen Left Pallidum Left Hippocampus Left Amygdala Right Cerebral White Matter
	-10	-92	4	$T_{(29)}$= -4.897		
	-64	-48	-12	$T_{(29)}$= -4.886		
	-36	2	26	$T_{(29)}$= -4.825		
	12	4	-2	$T_{(29)}$= -4.465		
	-64	-50	-12	$T_{(29)}$= -6.048		
	12	4	-2	$T_{(29)}$= -5.795		
	-48	44	-8	$T_{(29)}$= -4.562		
	-36	6	26	$T_{(29)}$= -4.459		
	-36	-10	-24	$T_{(29)}$= -4.377		
	-8	-90	4	$T_{(29)}$= -3.999		

cluster	local peak in MNI			T value	cluster size	brain regions
	X	Y	Z			
						Right Cerebral Cortex Right Lateral Ventricle Right Thalamus Right Caudate Right Putamen Right Pallidum Right Accumbens
2	46	-60	-10	$T_{(29)}$= -4.404	1033	Middle Temporal Gyrus, posterior division Middle Temporal Gyrus, temporo-occipital part Inferior Temporal Gyrus, posterior division Inferior Temporal Gyrus, temporo-occipital part Lateral Occipital Cortex, inferior division Temporal Fusiform Cortex, posterior division Temporal Occipital Fusiform Cortex Occipital Fusiform Gyrus Cerebellum
	42	-44	-18	$T_{(29)}$= -4.740		
3	-52	-6	50	$T_{(29)}$= -4.274	777	Precentral Gyrus Postcentral Gyrus Supramarginal Gyrus, anterior division Central Opercular Cortex Parietal Operculum Cortex
	-60	-18	34	$T_{(29)}$= -4.512		
4	18	-2	-22	$T_{(29)}$= -4.687	760	Insular Cortex Temporal Pole Frontal Orbital Cortex Parahippocampal Gyrus, anterior division Planum Polare Right Putamen Right Pallidum Right Hippocampus Right Amygdala
	30	14	-12	$T_{(29)}$= -4.519		
5	36	-66	-38	$T_{(29)}$= -4.392	668	Cerebellum
	36	-66	-38	$T_{(29)}$= -4.562		
6	60	-14	30	$T_{(29)}$= -3.745	360	Postcentral Gyrus Supramarginal Gyrus, anterior division
	60	-22	42	$T_{(29)}$= -4.163		
7	60	4	30	$T_{(29)}$= -4.250	289	Inferior Frontal Gyrus, pars triangularis Inferior Frontal Gyrus, pars opercularis Precentral Gyrus
	52	12	22	$T_{(29)}$= -4.195		
8	24	-36	-18	$T_{(29)}$= -4.641	268	Parahippocampal Gyrus, posterior division Lingual Gyrus Temporal Fusiform Cortex, posterior division Temporal Occipital Fusiform Cortex Cerebellum Brainstem
	26	-38	-16	$T_{(29)}$= -4.758		
9	-22	-64	36	$T_{(29)}$= -4.828	216	Superior Parietal Lobule Lateral Occipital Cortex, superior division
	-22	-64	36	$T_{(29)}$= -4.806		

cluster	local peak in MNI			T value	cluster size	brain regions
	X	Y	Z			
10	70	-22	4	$T_{(29)}$= -4.179	132	Superior Temporal Gyrus, posterior division Middle Temporal Gyrus, posterior division Central Opercular Cortex Parietal Operculum Cortex Heschl's Gyrus Planum Temporale
	70	-20	-2	$T_{(29)}$= -3.699		
11	32	32	2	$T_{(29)}$= -3.600	126	Frontal Pole Insular Cortex Inferior Frontal Gyrus, pars triangularis Frontal Orbital Cortex Frontal Operculum Cortex
	32	30	2	$T_{(29)}$= -3.414		
12	-14	-48	-32	$T_{(29)}$= -5.029	109	Cerebellum Brainstem
	-18	-50	-34	$T_{(29)}$= -5.476		
13	50	46	14	$T_{(29)}$= -3.829	73	Frontal Pole
	52	46	2	$T_{(29)}$= -3.716		
14	0	-56	38	$T_{(29)}$= -3.457	52	Precuneous Cortex
	0	-56	36	$T_{(29)}$= -4.501		
15	-30	40	-8	$T_{(29)}$= -3.691	48	Frontal Pole Frontal Orbital Cortex
	0	-56	36	$T_{(29)}$= -4.326		
16	-2	-4	-14	$T_{(29)}$= -3.780	42	Brainstem
	0	-56	36	$T_{(29)}$= -4.378		
17	-44	0	0	$T_{(29)}$= -2.978	31	Insular Cortex Central Opercular Cortex Planum Polare
	-46	-2	-2	$T_{(29)}$= -3.232		
18	-2	-56	-20	$T_{(29)}$= -4.681	24	Cerebellum
	-2	-56	-20	$T_{(29)}$= -4.122		
19	-38	-44	-34	$T_{(29)}$= -3.596	17	Cerebellum
	-38	-44	-34	$T_{(29)}$= -3.819		
20	-12	-32	-42	$T_{(29)}$= -5.170	12	Brainstem
	-12	-32	-40	$T_{(29)}$= -4.458		

CHAPTER 4

Mapping context-dependent value structures in the hippocampal-orbitofrontal system

This chapter is in preparation as:
A. N. de Haas, M. Garvert, A. Nitsch, R. Cools, N. W. Schuck, C. F. Doeller. Mapping context-dependent value structures in the hippocampal-orbitofrontal system.

Abstract

The hippocampus plays a crucial role (among other things) in navigation and spatial cognition. One core claim of the idea of cognitive mapping is that hippocampal mechanisms supporting navigation are also used in other domains. In recent years, first proof-of-principle studies have demonstrated hippocampal coding of abstract spaces along physical feature dimensions. Here, we wanted to extend these findings, by testing whether the hippocampus processes distances in a non-physical, conceptual 2-dimensional (2D) abstract space akin to distances in real space. We argue that numerical values are of particular interest for studying non-physical, conceptual abstract spaces. Numerical values are not only a constant reappearing concept in our everyday lives; they also inherently form a continuous axis. To this end, we tested whether a value map emerged after a binary decision making task. Participants had to learn associations between everyday objects and two independent values (value A and value B) in order to make optimal choices. The two values span a 2D value space, but can also be mapped onto a 1-dimensional (1D) space reflecting the global expected value. We hypothesised that the hippocampus may form a map of the objects according to their value differences and its activity may accordingly reflect distances in the 2D value space. Yet, we found no evidence for the emergence of a hippocampal representation of distances in a 2D value space. However, as is expected based on its known role in value-based decision making, distance representations in a global 1D value space emerged in the OFC. Furthermore, during the decision making task we found complementary roles of the hippocampus and OFC. Both areas coded – albeit in different directions, for the difference between the chosen and unchosen value during decision making. These results suggest that not all abstract feature dimensions may be represented in a hippocampal cognitive map and raises questions about the preconditions for hippocampal mapping.

Introduction

The hippocampus and adjacent entorhinal cortex are known to be highly involved in geometric computations during spatial navigation. Spatially tuned cells are thought to be the driving force behind these computations (Moser et al., 2008; O'Keefe & Nadel, 1978; Schiller et al., 2015). Prominent examples of these types of cells are hippocampal place cells and entorhinal grid cells (Hafting et al., 2005; O'Keefe & Burgess, 1996). These cells show firing patterns that are driven by the location of the navigator in the 2D plane. A place cell only fires at one specific location in a closed environment, with different place cells firing at different locations (O'Keefe & Burgess, 1996; O'Keefe & Nadel, 1978). In the same environment, a grid cell has periodical firing fields, which form a hexagonal grid (Doeller et al., 2010; Hafting et al., 2005). Grid cells differ in their orientation, phase and spacing of their firing fields. These and other properties of place and grid cells are thought to enable geometric computations underlying goal-orientated navigation. For instance distance coding, path integration and coding of relevant locations (Bush et al., 2015; Deuker et al., 2016; O'Keefe & Nadel, 1978; Spiers & Barry, 2015).

Historically, these properties of the hippocampus and entorhinal cortex have been rigorously studied and discussed for navigating our environment. However, according to the idea of cognitive mapping, computations supporting navigation are also utilized by other cognitive domains (Behrens et al., 2018; Bellmund, Gärdenfors, et al., 2018; Epstein et al., 2017; Schiller et al., 2015; Stachenfeld et al., 2017; Tolman, 1948). A cognitive map is in its essence a relational map between different states. These states can theoretically be any meaningful entity, from concrete positions in space or time to abstract concepts. It is no surprise then, that the coding mechanisms underlying navigating physical space are thought to also allow geometric computations in abstract cognitive maps (Behrens et al., 2018; Bellmund, Gärdenfors, et al., 2018; Epstein et al., 2017; Schiller et al., 2015; Stachenfeld et al., 2017).

Even though the behavioural basis of the idea of a cognitive map has been already proposed and demonstrated in the late 1940s (Tolman, 1948), the first proof-of-principle studies of hippocampal coding of abstract spaces have only been published in recent years. These studies showed involvement of the hippocampus and/or entorhinal cortex in mapping of e.g. time, concepts, social hierarchies and sound frequency (Aronov et al., 2017; Constantinescu et al., 2016; Garvert et al., 2017; Tavares et al., 2015; Theves et al., 2019). Furthermore, both evidence for coding mechanisms akin to grid cells and place cells has been found in the representation of these abstract cognitive maps (Aronov et al., 2017; Constantinescu et al., 2016).

Strikingly, many of these experiments used cognitive maps that mimic physical space in the sense that they can be described along continuous feature dimensions in 2D. These features (e.g. length of the leg of a bird) are based in the physical world. If any physical feature dimension can be organized with a hippocampal map, this principle might also apply to more abstract concepts. We argue that numeric values are a good candidate for examining hippocampal coding of these more abstract (non-physical) maps. Values are not a sensory/physical feature, but a constant appearing concept in our everyday lives. At the same time values also form inherently a continuous axis. These two features facilitate an experimental design of a meaningful value map.

Importantly, values are known to be coded in more frontal areas, such as the OFC, especially during value-based decision making (FitzGerald et al., 2009; Pelletier & Fellows, 2019). The OFC seems to be especially involved in tracking values of predictive cues or states (FitzGerald et al., 2009; Gottfried et al., 2003; Kaplan et al., 2017). These cue values or state values incorporate and summarize experienced reward contingencies. Such a summarizing value is important for flexible and adaptive behaviour. However, these value representations lose information about underlying complex reward structures. Often a cue or state is not only associated with one, but several rewards. In that case, it might be beneficial to have an additional representation such as a value map, which can incorporate all possible reward outcomes. Furthermore, a hippocampal value map of reward contingencies could allow geometric computations like distance coding between cues or states. These neural geometric computations might facilitate value-based decision making. Importantly, we propose that such a multidimensional value map representation in the hippocampus would exist next to and perhaps interact with the known unidimensional value representations in frontal areas. Interestingly, this proposition also dovetails with the already known involvement of the hippocampus in model-based decision making (Bornstein & Daw, 2013; Johnson et al., 2007; Shohamy & Daw, 2015; Vikbladh et al., 2019; Wikenheiser & Schoenbaum, 2016; Wimmer & Shohamy, 2012). Previous studies indicate that the hippocampus might play a substantial role in representing task contingencies (Bornstein & Daw, 2013; Duncan et al., 2018; Wimmer & Shohamy, 2012). These representations are thought to be necessary to form a flexible model (or map) that allows to plan and execute decisions that involve multiple steps (Bornstein & Daw, 2013; Doll, Shohamy, et al., 2015; Duncan et al., 2018; Johnson et al., 2007; Shohamy & Daw, 2015; Vikbladh et al., 2019; Wikenheiser & Schoenbaum, 2016; Wimmer & Shohamy, 2012).

Here, we aim to extend these findings by exploring complementary roles of the OFC and hippocampus in value representations. In the present study, we want to test the idea that the hippocampus can represent complex value structures via an abstract space, while the OFC incorporates these structures into a global value.

Akin to a previous study of physical feature space, we ask the question whether the hippocampus can code distances in non-physical value space (Theves et al., 2019). To this end, we combined fMRI with a behavioural value-based decision making task. Participants performed a binary decision making task in which they had to make a choice between the same two options in every trial. Each choice was rewarded with a numeric value. The choice-reward contingency was 100% predicted by a context object shown before each decision (in total five different context objects, each predicting a unique combination of choice-reward contingencies across both choices). With this task design, each context object was associated with two different types of values. These associations can be represented in a 2D value space, where one axis represents value of choice A and the other axis value of choice B (Figure 2). Additionally, both of these axes can be incorporated into a 1D representation. The one dimension here is the expected value of the context object (defined as probability of choice A * the expected value of choice A + probability of choice B * the expected value of choice B under the given context object). Importantly, before and after the decision making task, we presented all context objects in a randomized order. This allowed us to detect changes of across-voxel pattern similarity for all pairs of context objects as a function of distances in 2D and 1D value space, respectively (Kriegeskorte et al., 2008). We hypothesized that distances in 2D value space are represented in the hippocampus and distances in 1D expected value space in the OFC.

Methods

Participants

34 (20 women) healthy participants completed the experiment. Participants were between 18 and 33 years old (mean age= 23, sd= 2.9). At the beginning of the experiment, participants gave written consent to participate in the study and filled in a screening form to ensure that they did not meet any exclusion criteria for the MRI and behavioural labs. Participants were compensated for their time and could earn extra money (up to 5 Euros) based on their performance in the experiment. The study was approved by the local ethics committee (CMO Regio Arnhem-Nijmegen, The Netherlands, nr. 2014/288).

General procedure

Participants performed three tasks in the MRI scanner (Figure 1). During a pre- and post-block participants performed a picture viewing task (PVT) in order to measure the change in neural similarity between object pairs and to test whether this change scales as a function of distance in 1D and 2D value space. Between these pre- and post-blocks, participants performed a binary decision making task, which introduced

them indirectly to the position of objects in both types of abstract value spaces (Figure 2).

After scanning, participants' memory about the previous binary decision making task was tested in two different ways. First, participants completed a recognition memory task about context dependent reward contingencies. The second memory test was the first and only direct presentation of the 2D value space to the participants. Here, participants had to place context objects in the 2D value space. Lastly, participants' navigational abilities were tested with the Santa Barbara Sense of Direction Scale (SBSOD) and an object-location task. For an illustration of the general procedure, see Figure 1.

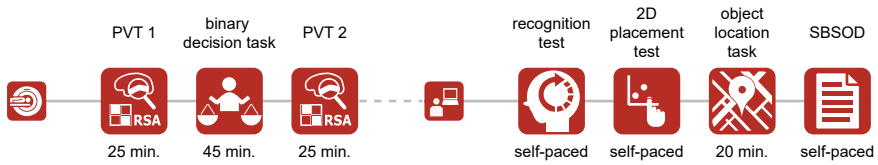

Figure 1 | General procedure of experiment
Participants performed three tasks in the MRI scanner: a pre picture viewing task (PVT 1), a binary decision making task and a post-PVT (PVT 2). Afterwards, participants finished four behavioural tasks: a recall test about the binary decision making task, a placement task in 2D value space, an object-location task, and the Santa Barbara Sense of Direction Scale (SBSOD). If tasks were not self-paced their duration is indicated in minutes underneath their icon.

Binary decision making task

Between the pre- and post-blocks of the PVT, participants performed a binary decision making task in the scanner. The task consisted of 400 choice trials, divided into 320 free-choice trials and 80 forced-choice trials. Each free-choice trial consisted of three phases (Figure 2A). In the first phase, participants saw one of the five possible context objects at the centre of a black screen for 1.5 seconds (all objects are shown in Supplementary Figure 1). In the second phase, participants always had to make a decision between a chair and lamp by pressing one of two buttons with the right index and middle finger, respectively. Index finger button presses indicated choice of the object presented on the left side of the screen and middle finger button presses indicated choice of the object presented on the right side of the screen. Chair and lamp positions were counterbalanced across all trials of the task, so that there was no action bias. Images of the chair and the lamp had a size of 246 by 246 pixels and edges of the options presented on either side were approximal 50 pixels form the centre, respectively. The chair and lamp were presented until the participant responded or 1.5 seconds elapsed. If the participant did not respond within 1.5 seconds, they received no reward for this trial. In the third phase, participants received feedback about their

choice for 1 second, followed by a white fixation cross which was shown randomized for either 1.5, 3, or 4.5 seconds (size of fixation cross was 52 by 52 pixels). During the feedback, they saw a reward in the form of a numerical value on the screen for the choice they made (text in stimuli was created with a font size of 150). Simultaneously they were presented with the reward for the non-chosen option. The reward for each choice was presented at the location that the choice object (lamp/chair) was presented at during the second phase of that trial (see also Figure 2B for all possible reward combinations).

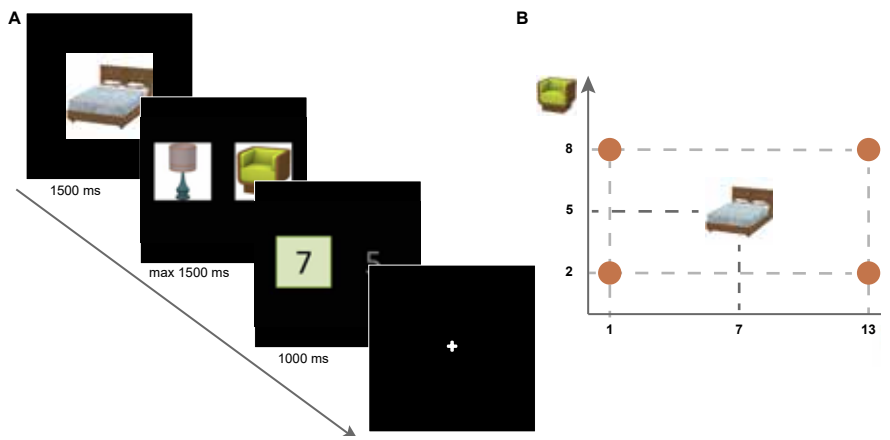

Figure 2 | Free-choice trials of the binary decision making task and context object placement in 2D value space
(A) Free-choice trials of the binary decision making task were divided into three phases. In the first phase one of five different context objects were shown (here the bed) for 1500 ms. In the second phase the two choice objects (chair and lamp) were presented until the participant made a choice or 1500 ms elapsed. In the third phase, the participant was presented with a feedback about the reward they received for their choice and the reward they would have gotten for the alternative choice. The received reward was indicated with a green box and the feedback was shown for 1000 ms. After each trial a white fixation cross was presented with a duration of either 1500, 3000, or 4500 ms.

(B) Representation of reward contingencies of context objects in a 2D value space. In the example in (A), the context object bed is associated with a certain reward for the choice of lamp and with the choice of chair, respectively. These two types of rewards can be represented as two independent dimensions of a 2D value space. The position of the bed is determined by the reward contingencies it predicts for either choice (here 7 for the choice of lamp and 5 for the choice of chair). All other possible positions in the 2D value space are marked with the golden circles (1|2, 1|8, 7|5, 13|2, 13|8).

The chosen reward was marked in a green box with a size of 238 by 224 pixels. Thus, throughout the experiment, participants learned reward contingencies for both, choice of lamp and choice of chair. Importantly, the reward contingency for either choice was 100% predicted by the context object in the first phase. Each context object predicted

a unique combination of choice-reward contingencies across both choices. This allowed each context object to be associated with two types of values (value for choice of lamp and value for choice of chair). These associations can be represented in a 2D value space, where one dimension represents the value for choice of lamp and the other dimension the value for choice of chair (Figure 2). Hence, positions of context objects in this 2D value space are a direct translation of the choice-reward contingencies they predict. Additionally, the task allows for both of these dimensions to be incorporated into a 1D representation. The one dimension here is the expected value of the context object (defined as probability of choice of lamp * the expected value of choice of lamp + probability of choice of chair * the expected value of choice of chair under the given context object). Combination of choice-reward contingencies were constant across participant, however which context object predicted which choice-reward contingency (i.e. their position in 2D value space) was randomized across participants.

Forced-choice trials were included in the task, to ensure that participants did not only associate context objects with their respective higher rewarded choice (Supplementary Figure 2). These trials differed from free-choice trials in that participants could not choose between the chair and the lamp, but were only given the option of the lower rewarded choice. Given the example shown in Figure 2 during a forced-choice trial for the context object bed, only the chair would have been given as an option.

All context objects appeared equally often across free and forced-choice trials. This equal distribution was pseudo-randomized so that the first and second half of the task had the same amount of free and forced-choice trials for all context objects. Furthermore, the order was pseudo-randomized so that all context objects appeared twice within a block of ten trials. Within each of these blocks of ten trials, the side on which the lamp and chair appeared on the screen was counterbalanced so that each configuration appeared once per context object. Exceptions were forced-choice trials in which only one option appeared on one side of the screen.

Additionally, to facilitate knowledge about choice-reward contingencies, participants had to complete a learning trial after every block of ten choice trials. During a learning trial, participants were asked to compare the outcome of a choice (e.g. chair) between two context objects (Supplementary Figure 3). They had to indicate via button press which of the two context objects predicted a higher reward for the given choice or whether they predicted the same outcome. The given choice (e.g. chair) was presented with an image of the object at the middle, upper part of the screen. Options were distributed on the screen, so that one context object was presented on the left side (answer with index finger), the other at the centre (answer with middle finger) and the option that both predict the same outcome on the right side of the screen (answer with ring finger). All images of objects had a size of 118 by 118 pixels. Participants had a maximum of 7 seconds to give an answer. After their response, participants received

feedback about whether their answer was correct for 1 second. If they did not respond within 7 seconds, they received negative feedback. Positive feedback showed a green positive smiley, while negative feedback showed a red negative smiley (size 243 by 249 pixels). Underneath the feedback smiley, participants either saw the message “Correct Answer. Keep paying attention to all possible rewards” or “Wrong answer. Pay more attention to all possible rewards” (font size in image was 32). Each possible combination of pairs of context objects and choice was presented twice during the experiment, resulting in 40 learning trials.

Due to the length of the task, the scanner was paused after half of the trials. Participants were allowed to take a small break in the scanner and then continued with the second half of the task.

The task was programmed in and presented with neurobs Presentation (version 16.4, www.neurobs.com/presentation).

Picture viewing tasks

Participants completed the identical picture viewing task (PVT, Figure 3) before (pre-block) and after (post-block) the binary decision making task. Participants were told that they would see a stream of objects (i.e. the context objects from the binary decision making task). Furthermore, participants were instructed to press one of two buttons every time they saw an object appear on the screen. Participants had to press one button if the object was different to the previously shown object (regular trial) and had to press the other button if the object was the same as the previously shown object (catch trial, Figure 3). Button-contingencies were randomized across participants, but always done with the right index and middle finger. This one-back task was orthogonal to later analyses of the PVTs and ensured that participants paid attention to the objects. Participants reached ceiling performance on the cover tasks in both PVTs (pre-PVT: mean= 93.8%, sd= 13.9, post-PVT: mean= 98.5%, sd= 1.3).

The five objects were presented during the PVT at the centre of the white screen (Supplementary Figure 1). Pictures of the objects had a pixel size of 512 by 512. Each object was presented 40 times in each PVT (total of 200 trials per PVT). Each trial had a duration of 2 seconds. Ten percent of trials were catch trials (self-repetitions) and these trials were evenly distributed across the five different objects. Each PVT was divided into four blocks. After each block, participants had a 20 second break, in which they received feedback about their performance in the previous block and a reminder of the button-contingencies.

The order of object presentation was pseudo-randomized across participants, but was the same for the pre- and post-PVT of the same participant. To be more specific, in every mini-block of five trials every object would appear once. Exception to this rule were catch trials (self-repetitions). Catch trials were pseudo-randomized in a manner

that they would appear twice within a block of 20 non-catch trials. Within these catch trial blocks an object could only appear maximally once as a catch trial. Additionally, for every participant the second trial of the PVT was always a catch trial. These pseudo-randomizations made sure that there was no temporal bias within the PVT, neither for catch trials, nor between objects.

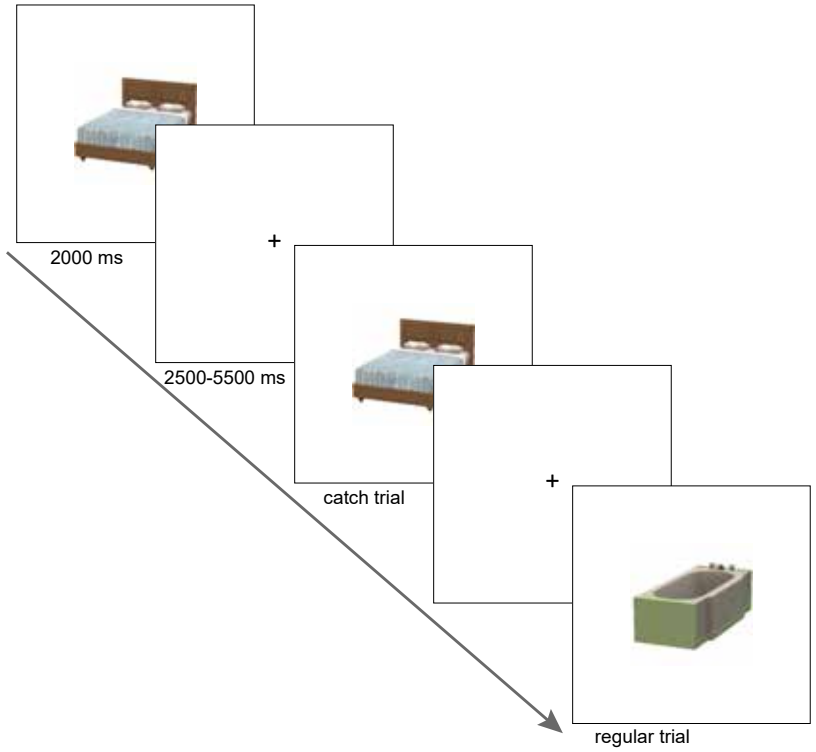

Figure 3 | Picture viewing task
The five different context objects of the binary decision making task were presented in random order during the PVT. Objects were presented for 2000 ms at the centre of the screen. Between object presentation a black fixation cross was presented at the centre of the screen. Duration of the fixation cross was either 2500, 4000 or 5500 ms. Participants had to press one of two buttons if the presented object was the same as the previous one (catch trial). They pressed the other button if the object was a different one from the previously presented object (regular trial). Button contingencies were randomized across participants.

After every object presentation, a black fixation cross appeared at the centre of the screen (fixation cross was presented as text object with a font size of 20). The duration of these inter-trial intervals (ITIs) was jittered between one and three scanner pulses (TR was 1.5 seconds) plus 1 second. The order of the ITI-durations was pseudo-randomized in a manner that all ITIs appeared equally often across all non-catch trials of an object (the ITI of a catch trial was randomly chosen). Furthermore, the average ITI duration of a block of 20 non-catch trials was not allowed to be more than half a second

different to the average ITI duration of the whole PVT. These pseudo-randomizations were introduced to make sure that there was no temporal bias of ITI duration between objects or within the PVT.
The task was programmed in and presented with neurobs Presentation (version 16.4, www.neurobs.com/presentation).

Memory tasks

Participants performed two memory tasks after completing the fMRI session (Figure 1). The first memory task contained ten trials, one for each possible combination of a context object and a choice object (Supplementary Figure 4). In each trial, participants saw an image of a context object at the middle upper part of the screen and the image of a choice object in middle lower part of the screen (each image size 256 by 256 pixels). Additionally, an instruction text was displayed above the context object, stating “If this object would be presented in the first phase:” and continuing above the choice object “How much money would you receive if you would choose this object in the second phase?” (text font size was 30). Below this instruction, participants saw a number array from 0 to 15, with each number being surrounded by a grey frame (frame with number in it had a size of 29 by 23 pixels). At the start of each trial the number 0 was placed in a red frame. Participants could move the red frame to the left and right by using the arrow keys. If the red frame was around the number they wanted to indicate as an answer, they could press enter and the next trial started. Each trial was completely self-paced and the participants did not receive any feedback about their performance. The score for this memory task was the percentage of trials in which participants remembered the correct answer.
The task was programmed in and presented with neurobs Presentation (version 16.4, www.neurobs.com/presentation).

For the second memory task, participants were asked to place the context objects in the 2D value space. To do this, they received a piece of paper on which the 2D value space was drawn on (Supplementary Figure 5). Underneath the 2D value space, they could see all context objects. Each context object had a number and participants were instructed to use this number to indicate its location in the 2D value space. Participants received no feedback on their performance. Before this memory task, participants never received any information about the 2D value space or how the choice-reward contingencies of the context objects could be represented in this manner. The score for the task was calculated by taking the average Euclidean distance between the remembered and actual locations of all context objects.

Spatial tasks

Object-location task

To measure participants' navigational skills, we asked them to do an object-location task (paradigm was adapted from the version used in Kunz et al. (2015), using Unreal Engine 2 Runtime software, Epic Games; Figure 4). They were instructed to learn the locations of six objects in a virtual arena. None of these objects appeared in the rest of the experiment. Participants could navigate in the virtual arena, either using the mouse (virtual head direction) and the W, A, S, and D keys (walking direction: W – walking forwards, S – walking backwards, A – striving to the left, D – striving to the right) or the arrow keys (virtual head direction – left and right arrows; walking direction – forward and backward arrows). The arena had a diameter of 8000 virtual distance points.

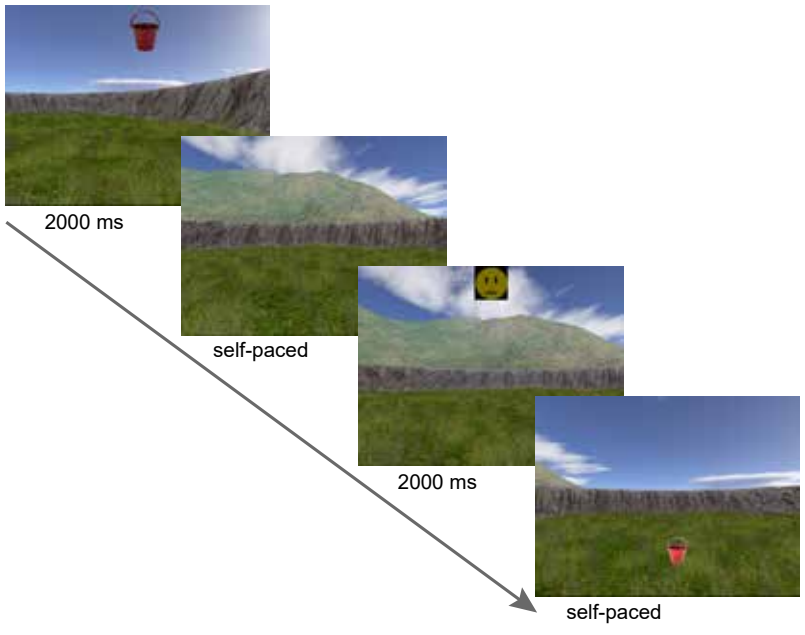

Figure 4 | Object-location task
After collecting every object at its correct location once, participants entered the second phase of the object-location task (shown here). In each trial, participants were first shown an image of the object they had to remember. The object was shown at the top of the screen for 2000 ms. Afterwards participants could freely navigate through the arena until they were at the location they remembered the object to be in. Once the participants indicated the location, they received feedback in the form of a smiley for 2000 ms. Depending on the distance between the remembered location and the actual location of the object, the smiley went from happy and green to sad and red. Here, the example shows a feedback for a neutral performance (yellow and neutral smiley). While the smiley was presented at the top of the screen, the object appeared at its actual location. The trial ended, when the participant collected the object from its actual location by walking over it.

In the first phase of the task, participants were instructed to learn the locations of the objects. To do so, an object appeared at its location and participants had to collect it by walking over it. As soon as an object was collected, the next object would appear. Participants had to collect every object once. In the second phase of the task participants had to place an object at its location. At the beginning of a trial, one of the six objects would appear at the most upper and central part of the screen for 2 seconds. Participants were instructed to navigate to the location, they thought the object belongs to and drop it there by pressing space. After dropping the object, participants received feedback in the form of a smiley at the most upper and central part of the screen for 2 seconds (Figure 4). Based on the distance between the correct location and the remembered location of the object, the smiley would change from green and happy, to yellow and neutral, and finally to red and sad. Participants received the most positive feedback for a distance error under 700 virtual distance points (less than 9% of arena diameter) and the most negative for distance error over 4500 virtual distance points (more than 56% of arena diameter). While participants received feedback in the form of the smiley, the object appeared at its correct location. To end the trial, participants had to collect the object by walking over it (as in the first phase of the task). After collection, the next trial would start. The task was completely self-paced and was ended by the experimenter after approximately 20 minutes. The score of the participants was calculated by taking the average of the Euclidean distance between the remembered and actual location of every object. The score is given in the virtual distance points of the software.

Santa Barbara Sense of Direction Scale

In the last part of the experiment, we asked participants to fill out the Santa Barbara Sense of Direction Scale (Hegarty, 2002). The SBSOD is a self-referential questionnaire about navigational abilities. Participants completed the questionnaire on a computer. The 15 Likert-type questions were subsequently presented at the centre of the screen (questions were text objects with font size 30). Participants could take as much time as they wanted per question. Under each question was a 7-point scale reaching from 'strongly agree' (1) to 'strongly disagree' (7). Each number on the scale was surrounded by a grey frame (frame with number in it had a size of 29 by 23 pixels). At the start of each trial '1' was within a red frame. Participants could move this red frame along the scale with the left and right arrow keys to indicate their answer. By pressing enter, they would confirm that the currently selected number was their final answer and the next question would appear. When scoring participants' answers, we reversed positive items, so that that a higher score translated to higher self-reported navigational abilities. The final score was the mean of all (reversed positive and non-reversed negative) items.
The task was programmed in and presented with neurobs Presentation (version 16.4, www.neurobs.com/presentation).

MRI Image acquisition

Functional T2*-weighted and anatomical images were acquired on a Magnetom Prisma 3 Tesla magnetic resonance tomograph (Siemens, Erlangen, Germany) with a 32-channel head coil. Functional images were acquired with a 4D multiband sequence with 84 slices (multi-slice mode, interleaved), TR= 1500 ms, TE= 28 ms, flip angle= 65 deg, acceleration factor PE= 2, FOV= 210 mm and an isotropic voxel size of 2 mm. An anatomical image of the brain was acquired, using a T1 sequence (MPRAGE) with TR= 2300 ms, TE= 3.03 ms, flip angle= 8 deg , FOV= 256 x 256 x 192 mm and an isotropic voxel size of 1 mm. If a time limit of 2 hours was not reached yet at the end of the scanning session two separate phase and magnitude images were acquired in order to correct for distortions with a gradient field map (multiband sequence with TR= 1020 ms, TE= 10 ms, flip angle= 45 deg and a voxel size of 3.5 x 3.5 x 2.0 mm).

fMRI preprocessing

Functional images of the four functional runs (one per PVT and two for the binary decision making task) were preprocessed with help of the FSL toolbox (version 5.0.4, http://fsl.fmrib.ox.ac.uk/fsl/fslwiki/). Motion correction and a high pass filter (cut-off: 100 s) were applied to the images. The anatomical scan of each participant was downsampled to the voxel size of the functional scans (2 mm isotropic). In order to have a common reference space for the first-level analyses, all four functional scans were linearly registered to the downsampled anatomical scan. After preprocessing, the functional output of each run was visually examined for artefacts (e.g. distortions throughout the whole brain). Participants were automatically excluded from any further analyses of the decision making task and/or the PVTs if the number of volumes that had to be excluded (i.e. regressed out in the later GLM) due to artefacts or too much movement (cut-off was 3 mm) exceeded 5% of the minimum number of volumes of a run. As a result, two participants had to be excluded from the further analyses of the PVT and one participant had to be excluded from all analyses. One additional participant was excluded from the analyses of the binary decision making task due to technical malfunctions during the recording of the logfiles. Another participant was excluded from further analyses of the PVTs due to not giving appropriate responses during the cover task (no correct responses to catch trials). This led us to doubt that this participant paid sufficient attention during the PVT. Taken together, 30 participants were included for further analyses of the PVTs and 32 participants were included for further analyses of the binary decision making task. For all participants we included the movement parameters into all first-level GLMs and if necessary additional regressors for each volume that had clear visual artefacts (on average 2.5 volumes with artefacts per run sd= 5.5).

First-level analyses

Pre and post PVT – Representational Similarity Analysis

We used representational similarity analysis to measure whether the similarity between two context objects changed as a function of distance in either 1D or 2D value space (Kriegeskorte et al., 2008). To this end, we set up a GLM in which we estimated context object-specific activation by modelling the onset and duration for each context object in a separate regressor (one GLM per PVT). We only included regular trials into these object-specific onset regressors. All catch trials were modelled in a single separate regressor. Additionally, we modelled button presses with the index and middle finger in two separate regressors.

For whole-brain analyses, we used the voxel-wise output of every object-specific onset regressor as input for a searchlight analysis. We included a grey-matter mask into the searchlight, which was based on the participant-specific (downsampled) anatomical scan. The searchlight had a radius of 3 voxels and was thresholded to include a minimum of 30 grey-matter voxels. Parameter regressor estimates of every context object were correlated with parameter regressor estimates of every other context object across all grey-matter voxels within a searchlight (Spearman's correlation coefficient). The resulting correlation matrix was written back into the centre voxel of the searchlight. The idea here is that the correlation matrix reflects neural similarity between the context objects. We then subtracted the neural similarity of the pre-PVT from the post-PVT to calculate the change in neural similarity between context objects. Finally, we could then estimate to what degree neural similarity of context objects changes as a function of their distance in either 1D or 2D value space. Hence, we created similarity matrices based on either distance. For the 1D distance, we calculated the difference in expected value for each pair of context object. The expected value for each context object was participant-specific, in the sense that we based it on the last trial of each context object in the binary decision making task. In more detail, we multiplied the probability of taking either choice (chair or lamp) with the expected value of either choice and took the sum across both weighted choices. The distance in 2D value space was calculated as the Euclidean distance between a pair of context objects. The position of a context object in the 2D value space was given by the rewards it predicted for either choice. To estimate the effect of either 1D and 2D distances, we correlated either prediction matrix with the data matrix of each searchlight.

For the ROI-analyses, we used each ROI as one searchlight. ROIs were based on MNI anatomical space. Therefore, the parameter regressor estimates of each context object (for both the pre- and post-PVT) were translated into MNI space. Subsequently, parameter regressor estimates of each context object were correlated with the parameter regressor estimates of every other context object across all voxels within an ROI. The rest of steps were in line with whole-brain analyses. However, additionally we introduced a multiple linear regression which included as predictors as constant

term, distances in 1D value space, distances in 2D value space and an interaction term between the two. This allowed us to control for shared variance between the two types of predictors.

Pre and post PVT – Adaptation Analysis

To further establish the neural effects of distance coding in 1D and 2D value space, we complemented the RSA analysis with a univariate analysis that leveraged repetition suppression (fMRI adaptation analysis). To this end, we set up a GLM for each PVT in which we set up a regressor for each possible pairing of context objects. In more detail, a regressor that for example models the pairing context object X – context object Y would contain the onset and duration of every presentation of context object Y under the condition that it was directly preceded by context object X. The idea here was that the univariate activity changes from pre-to post as a function of distance in either 1D or 2D value space. If an object is preceded by an object it has a low distance to, the activity should be lower than when preceded by an object with a high distance. This is based on the idea of fMRI repetition suppression, in which activity should be suppressed the greater the representational overlap between the current item and its predecessor (Barron et al., 2016; Grill-Spector et al., 2006; Kjelstrup et al., 2008). Additionally, we added regressors for catch trials of every context object and a regressor each for responses with the index and middle finger. For the subsequent ROI analyses, we transformed the whole-brain output of the parameter regressor estimates of each pair regressor into MNI space. We then calculated the mean response across all ROI voxels per parameter regressor estimates. To control for general different univariate responses of each context object we grouped all ROI regressor estimates where a context-object was the successor and subtracted the mean response. For all following analyses steps, we looked at the effects of both the demeaned and non-demeaned ROI regressor estimates. Importantly, we had one parameter regressor estimates per direction of each pair of context objects (X followed by Y and Y followed by X). We took the average of these two ROI regressor estimates to have a single estimation of the effect per pair. We then subtracted these averaged ROI parameter regressor estimates of the pre-PVT from the post-PVT. As a final step, we could then correlate this post-pre ROI data matrix with both distances in 1D and 2D value space, akin to the RSA analysis.

Binary decision making task

To model the fMRI data, we first estimated participant-specific behavioural parameters from the binary decision making task. For this purpose, we used a Rescorla-Wagner Model and a soft-max equation on the free-choice trials of the binary decision making task. We first did a grid search for every participant with every possible combination of 20 binned learning rates (alpha) between 0 and 1 and 15 binned temperatures (beta) between 0 and 15. We estimated on a trial-by-trial basis the context-dependent

expected value of the chosen option and the unchosen option given the current alpha ($expected\ value_{Context\ X,n+1} = expected\ value_{Context\ X,n} + \alpha^{*}(Outcome_{Context\ X,n}) - expected\ value_{Context\ X,n}$) and the context-dependent probability of the choice ($p_{Chosen,Context\ X} = \frac{\exp\left(\frac{expected\ value_{Chosen,Context\ X}}{\beta}\right)}{\exp\left(\frac{expected\ value_{Chosen,Context\ X}}{\beta}\right)+\exp\left(\frac{expected\ value_{Unchosen,Context\ X}}{\beta}\right)}$). We then calculated the temperature with the highest probability for every participant and took the group average of these winning temperatures (mean beta= 2.6667). Fixing the temperature for all participants was a compromise between taking the temperature into account and reducing the number of parameters for later analyses. Subsequently, we run our model again for every participant with 50 binned learning rates between 0 and 1 and a set temperature of the winning group average from the first round of modelling. For every participant, we chose the learning rate with the highest probability given the participant-specific data. This allowed us to estimate for every participant on a trial-by-trial basis the context-dependent expected value of the chosen and unchosen option and their probability.

We used the estimated context-dependent expected value of the chosen and unchosen option to model our fMRI data. In detail, we included the difference between the context-dependent expected value of the chosen and unchosen option as a parametric regressor on a trial-by-trial basis into our first-level GLM. This value regressor was modelled at the time point and with the duration of the presentation of each context object during free-choice trials. The value regressor was demeaned so that it was orthogonal to an onset regressor that we added for all context object presentations during free-choice trials. We also included into the GLM an onset regressor for context object presentation during forced-choice trials, an expected value regressor for the forced-choice, two separate regressors for both possible button presses, two separate regressors for the feedback of free-choice and forced-choice trials and two regressors for the learning trials and the feedback of the learning trials. We estimated the effect for every participant for the context-dependent chosen minus unchosen values by creating a contrast where the free-choice value regressor was set to 1 and all other regressors to 0. We set up a GLM for each functional run of the binary decision making task. We calculated the final effect per participant as the mean of the outputs of the two GLMs.

Second-level analyses

For whole-brain analyses, we used a one-sample permutation test. Output images from the first level analyses were entered as input, as well a whole-brain mask which only included voxels where all participants had an entry. 10000 random sign flips were performed to estimate the null distribution. We used threshold-free cluster enhancement and corrected for multiple comparison with family-wise error rate ($p_{FWE} < 0.05$).

This method for whole-brain analyses did not allow us to enter between-subject covariates. Therefore, we used a non-permuted one sample t-test to test for effects of covariates (e.g. memory scores). We entered the output images from the first-level and the covariate as input for this analysis. We corrected for multiple comparison with family-wise error rate (p_{FWE}< 0.05).
For the ROI analyses we had one entry per participant per test and used a simple one sample t-test.

Regions of interest

Based on our hypotheses, we used a-priori defined ROIs for the analyses of both the binary decision making task and the PVT blocks. We selected one mask for the hippocampus and OFC, respectively. Our hippocampus mask was based on the Harvard-Oxford subcortical structural atlas (https://fsl.fmrib.ox.ac.uk/fsl/fslwiki/Atlases). Included voxels had to fulfil two criteria: a minimum probability of 25% to be hippocampus voxels and no higher probability to belong to a region other than the hippocampus. Our OFC mask was based on the mask created by Kahnt et al. (2012) with unsupervised clustering techniques in fMRI.
We also created functional ROIs for the PVTs based on the results from the binary decision making task. The idea here was, to directly link areas within the hippocampus and OFC that code for value structures during decision making with potential uni- and multi-dimensional value map coding. We defined functional ROIs in the hippocampus and OFC as voxels that were significantly modulated by the context-dependent chosen minus unchosen values effect (small volume corrected, pFWE< 0.05). For some exploratory analyses we also defined clusters as ROIs that were modulated by the same effect and survived whole-brain correction (see Results section).

Results

Reaction times and optimal choice behaviour are modulated by context-dependent value differences of chosen and unchosen options

Participants performed the binary decision making task successfully. On average 84.30% (sd= 10.10) of participants chose the higher rewarded option per trial. Participants showed a rapid increase in performance. When evaluating average performance of participants every bin of 10 free-choice trials, we saw an average optimal choice behaviour of 48.13% in the first bin and a minimum optimal choice behaviour of 80% after the fourth bin – around 1/8th of all free-choice trials (Figure 5).

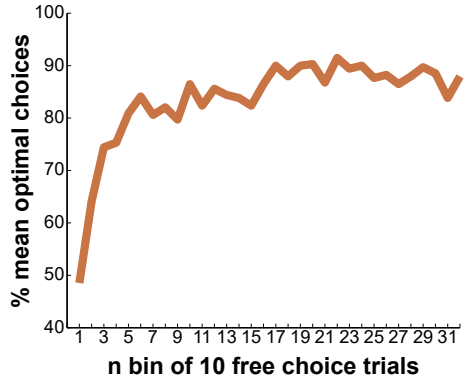

Figure 5 | Optimal choice behaviour rapidly increases over the course of the binary decision making task
Mean optimal choice behaviour was averaged for every bin of 10 free-choice trials across all participants. A trial was counted as optimal choice behaviour if a participant chose the option that led to the higher reward under the given context object of that trial. Mean optimal choice behaviour in the first bin was 48% and above 80% for every bin after the 4th bin (around 1/8th of the task).

Participants' performance during the binary decision making task was positively influenced by the context-dependent value differences between chosen and unchosen options. We performed participant-wise linear regressions for reaction times in which we included the trial-wise expected value for both the chosen and unchosen option as regressors, separately. We found a speeding effect for increasing chosen values ($T_{(29)}$= -6.5065, p< 0.0001, Figure 6A) and a slowing effect for the size of the unchosen value ($T_{(29)}$= 9.2575, p< 0.0001, Figure 6A). Furthermore, the speeding effect of the chosen value was significantly different from the slowing effect of the unchosen value

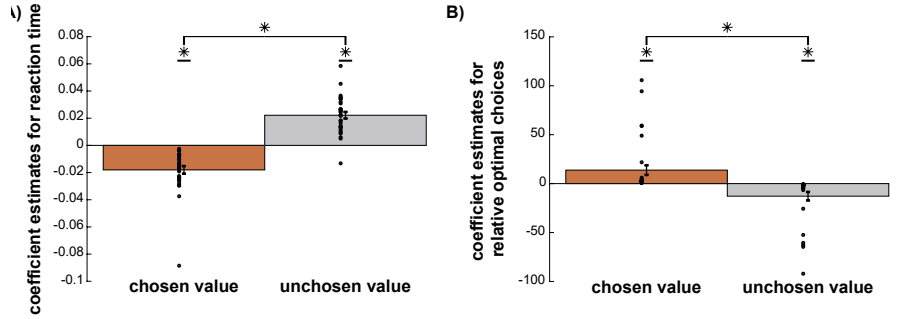

Figure 6 | Influence of chosen value and unchosen value on reaction time and optimal choice behaviour
(A) A participant-wise linear regression for reaction time was performed, with expected value of chosen and unchosen as separate regressors. Expected value of chosen option had a negative (i.e. speeding) effect on reaction times ($T_{(29)}$= -6.5065, p< 0.0001), whereas expected value of the unchosen option had a positive (i.e. slowing) effect on reaction times ($T_{(29)}$= 9.2575, p< 0.0001). The difference between the effect of expected value of chosen and unchosen was significant ($T_{(29)}$= -9.8011, p< 0.0001).

(B) A participant-wise multinomial linear regression for optimal choice behaviour was performed, with expected value of chosen and unchosen as separate regressors. Participants likelihood to choose the higher rewarded option over the lower rewarded option increased with the chosen value ($T_{(29)}$= 2.8070, p= 0.0086) and decreased with the unchosen value ($T_{(29)}$= -2.9721, p= 0.0057). The difference between the effect of chosen and unchosen value on optimal choice behaviour was significant ($T_{(29)}$= 2.9019, p< 0.0068).
Dots represent single participant values. Error bars show the standard error of the mean.

($T_{(29)}$= -9.8011, p< 0.0001, Figure 6A). We additionally performed participant-wise multinomial linear regressions for optimal choice behaviour in which we included the trial-wise expected value for both the chosen and unchosen option as regressors, separately. Participants likelihood to choose the higher rewarded option over the lower rewarded option increased with the chosen value ($T_{(29)}$= 2.8070, p= 0.0086, Figure 6B) and decreased with the unchosen value ($T_{(29)}$= -2.9721, p= 0.0057, Figure 6B). The increase in optimal choice behaviour caused by the chosen value was significantly different to the decrease in optimal choice behaviour caused by the unchosen value ($T_{(29)}$= 2.9019, p< 0.0068, Figure 6B).

Context-dependent choice-reward contingencies are tracked in the hippocampus and OFC

As a first step in our fMRI analyses, we wanted to test whether activity in the hippocampus and the OFC is modulated by context-dependent choice-reward contingencies during the binary decision making task. We modelled fMRI data during the presentation of the context objects on a trial-by-trial basis with participant-specific expected value differences between chosen and unchosen values. According to our hypothesis, we found that activity in both the OFC and hippocampus was modulated by the difference between chosen and unchosen values (both small volume corrected p_{FWE}< 0.05, Figure 7 and Supplementary Table 1).

We tested whether peak voxel activity in either ROI correlated with navigational abilities of the participants. We assessed navigational abilities with the help of an object-location task and the Santa Barbara Sense of Direction Scale (SBSOD), which participants completed after their scanning session. We included a constant term, the mean placement error of the object-location task and the score of the SBSOD, as well as an interaction term of the two into a multiple linear regression. Only the hippocampal peak voxel showed a significant effect (R^2= 0.2781, $F_{(2,29)}$= 3.5950 p= 0.0258), which seemed to be mainly driven by the mean placement error in the object-location task. We subsequently did two post-hoc correlations with only the SBSOD score and the mean placement error of the object-location task, respectively. Only the mean placement error of the object-location task was significantly related to peak voxel activity in the hippocampus (r= 0.4290, p= 0.0143, Figure 7C). Additionally, we ran a whole-brain analysis for an effect of context-dependent chosen minus unchosen values. We found two clusters, which extended the previously found bilateral OFC clusters into the insular cortex (among other areas, Figure 8 and Supplementary Table 1). An additional cluster was found, overlapping with several medial frontal areas, including the superior frontal gyrus and the anterior cingulate gyrus (Figure 8 and for a full list see Supplementary Table 1)

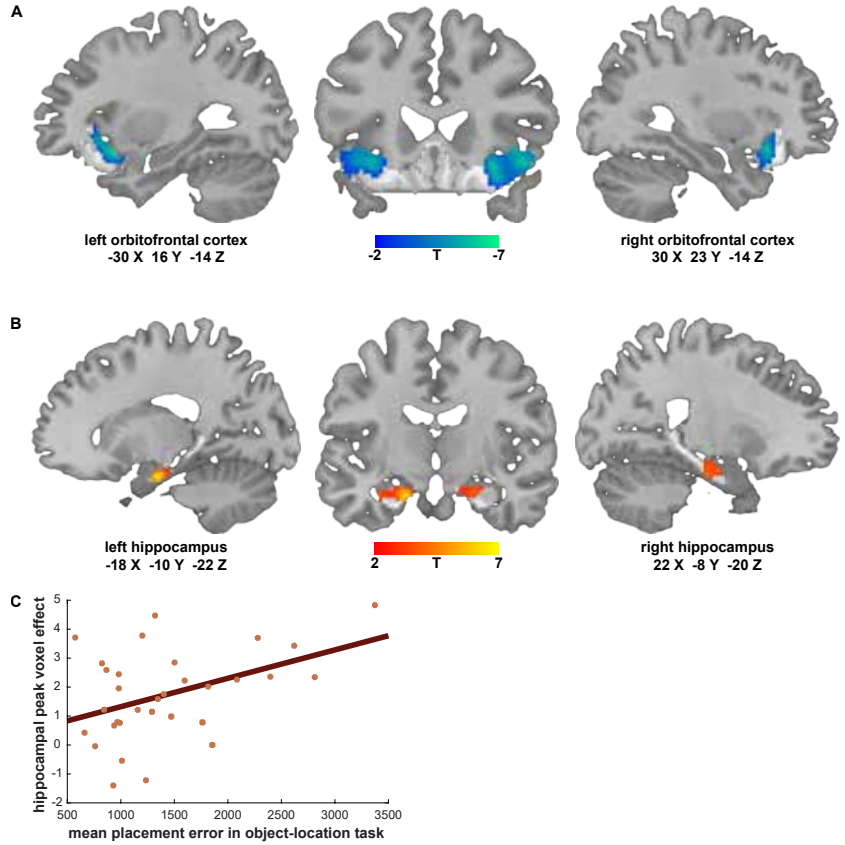

Figure 7 | Context-dependent chosen minus unchosen values modulation in the OFC and hippocampus

(A) Modulation of activity in the OFC by context-dependent chosen minus unchosen values. Bilateral clusters depicted survived small volume correction (p_{FWE}< 0.05, left cluster peak $T_{(31)}$= -6.586, right cluster peak $T_{(31)}$= -5.870). Both clusters showed a negative effect, meaning higher activity for a smaller difference between chosen and unchosen values. Coordinates for the peak voxels are given in MNI space. Image is masked for OFC voxels; see lighter area for outline of ROI. For more information, see Supplementary Table 1.

(B) Modulation of activity in the hippocampus by context-dependent chosen minus unchosen values. Bilateral clusters depicted survived small volume correction (p_{FWE}< 0.05, left cluster peak $T_{(31)}$= 6.402, right cluster peak $T_{(31)}$= 4.244). Both showed a positive effect, meaning higher activity for a bigger difference between chosen and unchosen values. Coordinates for the peak voxels are given in MNI space. Image is masked for hippocampal voxels; see lighter area for outline of ROI. For more information, see Supplementary Table 1.

(C) Hippocampal peak voxel (see B) correlation with mean placement error in the object-location task. Parameter estimates contrast effect was extracted for every participant from the hippocampal peak voxel of the context-dependent chosen minus unchosen values effect. The participant-specific peak voxel effect correlated positively with the participant-specific mean placement error in the object-location task (r= 0.4290, p= 0.0143). This means, the worse participants' average performance in the object-location task the higher the modulation of hippocampal peak voxel activity by context-dependent chosen minus unchosen values during the binary decision making task. Placement errors in the object-location task were measured with the Euclidean distance between the actual location of an object in the virtual arena and its remembered location (units are in virtual distance points).

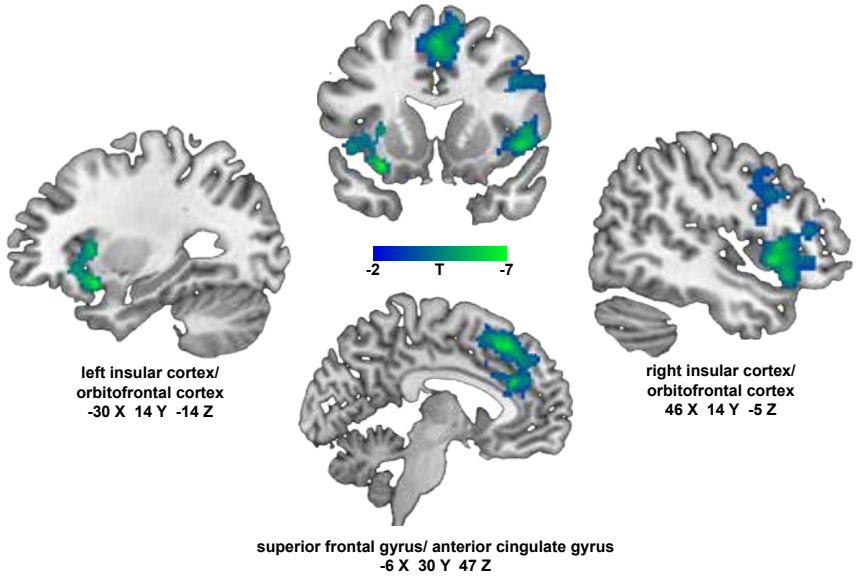

Figure 8 | Context-dependent chosen minus unchosen values modulation on whole-brain level
Clusters modulated by context-dependent chosen minus unchosen values. All clusters depicted survived whole-brain correction (p_{FWE}< 0.05, left insular/OFC cluster peak $T_{(31)}$= -7.091, right insular/OFC cluster peak $T_{(31)}$= -6.401, superior frontal gyrus/ACC cluster peak $T_{(31)}$= -6.728). All clusters showed a negative effect, meaning higher activity for a smaller difference between chosen and unchosen values. Coordinates of peak voxels are given in MNI space. Image is thresholded for whole-brain p_{FWE}< 0.05. For more information, see Supplementary Table 1.

No significant effects for distances in 2D value space in the hippocampus

We asked whether the neural pattern similarity of pairs of context objects in the hippocampus changes as a function of either distances in 1D or 2D value space. To bridge task-relevant activity and pre-post PVT representational similarity analysis (RSA) effects, we included voxels that were already significantly modulated (p_{FWE}< 0.05 svc in the hippocampus) by context-dependent chosen minus unchosen values during the binary decision making task into a functional ROI. We found neither an effect for distances in 2D value space ($T_{(29)}$= 0.5862, p= 0.5623), nor distances in 1D value space ($T_{(29)}$= 0.1121, p= 0.9115).

We also tested whether neural pattern similarity between context objects in the whole hippocampus was modulated by either distances in 1D or 2D value space. Therefore, we repeated the analyses from the functionally defined ROI for an anatomically defined ROI. Again we found no significant effect, neither for distances in 1D value space ($T_{(29)}$= 1.3417, p= 0.1901) nor in 2D value space ($T_{(29)}$= 1.3545, p= 0.1860). However it is worth noting, that we found a trend effect in the post-PVT block for distances in 2D value space ($T_{(29)}$= 1.7656, p= 0.0880, Figure 9) but not for distances in 1D value space ($T_{(29)}$=

1.4236, p= 0.1652), when exploring the data a bit further. Again, this effect vanished when controlling for the baseline pre-PVT block.

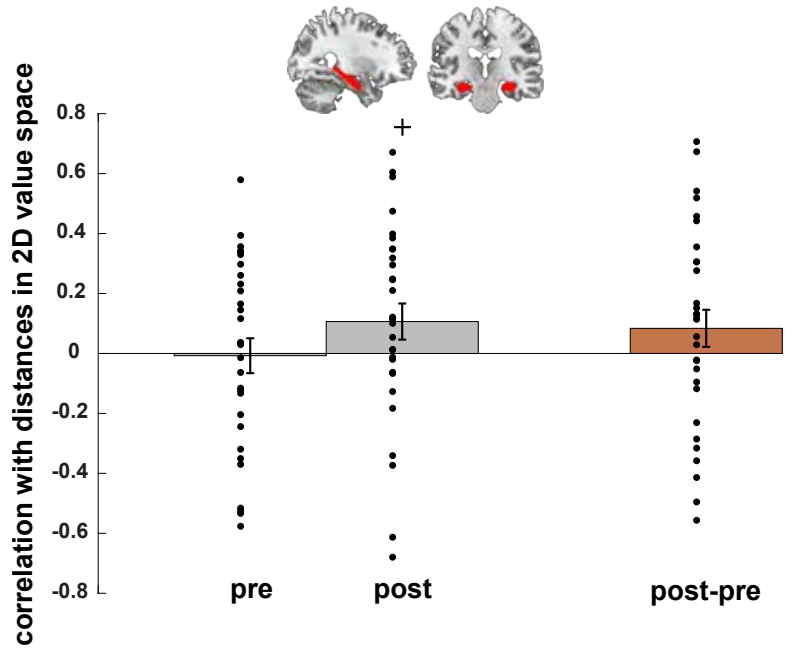

Figure 9 | Correlation of distances in 2D value space with neural pattern activity in the hippocampus
Correlation of distances in 2D value space with neural pattern similarity of anatomically defined hippocampus voxels. The ROI was used as one searchlight for the pre- and post-PVT. Within the searchlight, neural activity of each context object was correlated with the neural activity of every other context object. Pairwise neural similarity in the post-block showed a trend effect for a positive correlation with 2D distances in value space (T= 1.7656, p= 0.0880). For illustration purposes, the mean correlation is also shown for the pre-block and the change in similarity from pre- to post-block. Dots represent single participant values. Error bars show the standard error of the mean.

As an additional control, we tested a 2D value effect in the hippocampus with an adaptation analysis. Accordingly, univariate activity of an object should become lower the more of a neural representation it shares with the preceding object (Barron et al., 2016; Grill-Spector et al., 2006; Kjelstrup et al., 2008). It is important to note that we added this control analysis post-hoc, thus the randomization of the PVT blocks was not optimized for this type of analysis. In more detail, not every object preceded every other object equally amount of times, as would be ideal for adaptation analysis (as you measure the effect of the preceding object presentation on the current object presentation). A 2D value effect could also not be found with an adaptation analysis in the anatomically defined hippocampus, neither for post ($T_{(29)}$= 0.9817, p= 0.3343) nor for post minus pre ($T_{(29)}$= 0.4198, p= 0.6778). The same was true when correcting for

mean activation of every context object for both post ($T_{(29)}$= 0.9284, p= 0.3609) and post minus pre ($T_{(29)}$= 0.5503, p= 0.5863).

Lastly, we controlled whether pairs of objects that share the same optimal choice have a different change in neural similarity than pairs of objects with different optimal choices. We found neither an effect in the anatomically ($T_{(29)}$= -0.1306, p= 0.8970), nor functionally defined hippocampus ($T_{(29)}$= 0.0319, p= 0.9748).

Orbitofrontal cortex represents a one-dimensional value map

Next to the hippocampus, we tested whether the neural pattern similarity of pairs of context objects in the OFC changes as a function of either distances in 1D or 2D value space. We were particularly interested in whether voxels show an effect that are already significantly modulated (p_{FWE}< 0.05 svc in the OFC) by context-dependent chosen minus unchosen values. Therefore, we repeated the same analysis logic we applied for the hippocampus for the functional defined ROI in the OFC. We found a significant effect for distances in 1D value space ($T_{(29)}$= 2.9803, p= 0.0058, Figure 10), but not for 2D value space ($T_{(29)}$= -0.4161, p= 0.6804). The effect for distances in 1D value space was positive, meaning the greater the distance between pairs of context objects the greater their increase in neural similarity. To control for shared variance between both models, we included a constant term, the distances in 1D and 2D value space and an additional interaction term between the two as predictors in a multiple linear regression. This control analysis showed that the effect for distances in 1D value space survived ($T_{(29)}$= 2.2032, p= 0.0357) when controlling for shared variance with distances in 2D value space.

We repeated this analysis for an anatomically defined OFC ROI to test whether the effect extends beyond the previously functionally defined ROI in the OFC. We found the same pattern of results in the anatomically defined ROI, with a significant effect for distances in 1D value space ($T_{(29)}$= 2.5057, p= 0.0181, Figure 10), but not in 2D value space ($T_{(29)}$= -0.4740, p= 0.6391). However, the effect for distances in 1D value space did not survive when controlling for shared variance with distances in 2D value space as described above ($T_{(29)}$= 1.3676, p= 0.1819).

As an additional control, we tested whether we could replicate the effect with an adaptation analysis (see details above). Based on the previous RSA effect of 1D value space, univariate activity of an object should be lower if it was preceded by an object that is far away in 1D value space compared to close by. We could replicate the finding of an effect for distances in 1D value space in the functional ROI in the OFC ($T_{(29)}$= -2.1525, p= 0.0398), but not in the anatomically defined OFC ($T_{(29)}$= -0.8348, p= 0.3603). However, when correcting for the overall mean activation of each context object, there was neither an effect in the functional ROI in the OFC ($T_{(29)}$= -1.4267, p= 0.3219), nor in the anatomically defined OFC ($T_{(29)}$= -0.4732, p= 0.6396).

Lastly, we controlled whether pairs of objects that share the same optimal choice have

a different change in neural similarity than pairs of objects with different optimal choices. We found neither an effect in the anatomically ($T_{(29)}$= 1.0078, p= 0.6238), nor functionally defined OFC ($T_{(29)}$= 0.4958, p= 0.156).

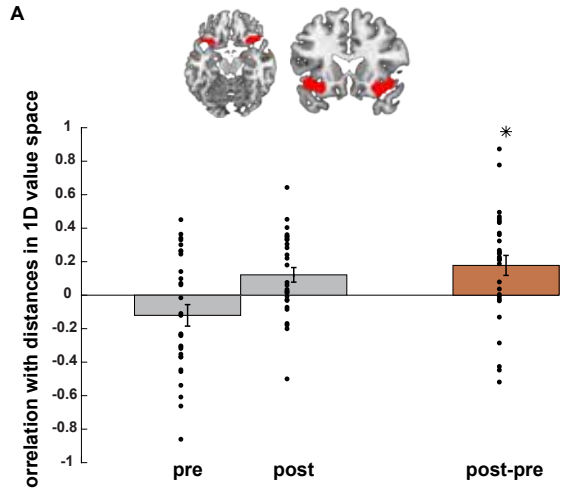

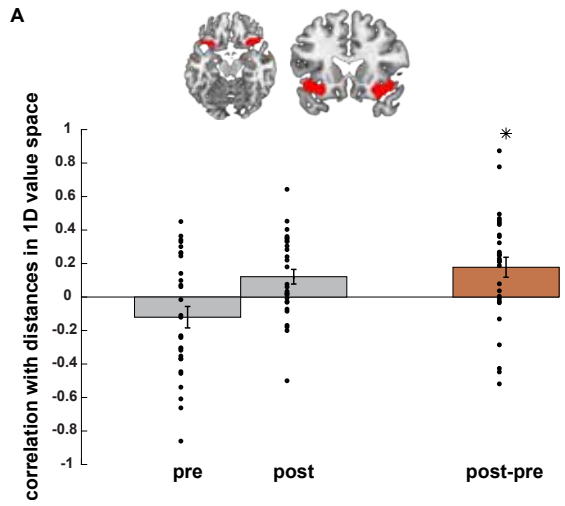

Figure 10 | Correlation of distances in 1D value space with changes in neural pattern activity in the OFC

(A) Correlation of distances in 1D value space with changes in neural pattern similarity in the functionally defined OFC ROI. The ROI included OFC voxels that were significantly modulated by context-dependent chosen minus unchosen values during the binary decision making task (p_{FWE}< 0.05). The ROI was used as one searchlight for the pre- and post-PVT. Within the searchlight, neural activity of each context object was correlated with the neural activity of every other context object. This change in pairwise neural similarity from pre to post was positively correlated with 1D distances in value space ($T_{(29)}$= 2.9803, p= 0.0058).

(B) Correlation of distances in 1D value space with changes in neural pattern activity in the anatomically defined OFC ROI. The ROI was used as one searchlight for the pre- and post-PVT. Within the searchlight, neural activity of each context object was correlated with the neural activity of every other context object. This change in pairwise neural similarity from pre to post was positively correlated with 1D distances in value space ($T_{(29)}$= 2.5057, p= 0.0181).

For illustration purposes, the mean correlation is also shown for the pre- and post-block, respectively. Dots represent single participant values. Error bars show the standard error of the mean.

Effects for distance in 1D and 2D value space on whole-brain level

Whole-brain analyses for distance coding in 2D and 1D value space yielded no effects that survived correction, respectively (p_{FWE}< 0.05, see Supplementary Figure 6 and Supplementary Figure 7 for unthresholded whole-brain maps).

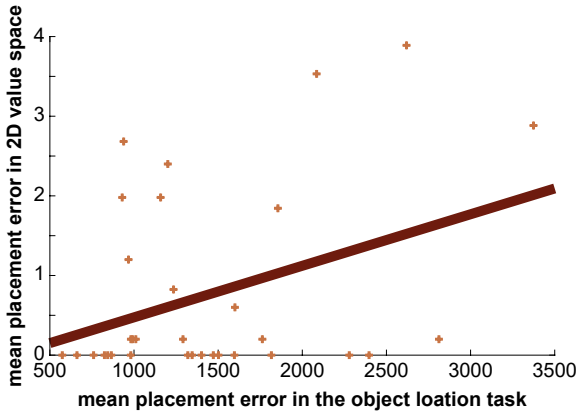

Figure 11 | Correlation of mean placement error in 2D value space with mean placement error in the object-location task
Mean placement error of context objects in 2D value space was positively correlated with mean placement error in an independent object-location task (r= 0.3679, p= 0.0352) across participants. Placement errors in 2D value space were measured with the Euclidean distance between the actual location of an object and its remembered location. Placement errors in the object-location task were measured with the Euclidean distance between the actual location of an object in the virtual arena and its remembered location (units are in virtual distance points).

Relationship between navigational abilities and remembering locations in 2D value space

We tested whether there is a relationship between navigational abilities and recall accuracy of locations in 2D value space. This was motivated by the hypothesis, that the neural mechanisms underlying spatial navigation and the representation of an abstract 2D value space are at least similar, if not shared. To this end, we used a multiple linear regression with a constant term, the scores from the SBSOD, mean placement error in the object-location task and an interaction term between the two as predictors for the mean placement error in 2D value space (R2= 0.1862, F= 2.2113, p= 0.1081). We performed two post-hoc tests, correlating the mean placement error in 2D value space with both, the SBSOD scores (r= -0.1507, p= 0.4025) and mean placement error in the object-location task (r= 0.3679, p= 0.0352, Figure 11). This suggests that if there is a relationship between navigational abilities and recall accuracy of locations in 2D value space, it is stronger for objective measurements, than self-reported navigational abilities.

Exploratory Analyses

We wanted to expand our analyses by exploring the dataset beyond our a-priori hypotheses. This gave us the opportunity to create new theories and to discuss possible explanations for lacking evidence for a robust distance coding effect in 2D value space

in the hippocampus. Although we report T and p stats in this section, we will not discuss significance since it is not informative in exploratory analyses. We added confidence intervals (CI) and standard deviation to give a clearer picture about effect sizes of the tests.

Contrasting high and low distances of 1D and 2D value space

We originally tested for parametric coding of distances in 1D and 2D value space in the hippocampus and OFC. We wanted to extend these analyses by exploring the effects of contrasting high and low distances in 1D and 2D value space. For this purpose, we performed a median-split for either type of distances. The idea was to test whether the change in similarity from pre- to post-PVT would be different for pairs of objects with high distances vs. pairs of objects with low distances between them.

The strongest, but still weak evidence for an effect of distances in 2D value space was in the anatomically defined ROI in the hippocampus ($T_{(29)}$= 1.4171, sd= 0.0158, p= 0.1671, CI= [-0.0018 0.0100], Supplementary Figure 8B). This effect was extensively weaker in the functionally defined ROI in the hippocampus ($T_{(29)}$= 0.1495, sd= 0.0312, p= 0.8822, CI= [-0.0108 0.0125], Supplementary Figure 8D). The effect in the anatomically defined hippocampus seems to be driven by a greater increase in similarity for pairs of objects with a high distance compared to pairs of objects with a low distance.

There was neither strong evidence for an effect of distances in 1D value space in the anatomically ($T_{(29)}$= 0. 1812, sd= 0.0111, p= 0.8575, CI= [-0. 0038 0.0045], Supplementary Figure 8A), nor in the functionally defined ROI in the hippocampus ($T_{(29)}$= -0.2709, sd= 0.0216, p= 0.7884, CI= [-0.0091 0.0070], Supplementary Figure 8C).

Exploratory analyses suggest a strong effect of distances in 1D value space in the anatomically defined ROI in the OFC ($T_{(29)}$= 2.1839, sd= 0.0123, p= 0.0372, CI= [0.0003 0.0095], Supplementary Figure 9A) and to a weaker extent in the functionally defined ROI in the OFC ($T_{(29)}$= 1.5855, sd= 0.0173 , p= 0.1237, CI= [-0.0015 0.0115], Supplementary Figure 9C). The effect seems to be driven by a greater increase in similarity for pairs of objects with a high distance compared to pairs of objects with a low distance. We found no strong evidence for an effect of distances in 2D value space in either the anatomically ($T_{(29)}$= -1.1329, sd= 0.0129 p= 0.2665, CI= [-0.0075, 0.0022], Supplementary Figure 9B) or functionally defined ROI in the OFC ($T_{(29)}$= 0.1325, sd= 0.174, p= 0.8955, CI= [-0.0061 0.0069], Supplementary Figure 9D).

These results are in line with the originally planned parametric analyses of distance effects in 1D and 2D value space (see above). Overall effects for distances in 1D value space in the OFC are most convincing. There was no strong evidence for distance coding in 2D value space in the hippocampus.

Inter-individual differences in representing distances in 1D and 2D value space

Since we did not find any strong evidence for a neural representation of distances in

2D value space, we wanted to explore whether this might be due to inter-individual differences. In detail, we were interested whether data suggest that inter-individual differences in representing distances in 2D value space is related to inter-individual differences in other parameters. A high variability in representing distances in 2D value space could be an explanation for the lack of strong evidence thereof. Based on this idea, we explored whether representation of distances in 2D value space correlated with mean placement error in 2D value space. In a nutshell, we explored, whether being able to place objects at their correct location in 2D value space could be related to the accuracy of how well distances are represented in the neural code. We did so in both, functionally and anatomically defined ROIs in the hippocampus and OFC. Additionally, we also correlated distances in 1D value space with the mean placement error in 2D value space as a control. Finally, we performed a whole-brain analyses in which we tested the effect of mean placement error in 2D value space by adding it as a covariate. We tested the effect of this covariate for both, correlation with distances in 1D and 2D value space with changes in neural similarity from pre to post. None of the ROI analyses showed a strong effect of mean placement error in 2D value space (Supplementary Table 2, Supplementary Figure 10 and Supplementary Figure 11). Neither were there particularly strong effects on whole-brain level (Supplementary Figure 12 and Supplementary Figure 13).

We further explored the data by repeating all of the analyses described above, but replacing mean placement error in 2D value space with optimal choice behaviour (the percentage of choices for the higher rewarded option; Supplementary Table 2, Supplementary Figure 14 and Supplementary Figure 15). The idea here was, that the representation of a 2D value space is based on differences between the context objects of the binary decision making task. Differences in context-based decision making might lead to different representation of the distances between these context objects. We found the strongest indication for such an effect in the functionally defined hippocampus (Supplementary Table 2 and Supplementary Figure 14D). Supplementary Figure 14D shows that participants who chose less often the higher rewarded option tended to have a negative effect of distance coding in 2D value space in the hippocampus. The effect for participants who chose the higher rewarded option more frequently tended to show the opposite effect, in that the pairs of objects seem to become more similar, the higher the distance in 2D value space was. There were no particularly strong effects of optimal choice behaviour on distance coding in 1D value space or 2D value space on whole-brain level (Supplementary Figure 16 and Supplementary Figure 17).

Coding of distances in 1D and 2D value space in binary decision making task related regions

For our original analyses of distance coding in 1D and 2D value space we defined functional ROIs in the hippocampus and OFC. The functional ROIs were defined by voxels that were significantly (small volume corrected) modulated by context-dependent chosen minus unchosen values during the binary decision making task. Here, we extended the analyses into ROIs that were defined by the same contrast and survived whole-brain correction (Figure 8 and Supplementary Table 1). We combined the two lateral clusters into one exploratory ROI. This ROI extended from the OFC into (amongst others) the insular cortex. As a second exploratory ROI, we used the more medial frontal cluster, covering among others the ACC and paracingulate gyrus. We repeated the pre-post RSA analyses for effects of 1D and 2D distances in value space in these two separate ROIs. The analysis steps were the same as described for the functionally and anatomically defined ROIs in the hippocampus and OFC. Results show a strong effect for coding of distances in 1D ($T_{(29)}$= 2.6153, sd= 0.3000, p= 0.0140, CI= [0.0312 0.2552]) but not 2D (T(29)= 1.4606, sd= 0.2859, p= 0.1551, CI= [-0.0305 0.1830]) value space in the medial frontal ROI (Supplementary Figure 18A & B). There was no convincing evidence for coding of distances in either 1D ($T_{(29)}$= 1.1738, sd= 0.3562, p= 0.2500, CI= [-0.0567 0.2093]) nor 2D ($T_{(29)}$= 0.2693, sd= 0.3207, p= 0.7896, CI= [-0.1040 0.1355]) value space in the bi-lateral frontal ROI (Supplementary Figure 18C & D).

Relationship between decision making and other behavioural parameters

We explored whether navigational abilities were related to performances during the binary decision making task. To this end we set up two multilinear regressions with a constant term, the scores from the SBSOD, scores from the object-location task and an interaction term between the two as predictors for either learning rate (R^2= 0.0723, F= 0.7536, p= 0.5293) or percentage of choices for the higher rewarded option (R^2= 0.0289, F= 0.2880, p= 0.8336). Neither test shows any strong indication that there is a relationship between navigational abilities and performance during the binary decision making task.

Furthermore, we explored whether remembering accurately context-dependent reward contingencies was related to performance during the binary decision making task. We used a constant term, learning rate, percentage of trials in which the higher rewarded option was chosen and an interaction term between the two as predictor in two multilinear regressions for the performance in the recognition memory task (R^2= 0.0666, F= 0.6900, p= 0.5655) and the mean placement error in 2D value space rate (R^2= 0.1190, F= 1.3053, p= 0.2916), respectively. Neither test shows any strong indication that there is a relationship between performance during the binary decision making task and remembering accurately context-dependent reward contingencies.

Discussion

We set out to test complementary roles of the OFC and hippocampus in representing values. During the decision making task, hippocampal activity was positively modulated by context-dependent differences between chosen and unchosen values. Interestingly, this contextual value modulation in the hippocampus was negatively related to navigational abilities across participants. We found no evidence for a 2D value map representation in the hippocampus from before (pre session) to after (post session) the decision making task.
The OFC showed the opposite activity pattern of the hippocampus during the decision making task. Activity in the OFC was negatively modulated by context-dependent differences between chosen and unchosen values. Furthermore, we found a multivariate value effect after (post session) compared to before (pre session) the decision making task. Neural pattern similarity in the OFC changed with the difference in the global expected value between context objects. However, this effect was in the opposite direction than we expected, with context objects becoming more similar the higher the difference in global expected values.

The hippocampus tracks context-dependent values during, but not after decision making

We found evidence for a positive modulation of the context-dependent difference between chosen and unchosen values in the bilateral hippocampus. We suspect that the hippocampus might signal here context-dependent value gains of the chosen over the unchosen choice. We know from contextual fear conditioning paradigms, that the hippocampus can perform context evaluation in the sense that it shows higher activity to negative contexts (i.e. associated with a negative outcome) than neutral or safe contexts (Alvarez et al., 2008; Maren et al., 2013; Marschner et al., 2008; Phillips & LeDoux, 1992). Our results extend these findings by demonstrating a much more fine-grained context-dependent value modulation in the hippocampus that is based on active decision making and not passive fear conditioning. Furthermore, our results expand on previous findings that show a critical role of the hippocampus during model-based decision making (Bornstein & Daw, 2013; Shohamy & Daw, 2015; Vikbladh et al., 2019). The idea here is, that the hippocampus represents task contingencies and successor representations that are used to enable flexible decision making, especially in multi-step decision making tasks (Stachenfeld et al., 2017). Our results show that the hippocampus might also code for context-dependent differences in expected value between possible options or successors.
Based on our main goal to test for a transfer of hippocampal navigational mechanisms to value representation, we correlated the context-dependent value effect in the hippocampal peak voxel with navigational abilities across participants. We used

average placement error in an object-location task as a proxy for navigational abilities. Previous studies have demonstrated a high involvement of the hippocampus in these types of virtual navigation tasks (Doeller et al., 2010; Guderian et al., 2015; Kaplan et al., 2012). Surprisingly, we found a negative relationship between navigational abilities and the size of the context-dependent value effect in the hippocampus. A recent patient study has found a positive relationship between model-based decision making and navigational abilities that seemed to be only present in controls that have an intact hippocampus (Vikbladh et al., 2019). Interestingly, we also found a positive relationship between navigational abilities and memory for context-dependent reward contingencies (Figure 11). It is important to note however, that we did not test for model-based decision making and have no direct measurement of hippocampal activity during the navigation test in our participants. Nevertheless, our results indicate that the relationship between hippocampal mechanisms in navigation and in value-based decision making might be more complex than previously thought. One interesting speculation is that hippocampal recruitment in context-dependent value representation is negatively related to hippocampal recruitment in map forming of environments or even model-based decision making. To further speculate, such a finding might speak to important inter-individual difference in the recruitment of hippocampal mechanisms like functional specialization across participants. This idea is also exciting in the light of our exploratory analysis that indicated inter-individual differences of a 2D value map representation in the functional hippocampal ROI. Optimal decision making was positively related with 2D value map representations. When looking closer, it seems that participants with less optimal choice behaviour represented a 2D value map via pattern completion (smaller distance in 2D value map results in higher neural similarity); whereas participants with more optimal decision behaviour represented a 2D value map via pattern separation (smaller distance in 2D value map results in lower neural similarity). Importantly, this exploratory analysis was based on a non-significant hippocampal value map effect and we did not have any prior hypothesis about this relationship. Nevertheless, these patterns of results accentuate the possibility that inter-individual differences might play a critical role in cognitive mapping, especially how and for what functions a cognitive map might be formed and utilized.

As mentioned above, our experiment resulted in a lack of clear evidence for a 2D value map in the hippocampus (or anywhere else in the brain). To explore the possibility of power issues, we performed a median split of object pairs based on their distances in 2D value space and compared the change in neural similarity between high and low distance object pairs. Here, we also found no indication of distance coding of a 2D value space in the hippocampus. One simple explanation for this lack of evidence might be that the hippocampus does not represent complex value structures in a map like

form. This line of thinking would support the idea that the previously demonstrated hippocampal coding of abstract maps is based on the continuous sensory features of the axes of these maps (e.g. change in tone frequency or change of leg length of a visual bird stimuli). However, we still think this explanation is less likely given that the hippocampus has been shown to also represent abstract maps that e.g. are based on discrete transition probabilities between stimuli (Garvert et al., 2017). What is unique to our study, however, is that there is no need for navigation or transitions between stimuli. In previous studies participants either navigated the abstract map actively by changing the configuration of sensory stimuli or passively by being presented with a transition structure between stimuli (Constantinescu et al., 2016; Garvert et al., 2017; Theves et al., 2019). In our study, however, there was no form of experienced transition structures (neither continuous nor discrete) between stimuli. If an experienced (active or passive) transition structure of an abstract map is a precondition for hippocampal involvement, this might be an important restriction as to what type of functions cognitive mapping can be applied to. Lastly, this would be in line with the recently proposed idea that the main function of the hippocampus is to form a predictive map that allows to make judgements about transition probabilities to future states from the current state (Stachenfeld et al., 2017).

The OFC tracks context values during and after decision making

The fact that we found evidence for value coding of contexts in the OFC during and after our binary decision making task dovetails with its known role in value-based decision making (FitzGerald et al., 2009; Gottfried et al., 2003; Jocham et al., 2011; Padoa-Schioppa & Assad, 2006; Pelletier & Fellows, 2019; Rangel et al., 2008). During the binary decision making task the lateral OFC was negatively modulated by the context-dependent difference between the chosen and unchosen values (opposed to the positive modulation in the hippocampus). This effect extended into other areas known to be involved in value coding like the insular cortex and the ACC (Doll, Duncan, et al., 2015; Preuschoff et al., 2008; Rushworth & Behrens, 2008). Importantly, we found behavioural modulation by the context-dependent difference between chosen and unchosen values as well. Participants had a higher likelihood to respond faster and more accurate the higher the expected value difference between chosen and unchosen objects. These behavioural patterns support our interpretation that the lateral OFC (and other areas such as the insular and ACC) does not merely code for values of different options under a context, but translate them into a context-dependent choice-difficulty signal. This is congruent with previous findings demonstrating that the lateral OFC (Doll, Duncan, et al., 2015; Tobler et al., 2007), ACC (Behrens et al., 2007; Rushworth & Behrens, 2008) and insular cortex (Preuschoff et al., 2008) are involved in coding for value-based uncertainty or choice probability. Furthermore, it has been shown that the lateral

OFC is functionally connected to the ACC and insular cortex, especially during the processing of reward (Zald et al., 2014). Surprisingly and incongruent with a vast amount of literature, we did not find any significant value effect during the decision making task in the medial OFC (FitzGerald et al., 2009; Hare et al., 2008; Noonan et al., 2010; Rangel et al., 2008; Rushworth et al., 2011; Rushworth & Behrens, 2008). We speculate that this absence of evidence might be (at least partially) due to participant's fast acquisition of optimal choice behaviour. As can be seen in Figure 5, participants' optimal choice behaviour was above 80% after already $1/8^{th}$ of all free-choice trials. Given that the medial OFC is especially known in coding expected values of a stimulus, the difference between chosen and unchosen values might not be a good predictor for such a modulation if choice behaviour is extremely biased towards one option (Rushworth et al., 2011).

We did however specifically test for coding of a global expected value in our pre- and post-blocks of the picture viewing task. We modelled the expected value of a context by incorporating both choice values, but weighted by the bias or probability to take one option over the other. We found that multivariate pattern similarity in both an anatomical and functional ROI of the OFC changed between context objects as a function of the difference of global expected values. In both ROIs, the neural code of context objects became less similar (from pre- to post-PVT) the lower the difference between global expected values. Importantly, the functional ROI we defined within the OFC could also be extended into a bigger cluster that extends into other areas, especially the insular cortex. Exploratory analysis shows a much weaker effect in this extended cluster. This suggests that the effect within the OFC is local. We did extend this exploratory analysis to a third ROI that covers medial frontal areas like the ACC and is also based on the univariate value effect during decision making. Here, results suggest a similar multivariate coding of context values as in the OFC.

In general, this multivariate pattern effect of expected value in the OFC nicely extends the previously established univariate effects of global expected value in the OFC (FitzGerald et al., 2009). Here, we found that the OFC integrates values of multiple reward contingencies within a context. This coincides with the crucial role the OFC has in integrating values from multi-attribute stimuli (J. D. Howard & Kahnt, 2017; Pelletier & Fellows, 2019). Additionally, our results show that these integrative value representations can be found without any active decision making or evaluating task component. During the PVT blocks, participants performed a visual comparison task that was orthogonal to our analyses and was unrelated to value-based decision making. We therefore argue that information about the global expected value of a context is reinstated automatically in the OFC and potentially other areas such as the ACC.

Interestingly, contexts were represented less similar in the OFC the more similar their global expected value was. This surprising pattern of results opens up the possibility that the OFC actively tries to separate contexts that have similar value information. If the OFC would only care about reward magnitude, we would have expected the opposite results. A recent fMRI study however has shown compelling evidence that one main function of the OFC might be to represent task states (Schuck et al., 2016). In the experiment, participants had to make judgements about the age (young vs. old) of two different categories (house or face) that were visually laid on top of each other. During a run participants had to evaluate the age of one category until the age of the previous trial did not match the current trial. In that case, participants had to start evaluating the age of the other category. This design resulted in 16 different states that could not be distinguished by sensory input, but had to be inferred through the task contingencies of category and value (in that case age). The authors could successfully decode these states from OFC activity during the task. We speculate that if the OFC distinguishes between states or contexts, this might have led to something like a pattern separation effect in our pre- to post-PVT comparison. Furthermore, this idea ties back to our univariate finding of (what we interpret as) a context-dependent value-based difficulty signal in the OFC during decision making. As a whole, our results suggest that the OFC signals for and distinguishes between context-dependent value similarities.

Conclusions

Our aim was to test complementary roles of the hippocampus and OFC in representing values. We were particularly interested, whether the hippocampus can represents distances in a 2D value space, akin to real space. For this, we found no supporting evidence. However, our results support the idea that the OFC and hippocampus have supporting roles during value-based decision making. While the hippocampus seems to signal the size of context-dependent gains between chosen and unchosen options, the OFC seems to signal for context-dependent choice difficulty. Furthermore, the OFC seems to represent global expected values of contexts after decision making and might differentiate contexts based on that value information.

Supplementary Behavioural Control Analyses

We tested participant's performance in three different domains: decision making, memory about context-dependent reward contingencies and navigational abilities. For each domain, we collected two parameters. To control for inner validity, we correlated the parameters within each domain.

Decision making

We obtained two parameters from the binary decision making task to evaluate participants' performance. The first parameter was percentage of free-choice trials in which a participant chose the higher reward option. On average participants chose the higher option in 84.15% of free-choice trials (sd= 0.1034). As a second parameter we estimated participant's learning rate with the help of a Rescorla-Wagner Model. Average learning rate was 0.2915 (sd= 0.2642).

These two parameters are not independent from each other, but we performed a correlation test as a sanity check to verify that the output from the Rescolar-Wagner model reflected choice behaviour. As expected, the correlation was significantly positive (r= 0.5889, p= 0.0003, Supplementary Figure 19).

Memory performance

Participants completed two memory tasks about the context-dependent reward contingencies. In a first recognition test, participants had to choose a value between 1 and 15 for every possible context–choice combination (5 context objects and two possible choices). Participants remembered on average 80% (sd= 22.6385) of trials the correct value. In a second memory test, participants were shown the abstract 2D value space with the axes 'value for choice of lamp' and 'value for choice of chair'. Participants were asked to indicate were in the 2D value space, a context object is located based on their reward contingencies. Participants were scored on the mean Euclidean distance between the correct and remembered location of a context object. Average mean placement error was 0.7581 (sd= 1.1709). Importantly, a higher score indicated lower memory.

As a sanity check, we correlated the score from the recognition memory test with the mean placement error in 2D value space. As expected, the correlation was significantly negative (r= -0.8027, p< 0.0001, Supplementary Figure 20). The same relationship between the memory scores was conserved when we scored the recognition task with the average difference between the real value and remembered value (r= 0.7050, p< 0.0001). Overall, these high memory scores indicate that participants learned the context-dependent reward contingencies.

Navigational abilities

Participants completed two tasks to estimate navigational abilities. The first task was the Santa Barbara Sense of Direction Scale (SBSOD), which allowed participants to score their own navigational abilities on 15 different questions. Possible score range was 1 to 7, with a higher number indicating higher self-reported navigational abilities. On average, participants had a score of 4.2848 (sd= 0.9901). The second task was an object-location task, which tested how accurately participants learned the location of different objects in a virtual arena. During probe trials, participants could navigate during the arena and indicate with a button press when they thought they were at the location of the current object. After each probe trial, they received feedback about the actual location of an object. Participants' performance was scored by the mean Euclidean distance between the remembered location and the correct location of an object, with a higher score indicating lower navigational abilities. On average, participants had a mean placement error of 1437.8 (distance given in virtual distance points, sd= 665.5389).

As a sanity check, we correlated SBSOD scores with object-location task scores. As expected, the correlation was significantly negative (r= -0.4094, p= 0.0180, Supplementary Figure 21). This indicates that subjective and objective navigational abilities were related across these two tasks.

Supplementary figures

Supplementary Figure 1 | Context objects
Five different objects were presented during the (pre and post) picture viewing task. These objects were used as context objects during the binary decision making task. The idea was to measure the change in neural pattern similarity between the context objects from pre to post as a function of their distance in 1D and 2D value space. The objects were a bed, a desk, a bathtub, a trash can and a bookshelf. The location of context objects in the different kinds of value spaces was randomized across participants. The gray frame around the object images is used here for illustration purposes and was not part of the object images during the experiment.

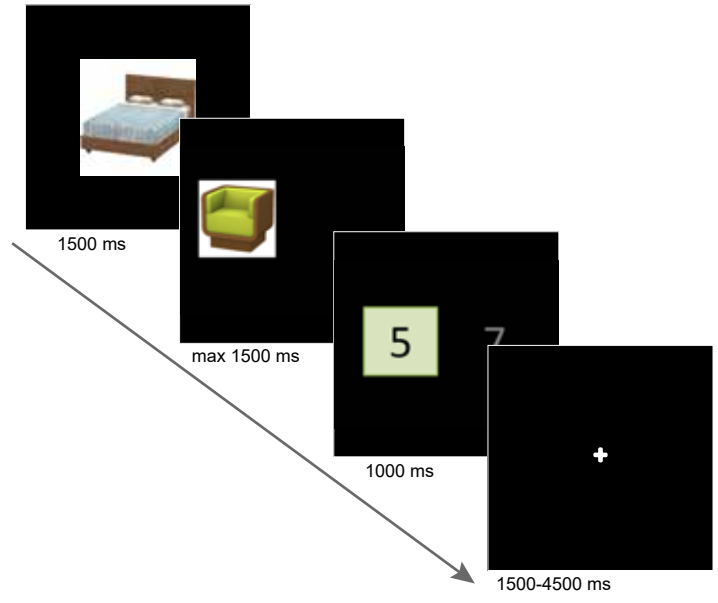

Supplementary Figure 2 | Forced-choice trial of binary decision making task
Forced-choice trials of the binary decision making task were structured in three phases. In the first phase one of five different context objects was shown (here the bed) for 1500 ms. In the second phase only the choice object that was lower rewarded was presented until the participant made a forced-choice or 1500 ms elapsed. In the third phase, the participant was presented with a feedback about the reward they received for their forced-choice and the reward they could not receive in this trial. The received reward was indicated with a green box and the feedback was shown for 1000 ms. After the trial ended a white fixation cross was presented with a duration of either 1500, 3000, or 4500 ms.

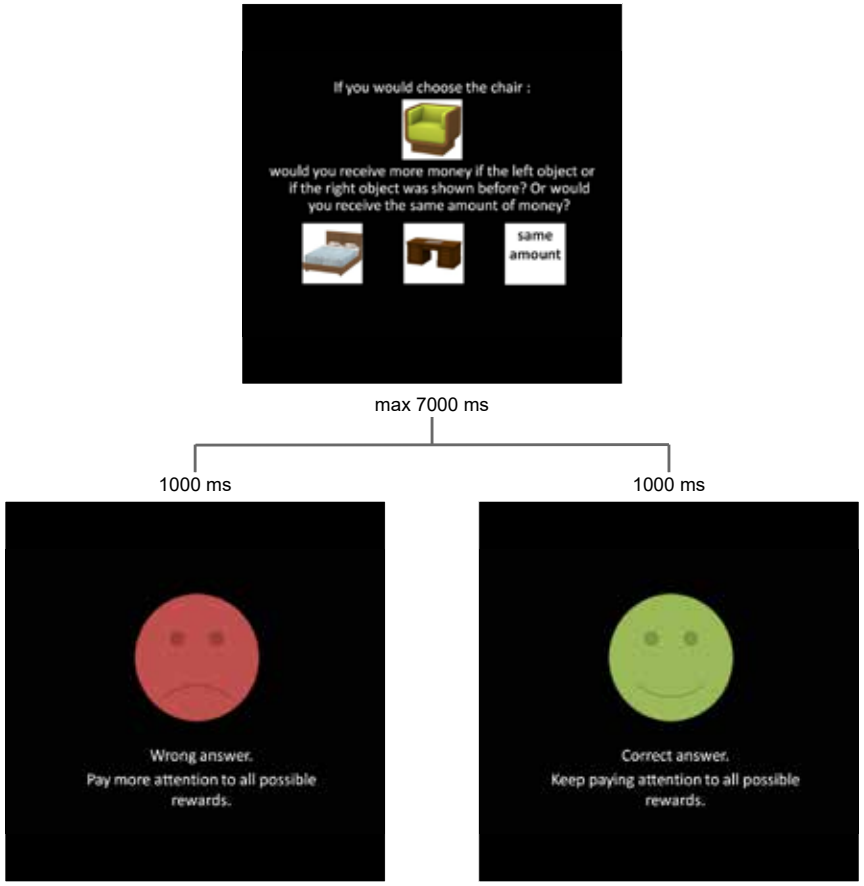

Supplementary Figure 3 | Learning trial of the binary decision making task
Learning trials of the binary decision making task were structured in two phases. In the first phase, participants were asked to compare the outcome of two context objects for a given choice. In the example shown, the participant would give an answer of whether they would receive more reward for the choice of chair under the context object bed or the context object desk. As a third option, participants could answer that both context objects predict the same reward for the option chair. The question was presented until the participant responded or 7000 ms elapsed. In the second phase, participants were presented with a feedback about their answer for 1000 ms. If the answer was incorrect or a participant did not give an answer during phase one, they received a negative feedback (red smiley). If the answer was correct, participants received a position feedback (green smiley).

Supplementary Figure 4 | Recognition test of context dependent reward contingencies
Participants were shown each possible combination of context objects and choice objects separately in 10 trials (5 context objects paired with 2 choice objects). Participants were asked how much reward they would receive for each context and choice combination. Participants could choose a value between 0 and 15 by moving the red box along the value scale shown below the instruction. Participants used the left and right arrow key to navigate along the value scale and could indicate their final answer by pressing enter. The task was completely self-paced and participants received no feedback.

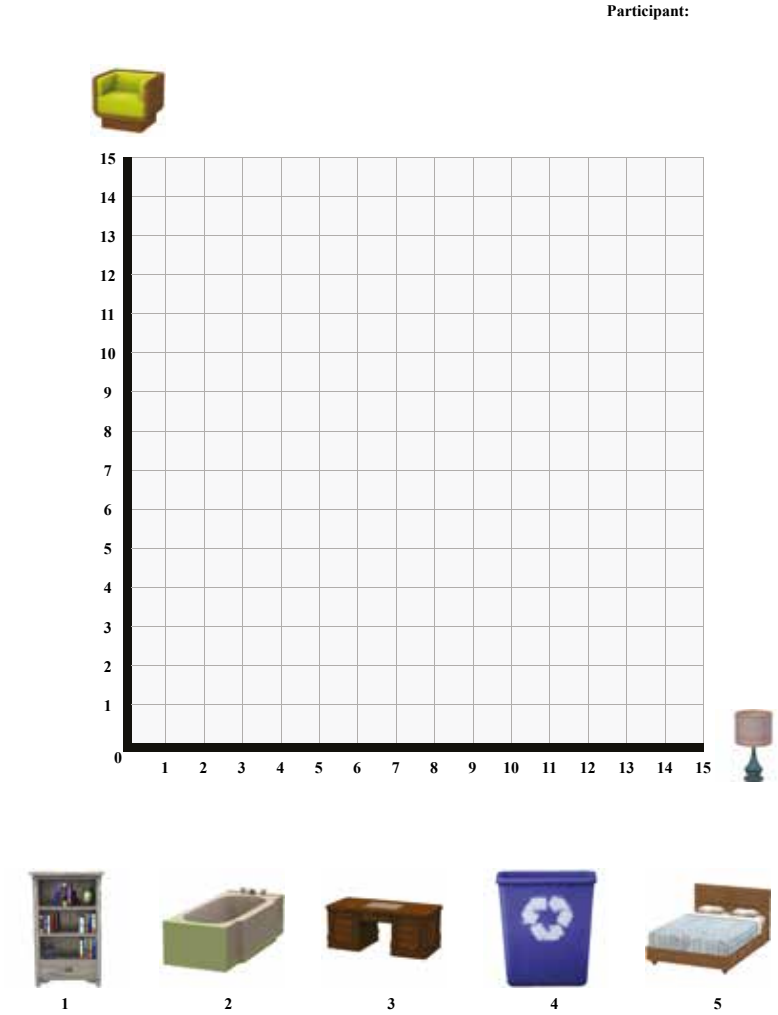

Supplementary Figure 5 | Placement task in 2D value space
Participants were given a sheet of paper with the 2D value space drawn on. The dimension for either choice (lamp and chair) ranged from 0 to 15. Underneath, participants saw all five context objects, which were numbered 1 to 5. Participants were instructed to use this number to indicate the location of a context object in the 2D value space.

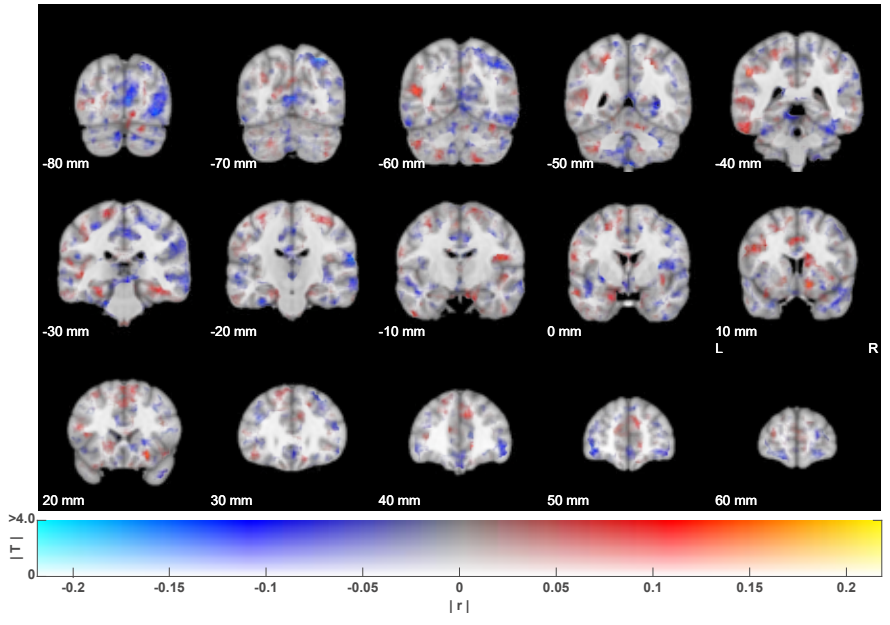

Supplementary Figure 6 | Change in neural pattern similarity as a function of distances in 2D value space
The change in neural pattern similarity between context objects from pre-PVT to post-PVT was correlated with their distances in 2D value space. No effect survived whole-brain correction. The image was created using a dual-coded design (Allen et al., 2012; Zandbelt, 2017). This allowed showing both, the correlation value (blue-red) and the T stats (opacity). Y-coordinates are in MNI space.

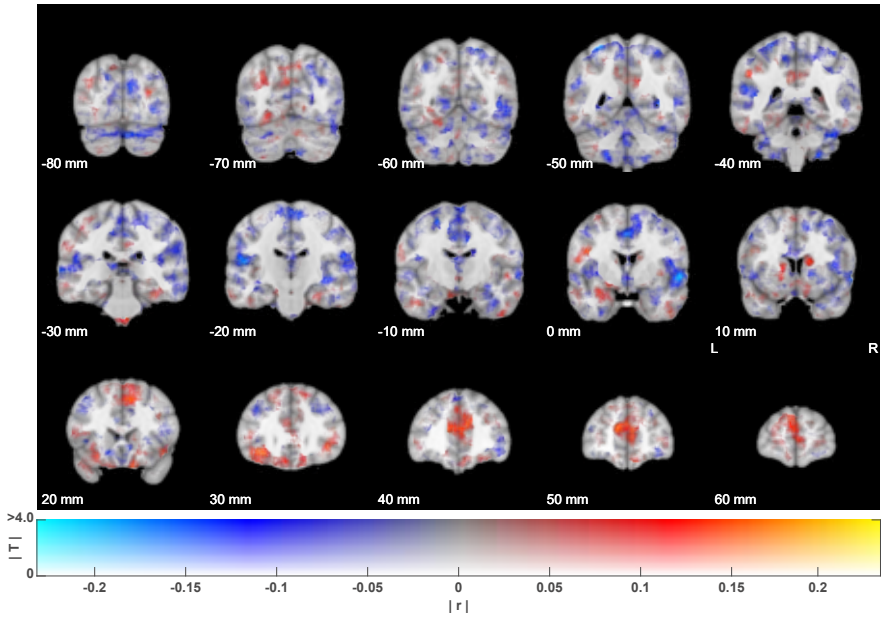

Supplementary Figure 7 | Change in neural pattern similarity as a function of distances in 1D value space

The change in neural pattern similarity between context objects from pre-PVT to post-PVT was correlated with their distances in 1D value space. No effect survived whole-brain correction. The image was created using a dual-coded design (Allen et al., 2012; Zandbelt, 2017). This allowed showing both, the mean correlation coefficient (blue-red) and the T stats (opacity). Y-coordinates are in MNI space.

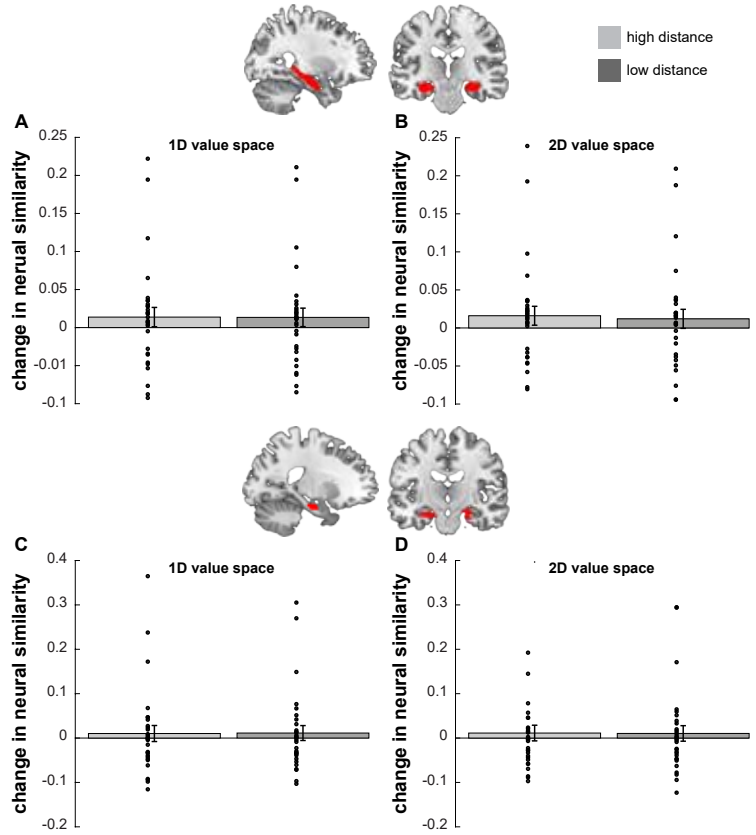

Supplementary Figure 8 | Effects of high and low distances in the anatomically and functionally defined hippocampus

(A) Pairs of objects were grouped into high distance and low distance by a median split along the distances in 1D value space. Anatomically defined voxels in the hippocampus were included into one searchlight for the pre- and post-PVT.

(B) Pairs of objects were grouped into high distance and low distance by a median split along the distances in 2D value space. Anatomically defined voxels in the hippocampus were included into one searchlight for the pre- and post-PVT.

(C) Pairs of objects were grouped into high distance and low distance by a median split along distances in 1D value space. Functionally defined voxels in the hippocampus were included into one searchlight for the pre- and post-PVT. The ROI was defined by hippocampal voxels that were significantly modulated by context-dependent differences in chosen minus unchosen values during the binary decision making task.

(D) Pairs of objects were grouped into high distance and low distance by a median split along distances in 2D value space. Functionally defined voxels in the hippocampus were included into one searchlight for the pre- and post-PVT. The ROI was defined by hippocampal voxels that were significantly modulated by context-dependent differences in chosen minus unchosen values during the binary decision making task.

Mean change of neural similarity from pre to post is shown for both, pairs of objects with high and with low distances, respectively.
Dots represent single participant values. Error bars show the standard error of the mean.

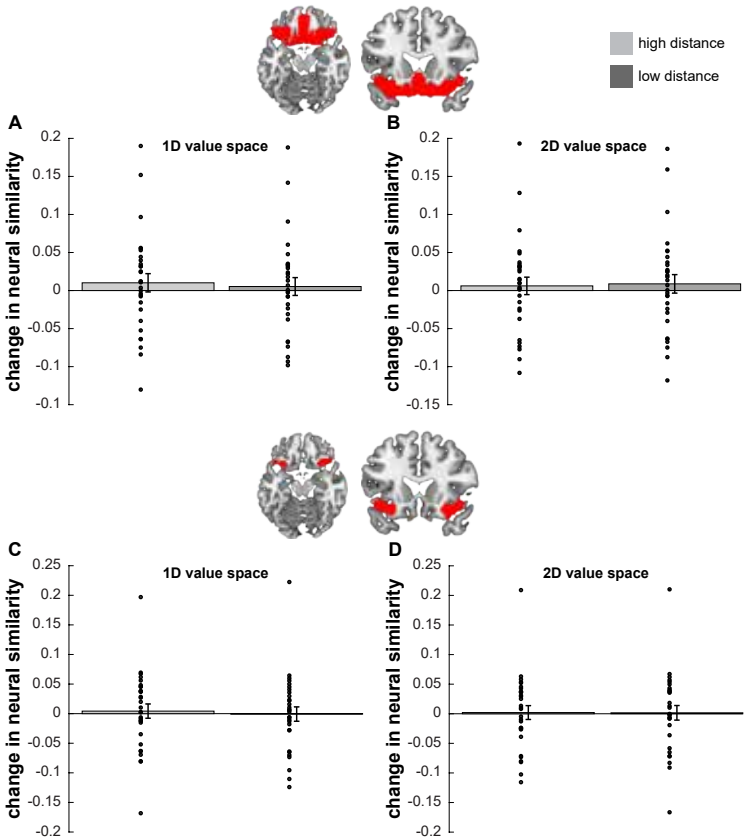

Supplementary Figure 9 | Effects of high and low distances in the anatomically and functionally defined OFC
(A) Pairs of objects were grouped into high distance and low distance by a median split along the distances in 1D value space. Anatomically defined voxels in the OFC were included into one searchlight for the pre- and post-PVT.

(B) Pairs of objects were grouped into high distance and low distance by a median split along the distances in 2D value space. Anatomically defined voxels in the OFC were included into one searchlight for the pre- and post-PVT.

(C) Pairs of objects were grouped into high distance and low distance by a median split along the distances in 1D value space. Functionally defined voxels in the OFC were included into one searchlight for the pre- and post-PVT. The ROI was defined by OFC voxels that were significantly modulated by context-dependent differences in chosen minus unchosen values during the binary decision making task.

(D) Pairs of objects were grouped into high distance and low distance by a median split along the distances in 2D value space. Functionally defined voxels in the OFC were included into one searchlight for the pre- and post-PVT. ROI was defined by OFC voxels that were significantly modulated by context-dependent differences in chosen minus unchosen values during the binary decision making task.

Mean change of neural similarity from pre to post is shown for both, pairs of objects with high and with low distances, respectively.

Dots represent single participant values. Error bars show the standard error of the mean.

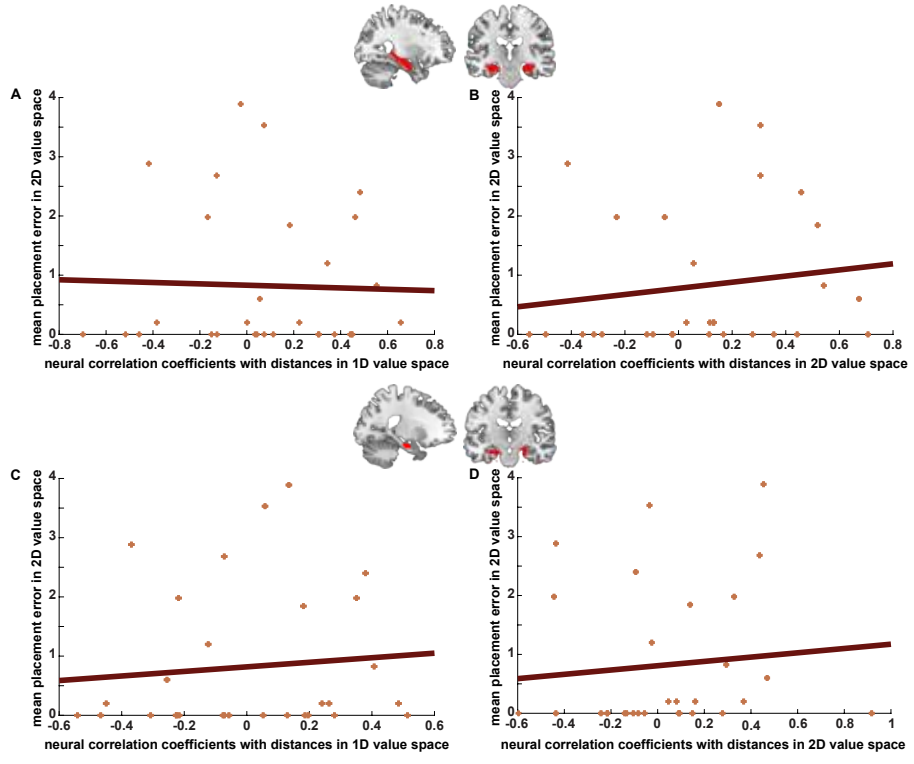

Supplementary Figure 10 | Correlation of (1D and 2D) distance effects in the anatomical and functional hippocampus ROI with mean placement error in 2D value space
(A) Correlation of 1D distance effect in the anatomical hippocampus ROI with mean placement error in 2D value space (r= -0.0329, p= 0.8630).

(B) Correlation of 2D distance effect in the anatomical hippocampus ROI with mean placement error in 2D value space (r= 0.1451, p= 0.6053).

(C) Correlation of 1D distance effect in the functional hippocampus ROI with mean placement error in 2D value space (r= 0.0938, p= 0.6218). The ROI was defined by hippocampal voxels that were significantly modulated by context-dependent differences in chosen minus unchosen values during the binary decision making task.

(D) Correlation of 2D distance effect in the functional hippocampus ROI with mean placement error in 2D value space (r= 0.0983, p= 0.6053). The ROI was defined by hippocampal voxels that were significantly modulated by context-dependent differences in chosen minus unchosen values during the binary decision making task.

1D and 2D distance effects are estimated by the correlation of changes in neural pattern similarity between context object from pre- to post-PVT with distances in 1D and 2D value space, respectively.
Placement errors in 2D value space were measured with the Euclidean distance between the actual location of an object and its remembered location. A low score reflects better memory.

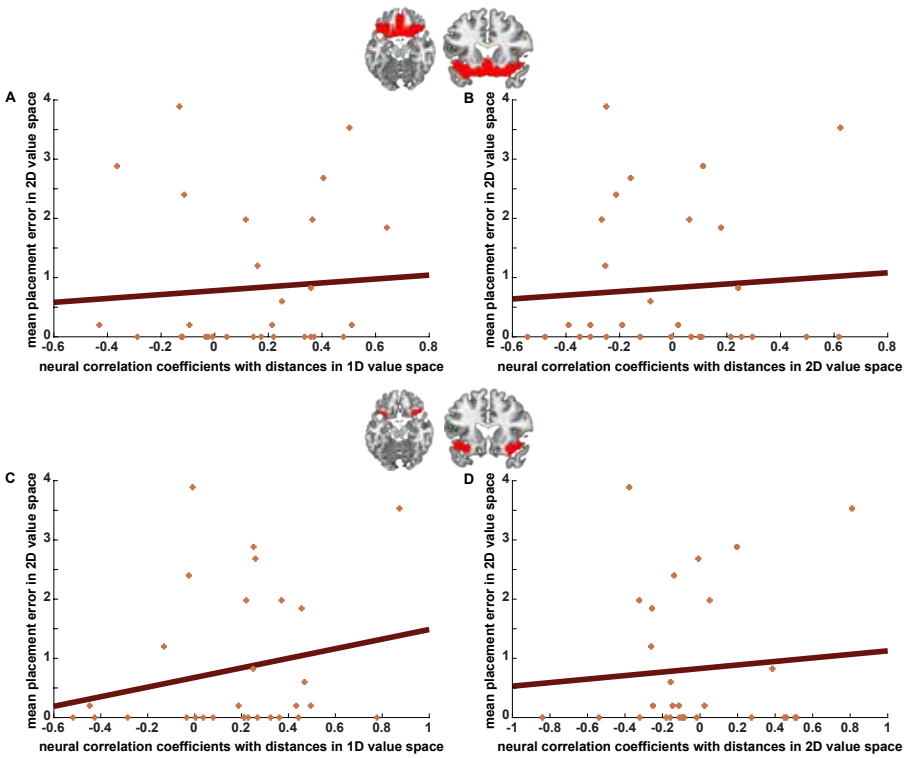

Supplementary Figure 11 | Correlation of (1D and 2D) distance effects in the anatomical and functional OFC ROI with mean placement error in 2D value space
(A) Correlation of 1D distance effect in the anatomical OFC ROI with mean placement error in 2D value space (r= 0.0749, p= 0.6939).

(B) Correlation of 2D distance effect in the anatomical OFC ROI with mean placement error in 2D value space (r= 0.0796, p= 0.6759).

(C) Correlation of 1D distance effect in the functional OFC ROI with mean placement error in 2D value space (0.2186, p= 0.2458). The ROI was defined by OFC voxels that were significantly modulated by context-dependent differences in chosen minus unchosen values during the binary decision making task.

(D) Correlation of 2D distance effect in the functional OFC ROI with mean placement error in 2D value space (r= 0.0861, p= 0.6511). The ROI was defined by OFC voxels that were significantly modulated by context-dependent differences in chosen minus unchosen values during the binary decision making task.

1D and 2D distance effects are estimated by the correlation of changes in neural pattern similarity between context object from pre- to post-PVT with distances in 1D and 2D value space, respectively.
Placement errors in 2D value space were measured with the Euclidean distance between the actual location of an object and its remembered location. A low score reflects better memory.

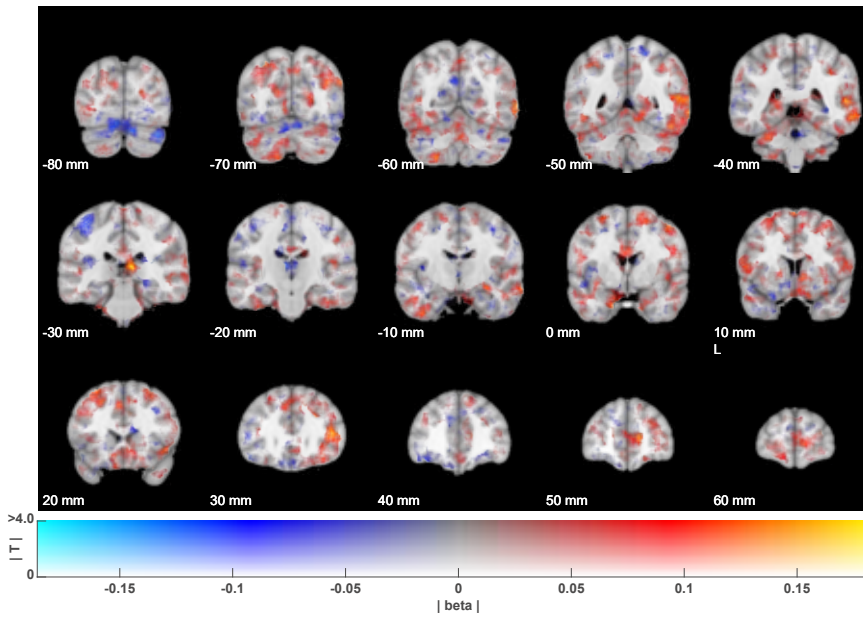

Supplementary Figure 12 | Change in neural pattern similarity as a function of distances in 1D value space weighted by mean placement error in 2D value space
The change in neural pattern similarity between context objects from pre-PVT to post-PVT was correlated with their distances in 1D value space. Participants' correlation coefficients were weighted with their mean distance error in 2D value space. Placement errors in 2D value space were measured with the Euclidean distance between the actual location of an object and its remembered location. A low score reflects better memory. The image was created using a dual-coded design (Allen et al., 2012; Zandbelt, 2017). This allowed showing both, the beta value/ weighted mean correlation coefficient (blue-red) and the T stats (opacity). Y-coordinates are in MNI space.

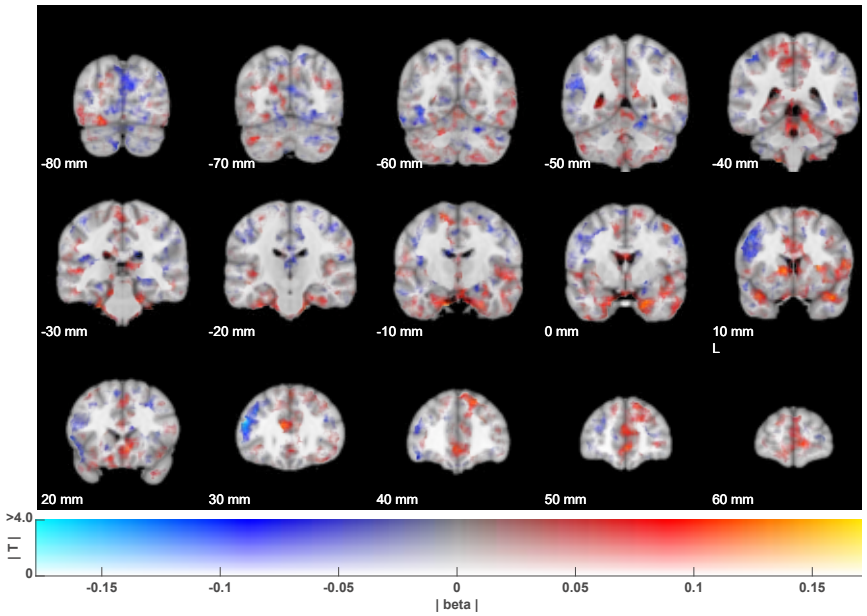

Supplementary Figure 13 | Change in neural pattern similarity as a function of distances in 2D value space weighted by mean placement error in 2D value space
The change in neural pattern similarity between context objects from pre-PVT to post-PVT was correlated with their distances in 2D value space. Participants' correlation coefficients were weighted with their mean distance error in 2D value space. Placement errors in 2D value space were measured with the Euclidean distance between the actual location of an object and its remembered location. A low score reflects better memory. The image was created using a dual-coded design (Allen et al., 2012; Zandbelt, 2017). This allowed showing both, the beta value/ weighted mean correlation coefficient (blue-red) and the T stats (opacity). Y-coordinates are in MNI space.

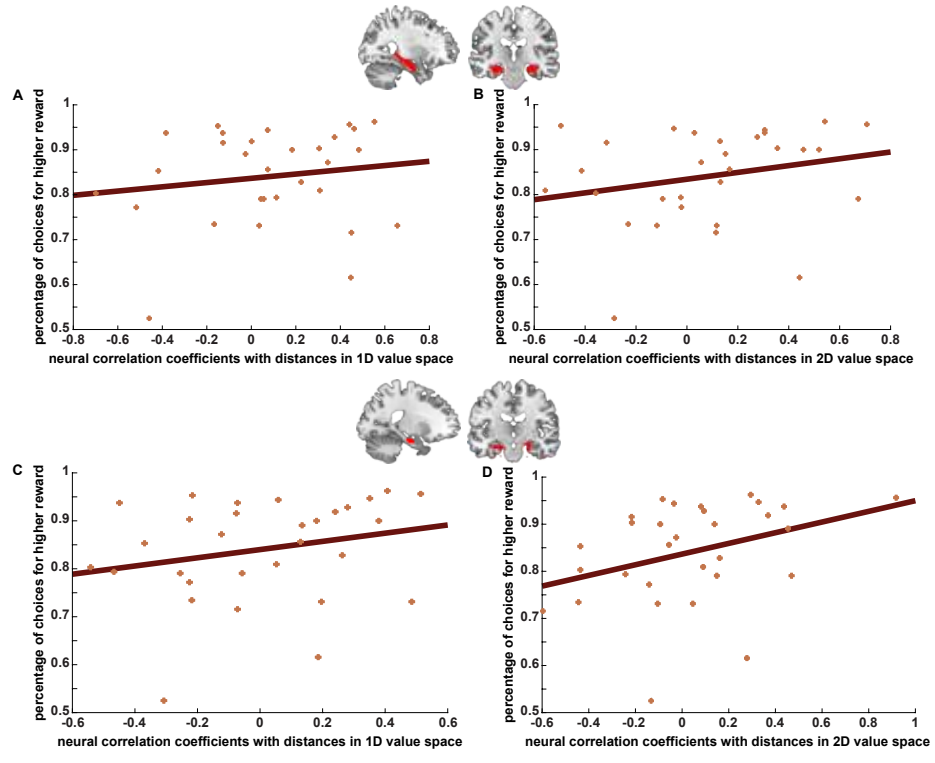

Supplementary Figure 14 | Correlation of (1D and 2D) distance effects in the anatomical and functional hippocampus ROI with percentage of choices for higher rewarded option
(A) Correlation of 1D distance effect in the anatomical hippocampus ROI with percentage of choices for higher rewarded option (r= 0.1536, p= 0.4178).

(B) Correlation of 2D distance effect in the anatomical hippocampus ROI with percentage of choices for higher rewarded option (r = 0.2401, p= 0.2013).

(C) Correlation of 1D distance effect in the functional hippocampus ROI percentage of choices for higher rewarded option (r= 0.2360 p= 0.2092). The ROI was defined by hippocampal voxels that were significantly modulated by context-dependent differences in chosen minus unchosen values during the binary decision making task.

(D) Correlation of 2D distance effect in the functional hippocampus ROI with percentage of choices for higher rewarded option (r= 0.3455, p= 0.0615). The ROI was defined by hippocampal voxels that were significantly modulated by context-dependent differences in chosen minus unchosen values during the binary decision making task.

1D and 2D distance effects are estimated by the correlation of changes in neural pattern similarity between context object from pre- to post-PVT with distances in 1D and 2D value space, respectively.
Percentage of choices for the higher reward options was calculated from all free-choice trials during the binary decision making task.

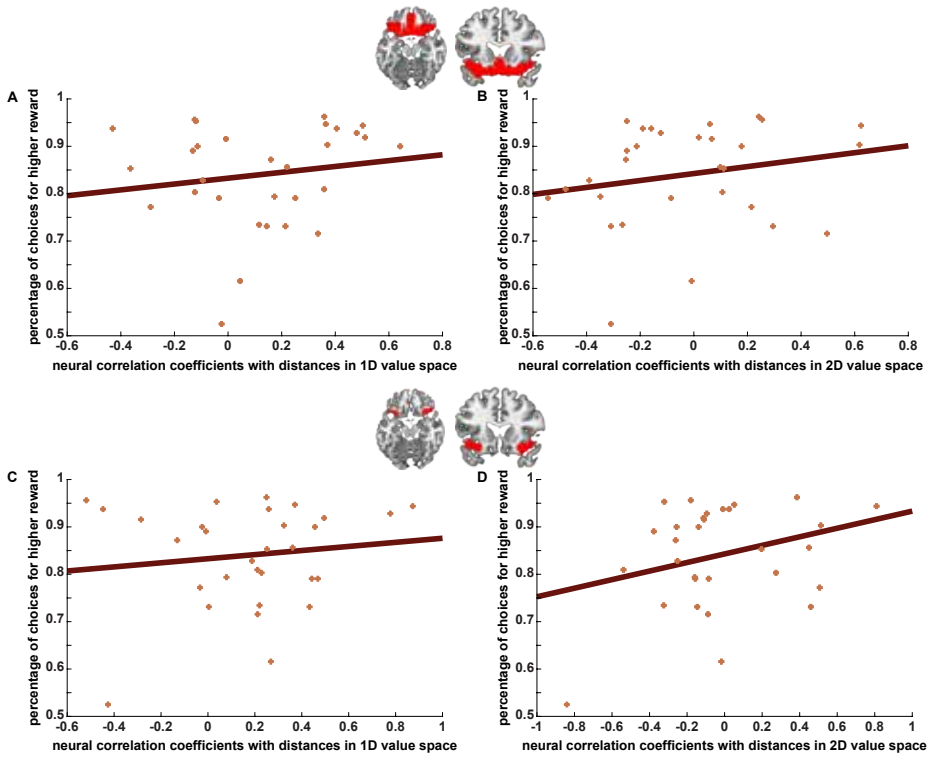

Supplementary Figure 15 | Correlation of (1D and 2D) distance effects in the anatomical and functional OFC ROI with percentage of choices for higher rewarded option
(A) Correlation of 1D distance effect in the anatomical OFC ROI with percentage of choices for higher rewarded option (r= 0.1599, p= 0.3986).

(B) Correlation of 2D distance effect in the anatomical OFC ROI with percentage of choices for higher rewarded option (r= 0.2096, p= 0.2662).

(C) Correlation of 1D distance effect in the functional OFC ROI percentage of choices for higher rewarded option (r= 0.1321, p= 0.4866). The ROI was defined by OFC voxels that were significantly modulated by context-dependent differences in chosen minus unchosen values during the binary decision making task.

(D) Correlation of 2D distance effect in the functional OFC ROI with percentage of choices for higher rewarded option (r= 0.2959, p= 0.1124). The ROI was defined by OFC voxels that were significantly modulated by context-dependent differences in chosen minus unchosen values during the binary decision making task.

1D and 2D distance effects are estimated by the correlation of changes in neural pattern similarity between context object from pre- to post-PVT with distances in 1D and 2D value space, respectively.
Percentage of choices for the higher reward options was calculated from all free-choice trials during the binary decision making task.

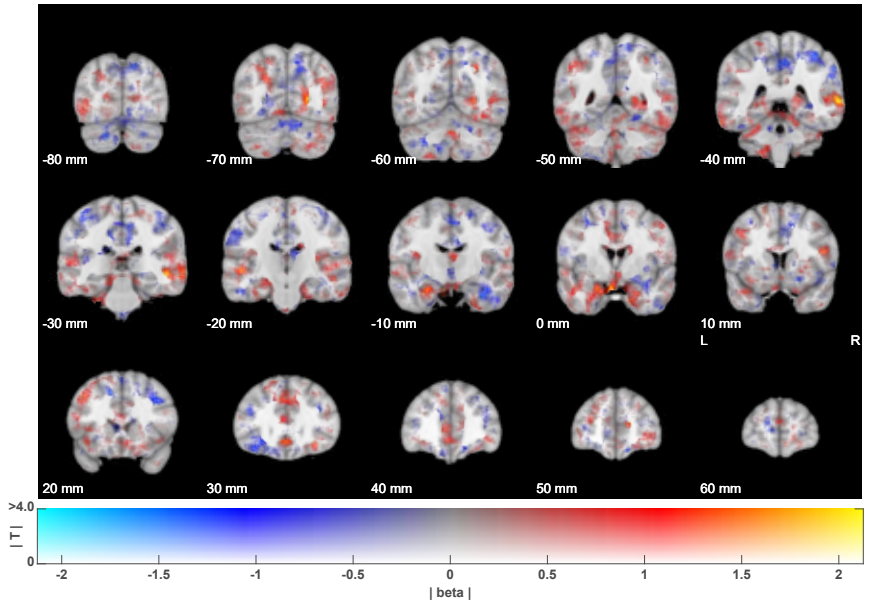

Supplementary Figure 16 | Change in neural pattern similarity as a function of distances in 1D value space weighted percentage of choices for the higher rewarded option
The change in neural pattern similarity between context objects from pre-PVT to post-PVT was correlated with their distances in 1D value space. Participants' correlation coefficients were weighted with their percentage of choices for the higher rewarded option. Percentage of choices for the higher reward options was calculated from all free-choice trials during the binary decision making task. The image was created using a dual-coded design (Allen et al., 2012; Zandbelt, 2017). This allowed showing both, the beta value/weighted mean correlation coefficient (blue-red) and the T stats (opacity). Y-coordinates are in MNI space.

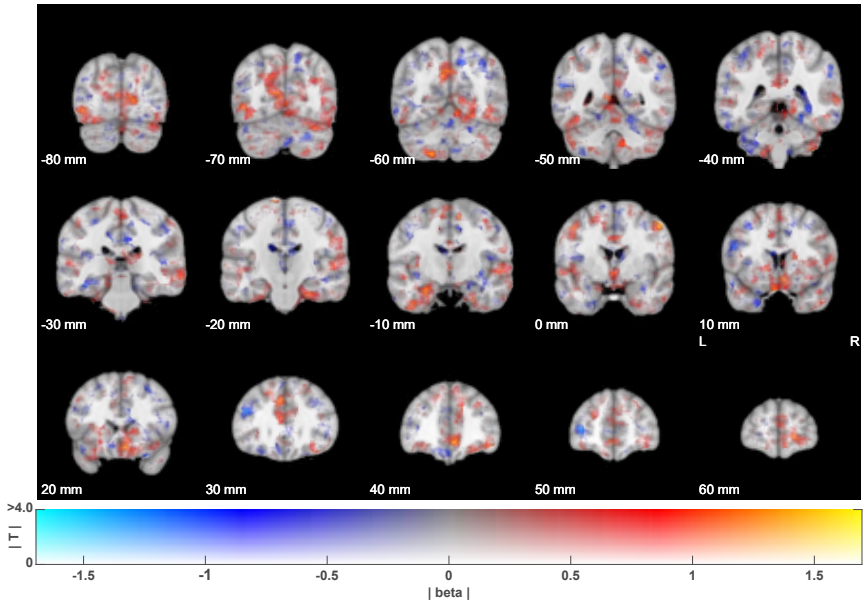

Supplementary Figure 17 | Change in neural pattern similarity as a function of distances in 2D value space weighted percentage of choices for the higher rewarded option
The change in neural pattern similarity between context objects from pre-PVT to post-PVT was correlated with their distances in 2D value space. Participants' correlation coefficients were weighted with their percentage of choices for the higher rewarded option. Percentage of choices for the higher reward options was calculated from all free-choice trials during the binary decision making task. The image was created using a dual-coded design (Allen et al., 2012; Zandbelt, 2017). This allowed showing both, the beta value/weighted mean correlation coefficient (blue-red) and the T stats (opacity). Y-coordinates are in MNI space.

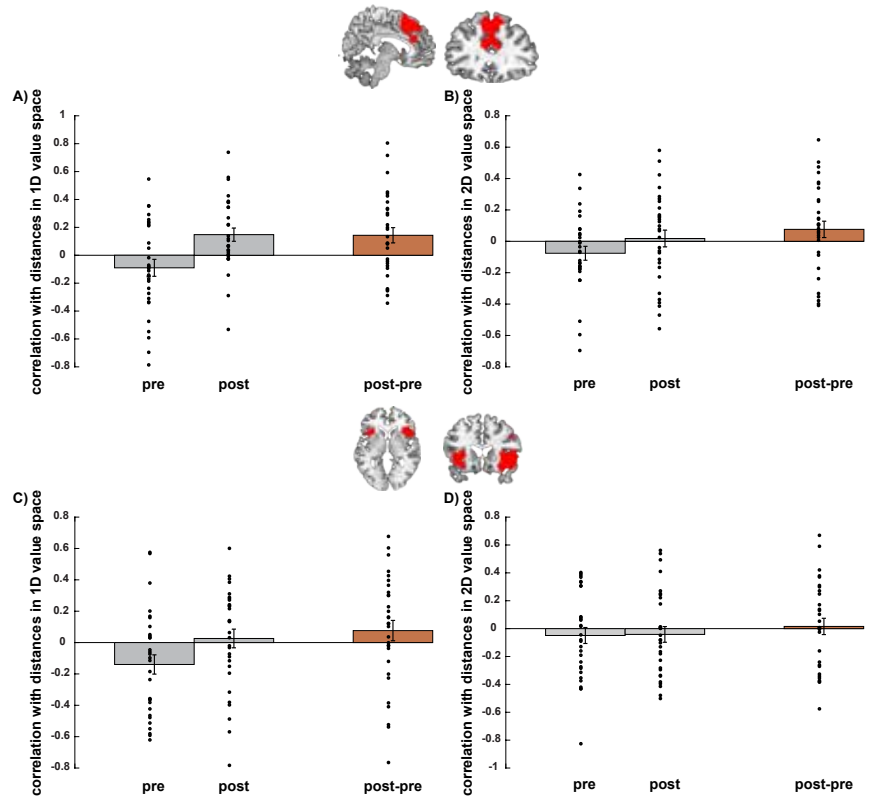

Supplementary Figure 18 | Correlation of distances in 1D and 2D value space with neural pattern activity in the medial frontal and lateral frontal ROI
(A) Correlation of distances in 1D value space with changes in neural pattern similarity in the medial frontal voxels related to the binary decision making task. The ROI included a medial frontal cluster that was significantly modulated by context-dependent chosen minus unchosen values during the binary decision making task.

(B) Correlation of distances in 2D value space with changes in neural pattern similarity in the medial frontal voxels related to the binary decision making task. The ROI included a medial frontal cluster that was significantly modulated by context-dependent chosen minus unchosen values during the binary decision making task.

(C) Correlation of distances in 1D value space with changes in neural pattern similarity in the lateral frontal voxels related to the binary decision making task. The ROI included a lateral frontal cluster that was significantly modulated by context-dependent chosen minus unchosen values during the binary decision making task.

(D) Correlation of distances in 2D value space with changes in neural pattern similarity in the lateral frontal voxels related to the binary decision making task. The ROI included a lateral frontal cluster that was significantly modulated by context-dependent chosen minus unchosen values during the binary decision making task.

The ROIs were used as one searchlight for the pre- and post-PVT. Within the searchlight, neural activity of each context object was correlated with the neural activity of every other context object. This change in pairwise neural similarity from pre to post was then correlated with distances in 1D and 2D value space, respectively. For illustration purposes, the mean correlation is also shown for the pre- and post-block, separately. Dots represent single participant values. Error bars show the standard error of the mean.

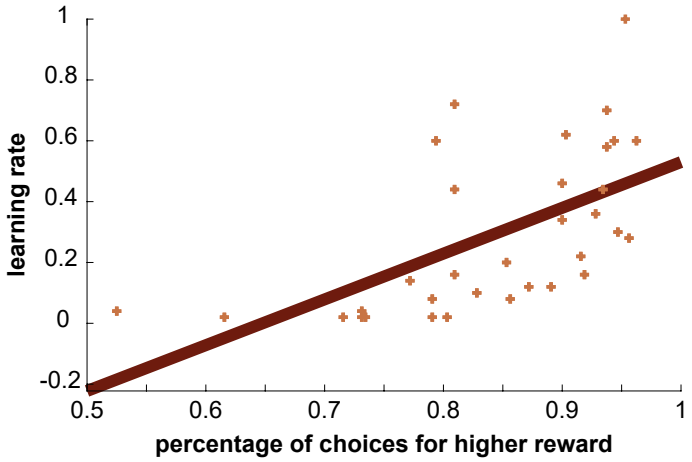

Supplementary Figure 19 | Correlation of learning rate with percentage of choices for the higher rewarded option
Learning rate correlated positively with the percentage of choices for the higher reward option across participants. (r= 0.5889, p= 0.0003). Learning rate was estimated from choice behaviour during free-choice trials of the binary decision making task with the help of a Rescolar-Wagner model. Percentage of choices for the higher reward options was calculated from all free-choice trials during the binary decision making task. Both measurements are inherently related and the correlation test was therefore a sanity check.

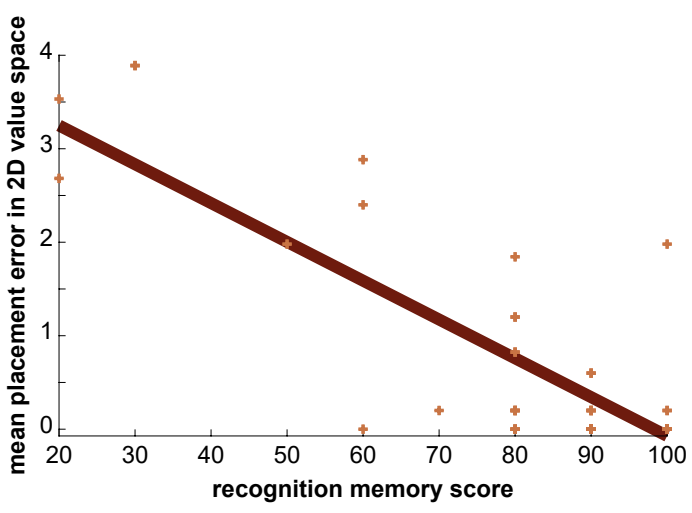

Supplementary Figure 20 | Correlation of mean placement error in 2D value space with recognition memory score
Mean placement error in 2D value space was negatively correlated with recognition memory score across participants (r= -0.8027, p< 0.0001). Placement errors in 2D value space were measured with the Euclidean distance between the actual location of an object and its remembered location. Therefore, a low score reflects better memory. The recognition memory score is the percentage of correct remembered rewards for each possible context-choice combination. Therefore, a high score reflects better memory. Both tasks rely on accurate recall of context-choice contingencies and the correlation test was therefore a sanity check.

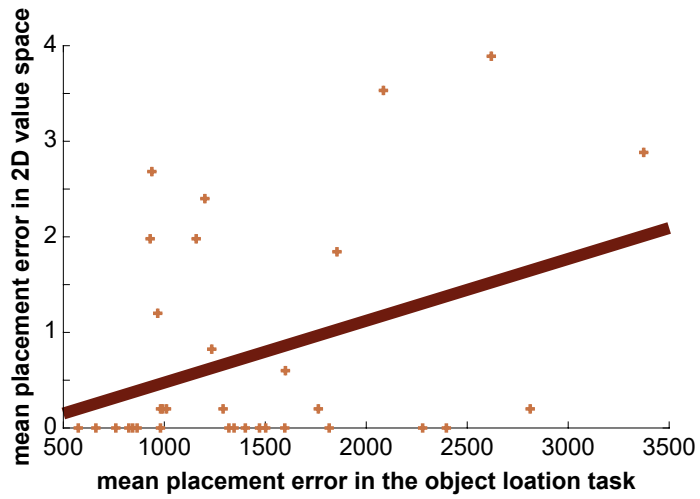

Supplementary Figure 21 | Correlation of SBSOD score with mean placement error in the object-location task
Scores from the Santa Barbara Sense of Direction Scale (SBSOD) were negatively correlated with mean placement error in an independent object-location task across participants (r= -0.4094, p= 0.0180). SBSOD score reflects mean self-reported navigational abilities ranging from 1 (lowest) to 7(highest). Placement errors in the object-location task were measured with the Euclidean distance between the actual location of an object in the virtual arena and its remembered location (units are in virtual distance points). Both tests measure navigational abilities and their correlation was a sanity check to verify that self-reported navigational abilities relate to objectively measured ones.

Supplementary Table 1 | Significant cluster for context-dependent chosen minus unchosen values effect

Voxels within the clusters survived family-wise error correction for the mask their listed under. Results are based on univariate modulation of activity by context-dependent chosen minus unchosen values during the binary decision making task. The peak position in MNI space and the T- and the p-value all refer to the voxel within the cluster with the highest T-value. Cluster size is the number of voxels within a cluster. Brain regions listed for the whole-brain mask are based on labels from the Harvard Oxford Cortical and Subcortical Brain Atlas.

mask	peak in MNI			T value and p_{FWE} value	cluster size	brain regions
	X	Y	Z			
OFC						
cluster 1	-30	16	-14	$T_{(31)}$= -6.586/ p< 0.001	396	OFC (left)
cluster 2	30	23	-14	$T_{(31)}$= -5.870/ p< 0.001	524	OFC (right)
hippocampus						
cluster 1	-18	-10	-22	$T_{(31)}$= 6.402/ p< 0.001	149	hippocampus (left)
cluster 2	22	-8	-20	$T_{(31)}$= 4.244/ p= 0.0028	110	hippocampus (right)
whole-brain						
cluster 1	-30	14	-14	$T_{(31)}$= -7.091/ p= 0.0039	650	frontal pole (left) insular cortex (left) inferior frontal gyrus, pars triangularis (left) inferior frontal gyrus, pars opercularis (left) temporal pole (left) OFC (left) frontal operculum cortex (left)
cluster 2	46	14	-5	$T_{(31)}$= -6.401/ p= 0.0016	1929	frontal pole (right) insular cortex (right) middle frontal gyrus (right) inferior frontal gyrus, pars triangularis (right) inferior frontal gyrus, pars opercularis (right) precentral gyrus (right) temporal pole (right) OFC (right) frontal operculum cortex (right) central opercular cortex (right)
cluster 3	-6	30	47	$T_{(31)}$= -6.728/ p< 0.001	2917	frontal pole (left/right) superior frontal gyrus (left/right) paracingulate gyrus (left/right) cingulate gyrus, anterior division (left/right)

Supplementary Table 2 | Correlation of behavioural parameters with distance effects of 1D and 2D value space in hippocampus and OFC ROIs

Parameters from two behavioural tasks were correlated with individual effects of distance coding of 1D and 2D value space in four different ROIs, respectively. Next to anatomical defined ROIs in the hippocampus and OFC, two functional ROIs were used for each region. Functional ROIs are based on voxels that are significantly modulated by context-dependent chosen minus unchosen values during the binary decision making task. In each ROI the distance in 1D and 2D value space was correlated with the change in neural similarity between context objects (from pre- to post-PVT). Presented here are the correlation coefficients and p-values of the correlation between each distance effect with mean placement error in 2D value space and percentage of choices for the higher rewarded option, respectively.

ROI	value space	mean placement error 2D value space		% of choices for higher rewarded option	
functional hippocampus	**1D**	r= 0.0938	p= 0.6218	r= 0.2360	p= 0.2092
	2D	r= 0.0983	p= 0.6053	r= 0.3455	p= 0.0615
anatomical hippocampus	**1D**	r= -0.0329	p= 0.8630	r= 0.1536	p= 0.4178
	2D	r= 0.1451	p= 0.4442	r= 0.2401	p= 0.2013
functional OFC	**1D**	r= 0.2186	p= 0.2458	r= 0.1321	p= 0.4866
	2D	r= 0.0861	p= 0.6511	r= 0.2959	p= 0.1124
anatomical OFC	**1D**	r= 0.0749	p= 0.6939	r= 0.1599	p= 0.3986
	2D	r= 0.0796	p= 0.6759	r= 0.2096	p= 0.2662

CHAPTER 5

General discussion

Summary

At the core of this thesis, I asked the question how the hippocampus can support a multitude of functions, especially episodic memory and spatial navigation. I approached this question in the light of a cognitive mapping framework. The term cognitive mapping has been around for decades and its scope and meaning has been continuously shaped and shifted (Behrens et al., 2018; Bellmund, Gärdenfors, et al., 2018; Epstein et al., 2017; O'Keefe & Nadel, 1978; Schiller et al., 2015; Stachenfeld et al., 2017; Tolman, 1948). For the purpose of this thesis, I broadly summarize cognitive mapping as the idea that the hippocampus uses general, domain-unspecific coding mechanisms to form integrative and flexible cognitive models/maps of our world.

In **chapter 2**, I expanded on previous studies showing hippocampal coding of spatial distances (Deuker et al., 2016; L. R. Howard et al., 2014; Morgan et al., 2011). More concretely, I wanted to test the idea that the hippocampus can map and *integrate* directly and indirectly experienced distances between goal locations. Furthermore, I tested whether it can update such a cognitive map flexibly, after changes in the environment occurred (Burgess et al., 2002; Deuker et al., 2016; L. R. Howard et al., 2014; McNaughton et al., 2006; Morgan et al., 2011; O'Keefe & Nadel, 1978; Spiers & Barry, 2015; Tolman, 1948). To this end, I let participants explore a large-scale virtual environment and trained them to walk the shortest possible routes between object-locations. The aim was to test the representation of the shortest path distance and the Euclidean distance between objects in the hippocampus. Behavioural results confirm that participants could recall (and distinguish between) path and Euclidean distances of object-pairs. To test the neural representations of these distances, I recorded fMRI data while presenting pictures of all objects before and after participants completed the object-location task. Leveraging representational similarity analysis (RSA) allowed me to measure the change in representational overlap between objects in the hippocampus (Kriegeskorte et al., 2008). As would be predicted by the idea of a cognitive map, results suggest that the (left) hippocampus forms an integrative map of path and Euclidean distances.

In order to investigate the flexibility of this map, participants completed a second object-location task in the same environment. However, here some (but not all) paths changed between object locations. As a result, shortest path distances could increase or decrease in comparison to the previous object-location task. The goal was to test the notion that the hippocampus cannot only form maps of our environment, but also update them flexibly when meaningful changes occur. Behavioural results show that the participants could update these new path distances successfully and distinguish them from the Euclidean distances. To test the effects of changed path distances on

neural representations, I again recorded fMRI data while presenting pictures of all objects and analysed the data with RSA (Kriegeskorte et al., 2008). Because the role of the hippocampus in detour problems is not well established, I also explored how navigational strategies might influence hippocampal remapping (Astur et al., 2016; L. R. Howard et al., 2014; Iglói et al., 2010, 2015; Spiers & Barry, 2015). Participants were therefore classified as response learners or place learners in an independent task (adapted from Astur et al., 2016). Interestingly, navigational strategies did have an effect on remapping. Response learners were more strongly affected by the changes in the environment than place learners. For them (but not for place learners), neural similarity between object-pairs adapted as a function of changed path distance in the (left) hippocampus. Response learners' navigation is largely based on egocentric responses (e.g. left and right turns) and therefore their hippocampal representations might be more sensitive to egocentric (i.e. path) changes in the environment. Taken together the results of **chapter 2** support the idea that the hippocampus can form integrative and flexible maps of our environment.

In **chapter 3**, I expanded on the findings of **chapter 2** and investigated across-domain mechanisms of the hippocampus. Two domains of central interest for this aim are episodic memory and spatial cognition/navigation. Both research fields show decades of evidence of hippocampal involvement (Buzsáki & Moser, 2013; Eichenbaum et al., 1992; O'Keefe & Nadel, 1978; Scoville & Milner, 1957). I classified theories about how the hippocampus can play a major role in both domains into two broader ideas. I summarized the first idea under the term *common coding mechanism*. This idea proposes that the hippocampus integrates spatial and episodic information (Bellmund, Gärdenfors, et al., 2018; Eichenbaum, 2017; Eichenbaum & Cohen, 2014; Epstein et al., 2017; Schiller et al., 2015). The second idea I explored here is a *parallel processing mechanism* according to which the hippocampus can be segregated into functional subregions which specialize in either episodic memory *or* spatial memory (Burgess et al., 2002; Kühn & Gallinat, 2014; Poppenk et al., 2013). Based on previous literature, I assessed differences between hemispheres (left vs. right hippocampus) and along the longitudinal axis (anterior vs. posterior) of the hippocampus (for an overview see Kühn & Gallinat, 2014).

Participants had to complete two tasks, in which objects were associated with one of two episodic contexts (episodic task) and one of two spatial contexts (spatial task), respectively. These task manipulations resulted in a 2x2 design, with pairs of objects either sharing no context at all, only a spatial context, only an episodic context or both an episodic and a spatial context. In order to test the effects of these spatial and episodic relationships between objects on their representational overlap, fMRI data were recorded while all objects were presented. Representational overlap was

measured after the spatial task and the episodic task, respectively (order of tasks was counterbalanced across participants). Leveraging fMRI adaptation analysis (Barron et al., 2016; Grill-Spector et al., 2006; Krekelberg et al., 2006), I assessed representational overlap in the hippocampus between objects as a proxy for memory integration. There was no evidence supporting the idea of a parallel processing mechanism in the hippocampus for spatial and episodic memory. However, the results of **chapter 3** concur with an integration of spatial and episodic memory in the hippocampus. In more detail, adaptation effects scaled with the amount of spatial and episodic context overlap (no context shared, episodic *or* spatial context shared, episodic *and* spatial context shared). This is in line with the idea of a common coding mechanism of episodic and spatial memory and supports the claim that hippocampal processing mechanisms are not bound to one cognitive domain.

In **chapter 4**, the aim was to test the question how hippocampal mechanisms supporting navigation are also used in other cognitive domains (Behrens et al., 2018; Bellmund, Gärdenfors, et al., 2018; Epstein et al., 2017; Schiller et al., 2015; Stachenfeld et al., 2017). There is growing evidence, showing that the hippocampus can map abstract spaces that are defined along e.g. physical feature dimensions, like the length of a bird's leg and neck (Aronov et al., 2017; Constantinescu et al., 2016; Garvert et al., 2017; Tavares et al., 2015; Theves et al., 2019). The work of **chapter 4** builds on these important proof-of-principle studies and tested whether the same principles can be applied to maps that are based on more conceptual, non-physical dimensions. Values in the form of numerical rewards were the concept of choice in **chapter 4**. I opted for values for two reasons: First, numerical values are a constantly appearing concept in our everyday lives and second, these values form by their own nature a continuous axis. As I was interested in a potential hippocampal representation of an abstract value space, participants first needed to learn relevant numerical value/reward associations. To this end, participants completed a binary decision task, in which context objects were associated with two independent numerical rewards (reward for option A and reward for option B). These two reward associations defined the axes of a two-dimensional value space (axis A represents the reward for option A, axis B represents the reward for option B). Akin to **chapter 2**, I tested for hippocampal mapping of (Euclidean) distances between these objects. Accordingly, all objects were presented before and after the binary decision task and fMRI data were recorded. Leveraging both RSA (Kriegeskorte et al., 2008) and adaptation analysis (Barron et al., 2016; Grill-Spector et al., 2006; Krekelberg et al., 2006), I tested whether representational overlap between objects changed in the hippocampus as a function of their distance in a value space. There was no evidence for hippocampal distance coding in such an abstract (non-physical) value space.

Taken together, **chapter 2** and **chapter 3** provide evidence that the hippocampus is able to form integrative and flexible cognitive maps within and between the domains of spatial navigation and episodic memory. Results of **chapter 4** do not support the notion that these principles can be applied to value maps.

Hippocampal maps for spatial and episodic memory

Although the results of **chapter 2** and **chapter 3** support the idea of flexible mapping mechanisms that are shared across spatial and episodic memory, it is important to take the limitations of these studies into account. In the following, I will first discuss common design features across these chapters and how they can (and cannot) inform us about hippocampal mechanisms. Afterwards, I will review how either chapter adds into the bigger understanding of hippocampal mechanisms and debate potential open questions.

Measuring (passive) representations with a task-offline design

One main feature of the work of **chapter 2** and **chapter 3** is the use of vivid, life-simulating techniques like virtual reality and 'the Sims'. The goal was to create tasks mimicking the naturalistic experiences underlying episodic memory and navigation. However, hippocampal representations were not measured while participants were performing these tasks. Rather, fMRI data were collected 'offline' from episodic and spatial experiences during picture viewing tasks. This type of design has been used before and has several advantages (e.g. Collin et al., 2015; Deuker et al., 2016; Milivojevic et al., 2015; Schapiro et al., 2012; Schlichting et al., 2015). Most importantly, representational changes are measured using an independent data set and therefore the identical stimulus material can be used to measure effects of different tasks or task conditions. This was essential for the multi-task designs of **chapter 2** and **chapter 3**. In both chapters, relationships between objects changed across multiple association tasks. By measuring neural effects on identical picture viewing tasks after each association task, results are easily comparable. Another benefit of using picture viewing tasks is that the stimulus material (pictures of objects) does not inherently contain spatial or episodic information, at least arguably not to the extent that walking in a virtual environment or watching a virtual character does. Therefore, neural effects cannot be explained by general perceptual attributes of the association tasks. Furthermore, this type of design is ideally suited for RSA and adaptation analysis. Because the fMRI signal is sluggish and slow it is important to exclude temporal biases between conditions (Deuker et al., 2016). Imagine, for example, I would have performed RSA on the navigation tasks of **chapter 2** instead of the picture viewing tasks. Obviously, when navigating from one object to another, the temporal duration between object

presentations will be biased by spatial distance (i.e. it takes longer to walk greater distances). This might have biased the results, because representational overlap might have been affected by a higher temporal overlap of the BOLD responses of objects that are closer together in space. The problem of temporal bias is amplified in the episodic task of **chapter 3**. One feature of stories/events is that they have a temporal order of events. Adaptation analysis however requires (maybe even more so than RSA) that the temporal duration and order between different object presentations not to be biased. This is due to the fact that adaptation analysis (as implemented here) is based on the effect of one object presentation on the univariate BOLD response elicited by its successor.

All of the aforementioned advantages are reasons for using such a task-offline design as described here. However, such a design also comes at the cost of ambiguity regarding what cognitive aspects of spatial and episodic memory are captured in the neural data. Participants were not asked to specifically think about the (spatial or episodic) task aspects they encountered before a picture viewing task. In order to sustain attention, participants had to do a cover task (e.g. an oddball detection task) during the picture viewing tasks. Therefore, probably no active, conscious components of spatial and episodic memory were measured, but rather passive representational signatures of spatial and episodic associations. I argue that **chapter 2** and **chapter 3** provide evidence for integrative and flexible representations in the hippocampus across space and episodes. However, this comes with the important limitation that these chapters do not allow to make direct statements about hippocampal mechanisms of e.g. *active* retrieval or encoding of spatial and episodic memory. The endeavour to understand domain-general mechanisms of the hippocampus will depend on the comparison of all stages (from encoding to recall or even forgetting) of episodic and spatial memory.

The hippocampus as focus area – does the rest of the brain matter?

As mentioned numerous times, the aim of this thesis was to understand how the hippocampus can support a multitude of functions, such as episodic and spatial memory. The hippocampus (and potential subregions) was therefore defined as region of interest (ROI) in the studies of this thesis. Even though I also included whole-brain analyses, it is important to recognize that this approach focuses less on the involvement of other brain areas in episodic memory and spatial cognition & navigation. For instance, in **chapter 2** and **chapter 3** the entorhinal cortex and PFC might have played an important role. The entorhinal cortex has been shown to code for space and time and the PFC is known to be involved in solving detour problems and monitoring episodic memory retrieval (Bellmund et al., 2019; Doeller et al., 2010; Henson et al., 1999; Spiers & Gilbert, 2015; for an overview see Eichenbaum, 2017). Coming from the specific question of *hippocampal* mechanisms supporting memory and spatial cognition one might thus ask the broader question how the brain as a

whole achieves these functions. This more general question surely will involve all of the above regions (and potential further ones) and their interplay. Understanding the neural mechanisms of these cognitive functions will therefore require *both* studies such as the ones presented here – maximising power for a detailed understanding of a focus area – and studies specifically investigating the functional connectivity across these areas (e.g. Ranganath et al., 2005; Zhang et al., 2014). Given that no brain area works in isolation, to fully understand the hippocampus will necessarily include such a network perspective (Rubin et al., 2017).

Path distance: time or space?

As has been described above, the results of **chapter 2** seem to indicate that the hippocampus forms an integrative distance map – containing information about both, the Euclidean distance and path distance between goal locations. Both types of distances represent a form of spatial relationship in our environment. However, path distance can also be understood as a temporal relationship between two locations (Deuker et al., 2016; Morgan et al., 2011). As the speed was constant in the navigation tasks of **chapter 2**, travelled distance was naturally highly related to the travel duration. One could argue, that therefore the results of **chapter 2** might point towards an integrative map across space and time (Eichenbaum, 2017; Eichenbaum & Cohen, 2014; Epstein et al., 2017; Schiller et al., 2015).

It might be beneficial to address the spatial and temporal aspects of path distance more directly in future studies. Inspiration for study designs can be drawn from real life. For example, I can break down my bicycle commute to the office into two parts. The first part is from my house to the train station and the second from the train station to the university. The travelled distance from my house to the train station is much shorter than the residual trip from the train station to the office. However, because there are numerous big intersections between my home and the train station, both parts of the commute take about the same time. I propose that incorporating waiting times, through e.g. traffic lights into a navigation task (akin to the one in **chapter 2**) might enable us to understand hippocampal coding of path distances in more depth. Such a design can create routes with comparable spatial distances, but different durations and vice versa. With this, one could test whether the hippocampus can code and integrate both the spatial and temporal aspects of routes in such a design. Evidence for such spatio-temporal integration already comes from rodent studies, showing hippocampal coding for waiting times along running tracks (Kraus et al., 2013; Salz et al., 2016).

The influence of navigational strategies on hippocampal mapping

The results of **chapter 2** not only demonstrated that hippocampal mapping is integrative, but also that it is adaptive to changes in the environment. Adaptive behaviour in the

face of changes has been postulated as a core feature of cognitive maps (Tolman, 1948). Finding neural representations that reflect or signal changes in the environment is therefore a key element in understanding how the brain enables this flexible behaviour. A previous study found that the hippocampus signals changes in path distance during active navigation (L. R. Howard et al., 2014; Spiers & Barry, 2015). The results of **chapter 2** dovetail with this finding, showing that task-offline hippocampal representations adapt as a function of changes in path distance. However, this adaptive effect was only present in response learners and not in place learners. Response learners base their navigation on remembered egocentric sequences of left and right turns, whereas place learners base their navigation on allocentric relationships between locations (Burgess, 2006). It might be that, therefore, hippocampal representations of response learners are more sensitive to path changes, i.e. egocentric changes in the environment. I speculate that hippocampal representations of place learners might be more sensitive to allocentric changes in their environment. This leads to the question what role navigational strategies might play in cognitive mapping and if their influence is limited to spatial representations and behaviour. Interestingly, there is evidence that allocentric behaviour is related to model-based planning and that this relationship might be mediated by the hippocampus (Vikbladh et al., 2019). This emphasizes that our understanding of hippocampal mapping mechanisms might benefit from studies that explore further how navigational strategies (e.g. through pre-selecting extreme groups; de Haas, 2018) might affect hippocampal representations beyond the spatial domain.

The search of functional hippocampal subregions for spatial and episodic information

The results of **chapter 3** support the notion that the hippocampus forms integrative representations of spatial and episodic memory (Eichenbaum, 2017; Eichenbaum & Cohen, 2014). There was no evidence for functional subregions in the hippocampus that support one function more than the other. This is in line with previous studies showing spatio-temporal integration in the hippocampus, rather than subfield specialisation for spatial or episodic information (Deuker et al., 2016; Kyle et al., 2015; Nielson et al., 2015).

Even though we found no evidence for a parallel processing mechanism, there is a general pattern that studies from the episodic literature find activation in the left and anterior hippocampus while studies from the spatial literature report rather right and posterior activation (Burgess et al., 2002; Kühn & Gallinat, 2014). I argue that there are two important factors that need to be taken into account when comparing the pattern of results from these different sets of literature.

First, let's imagine an example in which a study found significant activity in the left hippocampus while participants completed an episodic task, but not in the right hippocampus. This simply means that activity in the left hippocampus met a (somewhat arbitrary) threshold, while activity in the right hippocampus did not. It is however neither evidence for no involvement of the right hippocampus in the task, nor evidence for a (significantly) higher involvement of the left than the right hippocampus in the task. What is necessary to make definitive statements about differences between hippocampal subregions is the *direct* (and statistical) comparison between them. Such a direct comparison was done in **chapter 3**. As the present study looked at four subregions (split by the hemisphere and by the anterior-posterior axis) and compared two types of memory (spatial vs. episodic), it might be that the lack of evidence (and lack of evidence from the aforementioned studies) is due to a lack of power. Moving forward, it might be beneficial to use larger sample sizes (here n= 36) or use fewer subregions within one study, e.g. just compare the left and the right hippocampus.
Furthermore, the example described above demonstrates why visualization techniques like dual-coding (as was employed in the presented work) might be beneficial to the fMRI field as a whole (Allen et al., 2012). This method simultaneously presents sub-thresholded fMRI data, while still clearly marking voxels that met the statistical significance threshold.

Second, comparing spatial and episodic processing will require well-matched tasks or well-matched spatial and temporal/episodic features of the same task. This is important, as the spatial and episodic literature vary largely in their methodological approaches and techniques. Studies of spatial memory or navigation often leverage virtual reality or capture real-world environments that the participants are highly familiar with (Bohil et al., 2011; Kühn & Gallinat, 2014; Spiers & Barry, 2015). In comparison, episodic memory is often assessed through learned associations between items, e.g. words or pictures (Davachi, 2006). Another important challenge is the fact that episodic memory has a spatial component – namely 'where' an event has taken place (Tulving, 2002). Therefore, controlling for spatial effects of episodic memory is crucial when comparing hippocampal (subfield) involvement between spatial and episodic memory. I approached this challenge in **chapter 3** by keeping spatial (dis) similarities constant across episodic contexts, meaning an object had a comparable spatial relationship to all other objects, regardless of whether it shared an episodic context with another object or not.

Taken together, answering the question whether the hippocampus has specialized subregions for spatial and/or episodic memory will require experiments with high power (or at least more power than the current and previous studies provided) and tasks that are well-matched and controlled in their spatial and episodic features. Life-

simulating techniques like 'the Sims' or virtual reality might be helpful tools to create such tasks. These techniques mimic the richness of spatial and episodic experiences, while at the same time offering experimental control of spatial environments and temporal events (Bohil et al., 2011). Furthermore, both of these techniques have successfully been used for studying other functional gradients in the hippocampus (Brunec et al., 2018; Collin et al., 2015).

Transition structure as precondition for hippocampal mapping

The idea of cognitive mapping in the hippocampus goes (nowadays) beyond the spatial and episodic domain (Behrens et al., 2018; Deuker et al., 2016; Epstein et al., 2017; Schiller et al., 2015; Stachenfeld et al., 2017). As discussed above, the coarse idea is that spatial codes underlying navigation are general domain-unspecific mechanisms and first proof-of-principle studies support this claim. These studies show spatial coding, like hexadirectional signalling or distance representation within abstract physical feature spaces (e.g. Aronov et al., 2017; Constantinescu et al., 2016; Theves et al., 2019). The aim of **chapter 4** was to expand these findings by exploring hippocampal distance coding in a non-physical abstract value space. However, the results provide no evidence for any form of value space representation in the hippocampus. I can only speculate what the reasons for such an absence of evidence might be. The study might have been underpowered or the design of the binary decision task was suboptimal to elicit a value space representation. Furthermore, it might be that the hippocampus only codes abstract spaces that are based on physical feature dimensions (e.g. the length of a bird's neck and leg). I hypothesize that one likely explanation is that there was no navigation or experience of transition structures in the task. Such a navigation or transition aspect is present in the other experiments studying abstract spaces. For example, the task structure of studies using abstract physical feature spaces are all similar in the sense that they require participants (or rodents) to gradually change the physical features of a stimulus, i.e. navigate along the feature dimensions of that stimulus space (e.g. Aronov et al., 2017; Constantinescu et al., 2016; Theves et al., 2019). At the same time, another study showed hippocampal coding of discrete stimulus transition structures (Garvert et al., 2017).

Although one could argue that numerical values have an inherent transition structure (3 follows 2 follows 1), participants only experience the position of each stimulus in the 2D value space, never a transition through this space from one stimulus to another. Interestingly, representing transition structures has been proposed as one of the main purposes of spatially tuned cells (Stachenfeld et al., 2017). The idea here is that the hippocampus can form predictive maps based on regularities in the environment. This

notion can be seen as an extension of the relational binding theory and the idea of a memory space (Davachi, 2006; Eichenbaum et al., 1992; Eichenbaum & Cohen, 2014). The idea of relational binding is that the role of the hippocampus in episodic memory is to bind events into their spatiotemporal context. Representing transition structures would provide a mechanistic explanation of integrative representations of spatial memory (i.e. transitions through space) and episodic memory (i.e. transitions through spacetime) or even representations of abstract spaces (e.g. transitions through physical features). Moving forward, it might be beneficial to test the influence of transition structures on hippocampal mapping of abstract spaces more directly. A proposition would be to replicate one of the previously published abstract feature space studies but with the addition of a non-transition condition. For example, Theves et al. (2019) showed hippocampal distance coding in a physical feature space. Participants had to navigate through this feature space by changing the configuration of a stimulus along two feature dimensions. Objects were then associated with specific locations (i.e. specific feature configurations of the stimulus) in the space. Akin to **chapter 2**, the authors demonstrated distance coding by tracking changes in hippocampal representations from pre to post the navigation task. I would suggest to add another condition to this experiment, in which participants associate objects with a specific feature configuration of a stimulus (i.e. location of the space), but never transition through the stimulus space. If one of the main mechanisms of the hippocampus is indeed representing transition structures, distance coding should only be possible in the transition condition (as shown in the previous study) and furthermore should be significantly stronger than in the non-transition condition.

Conclusions

The cognitive mapping framework is a powerful tool to understand and bridge different fields of hippocampal research, such as navigation and memory. At its core, it proposes that the hippocampus uses domain-unspecific mechanisms to form an integrative and flexible model or map of our world. This cognitive map allows us to connect experiences and draw inferences for future behaviour.

The combined work of this thesis provides evidence that the ideas of cognitive mapping hold true across the domains of navigation and episodic memory. Furthermore, I believe that the work of this thesis supports the idea that one core mapping mechanism of the hippocampus is to code transition structures. In experiments where (temporal and spatial) transition structures were present, we found clear evidence for hippocampal involvement (**chapter 2** and **chapter 3**). Whereas the absence of transition structures in an experimental design resulted in an absence of evidence for hippocampal coding (**chapter 4**).

This underlines the need to address the preconditions and exact nature of hippocampal mapping mechanisms in future studies more directly. Understanding what elicits hippocampal mapping does not only deepen our knowledge about this structure, but also allows us to identify shared/similar features across cognitive domains.

Appendix

References

Allen, E. A., Erhardt, E. B., & Calhoun, V. D. (2012). Data visualization in the neurosciences: overcoming the curse of dimensionality. *Neuron, 74*(4), 603–608. https://doi.org/10.1016/j.neuron.2012.05.001

Alvarez, R. P., Biggs, A., Chen, G., Pine, D. S., & Grillon, C. (2008). Contextual fear conditioning in humans: cortical-hippocampal and amygdala contributions. *The Journal of Neuroscience : The Official Journal of the Society for Neuroscience, 28*(24), 6211–6219. https://doi.org/10.1523/JNEUROSCI.1246-08.2008

Alvernhe, A., Save, E., & Poucet, B. (2011). Local remapping of place cell firing in the Tolman detour task. *European Journal of Neuroscience, 33*(9), 1696–1705. https://doi.org/10.1111/j.1460-9568.2011.07653.x

Alvernhe, A., van Cauter, T., Save, E., & Poucet, B. (2008). Different CA1 and CA3 representations of novel routes in a shortcut situation. *The Journal of Neuroscience : The Official Journal of the Society for Neuroscience, 28*(29), 7324–7333. https://doi.org/10.1523/JNEUROSCI.1909-08.2008

Aronov, D., Nevers, R., & Tank, D. W. (2017). Mapping of a non-spatial dimension by the hippocampal--entorhinal circuit. *Nature, 543*(7647), 719. https://doi.org/10.1038/nature21692

Astur, R. S., Purton, A. J., Zaniewski, M. J., Cimadevilla, J., & Markus, E. J. (2016). Human sex differences in solving a virtual navigation problem. *Behavioural Brain Research, 308*, 236–243. https://doi.org/10.1016/j.bbr.2016.04.037

Barron, H. C., Garvert, M. M., & Behrens, T. E. J. (2016). Repetition suppression: a means to index neural representations using BOLD? *Philosophical Transactions of the Royal Society of London. Series B, Biological Sciences, 371*(1705). https://doi.org/10.1098/rstb.2015.0355

Behrens, T. E. J., Muller, T. H., Whittington, J. C. R., Mark, S., Baram, A. B., Stachenfeld, K. L., & Kurth-Nelson, Z. (2018). What Is a Cognitive Map? Organizing Knowledge for Flexible Behavior. *Neuron, 100*(2), 490–509. https://doi.org/10.1016/j.neuron.2018.10.002

Behrens, T. E. J., Woolrich, M. W., Walton, M. E., & Rushworth, M. F. S. (2007). Learning the value of information in an uncertain world. *Nature Neuroscience, 10*(9), 1214. https://doi.org/10.1038/nn1954

Bellmund, J. L. S. (2019). General introduction [Radboud University Nijmegen]. In *Hippocampal-entorhinal codes for space, time and cognition*. http://hdl.handle.net/2066/207524

Bellmund, J. L. S., Deuker, L., & Doeller, C. F. (2018). *Donderstown*. OSF. https://doi.org/10.17605/OSF.IO/78UPH

Bellmund, J. L. S., Deuker, L., & Doeller, C. F. (2019). Mapping sequence structure in the human lateral entorhinal cortex. *ELife, 8*. https://doi.org/10.7554/eLife.45333

Bellmund, J. L. S., Deuker, L., Navarro Schröder, T., & Doeller, C. F. (2016). Grid-cell representations in mental simulation. *ELife, 5*. https://doi.org/10.7554/eLife.17089

Bellmund, J. L. S., Gärdenfors, P., Moser, E. I., & Doeller, C. F. (2018). Navigating cognition: Spatial codes for human thinking. *Science (New York, N.Y.), 362*(6415), eaat6766. https://doi.org/10.1126/science.aat6766

Bohil, C. J., Alicea, B., & Biocca, F. A. (2011). Virtual reality in neuroscience research and therapy. *Nature Reviews Neuroscience, 12*(12), 752–762. https://doi.org/10.1038/nrn3122

Bornstein, A. M., & Daw, N. D. (2013). Cortical and hippocampal correlates of deliberation during model-based decisions for rewards in humans. *PLoS Computational Biology, 9*(12), e1003387. https://doi.org/10.1371/journal.pcbi.1003387

Bostock, E., Muller, R. U., & Kubie, J. L. (1991). Experience-dependent modifications of hippocampal place cell firing. *Hippocampus, 1*(2), 193–205. https://doi.org/10.1002/hipo.450010207

Brunec, I. K., Bellana, B., Ozubko, J. D., Man, V., Robin, J., Liu, Z.-X., Grady, C., Rosenbaum, R. S., Winocur, G., Barense, M. D., & Moscovitch, M. (2018). Multiple Scales of Representation along the Hippocampal Anteroposterior Axis in Humans. *Current Biology, 28*(13), 2129-2135.e6. https://doi.org/10.1016/j.cub.2018.05.016

Burgess, N. (2006). Spatial memory: how egocentric and allocentric combine. *Trends in Cognitive Sciences, 10*(12), 551–557. https://doi.org/10.1016/j.tics.2006.10.005

Burgess, N. (2014). The 2014 Nobel Prize in Physiology or Medicine: A Spatial Model for Cognitive Neuroscience. *Neuron, 84*(6), 1120–1125. https://doi.org/10.1016/j.neuron.2014.12.009

Burgess, N., Maguire, E. A., & O'Keefe, J. (2002). The Human Hippocampus and Spatial and Episodic Memory. *Neuron, 35*(4), 625–641. https://doi.org/10.1016/S0896-6273(02)00830-9

Burgess, N., Maguire, E. A., Spiers, H. J., & O'Keefe, J. (2001). A Temporoparietal and Prefrontal Network for Retrieving the Spatial Context of Lifelike Events. *NeuroImage, 14*(2), 439–453. https://doi.org/10.1006/nimg.2001.0806

Bush, D., Barry, C., Manson, D., & Burgess, N. (2015). Using Grid Cells for Navigation. *Neuron, 87*(3), 507–520. https://doi.org/10.1016/j.neuron.2015.07.006

Buzsáki, G., & Moser, E. I. (2013). Memory, navigation and theta rhythm in the hippocampal-entorhinal system. *Nature Neuroscience, 16*(2), 130–138. https://doi.org/10.1038/nn.3304

Cavanna, A. E., & Trimble, M. R. (2006). The precuneus: a review of its functional anatomy and behavioural correlates. *Brain : A Journal of Neurology, 129*(Pt 3), 564–583. https://doi.org/10.1093/brain/awl004

Clark, R. E., & Squire, L. R. (2013). Similarity in form and function of the hippocampus in rodents, monkeys, and humans. *Proceedings of the National Academy of Sciences, 110*(Supplement 2), 10365–10370. https://doi.org/10.1073/pnas.1301225110

Cohen, N. J., & Squire, L. R. (1980). Preserved learning and retention of pattern-analyzing skill in amnesia: dissociation of knowing how and knowing that. *Science (New York, N.Y.), 210*(4466), 207–210. https://doi.org/10.1126/science.7414331

Collin, S. H. P., Milivojevic, B., & Doeller, C. F. (2015). Memory hierarchies map onto the hippocampal long axis in humans. *Nature Neuroscience, 18*(11), 1562–1564. https://doi.org/10.1038/nn.4138

Collin, S. H. P., Milivojevic, B., & Doeller, C. F. (2017). Hippocampal hierarchical networks for space, time, and memory. *Current Opinion in Behavioral Sciences, 17*, 71–76. https://doi.org/10.1016/j.cobeha.2017.06.007

Constantinescu, A. O., O'Reilly, J. X., & Behrens, T. E. J. (2016). Organizing conceptual knowledge in humans with a gridlike code. *Science (New York, N.Y.), 352*(6292), 1464–1468. https://doi.org/10.1126/science.aaf0941

Davachi, L. (2006). Item, context and relational episodic encoding in humans. *Current Opinion in Neurobiology, 16*(6), 693–700. https://doi.org/10.1016/j.conb.2006.10.012

de Haas, B. (2018). How to Enhance the Power to Detect Brain-Behavior Correlations With Limited Resources. *Frontiers in Human Neuroscience, 12*, 421. https://doi.org/10.3389/fnhum.2018.00421

Deuker, L., Bellmund, J. L. S., Navarro Schröder, T., & Doeller, C. F. (2016). An event map of memory space in the hippocampus. *ELife, 5*. https://doi.org/10.7554/eLife.16534

Diba, K., & Buzsáki, G. (2007). Forward and reverse hippocampal place-cell sequences during ripples. *Nature Neuroscience, 10*(10), 1241–1242. https://doi.org/10.1038/nn1961

Dimsdale-Zucker, H. R., Ritchey, M., Ekstrom, A. D., Yonelinas, A. P., & Ranganath, C. (2018). CA1 and CA3 differentially support spontaneous retrieval of episodic contexts within human hippocampal subfields. *Nature Communications, 9*(1), 1–8. https://doi.org/10.1038/s41467-017-02752-1

Doeller, C. F., Barry, C., & Burgess, N. (2010). Evidence for grid cells in a human memory network. *Nature, 463*(7281), 657. https://doi.org/10.1038/nature08704

Doll, B. B., Duncan, K. D., Simon, D. A., Shohamy, D., & Daw, N. D. (2015). Model-based choices involve prospective neural activity. *Nature Neuroscience, 18*(5), 767. https://doi.org/10.1038/nn.3981

Doll, B. B., Shohamy, D., & Daw, N. D. (2015). Multiple memory systems as substrates for multiple decision systems. *Neurobiology of Learning and Memory, 117*, 4–13. https://doi.org/10.1016/j.nlm.2014.04.014

Duncan, K. D., Doll, B. B., Daw, N. D., & Shohamy, D. (2018). More Than the Sum of Its Parts: A Role for the Hippocampus in Configural Reinforcement Learning. *Neuron, 98*(3), 645-657.e6. https://doi.org/10.1016/j.neuron.2018.03.042

Eichenbaum, H. (2014). Time cells in the hippocampus: a new dimension for mapping memories. *Nature Reviews Neuroscience, 15*(11), 732–744. https://doi.org/10.1038/nrn3827

Eichenbaum, H. (2017). On the Integration of Space, Time, and Memory. *Neuron, 95*(5), 1007–1018. https://doi.org/10.1016/j.neuron.2017.06.036

Eichenbaum, H., & Cohen, N. J. (2014). Can We Reconcile the Declarative Memory and Spatial Navigation Views on Hippocampal Function? *Neuron, 83*(4), 764–770. https://doi.org/10.1016/j.neuron.2014.07.032

Eichenbaum, H., Dudchenko, P., Wood, E., Shapiro, M., & Tanila, H. (1999). The Hippocampus, Memory, and Place Cells. *Neuron, 23*(2), 209–226. https://doi.org/10.1016/S0896-6273(00)80773-4

Eichenbaum, H., Otto, T., & Cohen, N. J. (1992). The hippocampus---what does it do? *Behavioral and Neural Biology, 57*(1), 2–36. https://doi.org/10.1016/0163-1047(92)90724-I

Ekstrom, A. D., Kahana, M. J., Caplan, J. B., Fields, T. A., Isham, E. A., Newman, E. L., & Fried, I. (2003). Cellular networks underlying human spatial navigation. *Nature, 425*(6954), 184–188. https://doi.org/10.1038/nature01964

Ekstrom, A. D., & Ranganath, C. (2018). Space, time, and episodic memory: The hippocampus is all over the cognitive map. *Hippocampus, 28*(9), 680–687. https://doi.org/10.1002/hipo.22750

Epstein, R. A., Patai, E. Z., Julian, J. B., & Spiers, H. J. (2017). The cognitive map in humans: spatial navigation and beyond. *Nature Neuroscience, 20*(11), 1504. https://doi.org/10.1038/nn.4656

Ezzati, A., Katz, M. J., Zammit, A. R., Lipton, M. L., Zimmerman, M. E., Sliwinski, M. J., & Lipton, R. B. (2016). Differential association of left and right hippocampal volumes with verbal episodic and spatial memory in older adults. *Neuropsychologia, 93*, 380–385. https://doi.org/10.1016/j.neuropsychologia.2016.08.016

Felleman, D. J., & van Essen, D. C. (1991). Distributed hierarchical processing in the primate cerebral cortex. *Cerebral Cortex (New York, N.Y. : 1991), 1*(1), 1–47. https://doi.org/10.1093/cercor/1.1.1

FitzGerald, T. H. B., Seymour, B., & Dolan, R. J. (2009). The role of human orbitofrontal cortex in value comparison for incommensurable objects. *The Journal of Neuroscience : The Official Journal of the Society for Neuroscience, 29*(26), 8388–8395. https://doi.org/10.1523/JNEUROSCI.0717-09.2009

Foster, D. J., & Wilson, M. A. (2006). Reverse replay of behavioural sequences in hippocampal place cells during the awake state. *Nature, 440*(7084), 680–683. https://doi.org/10.1038/nature04587

Frankland, P. W., Cestari, V., Filipkowski, R. K., McDonald, R. J., & Silva, A. J. (1998). The dorsal hippocampus is essential for context discrimination but not for contextual conditioning. *Behavioral Neuroscience, 112*(4), 863–874. https://doi.org/10.1037/0735-7044.112.4.863

Garvert, M. M., Dolan, R. J., & Behrens, T. E. J. (2017). A map of abstract relational knowledge in the human hippocampal-entorhinal cortex. *ELife, 6*. https://doi.org/10.7554/eLife.17086

Ghaem, O., Mellet, E., Crivello, F., Tzourio, N., Mazoyer, B., Berthoz, A., & Denis, M. (1997). Mental navigation along memorized routes activates the hippocampus, precuneus, and insula. *Neuroreport: An International Journal for the Rapid Communication of Research in Neuroscience.*

Gottfried, J. A., O'Doherty, J., & Dolan, R. J. (2003). Encoding predictive reward value in human amygdala and orbitofrontal cortex. *Science (New York, N.Y.), 301*(5636), 1104–1107. https://doi.org/10.1126/science.1087919

Greenberg, D. L., Rice, H. J., Cooper, J. J., Cabeza, R., Rubin, D. C., & LaBar, K. S. (2005). Co-activation of the amygdala, hippocampus and inferior frontal gyrus during autobiographical memory retrieval. *Neuropsychologia, 43*(5), 659–674. https://doi.org/10.1016/j.neuropsychologia.2004.09.002

Grill-Spector, K., Henson, R., & Martin, A. (2006). Repetition and the brain: neural models of stimulus-specific effects. *Trends in Cognitive Sciences, 10*(1), 14–23. https://doi.org/10.1016/j.tics.2005.11.006

Guderian, S., Dzieciol, A. M., Gadian, D. G., Jentschke, S., Doeller, C. F., Burgess, N., Mishkin, M., & Vargha-Khadem, F. (2015). Hippocampal Volume Reduction in Humans Predicts Impaired Allocentric Spatial Memory in Virtual-Reality Navigation. *The Journal of Neuroscience : The Official Journal of the Society for Neuroscience, 35*(42), 14123–14131. https://doi.org/10.1523/JNEUROSCI.0801-15.2015

Hafting, T., Fyhn, M., Molden, S., Moser, M.-B., & Moser, E. I. (2005). Microstructure of a spatial map in the entorhinal cortex. *Nature, 436*(7052), 801. https://doi.org/10.1038/nature03721

Hare, T. A., O'Doherty, J., Camerer, C. F., Schultz, W., & Rangel, A. (2008). Dissociating the role of the orbitofrontal cortex and the striatum in the computation of goal values and prediction errors. *The Journal of Neuroscience : The Official Journal of the Society for Neuroscience, 28*(22), 5623–5630. https://doi.org/10.1523/JNEUROSCI.1309-08.2008

Hartley, T., Lever, C., Burgess, N., & O'Keefe, J. (2014). Space in the brain: how the hippocampal formation supports spatial cognition. Philosophical Transactions of the Royal Society of London. *Series B, Biological Sciences, 369*(1635), 20120510. https://doi.org/10.1098/rstb.2012.0510

Hayes, S. M., Nadel, L., & Ryan, L. (2007). The effect of scene context on episodic object recognition: parahippocampal cortex mediates memory encoding and retrieval success. *Hippocampus, 17*(9), 873–889. https://doi.org/10.1002/hipo.20319

Hegarty, M. (2002). Development of a self-report measure of environmental spatial ability. *Intelligence, 30*(5), 425–447. https://doi.org/10.1016/S0160-2896(02)00116-2

Henson, R. N. A., Shallice, T., & Dolan, R. J. (1999). Right prefrontal cortex and episodic memory retrieval: a functional MRI test of the monitoring hypothesis. *Brain, 122*(7), 1367–1381. https://doi.org/10.1093/brain/122.7.1367

Hirshhorn, M., Grady, C., Rosenbaum, R. S., Winocur, G., & Moscovitch, M. (2012). Brain regions involved in the retrieval of spatial and episodic details associated with a familiar environment: An fMRI study. *Neuropsychologia, 50*(13), 3094–3106. https://doi.org/10.1016/j.neuropsychologia.2012.08.008

Howard, J. D., & Kahnt, T. (2017). Identity-Specific Reward Representations in Orbitofrontal Cortex Are Modulated by Selective Devaluation. *The Journal of Neuroscience : The Official Journal of the Society for Neuroscience, 37*(10), 2627–2638. https://doi.org/10.1523/JNEUROSCI.3473-16.2017

Howard, L. R., Javadi, A. H., Yu, Y., Mill, R. D., Morrison, L. C., Knight, R., Loftus, M. M., Staskute, L., & Spiers, H. J. (2014). The Hippocampus and Entorhinal Cortex Encode the Path and Euclidean Distances to Goals during Navigation. *Current Biology, 24*(12), 1331–1340. https://doi.org/10.1016/j.cub.2014.05.001

Iglói, K., Doeller, C. F., Berthoz, A., Rondi-Reig, L., & Burgess, N. (2010). Lateralized human hippocampal activity predicts navigation based on sequence or place memory. *Proceedings of the National Academy of Sciences of the United States of America, 107*(32), 14466–14471. https://doi.org/10.1073/pnas.1004243107

Iglói, K., Doeller, C. F., Paradis, A.-L., Benchenane, K., Berthoz, A., Burgess, N., & Rondi-Reig, L. (2015). Interaction Between Hippocampus and Cerebellum Crus I in Sequence-Based but not Place-Based Navigation. *Cerebral Cortex (New York, N.Y. : 1991), 25*(11), 4146–4154. https://doi.org/10.1093/cercor/bhu132

Jacobs, J., Weidemann, C. T., Miller, J. F., Solway, A., Burke, J. F., Wei, X.-X., Suthana, N., Sperling, M. R., Sharan, A. D., Fried, I., & Kahana, M. J. (2013). Direct recordings of grid-like neuronal activity in human spatial navigation. *Nature Neuroscience, 16*(9), 1188–1190. https://doi.org/10.1038/nn.3466

Javadi, A.-H., Patai, E. Z., Marin-Garcia, E., Margolis, A., Tan, H.-R. M., Kumaran, D., Nardini, M., Penny, W., Duzel, E., Dayan, P., & Spiers, H. J. (2019). Prefrontal Dynamics Associated with Efficient Detours and Shortcuts: A Combined Functional Magnetic Resonance Imaging and Magnetoencenphalography Study. *Journal of Cognitive Neuroscience, 31*(8), 1227–1247. https://doi.org/10.1162/jocn{\textunderscore }a{\textunderscore }01414

Jocham, G., Klein, T. A., & Ullsperger, M. (2011). Dopamine-mediated reinforcement learning signals in the striatum and ventromedial prefrontal cortex underlie value-based choices. *Journal of Neuroscience, 31*(5), 1606–1613. https://doi.org/10.1523/JNEUROSCI.3904-10.2011

Johnson, A., van der Meer, M. A. A., & Redish, A. D. (2007). Integrating hippocampus and striatum in decision-making. *Current Opinion in Neurobiology, 17*(6), 692–697. https://doi.org/10.1016/j.conb.2008.01.003

Kahnt, T., Chang, L. J., Park, S. Q., Heinzle, J., & Haynes, J.-D. (2012). Connectivity-based parcellation of the human orbitofrontal cortex. *The Journal of Neuroscience : The Official Journal of the Society for Neuroscience, 32*(18), 6240–6250. https://doi.org/10.1523/JNEUROSCI.0257-12.2012

Kaplan, R., Doeller, C. F., Barnes, G. R., Litvak, V., Düzel, E., Bandettini, P. A., & Burgess, N. (2012). Movement-related theta rhythm in humans: coordinating self-directed hippocampal learning. *PLoS Biology, 10*(2), e1001267. https://doi.org/10.1371/journal.pbio.1001267

Kaplan, R., Schuck, N. W., & Doeller, C. F. (2017). The Role of Mental Maps in Decision-Making. *Trends in Neurosciences, 40*(5), 256–259. https://doi.org/10.1016/j.tins.2017.03.002

Kennedy, P. J., & Shapiro, M. L. (2004). Retrieving memories via internal context requires the hippocampus. *The Journal of Neuroscience : The Official Journal of the Society for Neuroscience, 24*(31), 6979–6985. https://doi.org/10.1523/JNEUROSCI.1388-04.2004

Kjelstrup, K. B., Solstad, T., Brun, V. H., Hafting, T., Leutgeb, S., Witter, M. P., Moser, E. I., & Moser, M.-B. (2008). Finite scale of spatial representation in the hippocampus. *Science (New York, N.Y.), 321*(5885), 140–143. https://doi.org/10.1126/science.1157086

Klatzky, R. L. (1998). Allocentric and Egocentric Spatial Representations: Definitions, Distinctions, and Interconnections. In J. G. Carbonell, J. Siekmann, & G. Goos (Eds.), *Spatial Cognition* (pp. 1–17). Springer Berlin Heidelberg. https://doi.org/10.1007/3-540-69342-4{\textunderscore }1

Kolb, B., & Whishaw, I. Q. (2009a). Anatomy of the hippocampus. In *Fundamentals of human neuropsychology* (6th ed., pp. 500–501). Palgrave Macmillan.

Kolb, B., & Whishaw, I. Q. (2009b). Functional magnetic resonance imaging. In *Fundamentals of human neuropsychology* (6th ed., pp. 155–157). Palgrave Macmillan.

Kraus, B. J., Robinson, R. J., White, J. A., Eichenbaum, H., & Hasselmo, M. E. (2013). Hippocampal "Time Cells": Time versus Path Integration. *Neuron, 78*(6), 1090–1101. https://doi.org/10.1016/j.neuron.2013.04.015

Krekelberg, B., Boynton, G. M., & van Wezel, R. J. A. (2006). Adaptation: from single cells to BOLD signals. *Trends in Neurosciences, 29*(5), 250–256. https://doi.org/10.1016/j.tins.2006.02.008

Kriegeskorte, N., Mur, M., & Bandettini, P. A. (2008). Representational similarity analysis - connecting the branches of systems neuroscience. *Frontiers in Systems Neuroscience, 2*, 4. https://doi.org/10.3389/neuro.06.004.2008

Kühn, S., & Gallinat, J. (2014). Segregating cognitive functions within hippocampal formation: a quantitative meta-analysis on spatial navigation and episodic memory. *Human Brain Mapping, 35*(4), 1129–1142. https://doi.org/10.1002/hbm.22239

Kumaran, D., & Maguire, E. A. (2005). The Human Hippocampus: Cognitive Maps or Relational Memory? *Journal of Neuroscience, 25*(31), 7254–7259. https://doi.org/10.1523/JNEUROSCI.1103-05.2005

Kunz, L., Schröder, T. N., Lee, H., Montag, C., Lachmann, B., Sariyska, R., Reuter, M., Stirnberg, R., Stöcker, T., Messing-Floeter, P. C., Fell, J., Doeller, C. F., & Axmacher, N. (2015). Reduced grid-cell-like representations in adults at genetic risk for Alzheimer's disease. *Science (New York, N.Y.), 350*(6259), 430–433. https://doi.org/10.1126/science.aac8128

Kyle, C. T., Smuda, D. N., Hassan, A. S., & Ekstrom, A. D. (2015). Roles of human hippocampal subfields in retrieval of spatial and temporal context. *Behavioural Brain Research, 278,* 549–558. https://doi.org/10.1016/j.bbr.2014.10.034

Leutgeb, J. K., Leutgeb, S., Treves, A., Meyer, R., Barnes, C. A., McNaughton, B. L., Moser, M.-B., & Moser, E. I. (2005). Progressive Transformation of Hippocampal Neuronal Representations in "Morphed" Environments. *Neuron, 48*(2), 345–358. https://doi.org/10.1016/j.neuron.2005.09.007

Lie, C.-H., Specht, K., Marshall, J. C., & Fink, G. R. (2006). Using fMRI to decompose the neural processes underlying the Wisconsin Card Sorting Test. *NeuroImage, 30*(3), 1038–1049. https://doi.org/10.1016/j.neuroimage.2005.10.031

MacDonald, C. J., Lepage, K. Q., Eden, U. T., & Eichenbaum, H. (2011). Hippocampal ``Time Cells'' Bridge the Gap in Memory for Discontiguous Events. *Neuron, 71*(4), 737–749. https://doi.org/10.1016/j.neuron.2011.07.012

Maguire, E. A., Burgess, N., Donnett, J. G., Frackowiak, R. S., Frith, C. D., & O'Keefe, J. (1998). Knowing where and getting there: a human navigation network. *Science (New York, N.Y.), 280*(5365), 921–924. https://doi.org/10.1126/science.280.5365.921

Maldjian, J. A., Laurienti, P. J., Kraft, R. A., & Burdette, J. H. (2003). An automated method for neuroanatomic and cytoarchitectonic atlas-based interrogation of fMRI data sets. *NeuroImage, 19*(3), 1233–1239. https://doi.org/10.1016/S1053-8119(03)00169-1

Maren, S., Phan, K. L., & Liberzon, I. (2013). The contextual brain: implications for fear conditioning, extinction and psychopathology. Nature Reviews Neuroscience, 14(6), 417. https://doi.org/10.1038/nrn3492

Marschner, A., Kalisch, R., Vervliet, B., Vansteenwegen, D., & Büchel, C. (2008). Dissociable roles for the hippocampus and the amygdala in human cued versus context fear conditioning. *The Journal of Neuroscience : The Official Journal of the Society for Neuroscience, 28*(36), 9030–9036. https://doi.org/10.1523/JNEUROSCI.1651-08.2008

McNaughton, B. L., Battaglia, F. P., Jensen, O., Moser, E. I., & Moser, M.-B. (2006). Path integration and the neural basis of the "cognitive map." *Nature Reviews Neuroscience, 7*(8), 663–678. https://doi.org/10.1038/nrn1932

Milivojevic, B., Vicente-Grabovetsky, A., & Doeller, C. F. (2015). Insight Reconfigures Hippocampal-Prefrontal Memories. *Current Biology, 25*(7), 821–830. https://doi.org/10.1016/j.cub.2015.01.033

Miller, J. F., Neufang, M., Solway, A., Brandt, A., Trippel, M., Mader, I., Hefft, S., Merkow, M., Polyn, S. M., Jacobs, J., Kahana, M. J., & Schulze-Bonhage, A. (2013). Neural activity in human hippocampal formation reveals the spatial context of retrieved memories. *Science (New York, N.Y.), 342*(6162), 1111–1114. https://doi.org/10.1126/science.1244056

Morgan, L. K., MacEvoy, S. P., Aguirre, G. K., & Epstein, R. A. (2011). Distances between Real-World Locations Are Represented in the Human Hippocampus. *Journal of Neuroscience, 31*(4), 1238–1245. https://doi.org/10.1523/JNEUROSCI.4667-10.2011

Morris, R. G. M., Garrud, P., Rawlins, J. N. P., & O'Keefe, J. (1982). Place navigation impaired in rats with hippocampal lesions. *Nature, 297*(5868), 681–683. https://doi.org/10.1038/297681a0

Moser, E. I., Kropff, E., & Moser, M.-B. (2008). Place cells, grid cells, and the brain's spatial representation system. *Annual Review of Neuroscience, 31*, 69–89. https://doi.org/10.1146/annurev.neuro.31.061307.090723

Moser, E. I., Moser, M.-B., & McNaughton, B. L. (2017). Spatial representation in the hippocampal formation: a history. *Nature Neuroscience, 20*(11), 1448–1464. https://doi.org/10.1038/nn.4653

Nadel, L., Hoscheidt, S., & Ryan, L. R. (2013). Spatial cognition and the hippocampus: the anterior-posterior axis. *Journal of Cognitive Neuroscience, 25*(1), 22–28. https://doi.org/10.1162/jocn{\textunderscore }a{\textunderscore }00313

Nau, M., Schröder, T. N., Bellmund, J. L. S., & Doeller, C. F. (2018). Hexadirectional coding of visual space in human entorhinal cortex. *Nature Neuroscience, 21*(2), 188–190. https://doi.org/10.1038/s41593-017-0050-8

Nielson, D. M., Smith, T. A., Sreekumar, V., Dennis, S., & Sederberg, P. B. (2015). Human hippocampus represents space and time during retrieval of real-world memories. *Proceedings of the National Academy of Sciences, 112*(35), 11078–11083. https://doi.org/10.1073/pnas.1507104112

Noonan, M. P., Walton, M. E., Behrens, T. E. J., Sallet, J., Buckley, M. J., & Rushworth, M. F. S. (2010). Separate value comparison and learning mechanisms in macaque medial and lateral orbitofrontal cortex. *Proceedings of the National Academy of Sciences of the United States of America, 107*(47), 20547–20552. https://doi.org/10.1073/pnas.1012246107

Nutt, D., & Railton, D. (2003). The Sims: Real Life as Genre. *Information, Communication & Society, 6*(4), 577–592. https://doi.org/10.1080/1369118032000163268

Nyberg, L., McIntosh, A. R., Houle, S., Nilsson, L.-G., & Tulving, E. (1996). Activation of medial temporal structures during episodic memory retrieval. *Nature, 380*(6576), 715–717. https://doi.org/10.1038/380715a0

O'Keefe, J., & Burgess, N. (1996). Geometric determinants of the place fields of hippocampal neurons. *Nature, 381*(6581), 425. https://doi.org/10.1038/381425a0

O'Keefe, J., & Dostrovsky, J. (1971). The hippocampus as a spatial map. Preliminary evidence from unit activity in the freely-moving rat. *Brain Research, 34*(1), 171–175. https://doi.org/10.1016/0006-8993(71)90358-1

O'Keefe, J., & Nadel, L. (1978). *The Hippocampus as a Cognitive Map*. Oxford University Press. https://repository.arizona.edu/handle/10150/620894

Olsen, R. K., Moses, S. N., Riggs, L., & Ryan, J. D. (2012). The hippocampus supports multiple cognitive processes through relational binding and comparison. *Frontiers in Human Neuroscience, 6,* 146. https://doi.org/10.3389/fnhum.2012.00146

Padoa-Schioppa, C., & Assad, J. A. (2006). Neurons in the orbitofrontal cortex encode economic value. *Nature, 441*(7090), 223–226. https://doi.org/10.1038/nature04676

Pelletier, G., & Fellows, L. K. (2019). A critical role for human ventromedial frontal lobe in value comparison of complex objects based on attribute configuration. *The Journal of Neuroscience : The Official Journal of the Society for Neuroscience.* https://doi.org/10.1523/JNEUROSCI.2969-18.2019

Persson, J., Stening, E., Nordin, K., & Söderlund, H. (2018). Predicting episodic and spatial memory performance from hippocampal resting-state functional connectivity: Evidence for an anterior-posterior division of function. *Hippocampus, 28*(1), 53–66. https://doi.org/10.1002/hipo.22807

Phillips, R. G., & LeDoux, J. E. (1992). Differential contribution of amygdala and hippocampus to cued and contextual fear conditioning. *Behavioral Neuroscience, 106*(2), 274–285. https://doi.org/10.1037/0735-7044.106.2.274

Poppenk, J., Evensmoen, H. R., Moscovitch, M., & Nadel, L. (2013). Long-axis specialization of the human hippocampus. *Trends in Cognitive Sciences, 17*(5), 230–240. https://doi.org/10.1016/j.tics.2013.03.005

Preuschoff, K., Quartz, S. R., & Bossaerts, P. (2008). Human insula activation reflects risk prediction errors as well as risk. *The Journal of Neuroscience : The Official Journal of the Society for Neuroscience, 28*(11), 2745–2752. https://doi.org/10.1523/JNEUROSCI.4286-07.2008

Ranganath, C. (2010). A unified framework for the functional organization of the medial temporal lobes and the phenomenology of episodic memory. *Hippocampus, 20*(11), 1263–1290. https://doi.org/10.1002/hipo.20852

Ranganath, C., Heller, A., Cohen, M. X., Brozinsky, C. J., & Rissman, J. (2005). Functional connectivity with the hippocampus during successful memory formation. *Hippocampus, 15*(8), 997–1005. https://doi.org/10.1002/hipo.20141

Rangel, A., Camerer, C., & Montague, P. R. (2008). A framework for studying the neurobiology of value-based decision making. *Nature Reviews Neuroscience, 9*(7), 545. https://doi.org/10.1038/nrn2357

Rubin, R. D., Schwarb, H., Lucas, H. D., Dulas, M. R., & Cohen, N. J. (2017). Dynamic Hippocampal and Prefrontal Contributions to Memory Processes and Representations Blur the Boundaries of Traditional Cognitive Domains. *Brain Sciences, 7*(7), 82. https://doi.org/10.3390/brainsci7070082

Rugg, M. D., & Vilberg, K. L. (2013). Brain networks underlying episodic memory retrieval. *Current Opinion in Neurobiology, 23*(2), 255–260. https://doi.org/10.1016/j.conb.2012.11.005

Rugg, M. D., Vilberg, K. L., Mattson, J. T., Yu, S. S., Johnson, J. D., & Suzuki, M. (2012). Item memory, context memory and the hippocampus: fMRI evidence. *Neuropsychologia, 50*(13), 3070–3079. https://doi.org/10.1016/j.neuropsychologia.2012.06.004

Rushworth, M. F. S., & Behrens, T. E. J. (2008). Choice, uncertainty and value in prefrontal and cingulate cortex. *Nature Neuroscience, 11*(4), 389. https://doi.org/10.1038/nn2066

Rushworth, M. F. S., Noonan, M. P., Boorman, E. D., Walton, M. E., & Behrens, T. E. (2011). Frontal cortex and reward-guided learning and decision-making. *Neuron, 70*(6), 1054–1069. https://doi.org/10.1016/j.neuron.2011.05.014

Salz, D. M., Tiganj, Z., Khasnabish, S., Kohley, A., Sheehan, D., Howard, M. W., & Eichenbaum, H. (2016). Time Cells in Hippocampal Area CA3. *Journal of Neuroscience, 36*(28), 7476–7484. https://doi.org/10.1523/JNEUROSCI.0087-16.2016

Sarel, A., Finkelstein, A., Las, L., & Ulanovsky, N. (2017). Vectorial representation of spatial goals in the hippocampus of bats. *Science (New York, N.Y.), 355*(6321), 176–180. https://doi.org/10.1126/science.aak9589

Schapiro, A. C., Kustner, L. V, & Turk-Browne, N. B. (2012). Shaping of Object Representations in the Human Medial Temporal Lobe Based on Temporal Regularities. *Current Biology, 22*(17), 1622–1627. https://doi.org/10.1016/j.cub.2012.06.056

Schiller, D., Eichenbaum, H., Buffalo, E. A., Davachi, L., Foster, D. J., Leutgeb, S., & Ranganath, C. (2015). Memory and Space: Towards an Understanding of the Cognitive Map. *The Journal of Neuroscience : The Official Journal of the Society for Neuroscience, 35*(41), 13904–13911. https://doi.org/10.1523/JNEUROSCI.2618-15.2015

Schlichting, M. L., Mumford, J. A., & Preston, A. R. (2015). Learning-related representational changes reveal dissociable integration and separation signatures in the hippocampus and prefrontal cortex. *Nature Communications, 6*(1), 1–10. https://doi.org/10.1038/ncomms9151

Schuck, N. W., Cai, M. B., Wilson, R. C., & Niv, Y. (2016). Human Orbitofrontal Cortex Represents a Cognitive Map of State Space. *Neuron, 91*(6), 1402–1412. https://doi.org/10.1016/j.neuron.2016.08.019

Scoville, W. B., & Milner, B. (1957). Loss of recent memory after bilateral hippocampal lesions. *Journal of Neurology, Neurosurgery, and Psychiatry, 20*(1), 11–21.

Seger, C. A., & Cincotta, C. M. (2002). Striatal activity in concept learning. *Cognitive, Affective, & Behavioral Neuroscience, 2*(2), 149–161. https://doi.org/10.3758/CABN.2.2.149

Seger, C. A., & Miller, E. K. (2010). Category learning in the brain. *Annual Review of Neuroscience, 33*, 203–219. https://doi.org/10.1146/annurev.neuro.051508.135546

Shastri, L. (2002). Episodic memory and cortico--hippocampal interactions. *Trends in Cognitive Sciences, 6*(4), 162–168. https://doi.org/10.1016/S1364-6613(02)01868-5

Sherrill, K. R., Erdem, U. M., Ross, R. S., Brown, T. I., Hasselmo, M. E., & Stern, C. E. (2013). Hippocampus and retrosplenial cortex combine path integration signals for successful navigation. *The Journal of Neuroscience : The Official Journal of the Society for Neuroscience, 33*(49), 19304–19313. https://doi.org/10.1523/JNEUROSCI.1825-13.2013

Shohamy, D., & Daw, N. D. (2015). Integrating memories to guide decisions. *Current Opinion in Behavioral Sciences, 5*, 85–90. https://doi.org/10.1016/j.cobeha.2015.08.010

Spiers, H. J., & Barry, C. (2015). Neural systems supporting navigation. *Current Opinion in Behavioral Sciences, 1*, 47–55. https://doi.org/10.1016/j.cobeha.2014.08.005

Spiers, H. J., Burgess, N., Maguire, E. A., Baxendale, S. A., Hartley, T., Thompson, P. J., & O'Keefe, J. (2001). Unilateral temporal lobectomy patients show lateralized topographical and episodic memory deficits in a virtual town. *Brain, 124*(12), 2476–2489. https://doi.org/10.1093/brain/124.12.2476

Spiers, H. J., & Gilbert, S. J. (2015). Solving the detour problem in navigation: a model of prefrontal and hippocampal interactions. *Frontiers in Human Neuroscience, 9*, 125. https://doi.org/10.3389/fnhum.2015.00125

Spiers, H. J., & Maguire, E. A. (2007). A navigational guidance system in the human brain. *Hippocampus, 17*(8), 618–626. https://doi.org/10.1002/hipo.20298

Squire, L. R. (1982). The neuropsychology of human memory. *Annual Review of Neuroscience, 5*, 241–273. https://doi.org/10.1146/annurev.ne.05.030182.001325

Squire, L. R. (1992). Declarative and nondeclarative memory: multiple brain systems supporting learning and memory. *Journal of Cognitive Neuroscience, 4*(3), 232–243. https://doi.org/10.1162/jocn.1992.4.3.232

Squire, L. R. (2009). The Legacy of Patient H.M. for Neuroscience. *Neuron, 61*(1), 6–9. https://doi.org/10.1016/j.neuron.2008.12.023

Squire, L. R., & Wixted, J. T. (2011). The cognitive neuroscience of human memory since H.M. *Annual Review of Neuroscience, 34*, 259–288. https://doi.org/10.1146/annurev-neuro-061010-113720

Squire, L. R., & Zola-Morgan, S. (1991). The medial temporal lobe memory system. *Science (New York, N.Y.), 253*(5026), 1380–1386. https://doi.org/10.1126/science.1896849

Stachenfeld, K. L., Botvinick, M. M., & Gershman, S. J. (2017). The hippocampus as a predictive map. *Nature Neuroscience, 20*(11), 1643–1653. https://doi.org/10.1038/nn.4650

Taube, J. S., Muller, R. U., & Ranck, J. B. (1990). Head-direction cells recorded from the postsubiculum in freely moving rats. I. Description and quantitative analysis. *Journal of Neuroscience, 10*(2), 420–435. https://doi.org/10.1523/JNEUROSCI.10-02-00420.1990

Tavares, R. M., Mendelsohn, A., Grossman, Y., Williams, C. H., Shapiro, M., Trope, Y., & Schiller, D. (2015). A Map for Social Navigation in the Human Brain. Neuron, 87(1), 231–243. https://doi.org/10.1016/j.neuron.2015.06.011

Theves, S., Fernandez, G., & Doeller, C. F. (2019). The Hippocampus Encodes Distances in Multidimensional Feature Space. Current Biology : CB, 29(7), 1226-1231.e3. https://doi.org/10.1016/j.cub.2019.02.035

Tobler, P. N., O'Doherty, J. P., Dolan, R. J., & Schultz, W. (2007). Reward value coding distinct from risk attitude-related uncertainty coding in human reward systems. *Journal of Neurophysiology, 97*(2), 1621–1632. https://doi.org/10.1152/jn.00745.2006

Tolman, E. C. (1948). Cognitive maps in rats and men. *Psychological Review, 55*(4), 189–208. https://doi.org/10.1037/h0061626

Tulving, E. (2002). Episodic memory: from mind to brain. *Annual Review of Psychology, 53*, 1–25. https://doi.org/10.1146/annurev.psych.53.100901.135114

Tulving, E., & Markowitsch, H. J. (1998). Episodic and declarative memory: Role of the hippocampus. *Hippocampus, 8*(3), 198–204. https://doi.org/10.1002/(SICI)1098-1063(1998)8:3<198::AID-HIPO2>3.0.CO;2-G

Viard, A., Doeller, C. F., Hartley, T., Bird, C. M., & Burgess, N. (2011). Anterior Hippocampus and Goal-Directed Spatial Decision Making. *Journal of Neuroscience, 31*(12), 4613–4621. https://doi.org/10.1523/JNEUROSCI.4640-10.2011

Vikbladh, O. M., Meager, M. R., King, J., Blackmon, K., Devinsky, O., Shohamy, D., Burgess, N., & Daw, N. D. (2019). Hippocampal Contributions to Model-Based Planning and Spatial Memory. *Neuron.* https://doi.org/10.1016/j.neuron.2019.02.014

Wikenheiser, A. M., & Schoenbaum, G. (2016). Over the river, through the woods: cognitive maps in the hippocampus and orbitofrontal cortex. *Nature Reviews Neuroscience, 17*(8), 513. https://doi.org/10.1038/nrn.2016.56

Wilson, M. A., & McNaughton, B. L. (1993). Dynamics of the hippocampal ensemble code for space. *Science, 261*(5124), 1055–1058. https://doi.org/10.1126/science.8351520

Wimmer, G. E., & Shohamy, D. (2012). Preference by association: how memory mechanisms in the hippocampus bias decisions. *Science (New York, N.Y.), 338*(6104), 270–273. https://doi.org/10.1126/science.1223252

Zald, D. H., McHugo, M., Ray, K. L., Glahn, D. C., Eickhoff, S. B., & Laird, A. R. (2014). Meta-Analytic Connectivity Modeling Reveals Differential Functional Connectivity of the Medial and Lateral Orbitofrontal Cortex. *Cerebral Cortex, 24*(1), 232–248. https://doi.org/10.1093/cercor/bhs308

Zandbelt, B. (2017). *Slice display*. Figshare. https://doi.org/10.6084/M9.FIGSHARE.4742866

Zhang, S.-J., Ye, J., Couey, J. J., Witter, M., Moser, E. I., & Moser, M.-B. (2014). Functional connectivity of the entorhinal-hippocampal space circuit. *Philosophical Transactions of the Royal Society of London. Series B, Biological Sciences, 369*(1635), 20120516. https://doi.org/10.1098/rstb.2012.0516

Research data management

This thesis research has been carried out under the institute research data management policy of the Donders Institute for Brain, Cognition and Behaviour. The appropriate guidelines can be found here: **https://www.ru.nl/donders/research/research-data-management/** (date of last access: 23-01-2020).

List of persistent identifiers of datasets

Chapter 2 **http://hdl.handle.net/11633/aac44hn3**
Chapter 3 **http://hdl.handle.net/11633/aac4cbvy**
Chapter 4 archived on discs HDD 1224 & 1225 with identifier 3012031.01

Nederlandse samenvatting

Net zoals waarschijnlijk alle promovendi, moest ik veel obstakels overwinnen om mijn scriptie af te ronden. Eén ding vond ik echter minder erg: het wonen en werken in Nijmegen. Dat komt natuurlijk omdat Nijmegen een aantal erg leuke cafés heeft. Maar ook doordat het, waar je ook woont, minder dan een kwartier duurt om naar je werk te fietsen. Ik vind het echter vooral leuk vanwege het jaarlijkse meerdaagse openluchtfestival. Miljoenen bezoekers uit de hele wereld verzamelen zich dan in deze middelgrote stad om te feesten. Ik heb erg mooie herinneringen aan dit evenement. Zo denk ik wel eens terug aan het moment dat ik met mijn vrienden aan de rand van de rivier zit. Het is een warme zomeravond en wij zitten in een massa van vrolijke mensen naar het vuurwerk te kijken. Maar, die massa mensen brengt soms ook wat problemen met zich mee. Kijk, de eigenlijke oorsprong van het festival is een vierdaagse mars. De deelnemers moeten elke dag een andere (extreem lange) route wandelen. Als gevolg daarvan wordt elke dag een andere reeks straten afgesloten voor het grote publiek. Dit geeft mij (en vele, vele anderen) de uitdaging om elke dag opnieuw een omweg naar het kantoor te plannen.
Op dit punt zou je je kunnen afvragen waarom ik dit verhaal vertel. En verder hoe dit alles in verband staat met het onderwerp van mijn scriptie. Ik heb een heel specifiek hersengebied bestudeerd: de hippocampus. Wat mij fascineert aan de hippocampus is dat hij betrokken is bij zeer verschillende aspecten van dit verhaal. Zo weten wij dat de hippocampus belangrijk is voor het onthouden van gebeurtenissen. Denk maar weer terug aan mijn herinnering bij de rivier. Waar ik samen met mijn vrienden naar het vuurwerk kijk. Tegelijkertijd speelt de hippocampus een grote rol voor het oplossen van navigatieproblemen. Bijvoorbeeld de fietstocht van mijn huis naar het kantoor. Dat brengt mij tot de kern van dit proefschrift: hoe ondersteunt de hippocampus blijkbaar verschillende functies als geheugen en navigatie? Hiervoor heb ik samen met mijn collega's drie experimenten uitgevoerd.

In het eerste experiment hebben we de mentale kaarten die de hippocampus vormt van onze omgeving onder de loep genomen. Denk terug aan het verhaal: ik fiets vaak van mijn huis naar kantoor. Hiervoor heb ik een mentale kaart van Nijmegen (of in ieder geval delen daarvan) nodig. Als ik een kaart van Nijmegen voor je zou leggen, zou ik een rechte lijn kunnen trekken tussen mijn huis en het kantoor. Dit is de Euclidische afstand. Ik zou ook de route kunnen tekenen die ik moet fietsen om naar het kantoor te komen. Dit is de route afstand. Nota bene kon ik mijn regulaire route zelfs aanpassen toen ik tijdens het festival nieuwe wegversperringen tegenkwam. Waaruit blijkt dat deze mentale kaart ook flexibel moet zijn. In de eerste studie hebben we gekeken naar representaties in de hippocampus van deze verschillende afstandsmetingen en hoe deze worden bijgewerkt wanneer er snelkoppelingen of omwegen worden ingevoerd.

Om navigeren uit het echte leven in het lab na te bootsen, lieten we de deelnemers een computerspel spelen. Zij moesten hun weg vinden in een grote virtuele stad. Zo konden we manipuleren welke routes de deelnemers van de ene naar de andere locatie konden nemen. Met behulp van functionele kernspintomografie (fMRI) hebben we gemeten hoe de hippocampus een mentale kaart van deze virtuele omgeving vormt en bijwerkt. Onze resultaten tonen aan dat de hippocampus zowel de Euclidische als de route afstand tussen belangrijke locaties kan coderen. Daarnaast liet het zien dat de mentale kaarten van de hippocampus kunnen worden geupdatet wanneer deelnemers nieuwe routes moesten bedenken om op hun bestemming te komen.

In het tweede experiment hebben we op hetzelfde moment gekeken naar hippocampale verwerking van navigatie en het episodisch geheugen. We hebben twee tegengestelde ideeën getest. Een idee is dat de hippocampus dezelfde coderingsmechanismen gebruikt bij navigatie als bij het episodisch geheugen. Het tweede idee gaat ervanuit dat verschillende subregio's in de hippocampus betrokken zijn bij een van de beide functies. De vraag is of de hippocampus mijn herinnering van het vuurwerk op dezelfde manier verwerkt als mijn fietstocht naar kantoor. Of zijn er verschillende delen van de hippocampus die voor het ene coderen, maar niet voor het andere? Om deze vraag te beantwoorden hebben we de ruimtelijke en episodische relaties tussen items gemanipuleerd. Tijdens een navigatietaak verschenen er items op twee verschillende locaties in een virtuele stad. Hierdoor waren items die op dezelfde locatie verschenen meer ruimtelijk verbonden dan items die op verschillende locaties verschenen. Gelijkwaardig verschenen de items in twee verschillende verhalen tijdens een episodische taak. Dit betekent dat items die in hetzelfde verhaal verschenen meer episodisch verbonden waren dan items die in verschillende verhalen verschenen. We gebruikten opnieuw fMRI om te meten hoe de hippocampus deze ruimtelijke en episodische relaties verwerkt. Onze resultaten ondersteunen het idee dat de hippocampus episodische en ruimtelijke relaties integreert en op dezelfde manier verwerkt. Maar we vonden geen bewijs, dat verschillende subregio's van de hippocampus navigatie meer verwerken dan geheugen of vice-versa.

In het derde en laatste experiment wilden we een stap verder gaan dan geheugen en navigatie. Wij stelden de vraag of de hippocampus dezelfde mechanismen ook gebruikt voor andere cognitieve functies. Tot nu hadden we onderzocht hoe de hippocampus een kaart vormt van onze werkelijke en fysieke omgeving. Nu testten we het idee dat de hippocampus bovendien ook 'abstracte' kaarten vormt van verschillende aspecten van onze wereld. Dit kan ik het makkelijkste uitleggen met weer het voorbeeld van de Nijmeegse zomerfeesten. Tijdens dit evenement heb je veel verschillende podia. Op deze verschillende plekken wordt tegelijk live muziek gespeeld. Ik moet dus mijn opties afwegen om te beslissen naar welke act ik wil gaan. Er kunnen verschillende criteria

zijn die mijn beslissing beïnvloeden. Zoals hoe leuk ik de muziekstijl van de act vind. Of hoe druk het zal zijn. Gezien het feit dat ik erg klein ben, vooral voor Nederlandse begrippen, is dit ook een belangrijk criterium. Er zijn meerdere manieren om deze twee criteria af te beelden. Een daarvan is het tekenen van een tweedimensionale abstracte ruimte. Daarbij geeft de ene as weer hoe leuk ik de muziekstijl vind. De tweede as geeft daarnaast aan hoe groot de kans is dat ik het podium kan zien. In het derde experiment wilden we het idee testen dat de hippocampus dezelfde mechanismen kan toepassen die hij gebruikt om de fysieke ruimte te representeren om zo'n abstracte ruimte te representeren. Tijdens het experiment associeerden de deelnemers items met twee soorten (numerieke) waarden. Net als in het voorbeeld vertegenwoordigde elk type waarde één as van een tweedimensionale "waarde-ruimte". Vervolgens hebben we met fMRI getest of de hippocampus afstanden in zo'n waarde ruimte kan weergeven. Net zoals in het eerste experiment, waarbij we ontdekten dat de hippocampus afstanden in een virtuele stad kan coderen. We vonden echter geen bewijs dat de hippocampus de mechanismen die we in het eerste experiment vonden, toepast op een abstracte waardenruimte.

Samengevat: wij weten dat de hippocampus belangrijk is voor zowel navigeren als herinneren. Het werk van dit proefschrift versterkt het idee dat de hippocampus vergelijkbare mechanismen gebruikt om deze twee functies te ondersteunen. Het laat zien dat de hippocampus flexibele kaarten vormt. En dat deze kaarten ruimtelijke en episodische informatie kunnen integreren. Het suggereert dus dat de hippocampus mijn herinnering aan het vuurwerken mijn fietstocht naar kantoor inderdaad op dezelfde manier verwerkt.
Tot slot ontstond de vraag of de hippocampus ook andere, meer abstracte functies in deze mentale kaarten kan verwerken. In mijn laatste experiment kon ik geen bewijs vinden voor representaties van abstracte kaarten in de hippocampus. Daarom denk ik dat dit wel een interessante vraag is voor toekomstig onderzoek. Onder welke specifieke omstandigheden vormt de hippocampus mentale kaarten en onder welke niet?

Acknowledgments

I was 14 or 15 when my brother Ben introduced me to cognitive neuroscience. He was a first year psychology student and asked me to give him feedback on a practice talk for one of his classes. He apparently did a pretty good job, as I was hooked. In the following years, him explaining me neuroscience and psychology interluded with my unsophisticated commentary became a stable part of our relationship. It's been 16 years and still one of my favourite things is to discuss science and research ideas with him. So Ben, thank you! I would neither be the person nor the scientist I am today without you.

When I think about my best memories of my time at the Donders, one that sticks out is Lonja's laugh. It's the kind of laugh you already hear from down the corridor – the kind that you recognize instantaneously and that you can't help but smile the second it hits your ear. There is also no person I have laughed with more than Lonja, even or maybe especially in the difficult times. Thank you Lonja for being the stupidest smart person. I know, that you know, that this is the highest compliment I can give.

I want to thank my supervisors Roshan, Mona and Christian for their support, input and guidance over the years and for giving me the freedom to develop my own ideas – even though a lot of them failed. I want to especially thank Roshan for letting me join her research group in the later half of my PhD – you became a mentor and a rolemodel and reminded me why I love research. Mona, even though we started working together pretty late into my PhD, you completely reshaped how I thought about cognitive mapping – thank you for the most inspiring and brilliant discussions and helping me with the (dreaded) analyses of this thesis.

I had the immense pleasure to collaborate with a broad range of scientists from junior to PI level on my projects. I want to thank all of the many interns, I was lucky enough to supervise and their contributions to the work in this thesis. Two of them stand out in their contributions and talent and I am proud to see that after their master thesis, they decided to continue our work with their own spin on it. Loes, you tackled together with me the most technical challenging project of this whole thesis with incredible dedication. I think spending so many afternoons in the weekend in a dark cellar together, collecting MRI data creates a special bond between people. I will never forget that you made a whole special cat edition of your thesis for me. Alex, I had the honour of supervising you twice – and both times I was just impressed by your smarts and joy for research. Even as a bachelor student you always went a step further than was expected of you. Thanks for all your hard work and your great input over the years. Last, but not least I want to thank Nico for collaborating on the value space project and

for all his incredible help, not only for modelling the data, but all the great discussions and insights about cognitive mapping and decision making.

Thanks to the entire Döller lab for all the interesting, creative and challenging talks and discussions. Even though, the majority of the lab was located in Norway and Germany, I always felt welcomed and part of the team during visits, lab outings and our annual travels to SfN. I especially want to thank the (current and former) lab members Jacob, Lorena, David, Tobias, Misun and Dörte – you all have not only been inspiring, but also fun to work with.

Thanks to the entire Cools lab and the BCS for taking me in, after the majority of my original lab had transferred away from the Donders. The strong strive of the team as whole towards more open science was and is inspiring to witness. Special thanks to Xiaochen for the great late afternoon brainstorms about the connection between cognitive mapping and language and science in general.

I want to thank the many people at the Donders, that always let me interrupt their work to grab a coffee. You made life at the Donders so much more colourful. For all the discussions, the great stories and distraction from my frustrations over Matlab: thank you. I want to give a special thanks to the following people: Monja, you were much more than an office mate, you became a good friend and also my favourite gym mate. Your humour, intelligence, and love for food continuously brightened up the mood of the whole office. Claudia, you are inspiring for how you manage to balance your life and how outspoken and active you are about social issues. I don't think I met anyone in my life, who is that structured and creative at the same time. Sophie, thanks for our many talks about food - I am still most impressed by the fact that you managed to make macarons. And Mats thanks to you, I know a lot more about Dutch carnival now – I still don't understand it though.

I want to thank my big, loud family, full of strong and unique characters – I love you all. Opa Vadder, I am always impressed by your wit, unbreakable spirit and deep curiosity about the world. Your continuous support opened many doors for me, including moving abroad to study cognitive neuroscience. Thanks for all the knowledge, anecdotes and laughs you have shared with me. Mama & Papa, thanks for all the incredible help and generosity over the years and most of all for creating a home where asking critical questions and finding your own conclusions was always encouraged and nourished. To my brothers and sisters (in law) Ricky, Maria, Sammy, Ben and Simone there is one thing for sure: life has never been boring with you. I am thankful to have you in my life, each allowing me access to a different perspective on the world. And last but not least a huge thank you to the next generation of de Haasen: Finn, Mika, Svea and Muthe.

Nothing let me forget the stress about this thesis better, than hanging out with you rascals.

Nanami and Mark, people often say "make yourself at home", however from my experience there are only a couple of places that can feel as comfortable as home. I know that the moment I enter through your door I can just be myself. Nanami, you have been with me for some of the happiest adventures of my life – thanks for being my partner (panda) in crime, the best motivator - during our runs & otherwise, for always lending an ear and watching trashy TV shows with me. Mark, thank you for all the honest, open and well thought out advice you have given me over the years and also for still not letting go of the disappointment of the Game of Thrones finale (still stings).

Anne, it all started on a grass field during introduction week – from there one we studied our Master's together, lived together for 2+ years, travelled together and went through our PhDs together. You are someone I can do both with: talk for hours and sit in complete, relaxed silence. Thank you for our weekly lunches, for our visits to the spa and for sharing all the ups and downs of our PhDs with each other. Dennis, hanging out with you is never boring and no matter what the situation is, we always manage to do something fun. However, I want to give you a special thank you for all the advice and pep talks you have given me to find out what is out there for me outside of academia.

Caprice and Nicole, it all started in the intern room at the DCCN and I am happy that years later we are still in each other's life. Caprice, my fellow crazy cat lady, thank you for the best games of cards against humanity, your amazing vegan desserts and for just hanging out. Nicole, thank you for the best memes, live messaging while watching RPDR and always picking the best places to eat at.

It's been almost 8 years since I left Germany and came to Nijmegen and I didn't know how central friendships in my life would change with this move. I never expected, however to be that lucky and to still be so close to that many people – no matter how long we haven't seen each other. Lennart, you are my oldest friend, and have been with me and supported me through all major milestones of my life. However, I especially value and want to thank you the 'little moments' – like cooking a meal together, taking long walks through the open fields between our houses, the stupid jokes and just sitting on the couch talking for hours. Tobi, Natalie, Biene & Fabi the Bachelor and Bochum wouldn't have been the same without you. Whether as PhDs or psychotherapists, we all had major academic achievements in the last year and it is special to be able to celebrate (once we are allowed to celebrate again) this with the people you started as an undergrad with. So Tobi thank you for all the enthusiastic discussions about

research, Nathalie for your calming presence, Biene for being the best host and Fabi for your unbreakable positive outlook on life.

I am very fortunate to have a life full with amazing people and unfortunately I could not name and thank everyone explicitly on these pages. Each person mentioned here has directly supported me during the creation of this thesis, let it be through their knowledge, wisdom, skills or by keeping me sane. After my thesis got approved for a defense (which is well over a year go) my life has only gotten better. I want to give a special thanks to Mitchell for enriching my life in so many ways since we met: I love you.

Donders Graduate School for Cognitive Neuroscience

For a successful research Institute, it is vital to train the next generation of young scientists. To achieve this goal, the Donders Institute for Brain, Cognition and Behaviour established the Donders Graduate School for Cognitive Neuroscience (DGCN), which was officially recognised as a national graduate school in 2009. The Graduate School covers training at both Master's and PhD level and provides an excellent educational context fully aligned with the research programme of the Donders Institute.
The school successfully attracts highly talented national and international students in biology, physics, psycholinguistics, psychology, behavioral science, medicine and related disciplines. Selective admission and assessment centers guarantee the enrolment of the best and most motivated students.
The DGCN tracks the career of PhD graduates carefully. More than 50% of PhD alumni show a continuation in academia with postdoc positions at top institutes worldwide, e.g. Stanford University, University of Oxford, University of Cambridge, UCL London, MPI Leipzig, Hanyang University in South Korea, NTNU Norway, University of Illinois, North Western University, Northeastern University in Boston, ETH Zürich, University of Vienna etc.. Positions outside academia spread among the following sectors: specialists in a medical environment, mainly in genetics, geriatrics, psychiatry and neurology. Specialists in a psychological environment, e.g. as specialist in neuropsychology, psychological diagnostics or therapy. Positions in higher education as coordinators or lecturers. A smaller percentage enters business as research consultants, analysts or head of research and development. Fewer graduates stay in a research environment as lab coordinators, technical support or policy advisors. Upcoming possibilities are positions in the IT sector and management position in pharmaceutical industry. In general, the PhDs graduates almost invariably continue with high-quality positions that play an important role in our knowledge economy.

For more information on the DGCN as well as past and upcoming defenses please visit:
http://www.ru.nl/donders/graduate-school/phd/

Curriculum Vitae

Anna Naomi de Haas was born on 23rd of August 1990 in Gieen, Germany. After obtaining her High School degree in 2010, she decided to study Psychology at the Ruhr-University Bochum, Germany. Here, Naomi majored in cognitive neuroscience and gathered first hands-on research experience. She worked as a research assistant in the cognitive psychology department of Prof. Dr. Oliver Wolf. Her work focused on studies about the influence of stress on memory and learning.

Based on these early research experiences, Naomi was driven to expand her theoretical and practical knowledge about cognitive neuroscience after completing her bachelor's in 2013. The research master's program of the Donders Institute gave her the perfect opportunity to do so. After her first year of the master's program, she joined the research group of Prof. Dr. Christian Doeller to conduct an fMRI study about the hippocampal processing mechanisms of episodic memory and navigation. The resulting master thesis was awarded with the Jan Brouwer Thesis Prize in the field humanities from the Royal Holland Society of Sciences and Humanities (KHMW).

Based on the results of her master thesis she wrote, in collaboration with Prof. Dr. Christian Doeller, a grant proposal for a 4-year PhD program. The application was rewarded with the Research Talent Grant from the Dutch Research Council (NWO) in 2015 and the work presented in this thesis is funded by this grant. During her PhD, Naomi also joined the research group of Prof. Dr. Roshan Cools to collaborate on projects expanding the idea of hippocampal mapping mechanisms beyond navigation and episodic memory. In addition to her own research activities, Naomi supervised several Bachelor and Master's students and was involved in teaching introductory courses about cognitive neuroscience.

During her academic career, Naomi developed a passion for academic writing and a general drive to work on broad and diverse topics. She decided to join the Life Sciences team of Hezelburcht - one of the largest grant consultancy agencies in the Netherlands - in 2020 to pursue this passion. Here, she helps academic researchers and industrial developers to bring their ideas to paper.